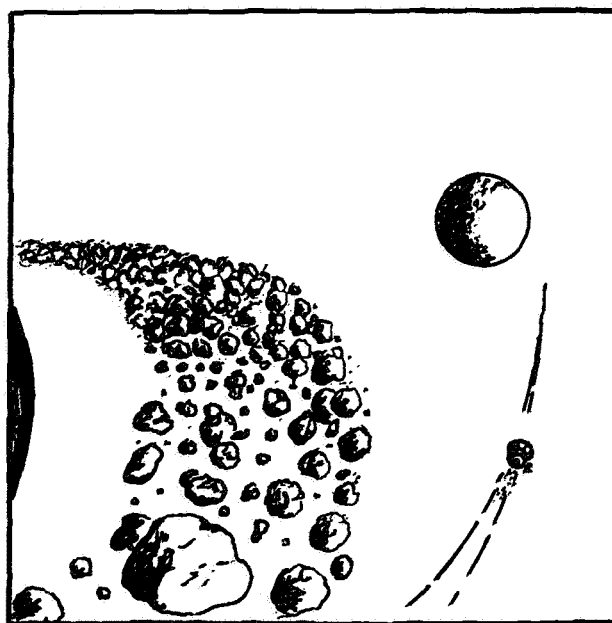Volume II

Final
Report

June 1976

Technical Report

A Titan Exploration Study - Science, Technology, and Mission Planning Options

MARTIN MARIETTA

MCR-76-186

NASA CR 137847

VOLUME II

FINAL REPORT

A TITAN EXPLORATION STUDY - SCIENCE,
TECHNOLOGY AND MISSION PLANNING OPTIONS

MAY 1976

SUMMARY

This study effort has examined new mission concepts and technology advancements that can be used in the exploration of the Outer Planet satellites. Titan, the seventh satellite of Saturn was selected as the target of interest. Science objectives for Titan exploration were identified and recommended science payloads for four basic mission modes were developed (orbiter, atmospheric probe, surface penetrator and lander). Trial spacecraft and mission designs were produced for the various mission modes using existing technology. Using these trial designs as a base, technology excursions were then made to find solutions to the problems resulting from these conventional approaches and to uncover new science, technology and mission planning options. The measure of worth of these new options is their contribution to mission performance, reliability and science value. Several interesting mission modes were developed that take advantage of the unique conditions expected at Titan. They include a combined orbiter, atmosphere probe and lander vehicle, a combined probe and surface penetrator configuration, and concepts for advanced remote sensing orbiters.

ACKNOWLEDGEMENT

STUDY TEAM

Program Manager	W. T. Scofield
Technical Directors	J. R. Mellin
	T. C. Hendricks
Technical Team	
Mission Analysis	A. L. Satin
Special Orbit Analyses	G. R. Hollenbeck
Technology Concepts	P. C. Carroll
	G. R. Hollenbeck
	W. H. Tobey
Science	B. C. Clark
Configuration	N. M. Phillips
Propulsion	R. Fearn
Thermal Control	T. Buna
	R. Giellis
Power	A. A. Sorensen
Guidance and Control	F. A. Vandenberg
Communications	R. E. Compton

CONTENTS

Figures (Cont'd)

CONTENTS (Cont'd)

CONTENTS (Cont'd)

LIST OF SYMBOLS

β	Ballistic Coefficient
γ	Flight Path Angle
γ_E	Flight Path Angle at Entry
ΔV	Delta-Velocity
ΔV_a	Delta-Velocity at Aphelion
ΔV_{SB}	Earth Swingby Delta-Velocity
θ_{AIM}	Approach Inclination
μ_m	Microns
ρ	Density
Ω	Ascending Node
$\mho$	Descending Node
ABS	Alpha Backscatter Spectometer
AMU	Atomic Mass Unit
APC	Apoapsis Plane Change
APM	Advanced Propulsion Module
ARSO	Advanced Remote Sensing Orbiter
BER	Bit Error Rate
bps	Bits-per-sec
C	Camera
C_3	Earth Departure Energy
CA	Cone Angle
CLA	Clock Angle
COSPAR	Commitee of Space Research
db	Decibel
DLA	Declination of Launch Aymptote
DR	Downrange
DSC	Differential Scanning Calorimetry
DV	Delta-Velocity
E_L	Earth Launch
GEX	Gas Exchange (ala Viking GEX Life Detection)
GC	Gas Chromatography
GCMS	Gas Chromatography Mass Spectrometer
h	Altitude
H/S	Heat Shield
i	Inclination
i_h	Approach Hyperbola Inclination

IR	Infrared
IUS	Interim Upper Stage
L	Lander
L/V	Launch Vehicle
mb	Millibars
MS	Mass Spectrometry
MSO	Mariner S/C Orbiter
NAS	National Academy of Sciences
O	Orbiter
OAST	Office of Aeronautics and Space Technology
P	Probe
P_A	Atmospheric Pressure
PAA	Probe Aspect Angle
Pg	Probability of Growth
PM	Propulsion Module
PSO	Pioneer S/C Orbiter
q	Dynamic Pressure
RCA	Radius of Closest Approach
RF	Radio Frequency
R_J	Radius of Jupiter
R_N	Radius of Nose Cone
R_F	Periapsis Radius
RPA	Retarding Potential Analyzer
R_S	Saturn Radius
RTG	Radioisotope Thermoelectric Generator
S/C	Spacecraft
SOI	Saturn Orbit Injection
SS	Space Storable
t	Time
T_A	Atmospheric Temperature
TOPL	Titan Orbiter/Probe/Lander
UV	Ultraviolet
V_∞	V-Infinity
V_E	Entry Velocity
V_{HP}	Hyperbolic Excess Velocity
W_{INJ}	Injected Weight
XR	Crossrange Distance
XRD	X-ray Diffractometry
XRFS	X-Ray Flourescence Spectrometer

I. INTRODUCTION

The principal objective of this study has been to identify new technology concepts that will contribute to the exploration of the outer planet satellites in general, and Titan in particular. Since only limited studies of Titan missions had been performed, it was necessary to first establish some baselines from which new technology requirements could be measured. This was done by compiling a consensus of Titan exploration science objectives and then devising four mission/spacecraft modes that attempted to meet these objectives. The four modes, orbiter, atmospheric probe, surface penetrator and lander, were developed into trial designs using conventional technology and applications of existing spacecraft. The orbiter mode was implemented both in a Mariner-class, three-axis stabilized configuration and a Pioneer-class, spin-stabilized version.* The atmospheric probe was based on the Ames Research Center's outer planets probe. The surface penetrator was derived from the Sandia Corporation devices used in Earth applications and studied for Mars exploration. The lander trial design used Viking technology as a base.

Figure I-1 shows the principal features of the orbiter mission trial design and Figures I-2, I-3 and I-4 illustrate the characteristics of the atmosphere probe, the surface penetrator and the lander baselines.

By examining the trial mission and spacecraft designs it became clear where mission performance, reliability and science value were being limited by the existing technology. In particular, the uncertainties in the Titan ephemeris, the wide range of possible atmosphere models,

* Existing designs(Ref B-4 and B-5) were used for trial mission orbiters.

I-1

112 to 144-day 1st orbit, 32-day 2nd orbit

Titan 16-day orbit

18 R_S

R_P (Saturn)

Saturn Orbiter	Spin Stabilized	3-Axis Stabilized
Science, kg	46	67
Vehicle (Including Science), kg	300	700
ΔV Propulsion, kg	390	777
(ΔV Available), km/s	(1.63)	(1.63)
Subtotal	690	1477.0
Payload Options		
Lander, kg	279.0	279
ATM Probe, kg	100	100
Penetrator, kg	92	92

Titan Encounter
Powered Swingby
ΔV = 1.6 km/s
Titan Flyby
RCA = 3700 km

Approach Hyperbola
V_{HP} = 5.5 km/s

Fig. I-1 Typical Titan Exploration Orbiter Mission
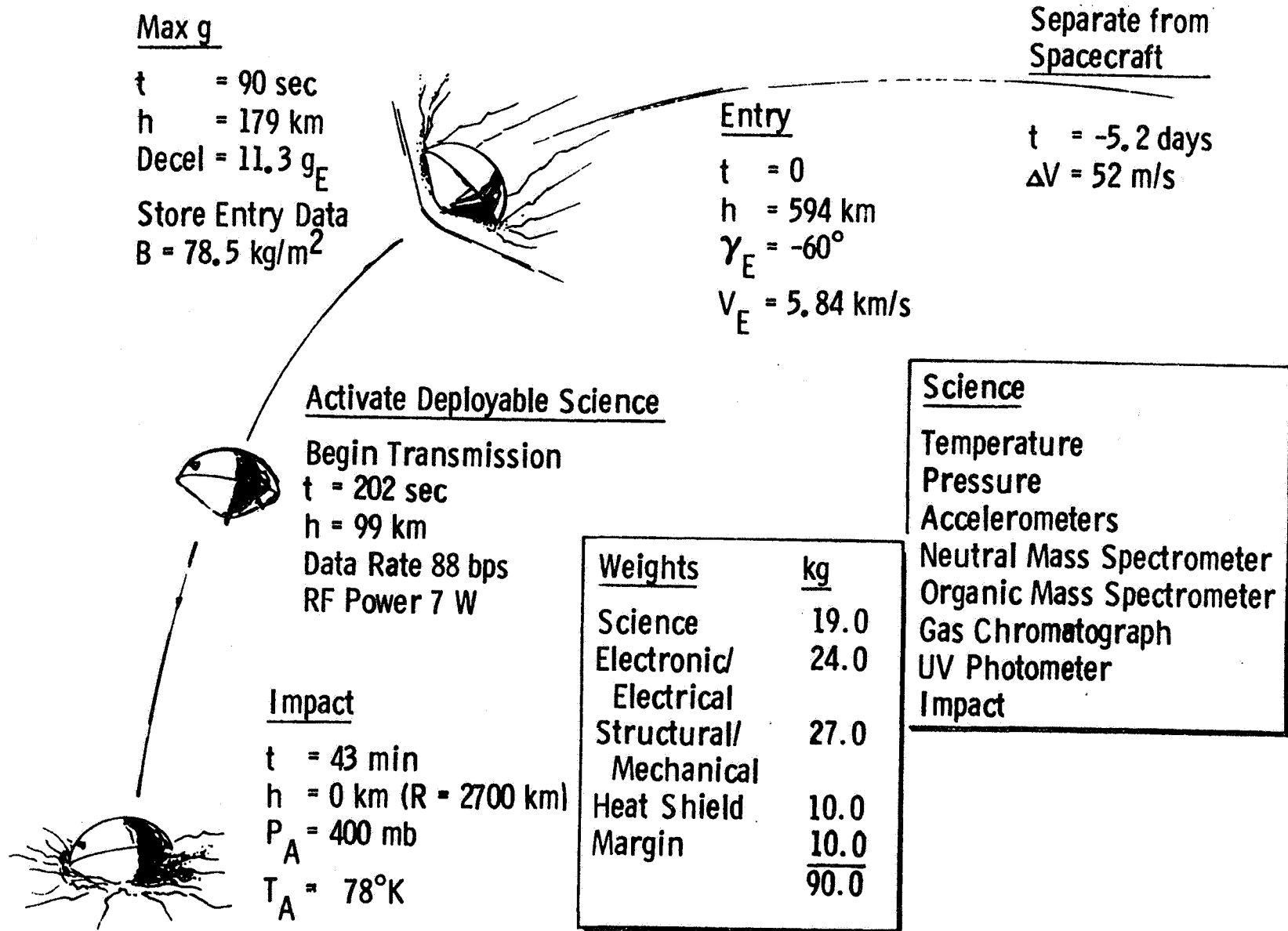
Fig. I-2   Typical Titan Atmosphere Probe Mission

Max g

$t = 90$ sec
$h = 179$ km
Decel $= 11.3$ g_E

Store Entry Data
$B = 78.5$ kg/m^2

Separate from Spacecraft

$t = -5.2$ days
$\Delta V = 52$ m/s

Entry

$t = 0$
$h = 594$ km
$\gamma_E = -60°$
$V_E = 5.84$ km/s

Activate Deployable Science

Begin Transmission
$t = 202$ sec
$h = 99$ km
Data Rate 88 bps
RF Power 7 W

Impact

$t = 43$ min
$h = 0$ km (R = 2700 km)
$P_A = 400$ mb
$T_A = 78°K$

Weights	kg
Science	19.0
Electronic/ Electrical	24.0
Structural/ Mechanical	27.0
Heat Shield	10.0
Margin	10.0
	90.0

Science

Temperature
Pressure
Accelerometers
Neutral Mass Spectrometer
Organic Mass Spectrometer
Gas Chromatograph
UV Photometer
Impact

Separate from Spacecraft

t = -5.2 days
ΔV = 100 m/s

Entry

t = 0 sec
h = 594 km
γ_E = -60°
V_E = 5.84 km/s

Max g

t = 90 s
10.6 g_E
h = 177 km
B = 63 kg/m^2

Stage Fairings

t = 246 s
h = 100 km
B = 13,000 kg/m^2

Impact

t = 10.5 min
h = 0 km (R = 2700 km)
Aft Section - 18,000 g
Forebody - 1,800 g
V_{impact} = 150 m/s
Data Rate 32 bps
RF Power 2 W
Lifetime 60 min

1 - 15 m

Weights	kg
Science	8.8
Electrical, Electronic	11.5
Structure Mechanical	42.9
	63.2
Entry Fairings	18.0
Margin	10.8
Total	92.0

Dia   = 12.7 cm
Length = 1.82 m

Science

Accelerometer
Temp Array
Mass Spectrometer

Fig. I-3 Typical Titan Penetrator Mission

Separate from S/C
t = -5 days
ΔV = 150 m/s

Entry

t = 0 s
h = 594 km
γ_E = 60°
V_E = 5.84 km/s

Max g

t = 90 s
h = 179 km
11.3 g_E
B = 47.1 kg/m^2

Deploy Chute,
Stage Aeroshell

t = 53 min
h = 2 km
B = 5.5 kg/m^2

Impact

t = 63 min
h = 0 km (R = 2700 km)
V_{impact} = 3 m/s
Data Rate = 16 - 88 bps
RF Power = 10 - 40 W
S-Band Direct Link

Weights	kg
Science	37.9
Electronic/Electrical	80.1
Structural/Mechanical	48.6
Landed Weight	166.6
Parachute/Mortar	13.2
Aeroshell, H/S	45.4
Deorbit Propulsion	15.0
Margin	39.0
Total	279.2

Science

GCMS/Life Detection
Atmospheric Sensor Array
(P, T, Wind, Sunlight)
Camera
Surface Sampler

Fig. I-4 Typical Titan Soft Lander Mission

and the lack of knowledge of the surface conditions, made it very difficult to plan conventional missions. These difficulties provided the stimuli and the direction for the search for new concepts.

Chapter II of this volume documents the results of the science studies done in support of this contract. The overall science objectives for Titan exploration, the required measurements, and the recommended payload instruments established the science guidelines for both the trial mission designs using existing technology, and the new concepts and technology advancements.

Chapter III is the main body of the report and describes the new technology recommendations and the advanced science, technology and mission planning options that offer promise of both enabling and/or enhancing the exploration of Titan.

The mission analysis and systems configuration work performed in the development of the trial mission/spacecraft designs is reported in Appendices A and B. Appendix A describes the performance requirements and the alternative strategies for: 1) trajectories from Earth to Saturn; 2) deflecting to a Titan encounter; 3) Titan entry; and, 4) Saturn orbit insertion and in-orbit strategies. It also discusses navigation and error analysis problems in performing these maneuvers. Appendix B contains the system and subsystem design data that support the trial spacecraft designs for the Titan atmospheric probe, surface penetrator and soft lander.

II. SCIENCE OBJECTIVES AND REQUIREMENTS FOR TITAN EXPLORATION

In recent years there has been an increasing interest in Titan. Armed with new astronomical data, planetary scientists have begun more active analytical evaluations of its atmospheris and geologic characteristics. NASA plans to obtain considerably more information about Titan from near flyby trajectories of both Pioneer 11 and the MJS '77 mission. The interest in this moon of Saturn is based on the discovery that it has a significant atmosphere with a relatively large methane to hydrogen ratio, thus presenting an environment similar to that which has been postulated for Earth during the beginnings of life. Although the atmospheric uncertainties are large at this time, preliminary analyses have shown that a spacecraft could survive entry and landing.

A. RECOMMENDED TITAN ENGINEERING MODELS

When this study was initiated in the summer of 1975, an engineering model for Titan was being developed under the cognizance of the GSFC and the principal author was Calvin P. Meyers of the Jet Propulsion Laboratory.[1] Since an engineering model was necessary as a guide to design in this study, discussions with Titan observers and particularly with C. Meyers and N. Divine of JPL provided the data upon which the preliminary model was formulated.

The atmosphere of Titan may be relatively thin (Caldwell model) or thick (Hunten model). An intermediate model, termed "nominal", has been proposed by Owen (see Section IIA-4) and currently appears to be the most probable. Hunten and Owen favor nitrogen over neon, though no experimental evidence demonstrates the existence of either. Ethane and acetylene have apparently been detected by Gillett.

_____

(1) NASA Space Vehicle Design Criteria (Environment) "The Environment of Titan (1975)" August 1975, NASA SP-81XX (To be Published)

Based on these considerations the following preliminary Titan engineering model is recommended for use in this study.

1. Atmosphere

    a. Composition

	Thin	Nominal	Thick
Methane	100%	2%	0 - 100%
Hydrogen	--	10%	--
Nitrogen	--	0 - 99%	0 - 100%
Neon	--	0 - 99%	--

    b. Assumed Molecular Weight

	Thin	Nominal	Thick
Weight	17	28	28

    c. Surface Conditions at 2700 km radius

	Thin	Nominal	Thick
Pressure, mb	17	400	1000
Temperature, $^{\circ}K$	78	78	125
Density, gm/liter	.042	1.7	2.7

Figures II-1, II-2 and II-3 present the pressure, temperature and density profiles consistent with the assumptions. All models of the temperature profile, Figure II-2, include an inversion layer with a peak temperature of $160^{\circ}K$ based upon 8 μm infrared measurements. Presumably this is a photochemical haze (smog) which heats the upper atmosphere by sunlight absorption. The nominal and thin models have no greenhouse effect, producing an extremely stable, permanently inverted atmosphere. The thick model allows greenhousing.

2. Surface Characteristics

Surface location: The radius of Titan is taken as 2700 km, based upon Veverka's occultation radius of 2900 $\pm$ 200 km, and Hunten's suggestion that even if Titan's atmosphere is not opaque, the limb effect would be approximately 200-300 km.
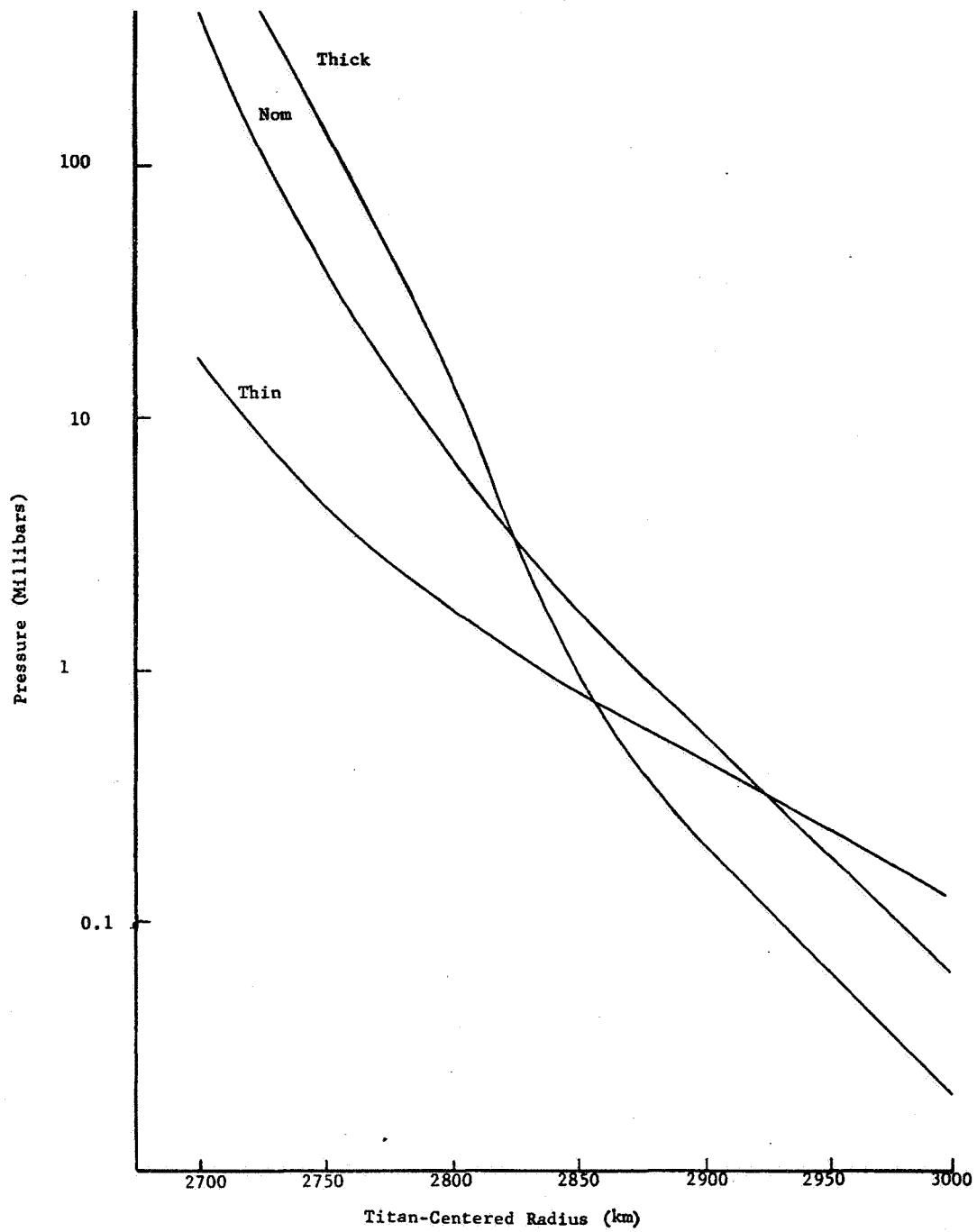
Fig. II-1 Titan Atmospheric Pressure

II-3

Preliminary Titan Atmospheric Models
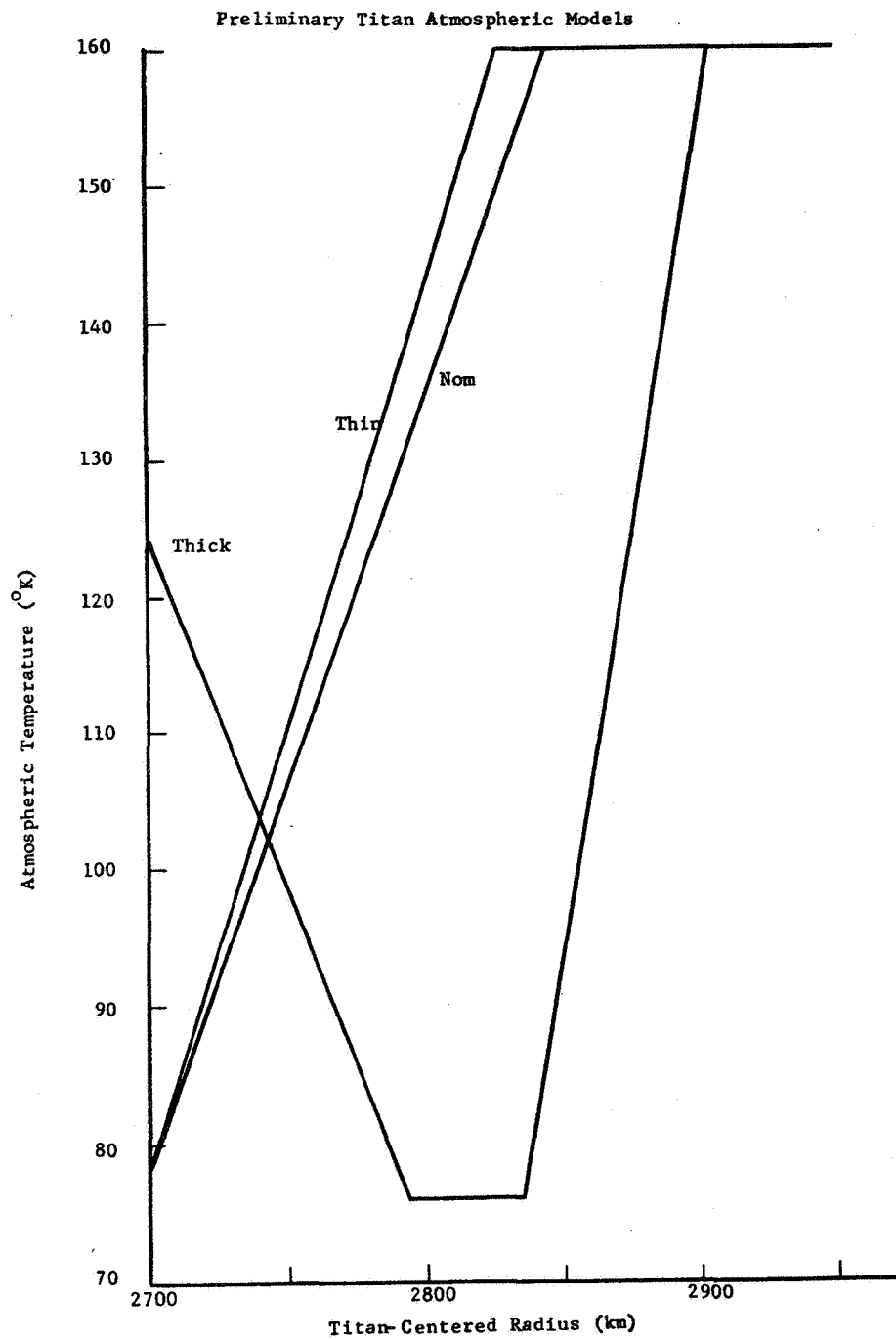
Fig. II-2 Titan Atmospheric Temperature
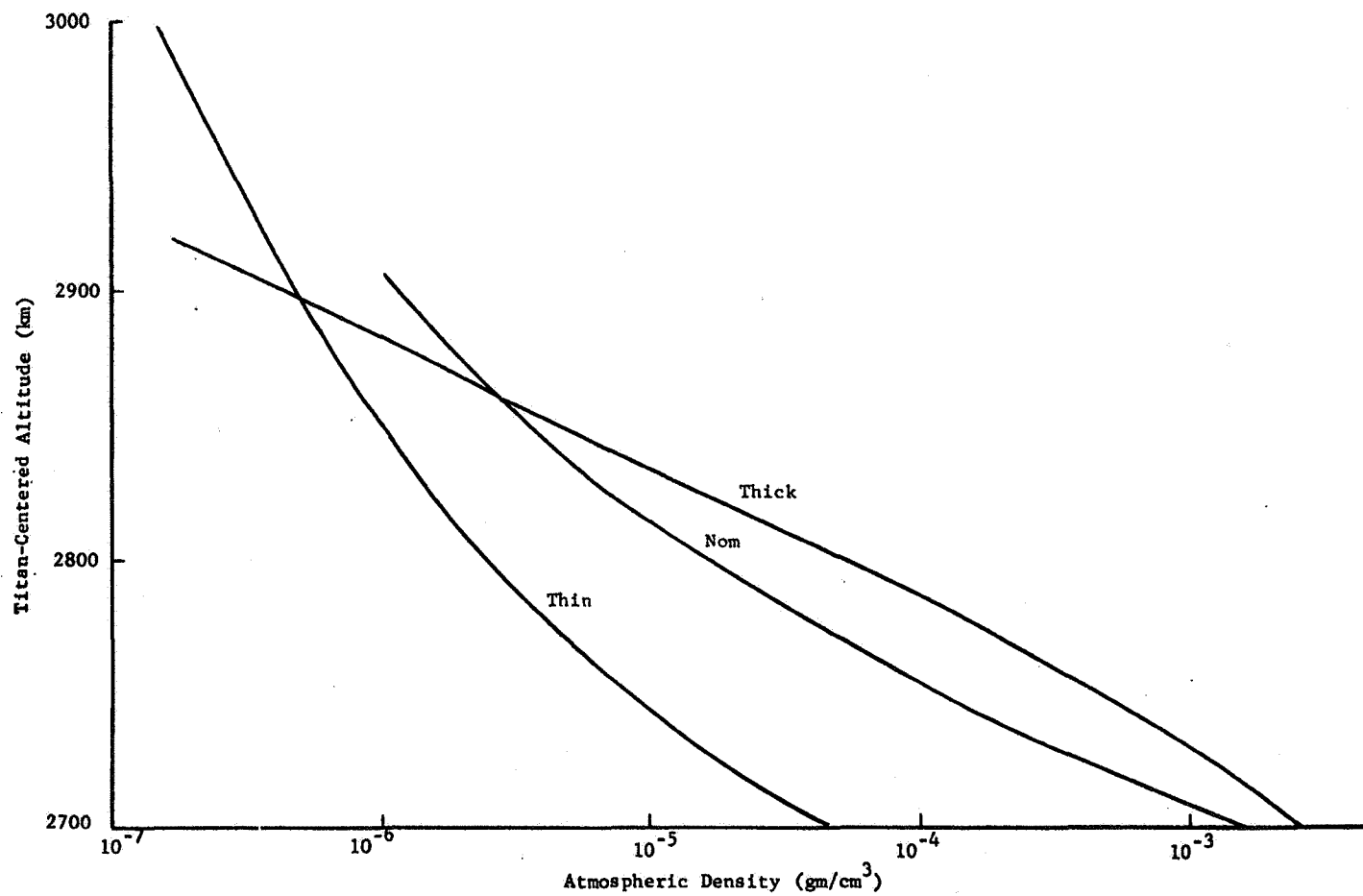
Fig. III-3 Titan Atmospheric Density

Surface State: For the time being, two surface compositions should be considered: (1) frozen methane, and (2) a solid surface of ices overlain with 1 to 100 meters of loose, unconsolidated dust (precipitated smog). The surface temperature may be as low as 78°K or as high as 125°K (greenhouse). An infrared brightness temperature at 34 μm has been reported at 95°K. Liquid methane is a possibility that should be considered; however, it is improbable.

3. Additional Data

Titan bulk density $\quad= 1.7 \pm 0.4$ gm/cm^3

Surface Acceleration $= 1.3 \pm 0.2$ m/s^2

$\qquad\qquad\qquad\quad = 0.133 \pm .02$ Earth g's

Rotational Period $\quad= 15.9$ Earth days

4. Comments on Titan Engineering Model by Tobius Owen

A meeting was held at Martin Marietta on July 1, 1975 with Professor Tobius Owen to discuss results of his Titan research and assessment of the value of Titan exploration. This meeting was at the beginning of the study and influenced the definition of the recommended Titan Engineering Model which was subsequently used in the study for spacecraft and probe design purposes.

A summary of Professor Owen's comments follows:

a. Atmsopheric Measurement - Owen's current estimate of methane abundance is 80 m-atm, based upon the weak bands at 0.543 μm. This translates to a surface partial pressure of 0.8 mb, or only 0.2% of the surface total pressure of 500 mb. These are Owen's estimates using Trafton's data. Owen has identified an additional methane band which is pressure-sensitive and hopes to refine the 400 mb estimate during future observations.

b. <u>Atmospheric Model</u> - Owen adopts the far IR (34 μm) brightness temperature of 93°K as that of the "surface", where quote marks are to indicate the uncertainty of whether the observation is of a true solid surface or merely cloud tops (Owen leans toward the solid-surface interpretation). He ascribes the temperature to a mild greenhouse induced by the atmosphere being predominently nitrogen (neon is still a possibility; hydrogen may have been eliminated by measurements by G. Munch). Clouds are indicated only by the polarization curve, which may really be due to loose fallout smog particles on the surface. The reddish color may indicate compounds containing either N or S, although P or Si are remote possibilities (phosphine and silane are unstable in the presence of water vapor).

B. SCIENCE OBJECTIVES FOR TITAN EXPLORATION

The fundamental science objectives in the exploration of the planetary and satellite bodies of the solar system are to obtain information on planetary formation, origin of life, and dynamic processes affecting planetary environments.

The specific science objectives for Titan exploration can be defined in terms of science questions, and the measurements or instruments required to answer them.

Science Questions - The fundamental questions are:

1. FORMATION

    When, how and of what was Titan formed?

2. EVOLUTION & DYNAMICS

    What processes are, or have been, at work at Titan since its formation?

3. LIFE

    Has prebiotic organic synthesis or life evolved at Titan?

This leads to many detailed science questions such as: Do complex organic compounds exist on Titan (on the surface, in the atmosphere)? If so what types? Are they the result of abiotic, photochemical synthesis, or . . . Does life exist on Titan (surface, subsurface, in atmosphere)?

What is the surface chemistry? How thick is the crust? Is the mantle liquid? What is its composition? Rocky core? Do convection cells exist?

When was Titan formed? Does the heat flow rate result from heating by radioactivity?

What is the composition of the atmosphere? Is it in chemical equilibrium with the surface? What is the structure of the atmosphere? Stable inversion? Greenhouse? Photochemical haze (smog)? Nature of clouds?

The types of science instruments or experiments needed to answer many of the above questions are placed in related groups and listed below.

II-8

Organics - Analytical instrumentation (gas chromatography (GC), mass spectrometry (MS), combined GC-MS, GCMS, organics detection, IR spectroscopy, differential scanning calorimetry (DSC), UV absorption amino acid detection and analysis).

Sampling techniques (scoops, vaporization--resistive heating or microwave induction, carrier gas sweep).

Origin of Organics, Life - Life detection (Viking biology experiments = gas exchange (GEX), label release (LR), pyrolytic release (PR); Unified Life Detection System - B. Kok mass spectrometer-based gas detection). Sampling technqiues.

Composition and Structure of Surface and Interior - Analytical instrumentation (GC, MS, alpha backscatter spectrometer (ABS), X-ray fluorescence spectrometer (XRFS), X-ray diffractometry (XRD)). Sampling techniques (ices, tars, meteorite debris). Active seismometry, microwave radiometry, imagery, radar altimetry, gravitational harmonics.

Formation - Age-dating. Heat-flow rates.

Atmosphere Composition - Composition (GC, MS, UV extinction, quartz-microbalance condensible vapors detector, retarding potential analyzer (RPA), etc.).

Atmospheric Structure, Dynamics - Meteorology, radio science, cloud and haze particle detection.

C. SCIENCE CONSULTANT'S REVIEW OF TITAN EXPLORATION STUDY

The Martin Marietta planetary science consultants' group met at Denver on November 2, 1975 and reviewed the approach being taken in the Titan Exploration Study. This meeting took place at about the midpoint in the study and served as a review of the recommended engineering model of Titan (Section II-2) and provided some additional inputs to the model and to scientific payloads to be considered.

Scientists present were:

Dr. Michael B. McElroy, Harvard University

Dr. Thomas Donahue, University of Michigan

Dr. Gordon H. Pettengill, MIT

Dr. Donald M. Hunten, Kitt Peak National Observatory

Dr. John S. Lewis, MIT

Dr. Alexander J. Dessler, Rice University

Mr. H. Julian Allen, Palo Alto, California

Mr. Harold Masursky, USGS/Flagstaff, Arizona

The Martin Marietta study team opened the meeting with a presentation that covered the following subjects:

1. Technology forecasting plan for Titan exploration.

2. Fundamental science questions for Titan exploration.

3. Descriptions of typical orbiter, probe, penetrator and lander missions for Titan exploration.

4. Best current description of Titan.

5. Science payloads for orbiter, probe, penetrator and lander missions.

6. Techniques for analyzing organic compounds and inorganic ices.

7. Titan exploration science value matrix.

During and after the presentation, the following comments and suggestions were offered by the consultants:

1. Scientific consensus seems to be favoring the 400 mb nominal atmosphere for Titan based principally on the observations and new laboratory calibration of methane signatures by Toby Owen et al.

2. Several of the scientists expressed the likelihood that the Titan surface is liquid methane. This is based on the model consisting of the Owen atmosphere above an opaque cloud and then more atmosphere below that down to a liquid surface that is not visible remotely.

3. The thought was advanced that Titan may be the only satellite we will be able to land on within the foreseeable future. A generalized approach to the landing problem was favored that can handle liquids and ices of various mixtures and consistencies.

4. Low temperature X-ray diffraction and neutron diffraction were suggested as possible experiment techniques for investigating the nature of Titan ices.

5. Recent work on predicting the lifetime of methane in the Titan atmosphere has suggested that methane should last only a short time compared with the age of Titan. This would mean a replenishing source exists.

6. According to predictions, a layer of photolysis products (CH_4, C_2H_6, C_3H_8, etc.) could exist on the surface of Titan that is on the order of 1 km thick.

7. Some doubts about the existence of organic molecules of any great complexity arose in the discussions. It was suggested that photolysis would probably stop after propane (C_3H_8) and perhaps something as complex as hexane (C_6H_{14}) could form by the joining of two propane molecules. The absence of circulation and vertical mixing in the Titan atmosphere probably prevents the re-exposure of heavier organics to UV for further photolysis and they settle to the surface. Therefore, microbes floating around in the atmosphere are unlikely.

8. It was recommended that the probe UV photometer needn't be solar pointing but that full hemispheric coverage would be satisfactory.

9. Sounding the surface and subsurface from orbit with a passive microwave radiometer was also suggested as a valuable experiment to detect the temperature signatures of the constituents.

10. It was recommended that the microwave radiometer measurements be made on repeated orbiter passes that provide different viewing geometry to maximize the usefulness of the data.

11. In attempting to come up with a method of age-dating the ices on Titan, the possibility of potassium-argon dating of the salts assumed to be present in the ices was suggested. This technique would be a very challenging new technology development.

12. One scientist thinks the upper limit on the crust thickness is 25 km. Convection cells will probably exist in the liquid below the crust that can be expected to cause bulges in the crust. The plasticity of the surface ices (if they exist) should otherwise keep the surface smooth.

II-12

13. Heat flow at Titan should be relatively large, only a few times less than at the Earth. This gives a high priority to heat flow experiments which will involve implanting subsurface temperature sensors and measuring the thermal conductivity and thermal gradient in the surface material.

14. Lewis offered a prioritization of the science objectives at Titan that was somewhat surprising in its downgrading of the search for organics. His order of importance:

   a. Atmospheric structure

   b. Atmospheric composition

   c. Surface chemistry

   d. Do complex organics exist?

   e. When was Titan formed?

   f. What kinds of organics? Life?

15. Active seismometry experiments were endorsed as valuable in developing knowledge of the internal structure of the satellite. A large impact or explosion diametrically opposite to a seismic recording station would be ideal.

16. Measurement of gravitational harmonics from orbit was suggested.

A science value matrix, Figure II-4, was presented for consideration by the consultant group, however, a unanimous agreement was not obtained on the assignment of science values for each category. The values shown only depict a typical evaluation.

TITAN EXPLORATION SCIENCE VALUE MATRIX

Measurement Type	Science Question	Measurement Regimes			
		Ionosphere	Atmosphere	Surface	Subsurface
Chemical	1. Formation	C	C	C	A
	2. Evolution	B (5)	A (15)	A (15)	A (15)
	3. Life	C	A	A	C
Physical	1. Formation	C	C	C	A
	2. Evolution	B (5)	A (11)	A (15)	A (15)
	3. Life	C	B	A	C
Biological	1. Formation	C	C	C	C
	2. Evolution	C (3)	B (11)	A (15)	B (11)
	3. Life	C	A	A	A

A = 7
B = 3
C = 1

A - Measurements of this type, made in this regime, will have great value in answering this question.

B - Measurements of this type, made in this regime, will have some value in answering this question.

C - Measurements of this type, made in this regime, will have little value in answering this question.

Fig. II-4 Titan Exploration Science Value Matrix

D. RECOMMENDED SCIENCE INSTRUMENT PAYLOADS

Recommended science instrument payloads have been identified for orbiter, probe, penetrator, and lander missions to be used in the system designs.

Each of these vehicles is best suited to certain types of experiments and, therefore, the most desirable science mission would include at least one of each type. The orbiter performs planet-wide experiments and obtains near-planet environmental data including such things as fields and particles, UV and photopolarimetry, radio, and IR spectrometer measurements. The probe is dedicated to atmospheric and cloud measurements down to the surface. The penetrator makes subsurface measurements including physical properties of the surface material, heat flow and thermal conductivity of soil, soil composition and seismometry. The lander provides the most sophisticated in situ measurements of all, including composition and life detection, meteorology, imagery, seismometry, and a host of other more complex detailed measurements. Therefore, a complete scientific investigation of Titan requires at least one of each type of these vehicles or possibly multipurpose vehicles to provide all of the desired measurements. The mission, engineering design, and program constraints probably will not allow simultaneous use of all four types of vehicles in one mission unless the advanced technology, combined-vehicle concepts discussed in Chapter III are found to be feasible.

1. Science Instrument Payload for an Orbiter

Two classes of orbiter missions were considered in this study. The first is a Saturn orbiter, which encounters Titan one or more times and supports the Titan mission through both data relay and remote measurements. The second is a Titan orbiter which necessarily has a severe weight constraint and therefore a much reduced science payload.

The Saturn orbiter science payload is based on current NASA planning for similar missions including the Mariner Jupiter orbiter and the Mariner and Pioneer flyby spacecraft configurations. Table II-1 presents a list of instruments.

<u>Table II-1   Candidate Science Payload - Orbiter</u>

1. Imaging Science

2. Radio Science

3. Cosmic Ray

4. Planetary Radio Astronomy

5. Plasma Wave

6. Low Energy Charged Particles

7. Photopolarimeter

8. UV Spectrometer

9. Magnetometer

10. IR Interferometer Spectrometer

11. Microwave Radiometer Probe

A small Titan orbiter might have a minimum science payload which could include a transponder for accurate tracking of the orbiter, a radiometer to investigate the surface ices, and imagery to map the surface.

<u>2. Science Instrument Payload for a Titan Atmospheric Probe</u>

Based upon discussions with Sagan, Lewis, Owen, Oyama, and others, the following probe payload is designed to answer those scientific questions of the greatest immediacy.

Science Strategy: Obviously the physical state of the atmosphere must be detailed, hence the need for temperature, pressure, and deceleration profile measurements. The light gases are best detected and assayed by a neutral mass spectrometer with a range of 1 to 50 AMU. More complex molecules, the products of presumed abiotic organic synthesis, should be studied by both a high molecular weight mass spectrometer (50 to 200-plus AMU) and a gas chromatograph. Study of the photochemical processes taking place in Titan's atmosphere will be greatly aided if the UV spectral intensity is measured as a function of depth in the atmosphere; this justifies inclusion of a UV multiband photometer. Location and nature of the solid surface are highly important. Not only for scientific reasons, but also to aid lander and penetrator mission designs. A contact indicator, radar altimeter, stroke penetrometer, or other device(s) should be considered. Of secondary priority, relative to the above, are instruments such as light attenuation detectors, cloud particle detectors (nephelometers), heavy element detectors (X-ray fluorescence, for phosphorous, sulfur, chlorine, etc.), ionospheric properties (ion mass spec, retarding potential analyzer, electron temperature probe, etc.), and magnetometers. If Titan is cloud-shrouded, imagery during descent below the cloud level would be invaluable since accurate imagery of the surface would not, in this case, be possible from orbit.

Table II-2 presents the recommended science payload for an atmospheric probe.

Table II-2 Titan Atmospheric Probe Science Payload

Instrument	Characteristics
Atmospheric MS	1-50 AMU, 3 meas./scale ht.
Organic MS	50-250 AMU, 1 meas./scale ht.
GC	1-3 analyses, up to 3-carbon
UV Photometer	Solar pointing, 220, 260, $>280\mu$ bands
Accelerometer	Entry
T, P Transducers	3 meas./scale ht.
Impact Transducer	Surface location, penetrability
Expanded Organic Analysis	
IR Radiometer	IR balance
Visible Light Monitor	Solar pointing
Nephelometer	Pioneer Venus
Cloud Particle Size Analyzer	Pioneer Venus
Ion MS	Ionosphere Meas.
RPA or Plasma Probes	Charged particles in ionosphere
X-ray Fluorescence Spectrometer	P, S, Cl, Ar Detection

Items Requiring Development: Several of these instruments or experiment concepts will require extensive development before becoming available for a Titan mission. Items:

1) Organic mass spectrometer (MS) - requires analysis of range of organic compounds expected and best type of spectrometer for analysis. Areas of experimental work include source optimization, inlet protection (prevent clogging by smog particles), avoidance of condensation trapping, and data interpretation and species identification (spectra will be complex and potentially ambiguous).

2) Gas chromatograph (GC) - detection of abiotic organics of relatively high molecular weight in the short time period available during a probe descent will require considerable laboratory studies in the areas of (a) column size and composition, (b) carrier gas, (c) detectors, (d) temperature programming, and (e) sampling technique.

3) UV broadband photometer - this instrument currently does not exist for this application, although most of the required technology may already exist. Bands desired include one at 260 μm (organics), 220 μm (ammonia, hydrogen sulfide, etc.),   280 μm (continium).

4) Impact indicator/penetrometer - measurement of surface properties in the short time interval of an impact is extremely challenging, but may be technically possible if sufficient development work is accomplished. Key ingredients would be a fast response time transducer (e.g., a spring loaded spike), high-rate data transmitter, and high-rate data receiver and storage device on the relay spacecraft.

3. Science Instrument Payload for a Titan Penetrator

The science payload proposed here must necessarily be taken in the context of what would be flown on the first mission to the surface of Titan since if a penetrator is employed, it is unlikely that a more sophisticated soft-lander mission will have preceded it. On the first such surface mission, the highest priority must be given to gross physical and chemical properties, providing the baseline for design of more sophisticated surface missions. This will undoubtedly be the first encounter of a surface which is icy rather than solid silicate (rock), and promises much greater chance of surprise than the surfaces of the inner planets.

a. Recommended Science Payload for First Penetrator Mission

(Based upon Mars-class penetrator with 35 kg science payload.)

1) Accelerometer -

Objective: Measurement of dynamic deceleration profile to derive physical properties of the surface.

Engr. Characteristics: 2 kg, 1 liter, 10 watts peak during landing (Sandia study).

2) Temperature Array -

Objective: Measurement of temperature - time profile at various points relative to the penetrator thermal source (power dissipation concentrations or RTG if employed).

Engr. Characteristics: 1 kg, 0.5 liters, 0.1 watt average, 10 bits/minute average

3) Mass Spectrometer -

Objective: Determination of major constituents of the surface, including frozen gases (ammonia, water, methane, etc.) and organics (10 to 300 AMU).

Engr. Characteristics: 5 kg, 3 liters, 20 watts each measurement sequence (1 hour per sequence, 3 sequences per mission), 2000 bits/minute during sequence.

Table II-3 presents an expanded list of instruments for a penetrator mission.

b. Development Requirements

A sampling device for the mass spectrometer will require extensive development to provide sample acquisition and volatilization. The mass spec itself will require careful design (and perhaps heating) to allow reliable measurement of water concentrations. The source filament may require development to ruggedize for penetrator deceleration loads. Work required on the temperature array includes ruggedized low temperature (80°K) thermometry techniques and theoretical modeling of penetrator-surface material interactions (including phase changes and fluid flows). The accelerometer may not require extensive development because of prior usage on terrestrial penetrators.

c. Rationale for Instruments not Included

A gas chromatograph (GC) would be highly desirable either in conjunction with or perhaps in place of a mass spectrometer (MS). It was not included in the recommended payload only because of the difficulty of accommodating both instruments and because of higher power and longer operating time required for the GC. Other candidate instruments which could compete with the GC or MS include: (1) differential scanning calorimeter, (2) gas-phase infrared spectrometer, and (3) chemically-sensitive quartz microbalance array. None of these latter techniques have been or are currently planned for flight usage on planetary missions, and are thus judged less developed. An alpha backscatter scatter spectrometer could detect the relative amounts of the light elements C, N, O, F, and others, but it is not accurate at pressures above about 100 mb, and would suffer extensive source degradation during the flight because of the short half-life radioisotope employed. An

TABLE II-3 Titan Penetrator Science Payload

INSTRUMENT	CHARACTERISTICS	MASS (Kg)	POWER (Watts)
Accelerometer	Physical Properties of Surface Material	0.3	1.0
Temperature Array	Soil temperature, thermal conductivity	2.0	0.1
MS	10-300 AMU	6.5	27.5
Expanded Organic Analysis *		8.8 Kg	28.6 Watts
Passive Seismometry	Viking		
Active Seismometry	Explosive Charges		
Neutron Activation	Elements, Isotopes		
Passive Gamma-ray Spectrometer	K, U, Activated Nuclides		
XRFS	Elements		
X-ray Diffractometer	Crystal Structures		
Heat Flow	Temperature Profile		
Magnetometer	Sensitivity?		

*The following instruments are optional

X-ray fluorescence experiment would be technically feasible, but of secondary scientific value since it would detect only elements above atomic number 11. Neutron activation techniques would be potentially quite informative, but are large and technically quite complicated. Seismometry appears feasible but of completely speculative importance.

4. Science Instrument Payload for a Titan Lander

The lander is assumed to be more sophisticated in its science payload relative to the penetrator, although one could as well conceive a minimum lander with a payload more like the penetrator (see Table II-4). The approach taken here is to mount a more complete and complex attack for the determination of the postulated abiotic organic synthesis as well as the possible existence of Titanic life forms.

a. Recommended Science Payload

1) Combined GCMS/Life Detection

Objective: Analyze samples obtained from surface material and atmosphere for organic compounds (GCMS) and for evidence of active metabolism (gas evolution and uptake using MS).

Engr. Characteristics: 30 kg, 35 x 30 x 45 cm, 7 watts standby, 15 watts during MS scans (6 times per day, 15 minutes each), 50 watts during GCMS mode (3 times for mission, 3 hr. per run), 2000 bits per MS scan, 100 kilobits per GCMS mode run.

2) Atmospheric Sensor Array

Objective: Monitor temperature, pressure, wind, and cloud cover (sunlight monitor).

Engr. Characteristics: Short boom (0.5 meter) with sensor array (2 kg, 15 x 10 x 10 cm), 5 watts during sampling period (6 times per day, 15 minutes per period), 2000 bits per period.

Fig. II-4 Titan Lander Science Payload

Instrument	Characteristics
Combined GCMS/Life Detection	Viking GCMS + Kok experiment
Meteorology	T, P, wind
Sunlight Monitor	Visible, UV?
Imagery	One panorama
Surface Sampler	Scoop/Chisel (viscid surface?)
Wet Chem. Amino Acid Analysis	ABLDI
Expanded Organic Analysis	
Seismometer	Passive, Active?
Neutron Activation, Scatter	Elements, Isotopes
Passive Gamma-ray Spectrometer	K, U, cosmic ray, nuclides
XRFS, X-ray Diffraction	Heavy elements, crystal structure
Heat Flow	Temp., gradient, thermal conduct.
Microwave Radiometer	Subsurface temperature profile
Sonar Sounder	Layer detection
Drill Sampler	1-10 meters
Particle Size Analyzer	Regolith characteristics
Age Dating	Ices, organics?
Upper Atmosphere Life Detect.	Sampler
Listening Devices	Audio, EM, lightning, thunder

3) Camera

   Objective: Obtain images of local topography and clouds.

   Engr. Characteristics: 6 kg, 15 watts per picture (20 pictures per mission, each picture requires 15 minutes), 1 megabit per picture.

4) Surface Sampler

   Objective: Obtain samples of surface material (and possibly airborne particulates) for analysis by combined GCMS/Life Detection experiment. Aid in determination of physical and thermal characteristics of surface material.

   Engr. Characteristics: 7 kg, 5 liters, 40 watts during acquisition (20 minutes each), 8000 bits per acquisition.

   Table II-4 presents the list of scientific instruments with additional desirable instruments listed.

b. Rationale for this Payload

   Based upon what is presently known about the various bodies of our solar system, Titan may be the only one on which the "natural" (i.e., non-biological, or abiotic) synthesis of complex organic compounds is on-going today. In this context, the Titan atmosphere may be chemically analogous, though not likely identical, to the primitive Earth. Accordingly, detections of 3-carbon and higher organics becomes the highest priority, with search for active organisms a close second.

   The first experiment recommended is a combination of two techniques recognized as excellent for each objective, viz., gas chromatograph separator with mass spectrometer analyzer (GCMS) and the "Kok method" of life detection which also requires a mass spectrometer - in this case for analysis of the gas composition in the head space above surface samples incubated with various nutrients. The engineering characteristics of this hypothetical

II-25

experiment are based upon a possible modification of a Kok-type life detection instrument presently being developed by Martin Marietta for NASA/Ames.

The proposed atmospheric sensor array is intended primarily to determine and monitor the physical state of the near-surface atmosphere, as well as monitor the cloud cover fluctuations (an adaptive mode wherein the sunlight sensor is continually "on" but records data only for signficant variations in light intensity would be desirable). The chemical state of the atmosphere can be determined by including an atmospheric inlet to the MS. Since it is presently anticipated that the surface of Titan will have a relatively static appearance (e.g., no dust storms), imagery need not be a monitoring function, but more of a one-shot study as compared, for example, with Mars exploration. A single camera is probably adequate. At present, we assume a solar-illuminated surface; if the surface is indeed occluded by optically dense clouds, artificial illumination, via flare or lamp, will be required.

c. New Technology Required

The feasibility and practicality of combining a GC module with the Kok life detection instrument, has not yet been studied. Thermal control of the incubation chambers and nutrient reservoirs may also be a serious problem requiring innovative design. The atmospheric sensor array may be attainable from adaptations of existing devices, and the Viking lander facsimile camera may be satisfactory for this application. However, the Viking sampler boom will be totally inadequate for sampling in this environment. Severe challenges are expected in design of a sampling device that can reliably obtain samples from a surface that may be anywhere from very hard to viscid (gooey), and operate at very low temperatures (80°K).

II-26

d. Alternate Instrument Candidates

A wet-chemistry experiment capable of analyzing amino acids and other organic compounds is currently under development for NASA/Ames by TRW. This instrument is an excellent candidate for Titan missions, although the current design emphasis is toward a future Viking-class Mars mission. It was not included here in the initial recommendation only because of the desire to keep the payload from being excessive and because a GCMS is a more generalized approach to measuring organics. A seismometer could also be included with very small weight penalty, but it remains to be seen whether a scientific rationale can be developed to justify its inclusion.

E. PLANETARY QUARANTINE CONSIDERATIONS FOR TITAN EXPLORATION MISSIONS

In October of 1975 we interviewed Dr. Richard S. Young at NASA Headquarters who performs the dual functions there of Chief of Exobiology and Chief of the Planetary Quarantine Program. Dr. Young stated that NASA has not yet established a firm position on the probability of growth (Pg) for Earth organisms at the outer planets and their satellites. He said that in several months such a policy would be recommended by a committee from the National Academy of Sciences and that it would then be offered at a special symposium at COSPAR next summer.

Prior to this time, several Planetary Quarantine Specification Sheets had been prepared by Exotech Systems, Inc., for the Planetary Quarantine Program in which the probability that a terrestrial microorganism that reaches a planetary satellite having an atmosphere would grow and proliferate was quoted at $Pg = 10^{-1}$. This figure compares with equivalent estimates for Mars of $Pg = 10^{-6}$ and for Saturn of $Pg = 10^{-7}$.

On the face of it, these estimates would imply that sterilization requirements for spacecraft designed to land on Titan would be five orders of magnitude more stringent than those used for the Viking mission to Mars.

Dr. Young, however, recommended that we not follow that logic, feeling that the Exotech estimates were purposely made ultra conservative for Titan pending the time when more careful thought could be given to the issue. It was his opinion that the Pg value for the outer planets would probably arrive at something like 10^{-9} and that the sterilization requirements for Titan spacecraft would be little if any more demanding than the Viking

protocol. He thought that in order to increase the lethality to the so called hardy organisms the terminal sterilization temperature requirements might be increased 3° or 4^oC. Otherwise, he was confident that the Viking design, manufacture, assembly and terminal sterilization procedures would be adequate for Titan mission hardware.

Having used the guidelines outlined above during this study, we checked back with Dr. Young just before publication of this report to determine whether or not the recommendations changed as the result of the National Academy of Sciences panel meeting. The NAS panel to review outer planet quarantine policies met during the week of March 8-12, 1976. The unofficial results did in fact reflect a further reduction in the recommended Pg value for Titan. The outer planet recommendations ranged from 10^{-7} to 10^{-10} and Titan was included in that range. These levels would not require sterilization of spacecraft. Dr. Young felt that the conditions at Titan may yet influence COSPAR, which will meet in June, to establish a special, higher, Pg value for that satellite.

Young did state that he would recommend clean room assembly and bioburden control procedures for all outer planet spacecraft equivalent to those employed on the Viking '75 program. This he said was good practice even though terminal sterilization is not required.

Dr. Young said finally, that the very low Pg values assigned to Titan do not mean that the search for life on that body is no longer a valid issue. The prediction that terrestial organism will not grow does not preclude the existence of indigenous life forms. Therefore, if a spacecraft is to carry any form of life detection experiment, then sterilization procedures will undoubtedly be imposed to prevent self-contamination.

For sterilized spacecraft, build and test cycles are such that final design and fabrication of science instruments must begin not later than 3 years prior to launch. Normally a bread board design and test phase of two or more years precedes final selection of payload instruments. Therefore, with flight times to Titan of 5 to 7 years, the span between instrument concept and obtained results is roughly one decade.

This emphasizes the need for planning missions designed to accomplish more in a single mission than has been the practice in the past.

III. APPLICATION OF NEW TECHNOLOGY TO TITAN EXPLORATION

A. KEY CHALLENGES AND STIMULI

In addition to achieving payload weights compatible with launch vehicle and spacecraft capabilities, three factors that most significantly influence the approach to Titan exploration from an engineering standpoint are:

o The long period between missions (10 years if each mission is based on results of previous missions).

o Uncertainties concerning Titan's ephemeris, atmospheric density, and surface.

o The long communication range to Earth.

The trial mission design studies (Appendix B) revealed that attempting to accommodate in a fixed design the uncertainties in the nature of Titan's atmosphere and its surface will result in an inefficient system. These uncertainties also present major challenges in the area of science instrument design and mechanization. Although it is unlikely that as large an uncertainty band will exist at the time Titan missions are initiated, the uncertainties are still a dominant factor in the planning and design of Titan missions.

Consideration of the above factors has led to some general conclusions about Titan exploration.

1) Due to the long wait between missions, it is desirable to develop the ability to obtain orbiter, probe, and landed science data in a single mission instead of sequentially.

2) As much data as possible should be obtained remotely in view of the risks to lander spacecraft survival imposed by the uncertainties in atmosphere and surface conditions. Therefore, advanced orbiters and/or flyby vehicles capable of detailed atmosphere and surface investigation should be developed.

3) Advanced probe and lander spacecraft capable of adaptively dealing with the uncertainties in atmospheric and surface conditions should be developed. This is desirable since all science objectives cannot be met with remote sensing techniques even with advanced technology spacecraft. The adaptive probe/lander spacecraft should however be designed to take advantage of updated information from the remote sensing spacecraft. The ultimate vehicle of this type would be one that initially performs remote sensing from orbit and subsequently effects an atmospheric entry and landing on Titan's surface.

Based on these conclusions, several approaches to Titan exploration appear to warrant emphasis. These are a combined orbiter/probe/lander vehicle, an advanced Titan-dedicated orbiting vehicle, and a combined penetrator/probe vehicle. In addition, a number of new techniques or extrapolations of existing techniques have been identified that either support the implementation of the above concepts or enhance the performance of the more conventional Titan exploration systems defined in the trial mission studies, Appendix B.

The following paragraphs contain descriptions of the concepts and ideas, evaluations of their potential benefit to Titan exploration, and recommendations as to their further development.

B. RECOMMENDED MISSION MODES

1. Titan Orbiter/Probe/Lander Vehicle (TOPL)

This multipurpose exploration vehicle concept is illustrated schematically in Figure III-1. Initially, step 1 of Figure III-1, the TOPL vehicle is carried into Saturn orbit by the Saturn orbiter which has served as the cruise vehicle or bus. This is feasible since it is estimated that the TOPL vehicle can be designed for 150 Kg or less. The period of this initial Saturn orbit is decreased by successive Titan Swingbys and small ΔV maneuvers until a more optimum situation exists for insertion of the TOPL into a close orbit about Titan, Step 2 of Figure III-1. From this orbit a period of remote sensing of Titan's surface and atmosphere takes place. This might include microwave radiometer readings to determine the nature of surface ices as well as high resolution surface imaging and gravity field experiments. An RTG powered, three-axis stabilized design is envisioned that can be oriented to focus the vehicle's instruments toward Titan or its antenna toward the mother spacecraft.

After completing the orbital phase, the TOPL vehicle is deflected into an entry trajectory, step 3. This is feasible for a vehicle designed essentially as an orbiter because of the low entry velocity ($\sim$ 1.7 km/sec), the shallow entry angle ($|\gamma| \lesssim 9^{o}$), and the large scale height of Titan's atmosphere. These factors result in peak entry heating, dynamic pressure, and decelerations that are very low, 0.6 watts/cm^2, 300 N/cm^2 and 0.4 Earth G's respectively. Therefore, no entry aeroshell or heatshield is required and vehicle attitude can be maintained during entry by the ACS system used for orbital operations.

1. Total System Inserted into Saturn Orbit

4. Lower Atmosphere Measurements
   Taken (Probe Type Data)

Saturn Orbit

3. Upper Atmosphere Measurements and
   Entry Data Obtained

Path of Titan

Saturn

Titan

30-45 Minute
Descent

$V_{Entry} = 1.7$ km/sec

Titan

2. TOPL Performs Orbital Science
   in Titan Orbit

$V = 1.6$ km/sec
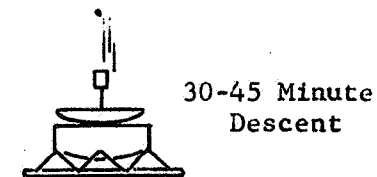
5. Landed Science Experiments

$V_{Impact} = 11$ m/s

Titan

.Microwave Radiometer
.Gravitational Harmonics
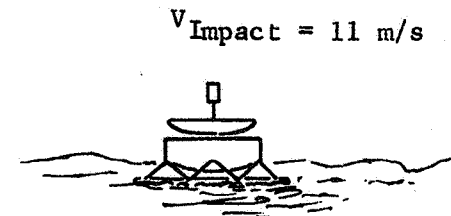
Fig. III-1   Titan Orbiter/Probe/Lander Vehicle (TOPL) Mission Phases

During descent, probe type data is collected, step 4, and after a relatively low velocity landing (11 m/s), the landed *science experiments* are initiated, step 5. During all phases of the mission after separation from the mother spaceship (Saturn orbiter), communications from the TOPL vehicle are via relay link through the mother ship.

Further descriptions of the various aspects of the TOPL concept are contained in the following paragraphs.

a. <u>Configuration and Mechanical Subsystems</u>

The keys to the feasibility of a spacecraft designed as an orbiter also entering and landing are the low velocity of the Titan orbiter and *hence, the low entry velocity, and the gradual build up of Titan's atmosphere* (its large scale height). It appears that a 1000 km periapsis altitude by 12-hour period elliptical orbit is appropiate for remote sensing (the orbit selection and insertion options are discussed in Section 2 that follows). Entry can be initiated directly from this 12-hour orbit or, to further reduce the entry severity, can be initiated after circularization at the 1000 Km altitude. For the latter case, the orbital velocity is only 1.58 km/sec (5,200 fps), with entry velocity being slightly greater depending on how far out the atmosphere extends.

The extent of Titan's atmosphere is illustrated in Figure III-2. Depending on the atmosphere model, it can be seen from this figure that the sensible atmosphere, $\rho = 10^{-9}$ gm/cm^3, *extends out to from 400 to 700* Km on Titan whereas on Earth and Mars it extends only to the order of 100 Km. The scale height of Titan's atmosphere, i.e., the altitude span in which density changes by a factor of e, is therefore large by comparison with Earth and Mars, 50 Km versus 6 or 7 Km. This significantly reduces the entry severity at Titan.
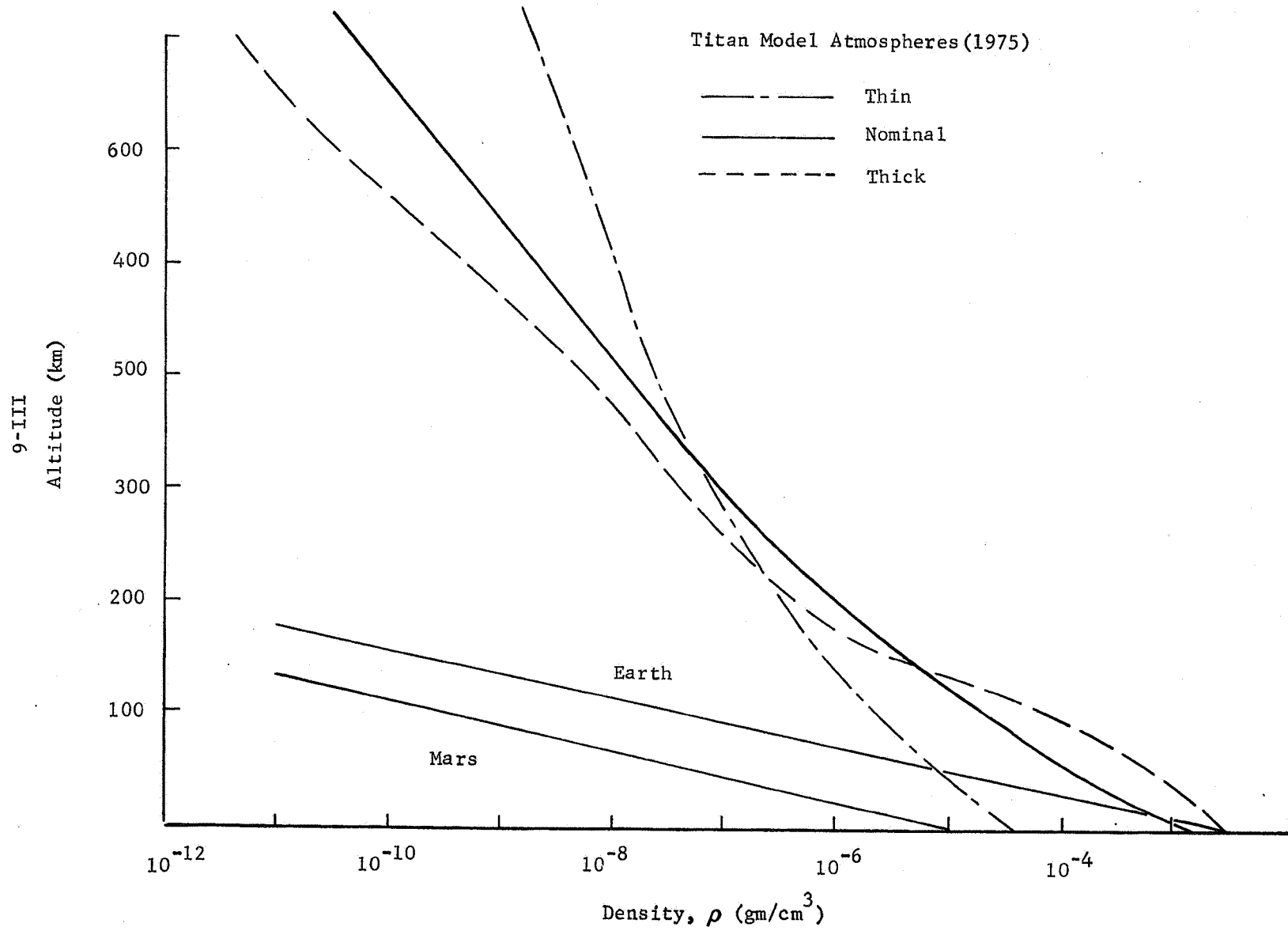
Fig. III-2 Titan Atmospheric Density Models

Several options are available for entering Titan's atmosphere from the 1000 Km circular orbit. The TOPL can be given a small retro impulse at apoapsis causing it to dip down during periapsis passage and skim through the outer edge of the atmosphere. Some energy would be removed although heating and dynamic pressures would be minimal due to the low velocity. Apoapsis would thus gradually be reduced and an orbital decay entry would result. Tracking this trajectory from the mother ship would, along with on-board accelerometer data, yield the atmospheric density profile. The potential for a large time-intergrated heat input exists for this type of entry, but for Titan entry the flux levels will be low enough that metal surfaces at moderate temperatures could reradiate most of the heat. Thus the vehicle would not experience a large integrated heat load.

A disadvantage of this entry mode is that final location of the ultimate vertical descent and landing would not be readily predictable. A second entry mode, and the one preferred, involves providing retro at apoapsis to lower periapsis altitude to zero. This orbit would intercept the outer edge of the atmosphere at a slightly steeper angle than in the orbital decay mode, depending on the actual extent of the atmosphere encountered, but the angle will still be small, see Figure III-3. For this mode, landing occurs about 120° to 150° from apoapsis. An enlarged view of the entry and descent region, Figure III-4, shows that for the Thick model atmosphere the effect of the atmosphere is felt at about 250 Km.

Since the feasibility of the TOPL concept depends to a large extend on not having to provide an entry vehicle with an aeroshell and heat shield, an entry trajectory was analyzed for the Thick model atmosphere which represents the worst case since it exhibits the smallest scale height.

POTENTIAL ENTRY CONDITIONS
AT VARIOUS ALTITUDES

γ_e(deg), V_e(km/sec)

-9.0, 1.69

-8.8, 1.75

-8.3, 1.81

-7.2, 1.87

-6.3, 1.96

500 KM
300
100

1000 KM

2700 KM

$V_p = 1.99$

$\gamma = 0$

III-8
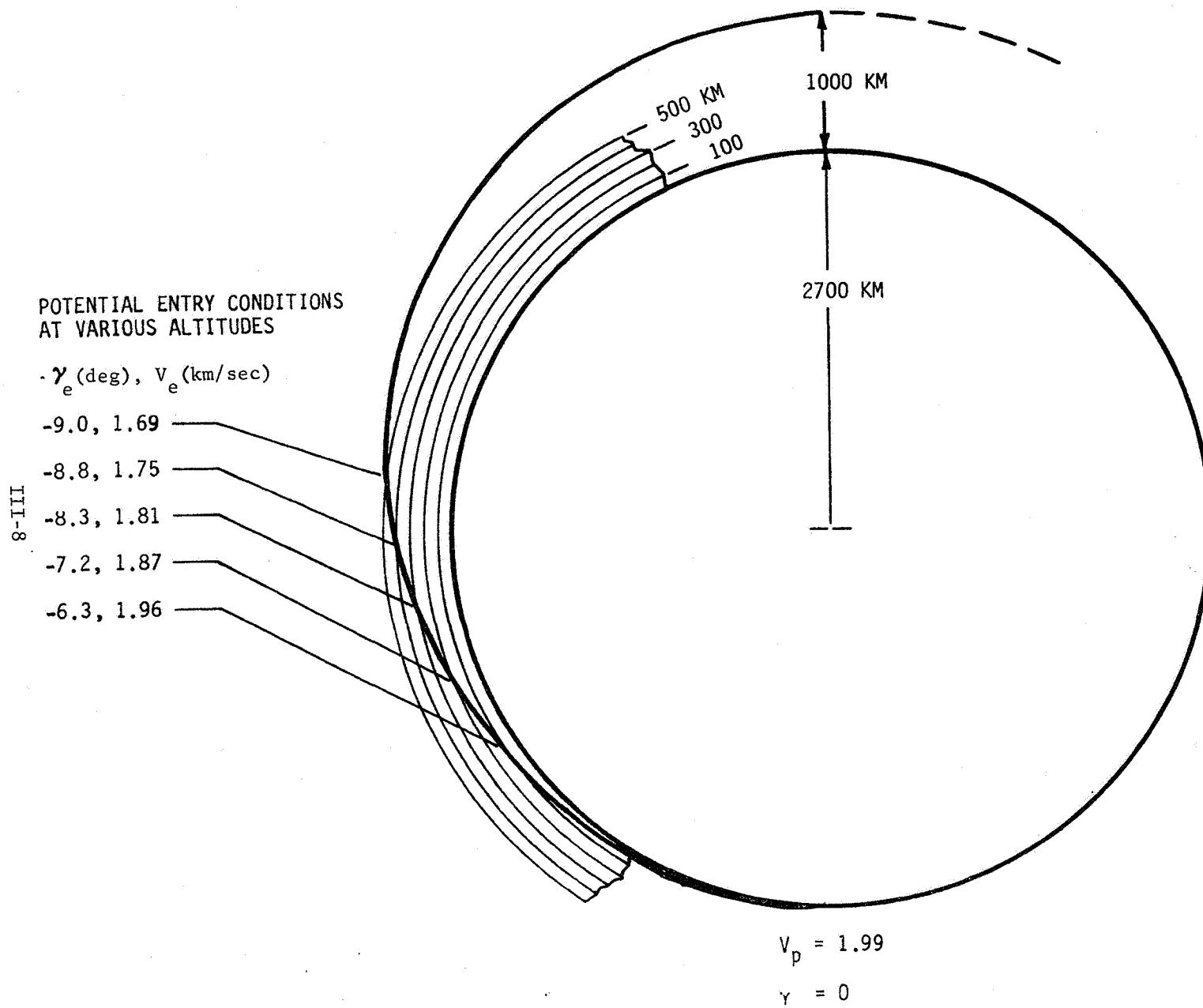
Fig. III-3   TOPL Deorbit Trajectory

$V_{500 \, km} = 1.69 \text{ km/sec}$

$\gamma_{500 \, km} = -9°$

500

400

300

200

100 KM

TITAN SURFACE

DESCENT TRAJECTORY IN "THICK" ATMOSPHERE MODEL

DEORBIT TRAJECTORY (IN ABSENCE OF ATMOSPHERE)

III-9
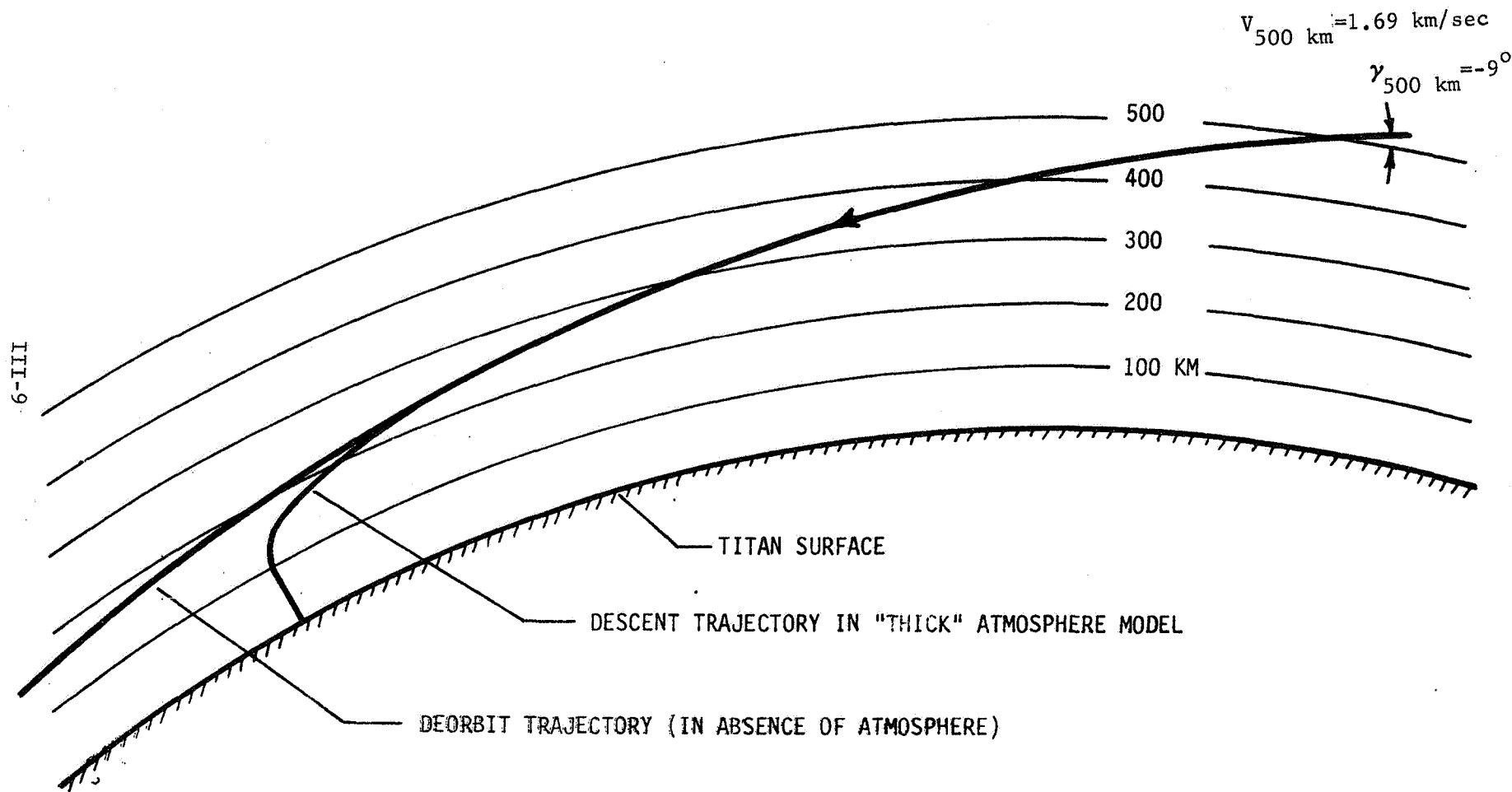
Fig. III-4 Entry from Zero-Periapsis-Altitude Ellipse

The resulting dynamic pressure and deceleration pulses for this case are plotted in Figure III-5, and the heating pulse is shown in Figure III-6. These figures show that peak heating (coldwall), peak g's, and peak dynamic pressure are .57 watts/cm^2, .398 g's, and 305 N/m^2, respectively. If the Thin atmosphere is encountered, the initial entry angle will be slightly steeper but the lower entry velocity (farther from periapsis) and larger scale height more than offset this effect and a less severe entry results. The peak coldwall heat flux on the body of the vehicle produces a surface equilibrium temperature of 260°C which is compatible with light-weight metal structures. Exposed truss members with small diameters would get hotter but would not exceed, unprotected, a value of 500°C. Spray coatings of subliming materials could be used to reduce this temperature, but these would induce the potential for contamination and consequently large diameter structural elements should be utilized.

The vehicle body axis can be kept aligned with the velocity vector through peak heating with the RCS system that performs orbital operations since the maximum dynamic pressure is small.

On reaching subsonic velocities a small, g-switch-operated-drogue device would orient the vehicle to the local vertical. This aerodynamically established local vertical direction would also be used to update the on-board gyro attitude reference system (by averaging the attitude through a number of oscillations). Mass spectrometer, pressure, tempterature, radiometer, and cloud sensor instruments would function during the descent. Their operation would be enhanced relative to conventional probe designs by the absence of outgassing from ablative heat shield materials.
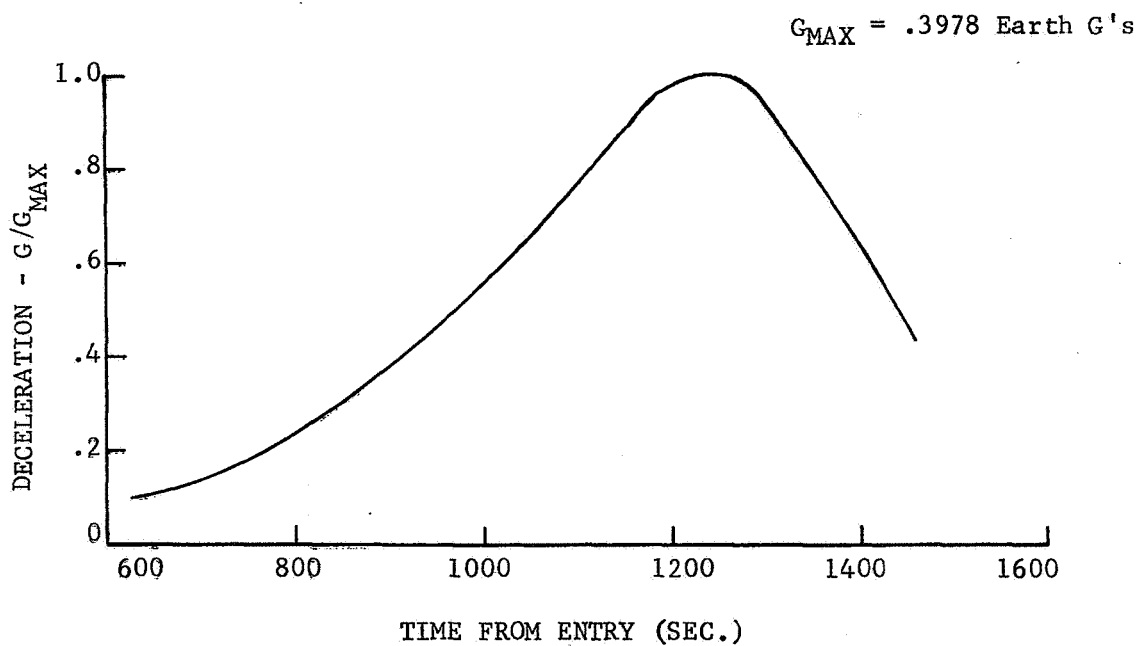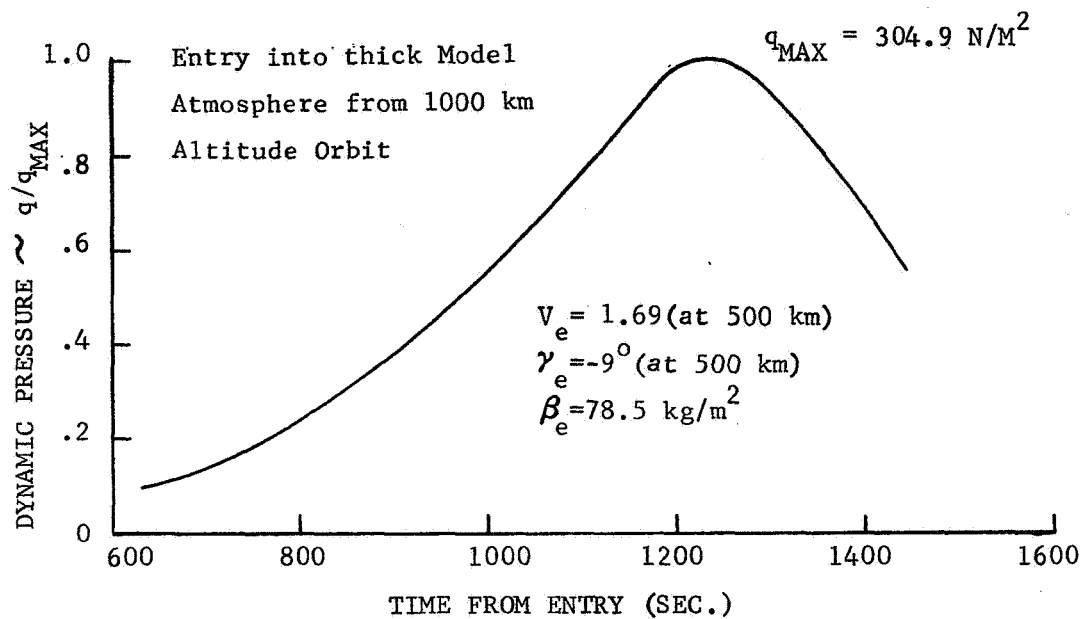
Fig. III-5 Dynamic Pressure & Deceleration During Entry

COLD WALL
HEATING RATE
BTU/FT^2 SEC

R_N = 0.91 m(Nose Radius)

β = 78.5 kg/m^2

V_E = 1.69 km/sec

γ_E = -9°

h_e = 500 km

watts/cm^2

TIME (SEC) FROM 500 KM ALTITUDE
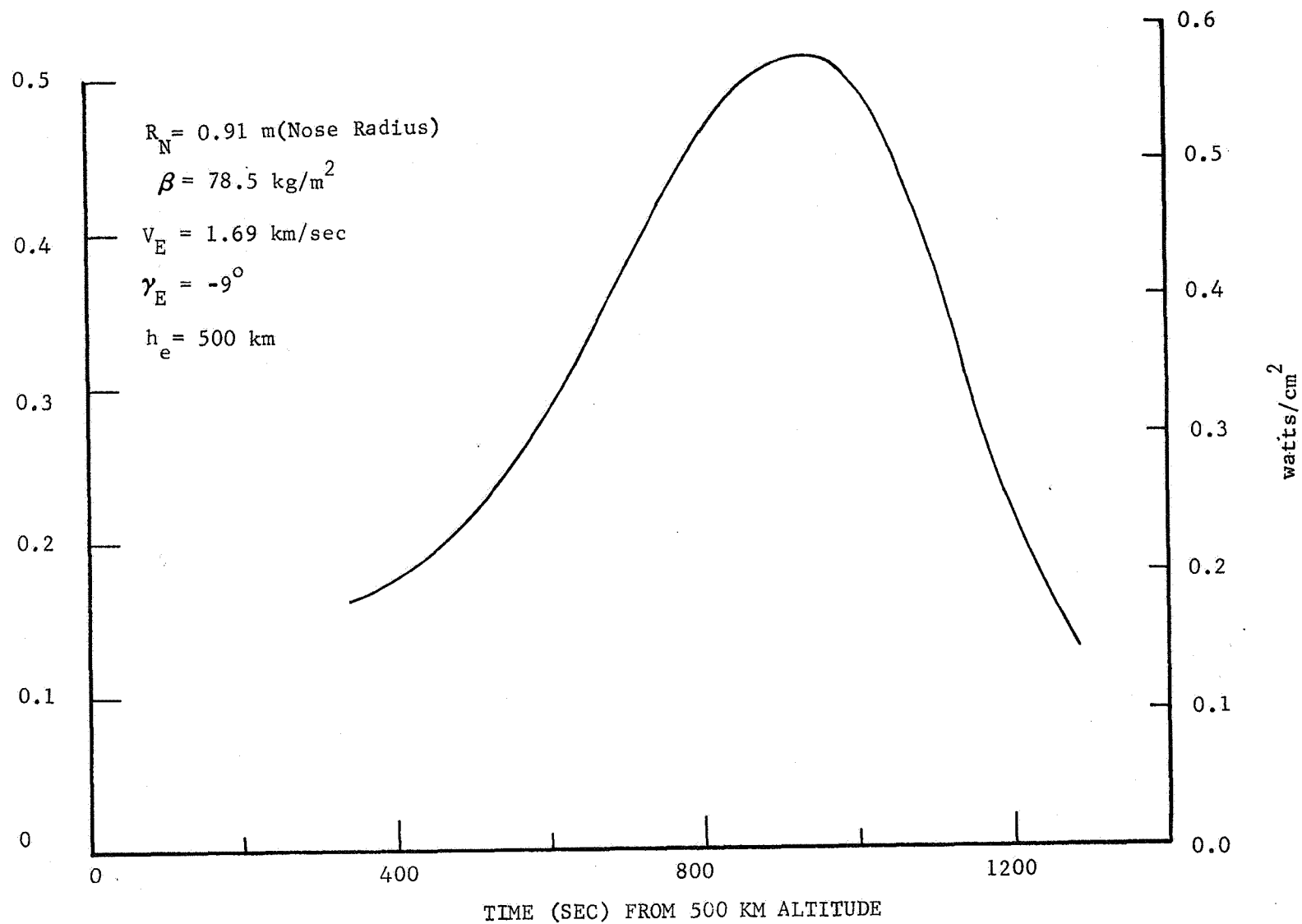
Fig. III-6   Heat Input During Entry From Circular Orbit - TOPL Vehicle

Landing velocity, for the nominal atmosphere, would be 11 m/s based on just the drag of the basic vehicle (this compares to the ~7 m/s velocity reported by the Soviets in their recent Venus landers and the 4 m/s planned for the Viking Lander). For this velocity a simple shock absorbing ring located forward of the vehicle could be designed to reduce landing loads to values compatible with landing stability and the operation of cameras and other landed science experiments and their supporting electronics. Such a ring could also be designed as a pontoon to serve as a flotation system in the event a liquid surface is encountered. Alternatively, a crushable pad could be provided that would also serve to insulate the body during the aero-heating phase. These options are shown in Figure III-7, and an estimated mass breakdown is given in Table III-1. Figure III-8 shows several possible versions of the vehicle during the descent phase, including a tractor rocket braking version and optional antenna configurations. The small drogue parachute shown in these views serves primarily to provide a vertical attitude reference but it also could be enlarged and serve as an alternative to propulsive braking in the event a thin model atmosphere is encountered.

From the foregoing evaluation, it appears that the features required to make a Titan orbiter also perform entry probe and lander functions can be kept to a bare minimum. The other critical aspects of the TOPL concept are the Titan orbit insertion requirements, discussed later in Section 2, and the applicability of using the mothership, in orbit around Saturn, as a relay communications station. This latter situation is discussed next.
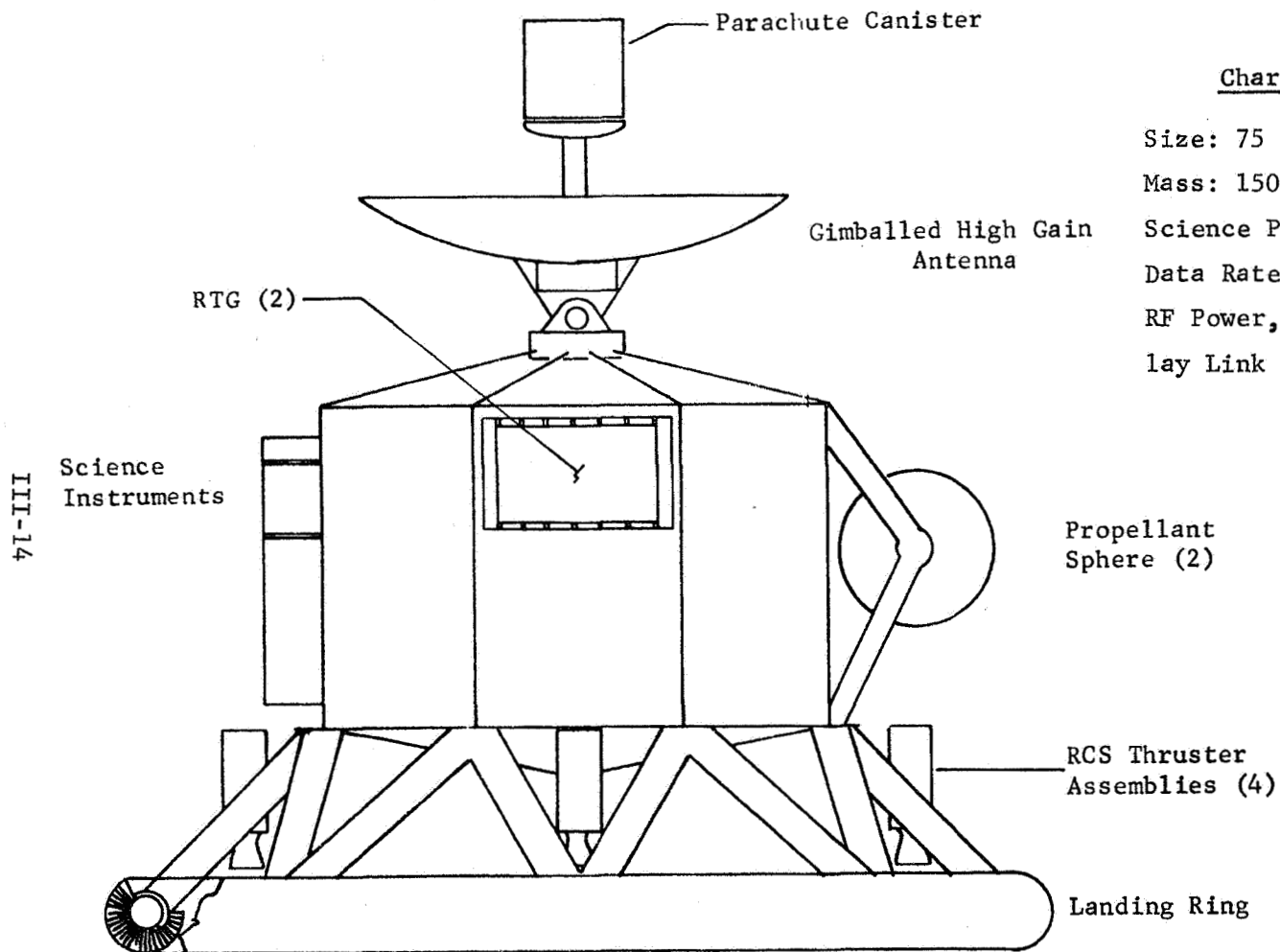
Parachute Canister

Gimballed High Gain
Antenna

RTG (2)

Science
Instruments

III-14

Propellant
Sphere (2)

RCS Thruster
Assemblies (4)

Landing Ring

Fig. III-7a Potential TOPL Configuration

Disc Antenna/
Parachute Canister

RTG (2)

Science
Instr

Propellant
Sphere (2)

RCS Thruster
Assemblies (4)

Landing Disc (Crushable Material)

III-15
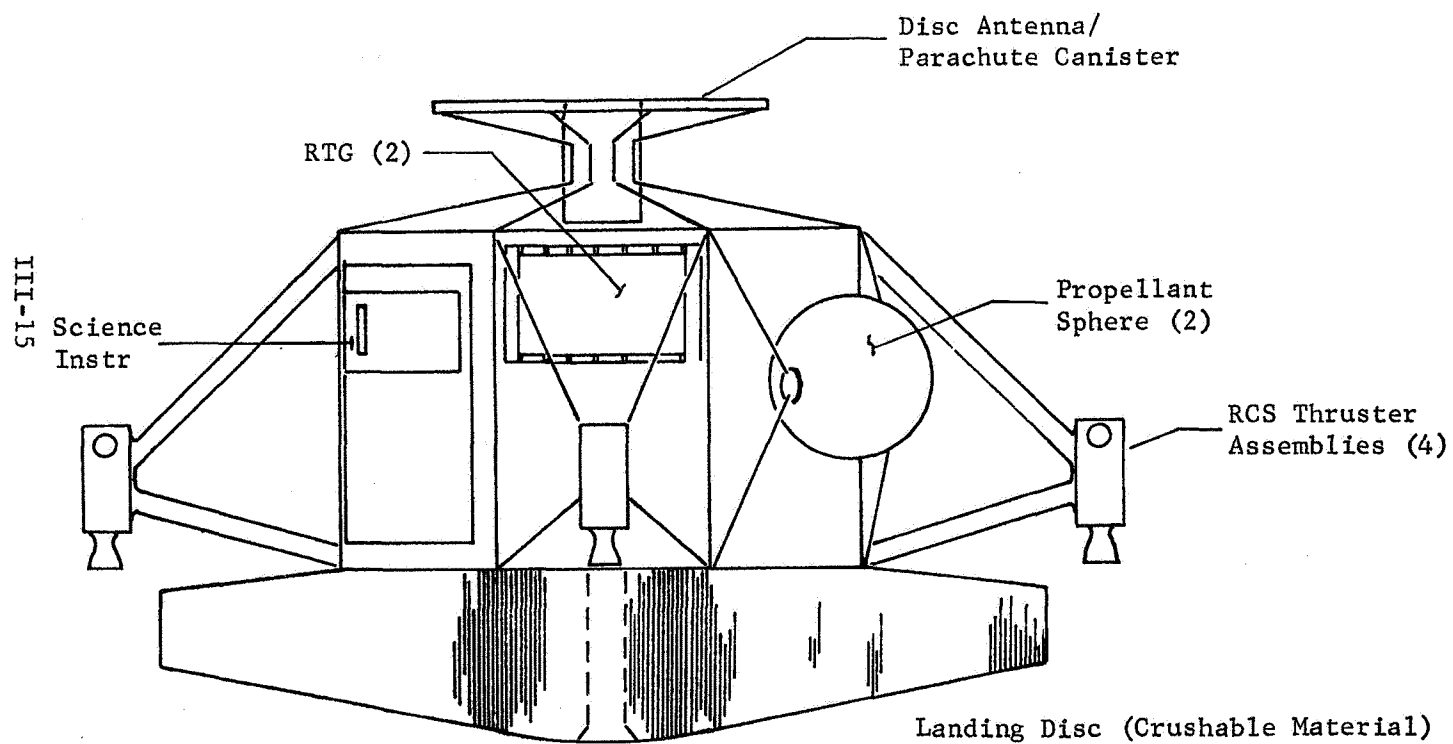
Fig. III - 7b TOPL Configuration (Alternate Design)

Table III - 1 Estimated Mass Breakdown for the TOPL Vehicle

ITEM	MASS, kg
Orbital Science	6
Descent Phase Science [1]	8
Landed Science [2]	22
Electronics Systems [2] (Communications, Power, Data Handling)	40
Structure and Mechanical Systems [2]	46
Attitude Control (including RCS system)	18
Terminal Descent Propulsion	10
TOTAL	150

(1) Assumes shared equipment with landed science, e.g.,

mass spectrometer

(2) Based on achieving factor of two improvement in

Viking '75 lander science mass and volume requirements

Retro Motor

Dish Antenna

Disk Antenna

Dish Antenna

Landing Disc

Landing Disc

Landing Ring
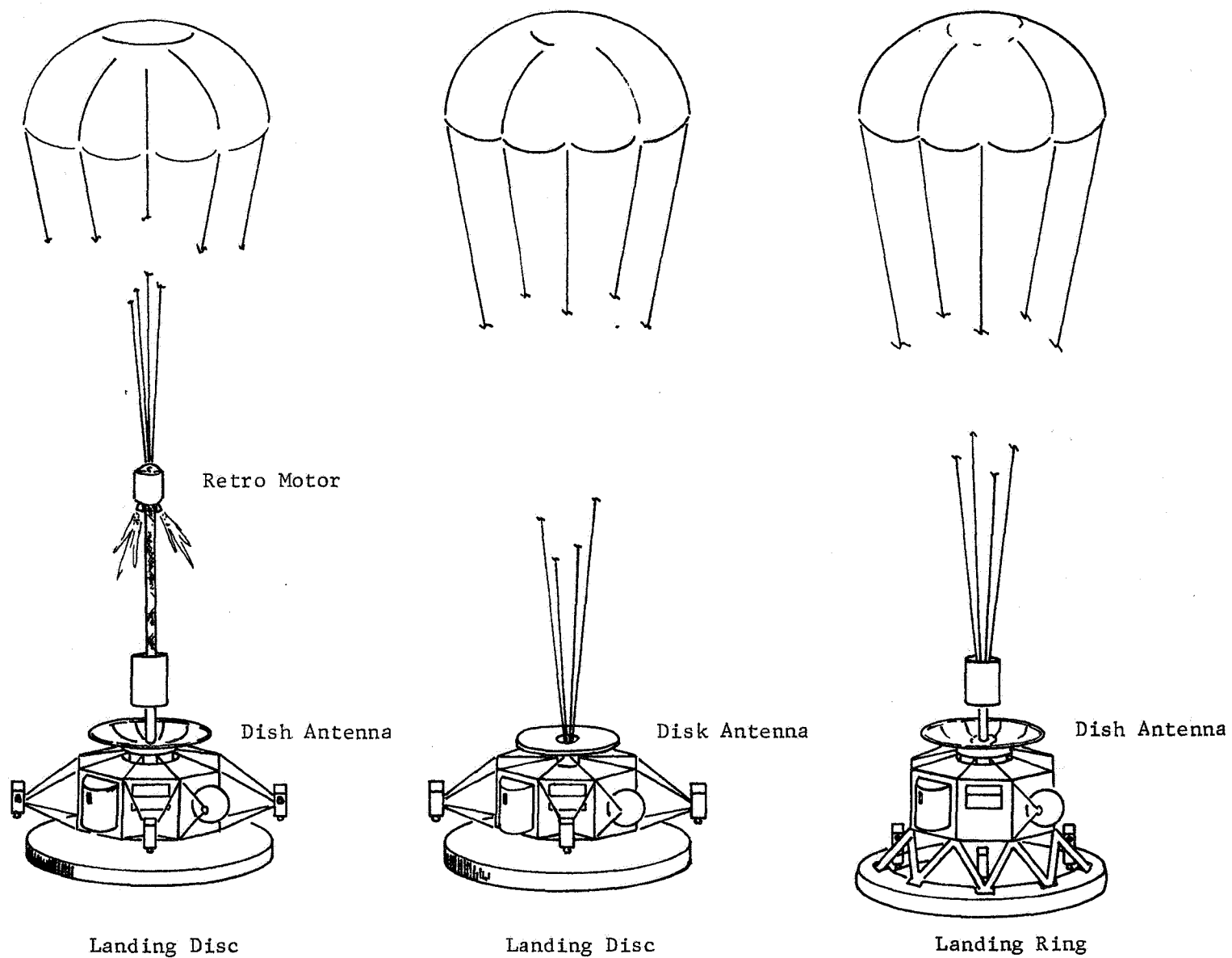
Fig. III - 8   TOPL Configuration Options in Descent Phase

b. Communications Geometry Between a Titan Lander and a Saturn Orbiter

Several options are possible for communicating between Earth and a Titan lander. It may be feasible to establish a direct link for periods approaching half the Titan day (about 8 Earth days if Titan is face-locked to Saturn) with comparable intervals of communication outage. If a supporting spacecraft is maintained in Titan orbit, lander communications could be relayed for several hours a day without long-duration interruptions. A third alternative would involve relay via a Saturn orbiting spacecraft positioned in an appropriate orbit. This latter option may be particularly applicable to the TOPL concept in which the entire Titan orbiter space-craft is subsequently committed to the Titan surface.

Typical Titan mission communications geometry begins with the approach to Titan from a coplanar orbit having a high apoapsis radius. Tangential Titan encounter for this case corresponds to a relative approach velocity of about 1.73 km/sec. Prior to Titan encounter, Titan orbiter and/or lander vehicles can be deployed from the primary Saturn spacecraft. Also, with slightly different targeting, the Saturn orbiter can utilize the Titan flyby to produce an orbit period three times that of Titan. This commensurate orbit was examined for communication relay characteristics.

Planetocentric motion of Titan and spacecraft following the Titan swingby are shown on Figure III-9. For this analysis, Titan gravity effects after the swingby were neglected; i.e., 3-body integrations were not performed. The resulting inaccuracy of relative motion while the space-craft orbit is near that of Titan is not of first-order significance to primary communication considerations.

III-18
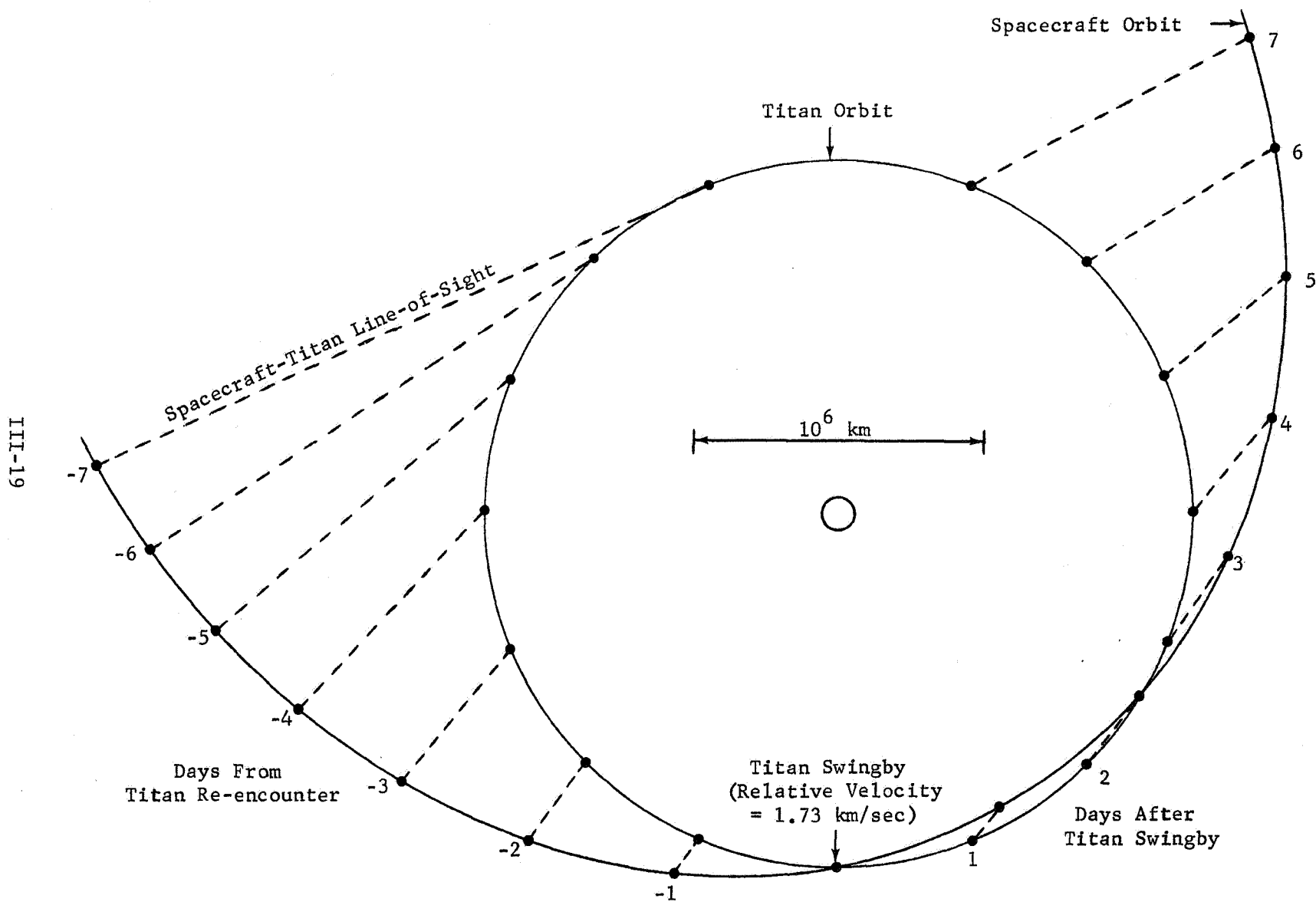
Fig. III-9 Spacecraft Orbit Period = 3 X Titan Orbit Period, Co-Planar With Titan

Separation distance between Titan and the spacecraft are shown for the first week following Titan encounter. Also, information regarding pointing angles from a fixed longitude on the Titan surface and from the Saturn orbiting spacecraft can be derived from the figure. The geometries depicted reflect the arbitrary choice of deflecting the Titan relative velocity inward with the result that the Saturn orbiter periapsis occurs shortly after the Titan swingby event. For the alternative case of outward deflection, apoapsis would occur first and periapsis would be deferred until shortly before the next Titan encounter.

About a week after Titan swingby, communication range exceeds 1 million km. Subsequently, at about 24 days, the Saturn orbiter and Titan are in Saturn opposition and separation has increased to over 5 million km. While communication at ranges of this magnitude may be feasible, primary interest has been directed at the shorter ranges, Such conditions occur again as the Saturn orbiter completes it approximately 48-day orbit.

Geometries for the week preceding Titan re-encounter are included in Figure III-9. This period is more likely to be relevant to surface communications if an interim Titan orbit, with associated time implications, has preceded the landing operation. Conversely, a direct entry lander could be supported by the earlier communication opportunity. As shown by the figure, the first period following Titan swingby favors communication with the forward hemisphere of Titan. At Titan re-encounter, the outward hemisphere dominates the short-range view. Such factors would be of importance to total mission design and would interact with other matters such as landing site preference. As mentioned earlier, the option exists before the Titan swingby (following observations from flybys) to reverse the swingby deflection and hence the sequence of the two geometry segments depicted on Figure III-9.

The orbit of the Saturn orbiting spacecraft could be adjusted prior to re-encounter for purposes of avoiding the Titan gravity field (to maintain the prior orbit) or to produce controlled deflection to a different orbit with superior communication relay characteristics. For example, a second Titan swingby can reduce the period of the Saturn orbiting spacecraft to that of Titan. As shown in Figure III-10, this latter orbit remains in closer proximity to Titan with a maximum communication range of about 1.5 million Km. Over the Titan period of about 16 days, the Saturn orbiter view of Titan shifts from the inside forward quadrant of Titan to the outside forward quadrant. Reversal of the view to favor the trailing hemisphere of Titan could be achieved if the outward deflection option had been elected for both the first and second swingbys.

Further improvement of communication geometry can be accomplished by using Titan gravity to deflect the relative velocity vector out of the Titan orbit plane. In the case of Titan relative velocity equal to 1.73 km/sec, two more Titan swingbys are required after the spacecraft orbit period has been reduced to that of Titan. The final inclined orbit is circular and the spacecraft orbit period remains equal to that of Titan. For another example case (discussed in Section 2 that follows) relative velocity is reduced to 0.95 km/sec, and a single Titan swingby is sufficient to deflect a co-planar orbit to the fully inclined condition.

Figure III-11 depicts relative motion of the foregoing cases for the first half orbit following establishment of Titan-period inclined orbits. As shown, the maximum communication ranges to Titan surface locations in the adjacent hemisphere are about 380,000 km and 210,000 km for the two examples. These distances correspond to about 140 and 80 Titan

III-21
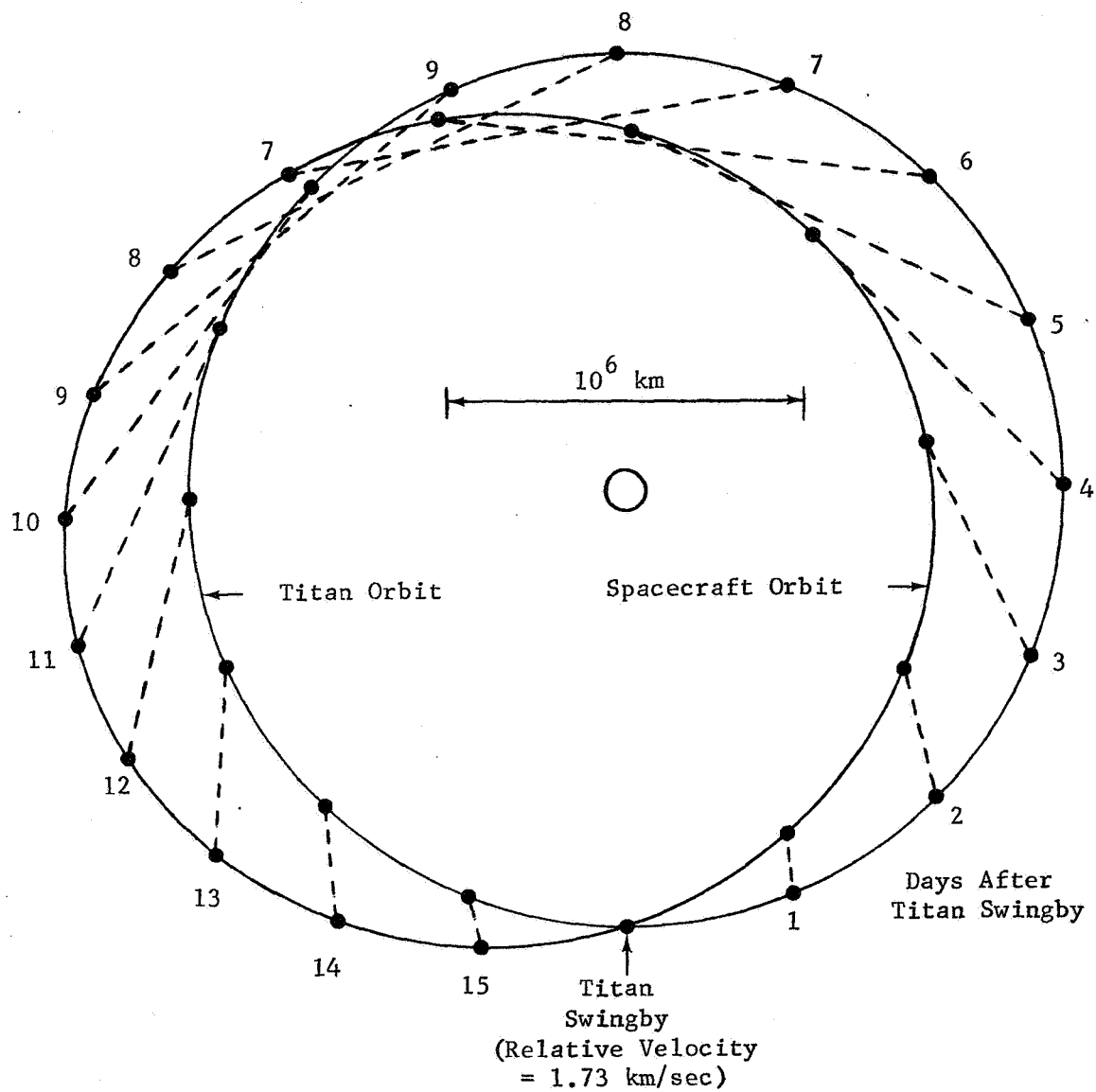
Fig. III-10   Spacecraft Orbit Period = Titan Orbit Period,
Co-Planar With Titan

radii respectively which place the Titan-orbiting spacecraft beyond the
region of appreciable Titan gravity. However, sufficient time would be
spent well within the Titan sphere of influence to introduce significant
error in the presentation of Figure III-11. Valid analyses would require
3-body treatment of the problems and are beyond the scope of this study.
In view of the apparent communication advantages of synchronous inclined
orbits, such analyses would be valuable for detailed mission design studies.
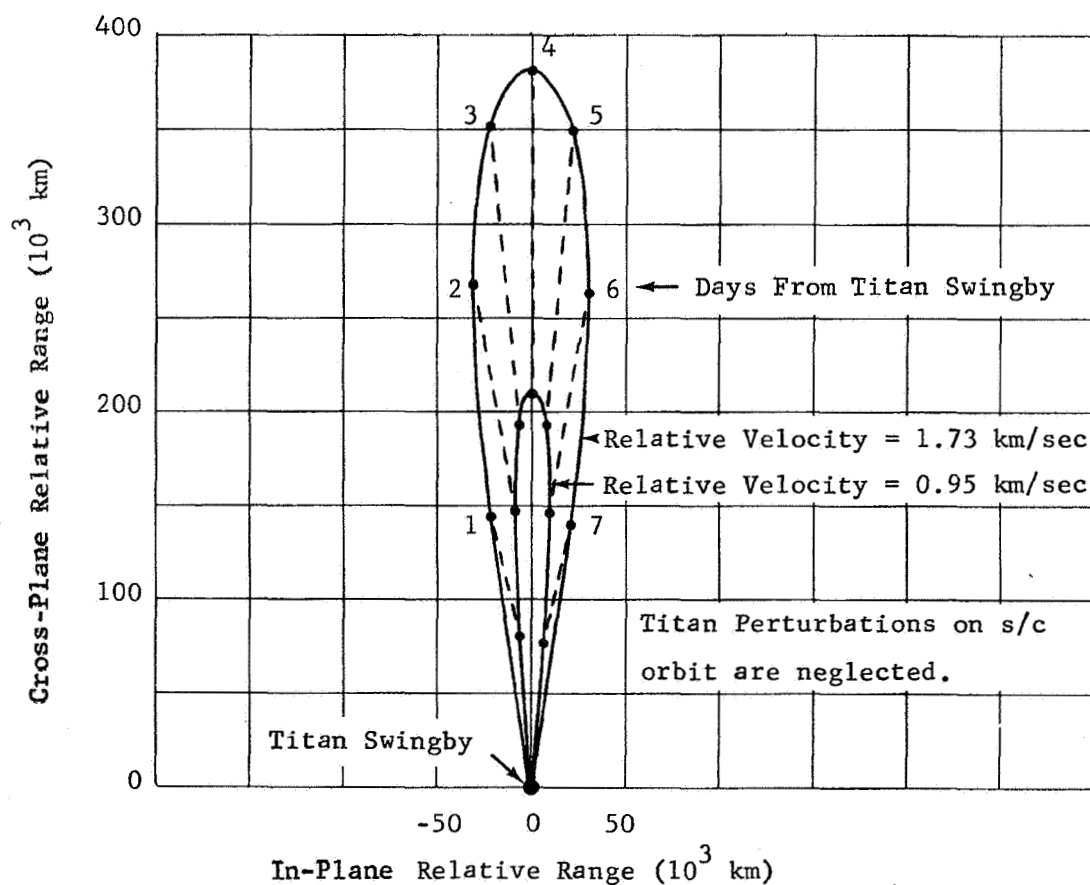
Fig. III-11   Relative Motion Between Titan and Circular, Inclined
Spacecraft Orbits With Period = Titan Period

Further improvement (and complexity) could be introduced by consideration of controlling Titan swingbys to produce somewhat imperfect synchronization with Titan; residual eccentricity, period discrepancy, etc. For these cases, subsequent small velocity maneuvers could establish semi-stable repeating orbits which would circulate in the vicinity of Titan without actually being in Titan orbit. Due to the significant mass of Titan, complete 3-body analyses would be necessary for meaningful assessment of such communication relay orbits.

c. Relay Data Links for a Titan Orbiter and Lander

To establish that the transmission of sizable amounts of data from a power limited Titan Orbiter, lander, or combination vehicle (TOPL) is feasible, relay data link designs were performed for several cases based on the relative geometry developed in the previous section.

1) Case 1 - Titan Orbiter to 48-day period Saturn Orbiter

Data link designs were performed for 80 W of RF power at 1 GHz with the communication geometries resulting from a 12-hour orbit for the Titan orbiter and a 48-day orbit for the Saturn orbiter, Figure III-9. The ranges and aspect angles for the second and fourth days were used to determine data rates for the fixed amount of output power. The results are shown in Table III-2. A 0.6 m (2-ft.) dish antenna was used on the Titan orbiter having the capability of tracking the Saturn orbiter. The Saturn orbiter is spin-stabilized with a 65° beamwidth antenna aligned parallel to the spin axis. As seen in the table, 80 W can sustain a data rate of 400 bps out to day 2 and 125 bps at day 4 where the range is rapidly increasing. These relatively high data rates result from the high gain of the Titan orbiter antenna which is oriented to track the Saturn orbiter during these periods.

TABLE III-2 Relay Link Designs for Titan Orbiter to Saturn Orbiter

NO.	PARAMETER	TO-SO 1 GHz Day 2	NOTE	TO-SO 1 GHz Day 4	NOTE	
1	TOTAL TRANSMITTING POWER (dBW) - - - - - - - - - - - -	19.0	80 W	19.0	80 W	
2	TRANSMITTING CIRCUIT LOSS (dB) - - - - - - - - - - - -	-0.5		-0.5		
3	TRANSMITTING ANTENNA GAIN (dB) - - - - - - - - - - - -	13.5	2' Dish $\emptyset=0°$	13.5	G=13.5db θ=	36°
4	COMMUNICATIONS RANGE LOSS (dB) - - - - - - - - - - - -	-202.0	3×10^5 Km	-205.5	4.5×10^5Km	
5	ATMOSPHERIC ABSORPTION & DEFOCUSING LOSSES (dB)- - -	0		0		
6	POLARIZATION LOSS (dB) - - - - - - - - - - - - - - - -	-00.4	AR=3/3 dB	-0.4		
7	ANTENNA PATTERN RIPPLE LOSS (dB) - - - - - - - - - -	- 0.5		-0.5		
8	RECEIVING ANTENNA GAIN (dB)- - - - - - - - - - - - -	8.2	θ=65° $\emptyset$=10°	6.7	$\emptyset$=25°	
9	RECEIVING CIRCUIT LOSS (dB)- - - - - - - - - - - - -	-1.0		-1.0		
10	NET LOSS (dB)(2+3+4+5+6+7+8+9) - - - - - - - - - - -	-182.7		-187.7		
11	TOTAL RECEIVED POWER (dBW)(1+10) - - - - - - - - - -	-163.7		-168.7		
12	RECEIVER NOISE SPECTRAL DENSITY (dBW/Hz) - - - - - -	-202.5	$T_s=400°$K	-202.5		
13	TOTAL RECEIVED POWER/N_o (dBW/Hz)(11-12)- - - - - - -	38.8	ADV=-1.3	33.8	ADV=-1.3	
	DATA CHANNEL					
14	FADING LOSS (dB) - - - - - - - - - - - - - - - - - - -	-0.3		-0.3		
15	PROCESSING LOSS (dB) - - - - - - - - - - - - - - - - -	-0.4		-0.4		
16	RECEIVED DATA POWER (dBW)(11+14+15)- - - - - - - - - -	-164.4		-169.4		
17	DATA BIT RATE (dB) - - - - - - - - - - - - - - - - - -	26.0	400 bps	21.0	125 bps	
18	THRESHOLD ENERGY PER DATA BIT -E_b/N_o (dB)- - - - - -	10.6	BER-5x10^{-4}	10.6		
19	THRESHOLD DATA POWER (dBW)(12+17+18)- - - - - - - - -	-165.9		-170.9		
20	PERFORMANCE MARGIN (dB)(16-19) or (13+14+15-17-18) -	1.5	ADV=-1.5	1.5	ADV = -1.5	
21	NET MARGIN (dB)(20-20 ADV) - - - - - - - - - - - - - -	0.0		0.0		

CONDITIONS: 1. Titan Orbiter-to-48 day period Saturn Orbiter relay link geometry
2. PCM/FSK/PM non-coherent modulation, BT=2
3. Spin-stabilized Saturn orbiter - fixed altitude during the 4 days considered
4. Convolutional encoding, Viterbi decoding, Rate = 1/2

NOTATIONS: θ = Beam width
∅ = Angle away from max gain point

2) Case 2 - Titan Lander to 48-Day Period Saturn Orbiter

The second case considers communication between a lander and the Saturn orbiter in a 48-day orbit around Saturn. The orbiter is again assumed to be spin-stabilized with a 65° beam width receiving antenna and the communication geometry is as described in Figure III-9, above. The major difference is that the lander antenna is here assumed to be fixed, and aspect angles to the orbiter therefore increase with each day from periapsis. The computed data rates at day 2 and 4 for 80 W of RF power are shown in Table III-3. A data rate of 225 bps is found to be sufficient to transmit 19.4 mega-bits of data in one day (enough to transmit 20 T.V. pictures). As seen from the table, the data rate is decreased to 7 bps at day 4 due to the increasing range and aspect angle to the Saturn orbiter. A tracking antenna on the lander would offer some improvement.

3) Case 3 - Titan Lander to Out-of-Plane Saturn Orbiter with a 16-Day Orbit Period (Period Equal to Titans)

The third case considered involves the geometry described in Figure III-11 wherein a range of 400,000 km is not exceeded at any time in the relay spacecraft's orbit and the aspect angle stays small. This situation is much better from the standpoint that data can be transmitted over a longer span since a biology mission requires 16 days (to assess life growth reactions) and seismology missions require much greater times. A disadvantage of this geometry lies in the fact that if the landing site is positioned to be optimum for one half of Titan's orbit, the relay S/C will be out of sight during the other half of the orbit. However, it may be possible to avoid this situation by further adjusting the orbit synchronization as discussed in Section b. above.

TABLE III-3 Relay Link Designs for Titan Lander and Saturn Orbiter

NO.	PARAMETER	TL-SO 1 GHz Day 2	Notes	TL-SO 1 GHz Day 4	Notes	
1	TOTAL TRANSMITTING POWER (dBW) - - - - - - - - - - - - -	19.0	80 W	19.0	80 W	
2	TRANSMITTING CIRCUIT LOSS (dB) - - - - - - - - - - - -	-0.5		-0.5	θ=33°,θ=36°	
3	TRANSMITTING ANTENNA GAIN (dB) - - - - - - - - - - -	11.0	2', $\emptyset$=15°	1.0	4, 5x10^5 Km	
4	COMMUNICATIONS RANGE LOSS (dB) - - - - - - - - - - -	-202.0	3x10^5 Km	-205.5		
5	ATMOSPHERIC ABSORPTION & DEFOCUSING LOSSES (dB)- - -	0		0		
6	POLARIZATION LOSS (dB) - - - - - - - - - - - - - - - -	-0.4	AR=3/3 dB	-0.4		
7	ANTENNA PATTERN RIPPLE LOSS (dB) - - - - - - - - - -	-0.5		-0.5		
8	RECEIVING ANTENNA GAIN (dB)- - - - - - - - - - - - -	8.2	θ=65°,$\emptyset$=10°	6.7		
9	RECEIVING CIRCUIT LOSS (dB)- - - - - - - - - - - - -	-1.0		-1.0		
10	NET LOSS (dB)(2+3+4+5+6+7+8+9) - - - - - - - - - - -	-185.2		-200.2		
11	TOTAL RECEIVED POWER (dBW)(1+10) - - - - - - - - - -	-166.2		-181.2		
12	RECEIVER NOISE SPECTRAL DENSITY (dBW/Hz) - - - - - -	-202.5	T_s=400°K	-202.5		
13	TOTAL RECEIVED POWER/N_o (dBW/Hz)(11-12)- - - - - - -	36.3	ADV=-1.3	21.3	ADV = -1.3	
	DATA CHANNEL					
14	FADING LOSS (dB) - - - - - - - - - - - - - - - - - -	- 0.3		- 0.3		
15	PROCESSING LOSS (dB) - - - - - - - - - - - - - - - -	- 0.4		- 0.4		
16	RECEIVED DATA POWER (dBW)(11+14+15)- - - - - - - - -	-166.9		-181.9		
17	DATA BIT RATE (dB) - - - - - - - - - - - - - - - - -	23.5	225 bps	8.5	7 bps	
18	THRESHOLD ENERGY PER DATA BIT -E_b/N_o (dB)- - - - - -	10.6	BER=5x10^{-4}	10.6		
19	THRESHOLD DATA POWER (dBW)(12+17+18)- - - -- - - - -	-168.4		-183.4		
20	PERFORMANCE MARGIN (dB)(16-19) or (13+14+15-17-18) -	1.5	ADV = -1.5	1.5	ADV = -1.5	
21	NET MARGIN (dB)(20-20 ADV) - - - - - - - - - - - - -	0		0		

CONDITIONS: 1. Titan lander to 48-day period Saturn orbiter geometry
2. PCM/FSK/PM non-coherent modulation, BT=2
3. Spin-stabilized Saturn orbiter
4. Convolutional encoding, Viterbi decoding, Rate = 1/2

For this relay geometry, a higher gain receiving antenna can be used on the relay spacecraft and the 80 W of lander RF power is found to sustain a data rate of 370 bps (see Table III-4) versus the 225 bps of the previous example. This is sufficient to send over 31 megabits of data in 24 hrs. Alternatively, if a data rate of 225 bps is adequate, only 48 W of RF power is required as opposed to 80 watts for the previous case. If the range is further reduced as appears possible, see Figure III-11, an RF power of 22 W will produce a data rate of 370 bps.

From these analyses the modest amount of mass allocated to the communications system in sizing the TOPL configurations in Section a appears reasonable even for fairly ambitious science objectives.

2. Advanced Remote Sensing Orbiters (ARSO)

The TOPL concept for Titan exploration described in the preceding section was developed to provide early answers to the important science questions and to function in spite of uncertainties in Titan atmosphere or surface conditions. There is another school of thought among those involved in planning planetary exploration missions that favors advanced orbiting vehicles to accomplish the same objectives. An orbiting vehicle would of course be less vulnerable to failure due to the uncertainties of the atmosphere or surface but the question is whether or not it can adequately answer the high priority science questions.

The spacecraft in this case might either be a Titan orbiter whose operation would be similar to the orbital phase of the TOPL vehicle mission, or a Saturn orbiter that remains in close proximity to Titan.

TABLE III-4 Close Titan Orbit Relay Link
PROBE TELEMENTRY DESIGN CONTROL TABLE

ITEM	PARAMETER	NOMINAL VALUE	ADVERSE TOLERANCE	REMARKS
1.	Total Transmitter Power, dBW	19.0	- 0.1	f= 1 GHz, 80 W
2.	Transmitting Circuit Loss, dB	- 0.5		
3.	Transmitting Antenna Gain, dB	12.0	- 0.2	2 ft Dish $\emptyset = 10^{\circ}$
4.	Antenna Pattern Ripple, dB	- 0.5	-	
5.	Space Loss, dB	-204.1	- 0.2	3.8×10^5 km, f= 1 GHz
6.	Planet Atmosphere Loss, dB	- 0		
7.	Polarization Loss, dB	- 0.4		AR = 3/3 dB
8.	Receiving Antenna Gain, dB	12.0	- 0.3	2 ft Dish $\emptyset = 10^{\circ}$
9.	Receiving Circuit Loss, dB	- 1.0		
10.	Net Circuit Loss, $\Sigma(2 \rightarrow 9)$, dB	-182.5	- 0.7	
11.	Total Received Power, (1+10), dBW	-163.5	- 0.8	
12.	Receiver Noise Spectral Density, N_o, dBW/Hz	-202.5	- 0.3	$T_s = 400^{\circ}K$
13.	Received Power/N_o, (11-12), dBW·Hz	39.0	- 1.1	

DATA CHANNEL

ITEM	PARAMETER	NOMINAL VALUE	ADVERSE TOLERANCE	REMARKS
14.	Fading Loss, dB	- 0.3		
15.	Processing Loss, dB	- 0.4		
16.	Received Data Power, (11+14+15), dBW	-164.2	- 0.8	
17.	Data Bit Rate, dB	25.7		Rate = 370 bps
18.	Threshold E_b/N_o, dB	10.6		BER = 5×10^{-4}
19.	Threshold Data Power, (12+17+18), dBW	-166.2	- 0.3	
20.	Performance Margin, (16-19) or (13+14+15-17-18), dB	2.0	- 1.1	
21.	Nominal Less Adverse Margin, (20-20 adv), dB	0.9		

Conditions:
1. Based on Titan lander to 16-day period Titan orbiter geometry
2. PCM/FSK/PM non-coherent modulation, BT = 2
3. 3-axis stabilized orbiter
4. Convolutional encoding, Viterbi decoding, Rate = 1/2

By optimizing the orbit insertion technique, the penalty for achieving a Titan orbit can be made relatively small as will be shown. This fact, along with the possibilities for reducing spacecraft weight with the advances in technology currently being forecast, Ref. III-7, make the Titan orbiter an attractive exploration mode. Such a vehicle, which is envisioned as being in the 130 kg class could perform some of the following experiments in addition to the "normal" orbiter experiments (optical imaging, gravity harmonics, etc).

o Multiple-location stimulation of the atmosphere - Determination of atmospheric composition by spectrographic analysis of wakes stimulated by small passive entry bodies.

o Occultation experiments performed in conjunction with the Saturn orbiter.

o Direct sampling and analysis of the upper atmosphere during periapsis passage.

These experiments are discussed further in a subsequent Section (IIIC). In general they require new technology development or the extrapolation of existing technologies. The Titan orbiting spacecraft itself will also require the development of new technologies, e.g., more capable on-board systems in the areas of optical guidance and data processing (robotics). Figure III-12 illustrates a possible 3-axis stabilized configuration for this class of Titan exploration vehicle. Communications would be accomplished by relay with a Saturn orbiter as described earlier.

Science Scan Platform

Propellant Sphere (2)

RTG

Gimballed High Gain Antenna

Science Boom (Stowed)

Thruster Assemblies (4)
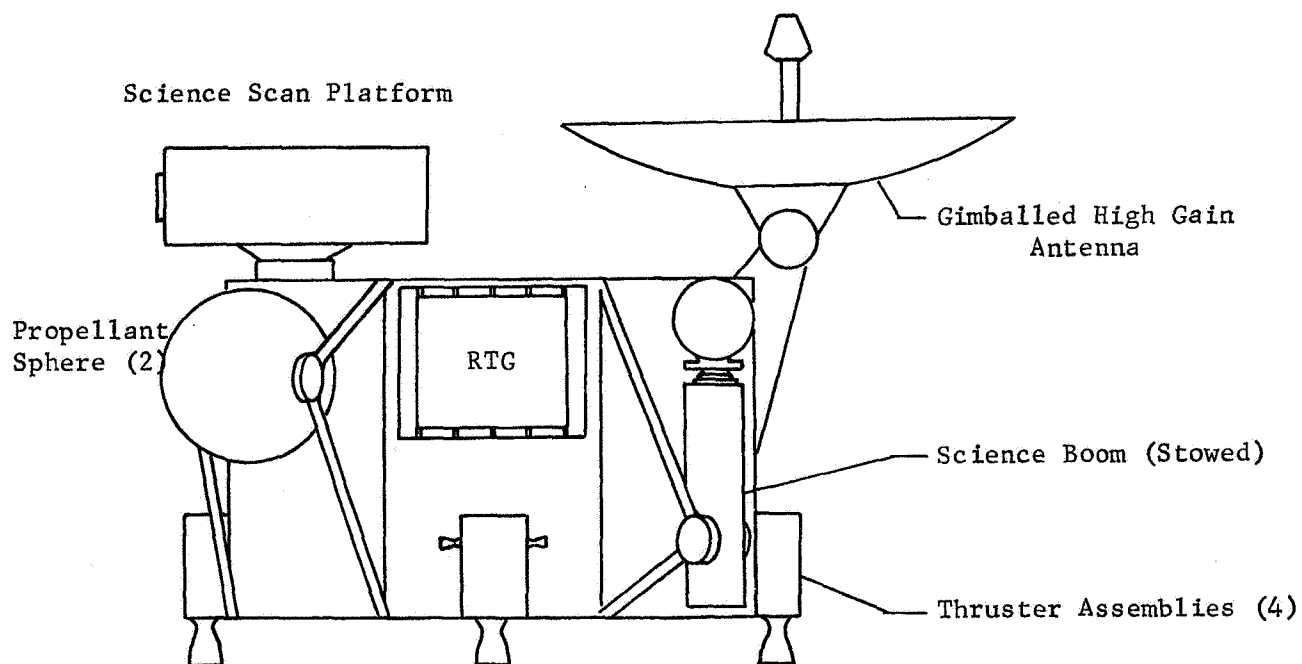
Mass ∼ 130 kg
Size ∼ 75 cm Diam.

Fig. III-12 Advanced Remote Sensing Titan Orbiter

In the case of a Saturn orbiter that remains in the vicinity of Titan although primarily under the influence of Saturn, a larger vehicle is possible due to the smaller insertion ΔV requirement relative to a Titan orbiter. It is therefore more appropriate for experiments requiring greater power, mass or size. The large diameter, high data rate, side looking radar experiment described in Section C is an example. The Saturn orbiter can also serve as the cruise vehicle for a lander or a small Titan orbiter. Figure III-13 shows a possible configuration for this class of Titan exploration vehicle. The major area of new technology required for the Saturn orbiter derives from its requirement for very accurately obtaining Titan's location and using that data to determine in real time the adjustments required to arrive in the "Titan stationkeeping" orbit and to maintain this orbit in the presence of Titan gravity forces.

Orbit Insertion Options

The maneuver strategies employed to transfer a vehicle from a Saturn approach hyperbola to a Saturn orbit, and then possibly to an orbit about Titan can be extremely complex and can involve compromise between conflicting requirements. A key requirement will be to allow for flexibility to respond to observations from repeated flybys in the Saturn orbit before insertion into Titan orbit. Orbit inclination, latitude of periapsis, etc., are all subject to efficient control if Titan swingbys and/or modest velocity maneuvers are employed. The primary disadvantage of these techniques is the time required to properly phase successive encounters.

The major factor affecting selection of orbit size and period is the stability (short term and long term) of Titan orbits of various orientations in such close proximity to Saturn. Analyses of the destabilizing effects require 3-body integrations and are beyond the scope of this study.

III-32

Relay Antenna

Titan Orbiter (ARSO)

Science Platform

Modified Propulsion Module
To Accommodate Titan Payload
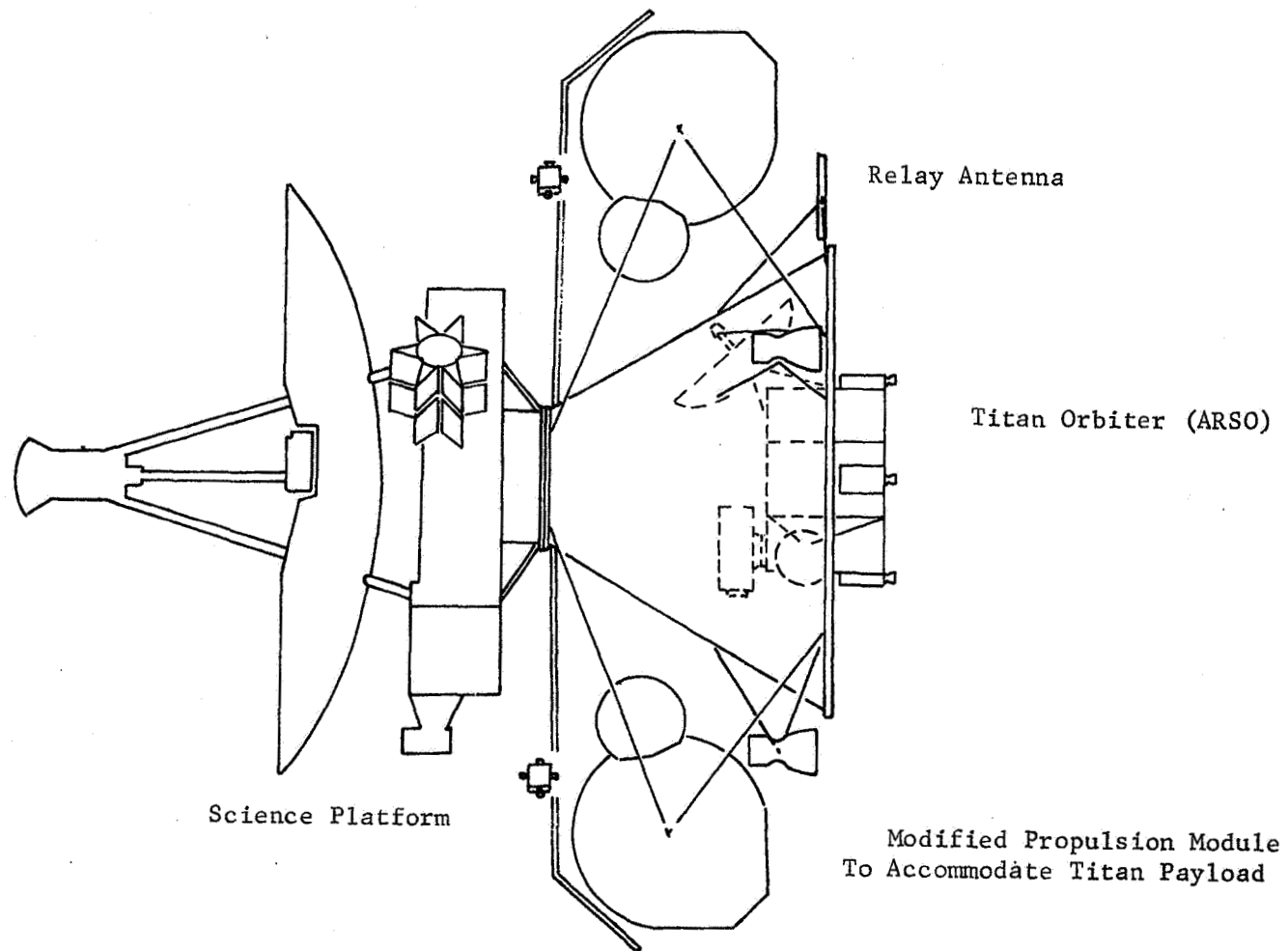
Fig. III-13   Saturn Orbiter and Bus (Based on "Multi-Mission" Modified Pioneer Spacecraft)

Therefore, Titan orbit calculations have been predicated on a representative orbit suggested in Reference III-1. The primary parameters of this presumably stable orbit are periapsis altitude = 1000 Km and period = 12 hours. Orientation options were assumed to be unconstrained prior to orbit insertion.

If initial Titan encounter occurs near periapsis of the Saturn approach hyperbola, direct insertion to Titan orbit could be accomplished which would typically involve a velocity maneuver of over 3 km/sec. Alternatively, Titan orbit can be achieved after Saturn orbit insertion. Reference III-1 relates a typical case for which the spacecraft velocity relative to Titan is 3.2 km/sec after Saturn orbit insertion with Titan gravity-assist. If, after a series of observational flybys, a Titan orbit were desired, a velocity maneuver of about 2 km/sec would be required. In combination with the prior Saturn orbit insertion maneuver, the Titan orbiter vehicle will have undergone over 3 km/sec velocity change. Thus the ΔV requirements for direct Titan orbit insertion and the orbiting of Titan via a Saturn orbit are comparable unless additional use is made of Titan gravity assist.

As pointed out in Reference III-1, these ΔV requirements can be reduced through use of Titan gravity effects and orbit change maneuvers. Controlled Titan swingbys are capable of producing co-planar conditions with two optional Titan encounter locations as shown in Figure III-14a. These encounters are not tangential, and a velocity maneuver at apoapsis to achieve tangential Titan encounter at the modified periapsis will also result in reduction of relative approach velocity. The alternate sequence depicted in Figure III-14b represents another possibility with differing performance characteristics.

T$_1$ and T$_2$: Optional Titan Encounter Positions (Initial Relative Velocity)

T$_3$: Titan Re-encounter After ΔV (Reduced Relative Velocity)

(a) Periapsis Raised to Titan Radius   (b) Apoapsis Lowered to Titan Radius
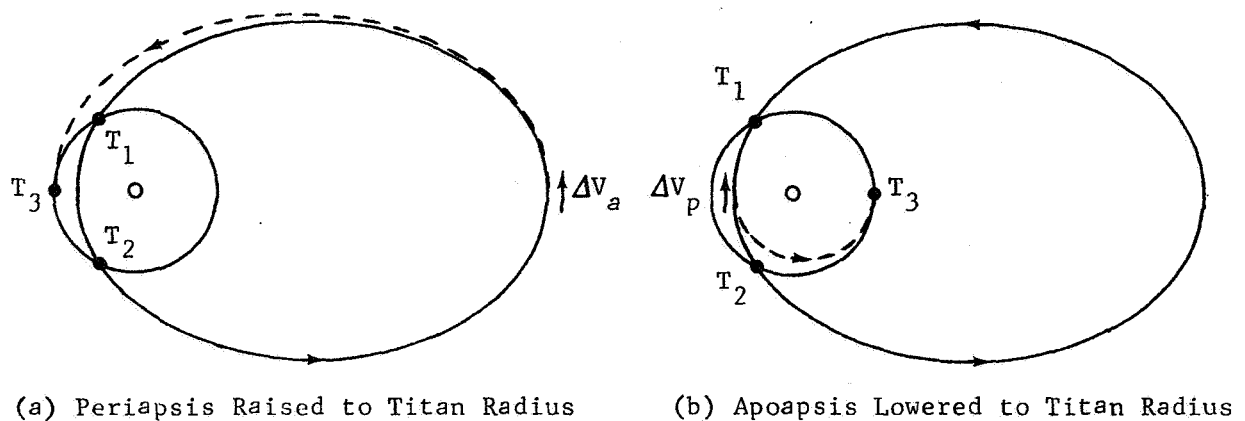
FIGURE III-14 Techniques for Reducing Titan Relative Velocity

Figure III-15 defines the swingby geometry parameters and presents data for the case of relative velocity = 3.2 km/sec and the technique of raising spacecraft orbit periapsis to Titan radius. As shown, the angle β is limited to values less than about 126 deg to avoid re-escaping Saturn. The corresponding periapsis radii are constrained well inside the Titan orbit. In the case of large but finite period orbits, raising periapsis radius to achieve tangential Titan encounter results in Titan approach velocities no greater than about 2.3 km/sec. For smaller β values, relative velocity can be further reduced at the expense of larger apoapsis maneuvers.
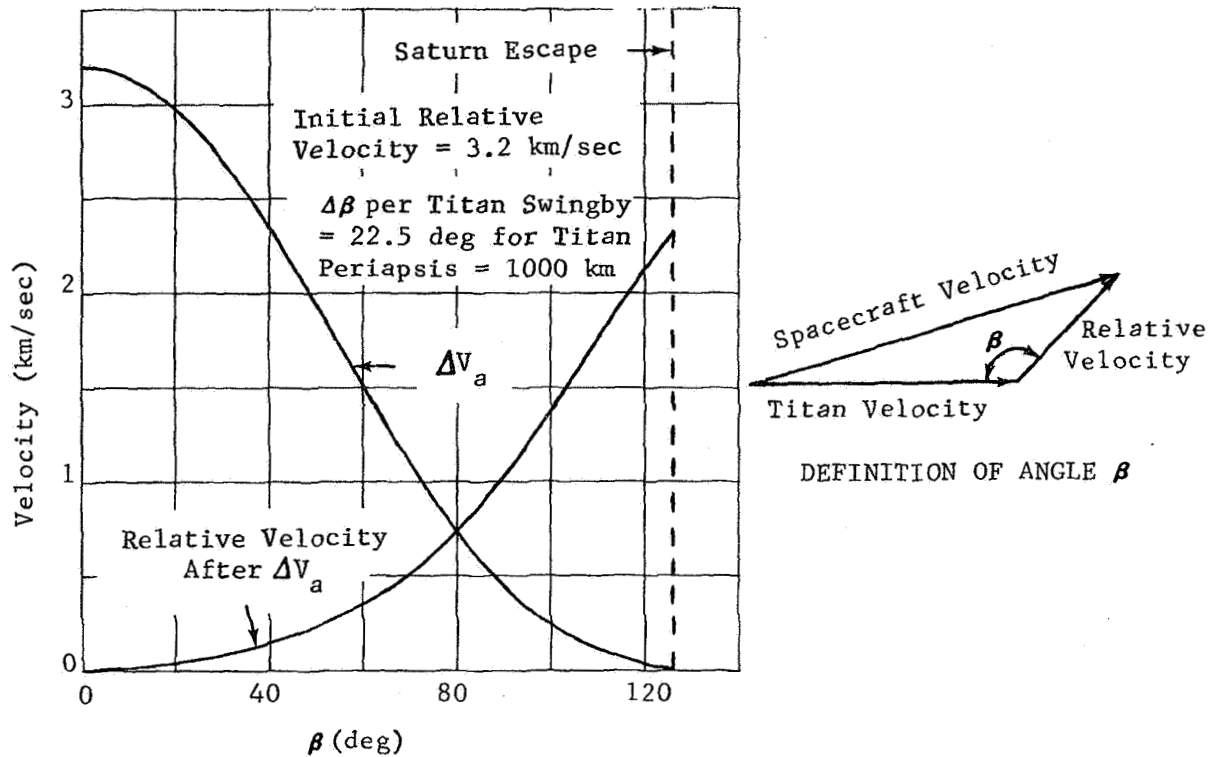
FIGURE III-15 ΔV Requirements for Reducing Titan Relative
Velocity, Periapsis Raised to Titan Radius

This technique can be employed to efficiently lower relative velocity
for purposes of enhancing flyby science observations or improving communi-
cations between a Saturn orbiter and Titan-dedicated vehicles (orbiter
and/or lander). Also, of course, reductions in Titan approach velocity
produce corresponding improvements in Titan orbit insertion requirements.
This latter consideration is presented in Figure III-16. As shown, the
sum of the two velocity increments exhibits a minimum. Interpretation of
these data requires knowledge of the relative masses intended for Titan
orbit and for retention in Saturn orbit. If significant mass is to be
retained in Saturn orbit, best overall performance results from conditions
to the right of the indicated minimum.

III-36
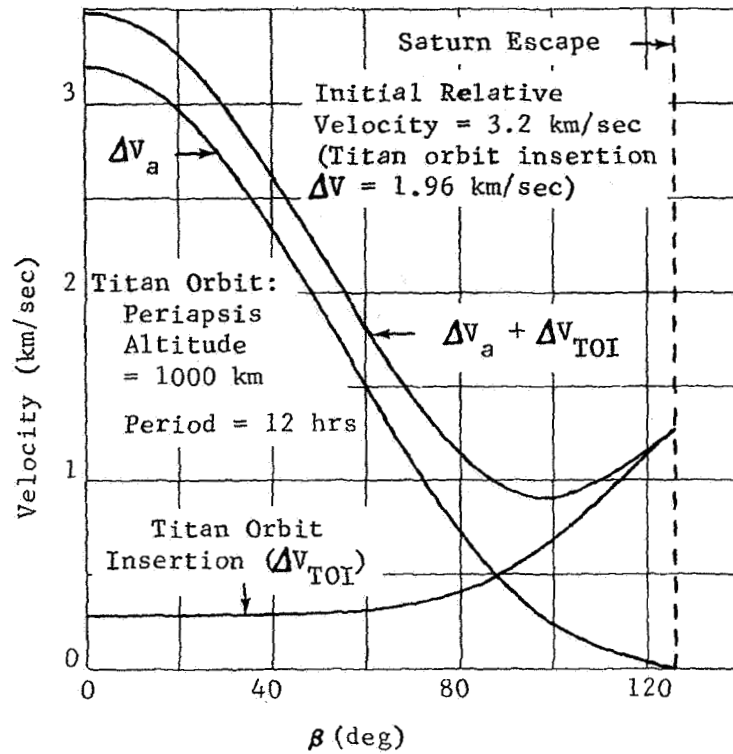
FIGURE III-16 ΔV Requirements for Titan Orbit Insertion,
Periapsis Raised to Titan Radius

Corresponding requirements for the technique of Figure III-14b are

compared in Figure III-17. While a minimum also occurs for this case, the

prior method is clearly superior.
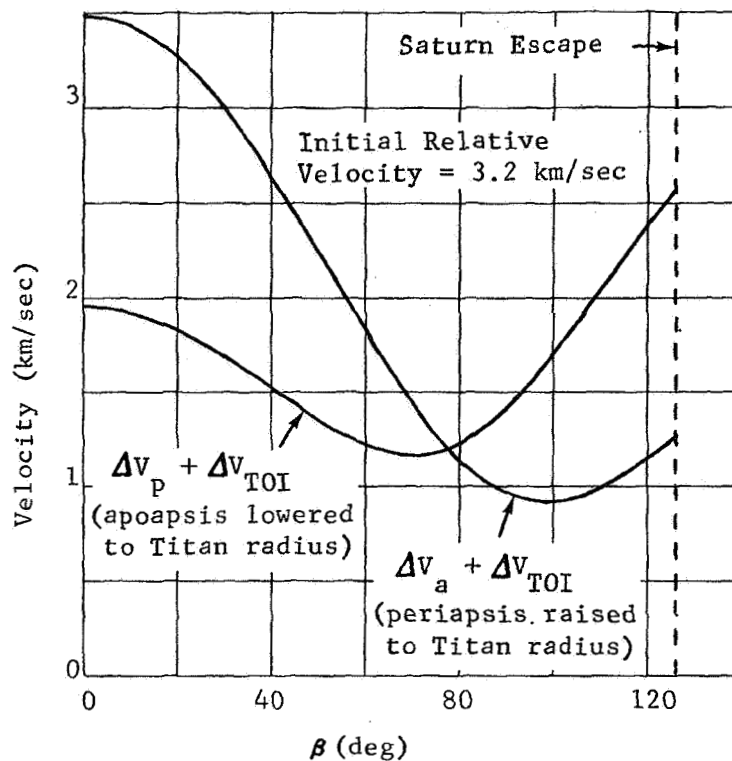
FIGURE III-17 Comparative ΔV Requirements for
Titan Orbit Insertion

The foregoing parametric data were not constrained by considerations
of orbit phasing requirements. To implement the techniques described, it
is necessary to determine the specific values of β which, after the orbit
change maneuver, will actually re-encounter Titan at the desired location.
Since the spacecraft orbit period is not an exact integral of that of Titan,
Titan does not complete an exact integral number of Saturn revolutions
between encounters. These matters are best illustrated with examples.

Reference III-1 relates a specific case corresponding to a post-Titan
swingby period slightly less than 9 times the Titan period ($\beta \sim$ 112 degrees).

Following a posi-grade maneuver at apoapsis of about 85 mps, the relative velocity at Titan re-encounter has been reduced from the initial 3.2 km/sec to about 1.73 km/sec. Net savings on Titan orbit insertion requirements amount to about 1 km/sec.

At Titan re-encounter, another swingby can reduce the spacecraft orbit period to the region of three times that of Titan. Since the resultant deflected orbit intersects that of Titan, options exist to apply a second apoapsis maneuver and further reduce relative velocity (and Titan orbit insertion requirements) at a subsequent tangential encounter with Titan. This process can be repeated indefinitely by using swingbys to produce orbits of appropriate period (near-integral multiples or fractions of the Titan orbit period). However, phasing time penalties are incurred as the price for the performance improvements. Also the benefits of repeated operations diminish rapidly.

A second example more representative of a practical mission is presented in Table III-5. The listed events and values have been iterated to maintain continuity of the sequence.

TABLE III-5   Typical Titan Swingby Sequence

	Titan Encounter		
	1	2	3
Relative Velocity at Titan Encounter (km/Sec)	3.2	1.494	.955
Spacecraft Revs to Next Titan Encounter / Titan Revs to Next Titan Encounter	1- / 4-	1- / 2-	1+ / 1+
Spacecraft Orbit Period After Titan Swingby / Titan Orbit Periods	3.784	1.946	.989
Velocity Maneuver at Apoapsis (km/sec)	.189	.072	.265
Relative Velocity at Next Titan Encounter (km/sec)	1.494	.955	.206
*Titan Orbit Insertion ΔV (km/sec)	.745	.487	.301
**Total ΔV through Titan Orbit Insertion (km/sec)	.934	.748	.827

*Periapsis altitude = 1000 km, period = 12 hours
**For relative velocity at Titan = 3.2 km, Titan Orbit Insertion ΔV = 1.961 km/sec

The sequence summarized in Table III-5 is initiated with a Titan swingby to establish an orbit period somewhat less than 4 times that of Titan. The transfer angle to tangential re-encounter with Titan is about 294 degrees (similar to the geometry depicted on Figure III-14a for departure from Titan position 2). These conditions correspond to a β value of about 103 degrees and are near the optimum indicated on Figure III-16 for a single apoapsis maneuver. Total velocity requirements through Titan orbit insertion, if performed at this time, are improved over the prior example by about 80 mps.

At re-encounter with Titan, the lowered relative velocity (about 1.5 km/sec) can be deflected to target a third Titan encounter after about 320 degrees of transfer angle and a time interval of slightly less than two Titan periods. Following a second apoapsis velocity maneuver, Titan approach velocity has been reduced to less than 1 km/sec. Titan orbit insertion at this time represents an additional savings of about 200 mps over the previous encounter when both apoapsis maneuvers are considered.

Gravity swingby at the third Titan encounter can produce a spacecraft orbit period equal to that of Titan if desired for communication purposes. Alternatively, another set of swingby and apoapsis maneuver operations could be attempted. However, as shown by Table III-5, no further reduction of Titan orbit requirements are attainable with short period phasing orbits.

The foregoing discussions of Titan gravity-assist for Titan orbit insertion are contingent on availability of adequate orbit determination capabilities. In view of the apparent benefits of this and other applications of Titan gravity-assist (Saturn orbit insertion, etc.), appropriate

technology developments are needed. A primary requirement will be on-board systems to permit navigation in terms of Titan relative motion. The same systems could be employed to remove Titan ephemeris uncertainties existing at the time of Saturn arrival.

3. Combined Penetrator and Probe Spacecraft Concept (Penetrobe)

For Atmospheric Entry Probe missions it is desirable to have a subsonic descent time of 30 to 50 minutes. This provides enough time for processing several gas chromatograph samples (the slowest of the several measurements being made) but is sufficiently brief to minimize the power and thermal control subsystem requirements. Unfortunately, for a fixed ballistic coefficient probe designed for a 45 minute descent time in the nominal atmosphere, the actual descent time could be as little as 7 minutes if the Thin model atmosphere is encountered or as much as 80 minutes if the Thick atmosphere model is encountered. (The density at the surface is 4×10^{-5} gm/cm^3 in the Thin model vs. 3×10^{-3} gm/cm^3 in the Thick model atmosphere.)

A similar problem exists with surface penetrator designs since for a fixed ballistic coefficient penetrator, the impact velocity varies from ~100 m/s to over 300 m/s depending on atmosphere model. In order to design the penetrator to achieve satisfactory penetration while avoiding excessive deceleration, it is necessary to control the penetrator impact velocity to be within much smaller tolerances than this 200 m/s.

Another problem with the penetrator concerns the atmospheric entry phase. No really efficient and reliable entry configuration has yet been developed. The extendible cylinder proposed in Ref. III-2 and baselined

for the Trial Mission Titan Penetrator, Appendix B, is relatively complex
and is potentially susceptible to tumbling or coming in end-on. The other
candidate configurations, flaps, inflatible after-bodies and umbrella-
like extendible forebodies have drawbacks as well.

Although it is possible to solve the above problems individually, one
solution is possible that involves combining the two vehicles. This
solution thus also meets the criterion of obtaining many different kinds
of measurements in a single mission. Combining the vehicles during the
entry and part of the descent phase provides a solution to the penetrator
entry configuration problem, permits some dual usage of science and engineering
subsystems, and affords a way of controlling the probe descent time and
penetrator impact velocity.

The concept is as follows: A surface penetrator is mounted initially
inside the probe along the probe center line as shown in Figure III-18.
It remains in the probe during the aeroheating portion of the entry.
The bare penetrator would be designed to achieve the desired surface
impact velocity in the thinnest anticipated density atmosphere. The
combined probe and penetrator would have a ballistic coefficient such that
in the Thick (most dense) atmosphere the descent time would be desired
45 minutes. If the Thick atmosphere is the one encountered (as sensed by
an on-board sensor) the penetrator is retained in the probe until the
probe is a few meters above the surface. At that time the penetrator is
accelerated to the desired impact velocity with a solid rocket motor
located in the base of the penetrator. If a thinner atmosphere, nearer
the Nominal, is encountered, the penetrator is staged out of the probe at
a higher altitude to reduce the probe ballistic coefficient and thus

Parachute for Thin Atmosphere

Nominal Probe Science & Engineering Complement

Pop-Up Antenna

Jettisonable H/S Nose Cap

Snap Out Fins

Note:
Staging occurs by means of differential ballistic coefficient

"Normal" Penetrator Payload

Proximity Fuse
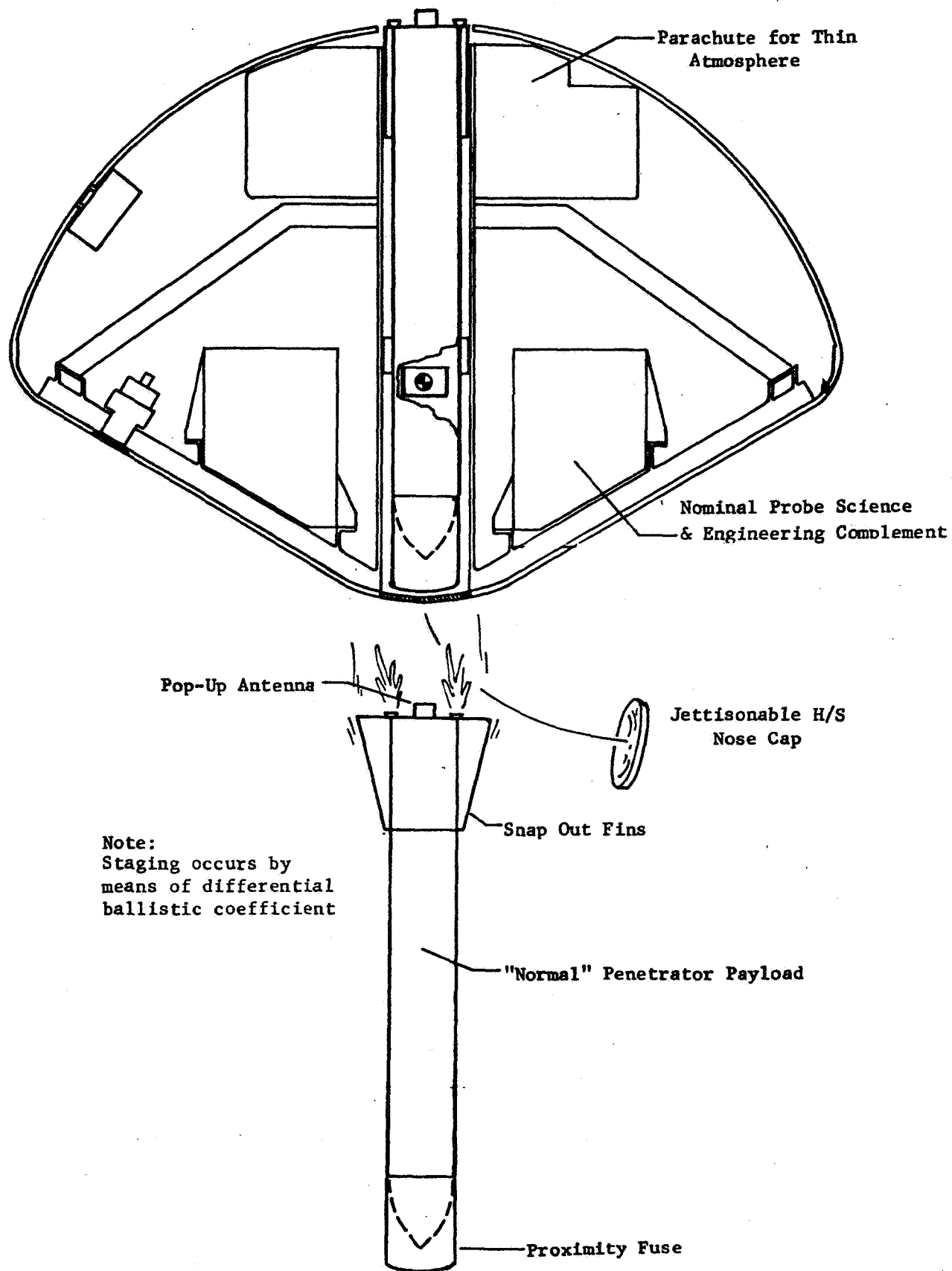
Fig. III-18   Integrated Probe & Penetrator Configuration (Penetrobe)

prevent the probe from descending as rapidly. In this case the penetrator achieves part of its required velocity during free fall and needs to use only a portion of its modularized solid rocket motor. These trajectories are compared in Figures III-19 and III-20.

Finally, if the thinnest model atmosphere is encountered, the penetrator is released at a still higher altitude, just after the entry heating phase is concluded. In this case the penetrator needs no auxiliary energy to attain the desired impact velocity and the rocket motor is not fired. The probe in this case will require a parachute even with its now-reduced mass to avoid falling to the surface faster than the planned science measurements can be taken, but the parachute will be much smaller than that required for the Trial Mission Thin atmosphere probe (4 meters in diameter or less vs 8 meters). This case is also illustrated in Figures III-19 and III-20.

This approach provides fairly accurate control of the penetrator impact velocity, which is crucial to its success, while providing somewhat coarser control of the probe descent time, which is sufficient since the probe requirements are not as severe as the penetrator's. A weight penalty is paid relative to the Trial Mission penetrator in terms of the added mass of the penetrator solid rocket motor, but this is offset by the fact that dual usage is made of probe and penetrator subsystems, e.g., aeroshell, heat shield, antenna, S/C adaptors, accelerometers among others. Also, this approach permits a fairly complex mission to be flown prior to narrowing the uncertainty of the atmosphere models to a small tolerance. Ideally, this concept requires the development of an on-board system for determining in real time what atmospheric density profile has been encountered.

Thin
Model

Entry

(High Altitude
Staging -
Parachute Augemented
Probe Descent)

Nominal
Model

Thick Model

(Low Altitude Staging)

(Free Fall
Penetrator
Descent)

(Free Fall
Probe
Descent)

(Partial Thrust
Augmentation)

(Full Thruster Augmentation)
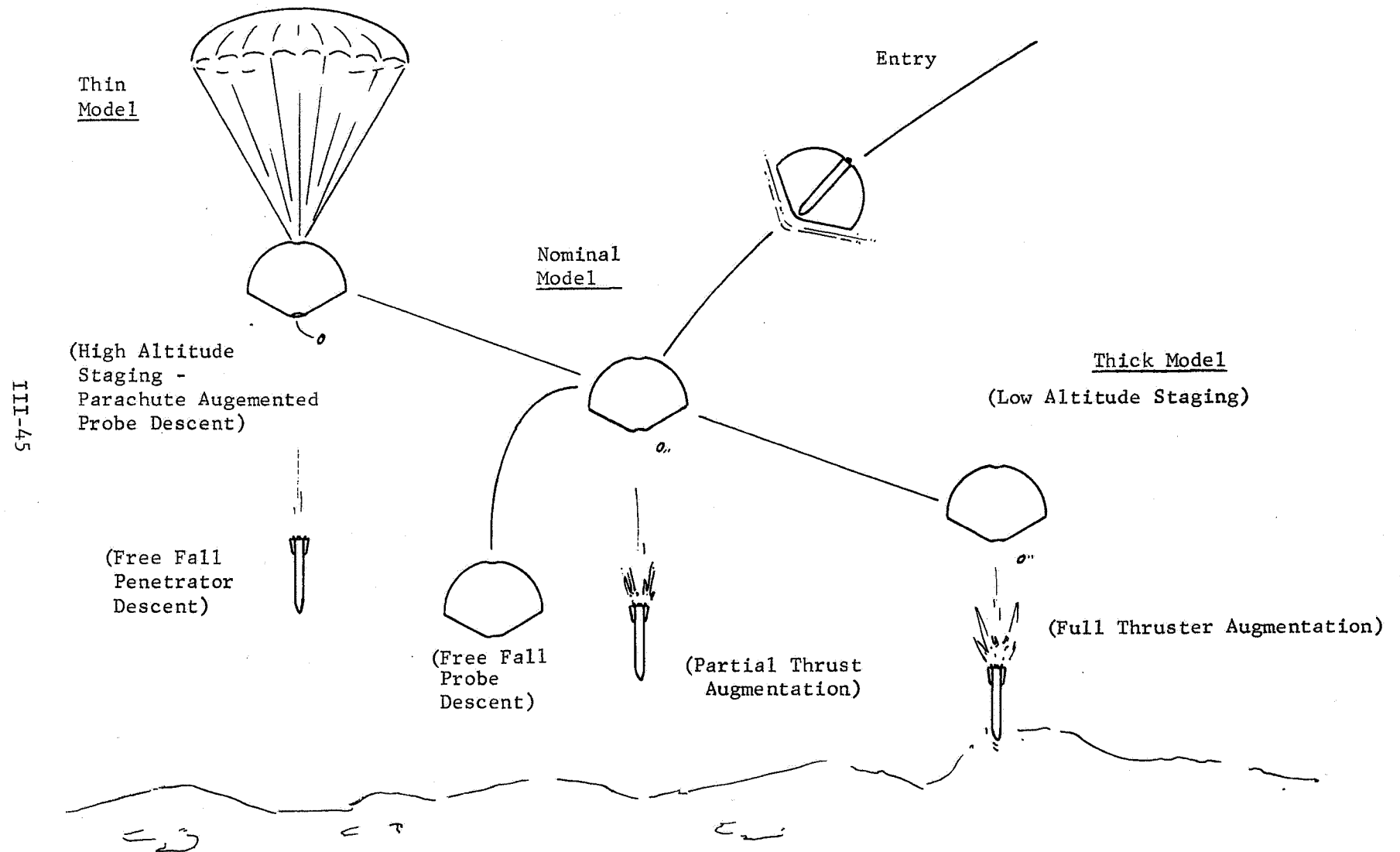
FIGURE III-19   Penetrobe Mission Sequence for Various Atmospheric Models
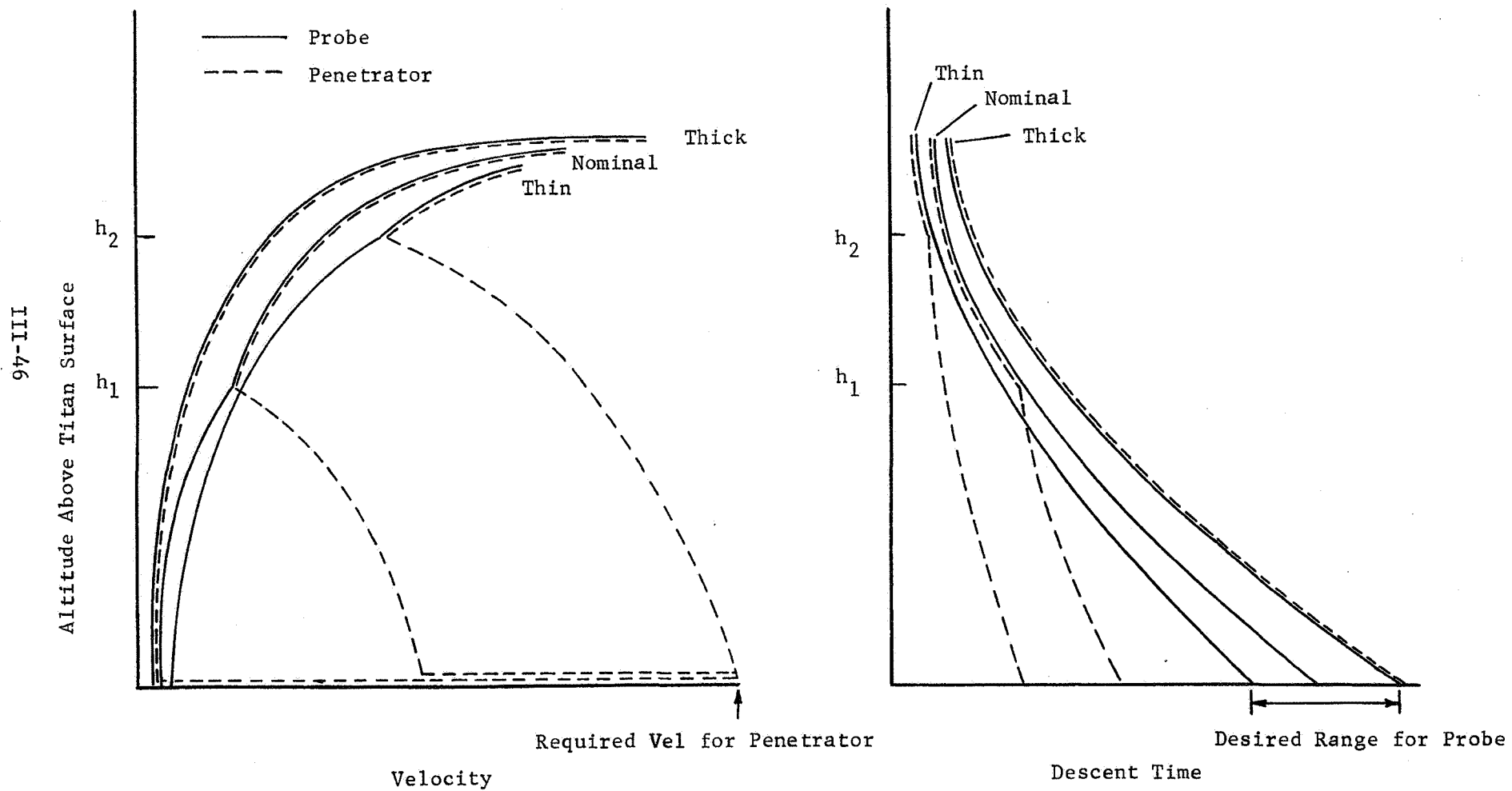
Fig. III-20 Descent Profiles for Probe & Penetrator in Integrated Design Approach

Such a system is discussed in Chapter III-C(Item 17). Even without the

development of a full blown atmosphere-profile-determining-technique, this

concept would be reasonably effective, i.e., it could be based on using

radar altimeter and velocity (Doppler radar) information compared with

precalculated values for given atmosphere models.

C. SUPPORTING TECHNOLOGY CONCEPTS

A number of new concepts have been identified in various technology areas that support the implementation of the three mission modes discussed in the previous section. Many of these ideas will also enhance the more conventional trial mission modes and systems of Appendix B. They range from items that are straight foward extensions of current devices to those representing completely new approaches or techniques. These items together with the new mission modes described earlier, represent many additional exploration options that should be useful in future Titan Mission planning.

The arrangement of this section is intended to allow a quick survey of the various concepts by means of a summary page provided for each topic. Additional information about each concept can be found in the pages that immediately follow the pictorial summary sheets.

The following technology concepts were identified:

1. Remote Surface Composition Using a Laser/Spectrometer Analyzer

PURPOSE

To provide remote determination of surface
material chemical composition

APPLICATION

*Making composition measurements of Planetary
surfaces from a soft lander or a low-
altitude orbiter.*

CONCEPT DESCRIPTION

*Laser emits pulses that vaporize the material
on which they impinge and periodically re-
excite the vapor cloud. Between pulses
the spectrometer obtains the spectral lines
emitted by the vapor.*

ESTIMATED CHARACTERISTICS

   Weight - 5 kg

   Size   - 50 cm x 15 cm dia

DESIRED PERFORMANCE

   Range 1-10 Km (Lander)
           500 - 1000 Km (Orbiter)
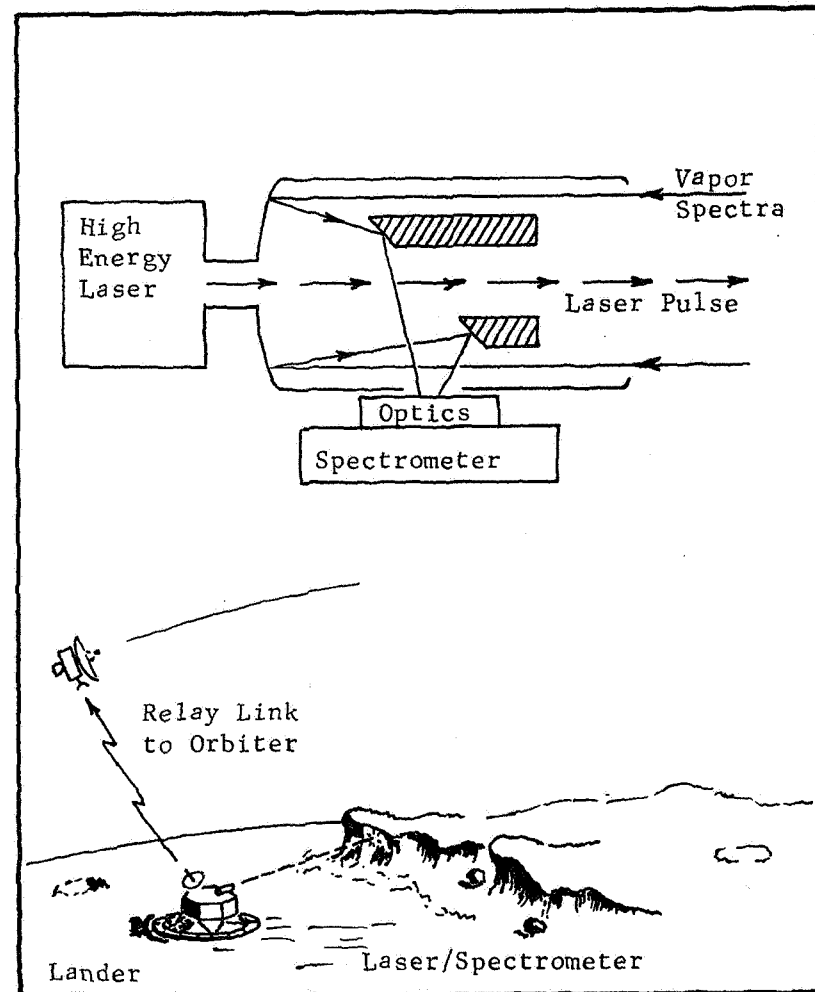
Fig. III-21 Laser/Spectrometer
Analyzer Schematic

Laser/Spectrometer Surface Material Analyzer

If large amounts of power can be made available for short periods of time (seconds) it may be possible to analyze surface materials remotely (meters or kilometers range) by laser vaporization and spectrographic analysis of the line spectra emitted by the vapor. A preliminary instrument layout is shown in Figure III-21. The laser, perhaps utilizing high-energy techniques being evolved by DOD, would emit pulses that would vaporize the surface on which they impinge and periodically re-excite the vapor cloud. Between laser pulses (to avoid the interference of back-scattered laser radiation), the spectrometer would obtain the spectral lines emitted by the vapor. This device could operate from either a lander or, with sufficient power and pointing stability, from an orbiter or flyby spacecraft provided clouds are not present. (Consideration was also given to using a laser beam from orbit to perform remote temperature sounding of Titan's atmosphere in a similar manner as has been proposed for Earth applications, Experiment CO-11 of Reference III-3. However, this experiment in Earth atmosphere depends on the apriori knowledge that the CO_2 and H_2O are uniformly mixed and that each has a pure rotational, infrared, spectra. For Titan the CH_4-molecule has no pure rotational spectrum and attempting to measure the rotational temperature of N_2 would likely result in unacceptable loss in return signal due to Rayleigh Scattering.

While much work on laser vaporization has been accomplished, the surface composition measurement concept proposed here would require an initial feasibility test program to determine if the spectra are available. If successful, these tests would aid in defining a development program for the instrument. Each of the principal parts (laser, optical train, and spectrometer) would require special attention to provide capabilities matched to each other and the characteristics of the supporting spacecraft.

2. Atmosphere Analysis by Artificial Stimulation

PURPOSE

To determine primary atmosphere properties
including composition and density profile.

APPLICATIONS

Global correlation of latitude and time-of-day
variations. Precursor to commitment of penetrators,
entry probes and surface landers.
Deployed prior to Saturn orbit insertion, from
Saturn orbit or from Titan orbit.

CONCEPT DESCRIPTION

Mechanical stimulation of atmosphere gases with
high velocity passive projectile. Constituent
spectra contained in radiation from heated,
ionized wake. Stimulater material selected to
avoid confusing data interpretation. Measured
heat pulse with known entry conditions and
ballistic coefficient of stimulater mass permit
estimates of density profile. Different ballistic
coefficients produce primary effects at different
altitudes. Hollow pressurized sphere transfers
most of kinetic energy to wake in upper atmosphere.
Solid sphere of same mass produces maximum wake
excitation at lower altitudes.

SUPPORT REQUIREMENTS

Wide-spectrum spectrometer and fast-response
radiometer on board spacecraft.
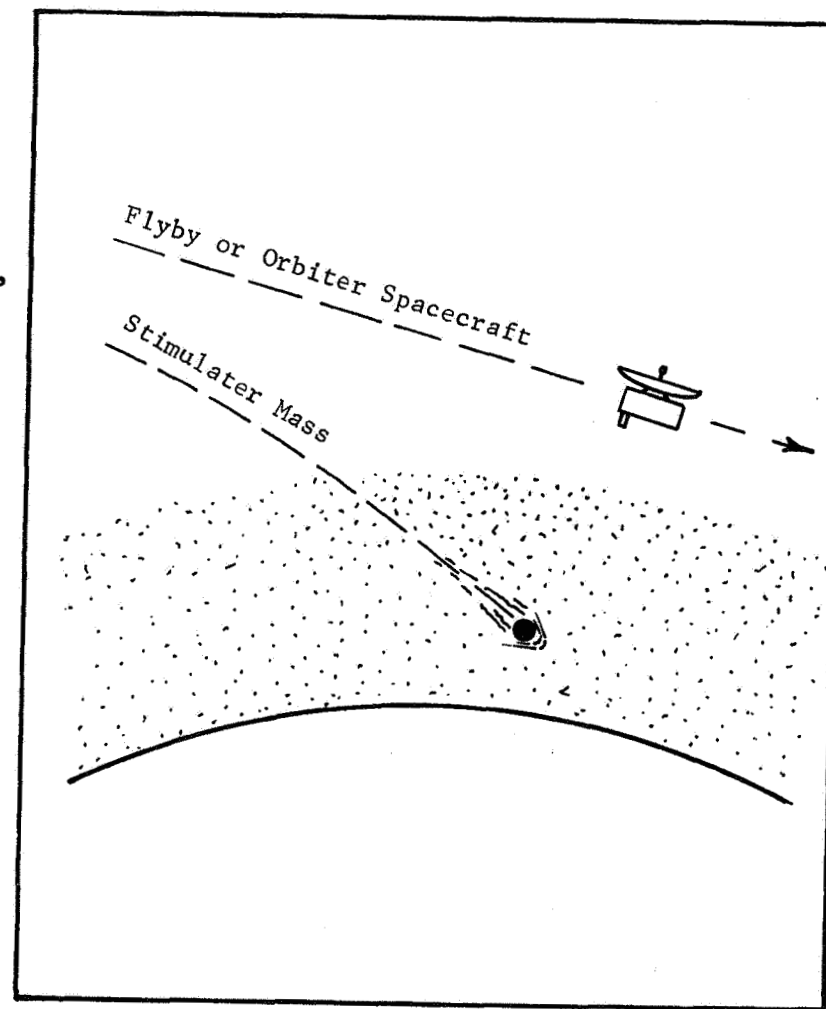
Fig. III-22 Atmosphere Analysis by Artificial
Stimulation

Atmosphere Analysis by Artificial Stimulation

Remote measurement of Titan atmosphere properties by Saturn orbiters or Titan orbiters are facilitated to some extent by stimulation of the atmospheric gasses by natural energy sources such as the Sun. Additional data may be derived from excitation of informative phenomona by artificial means. For example, high-intensity laser beams may evoke measurable responses from some constituents of the atmosphere.

A simpler and more general technique could be based on mechanical stimulation. If a high velocity projectile of known material is targeted to traverse the Titan atmosphere, the heated and ionized wake will radiate characteristic spectra of the atmosphere components. Science value of this experiment is dependent on the level of wake excitation (energy of the incoming projectile and energy transfer mechanisms) and the sensitivity of signal detection instruments. Also, the stimulater material must be properly selected to eliminate confusion in interpreting the data.

High entry velocities for the stimulater mass are desirable to produce high signal to noise ratio data. In this respect, the most efficient time to deploy the stimulater is prior to Saturn orbit insertion (Titan relative velocity 4.5 Km/sec, Titan entry velocity about 5.2 Km/sec). Alternatively, deployment from Saturn orbit in conjunction with repeated Titan flybys would be effective (Titan entry velocity typically 4.1 Km/sec). If the experiment is conducted from Titan orbit, efficient de-orbit of the stimulater would correspond to entry velocity of about 2.3 Km/sec. In this latter case, it may be necessary to apply a large ΔV to the stimulater mass to increase the entry velocity to effective levels.

A spherical shape for the stimulater mass would produce the most uniform and predictable wake effects. Also, this shape is compatible with a totally passive and inert object. With this approach the primary parameters affecting the wake data are the entry angle and the stimulater ballistic coefficient. The first variable determines the magnitude of the peak heating rate for a given ballistic coefficient. The second parameter provides flexibility to emphasize various altitude regions. For instance, a solid sphere of material would not lose significant energy to the upper atmosphere but would yield more data at the lower altitudes. Conversely, a thin-wall hollow sphere (pressurized for shape stability) would be more effective at high altitude.

If it can be established that measurable data can be derived from mechanical stimulation of the Titan atmosphere, the technique could be applied in multiple to determine atmospheric variations for a variety of locations (equator to poles) and different local times (noon to midnight). Another potential use would be as precursors to deployment of vehicles dependent on adequate knowledge of the atmosphere (probes, landers, etc.).

Feasibility of the artificial stimulation technique will probably depend on additional development of sensor technology; especially wide-spectrum spectrometers. In addition, a means of skin-tracking the stimulater (e.g., radar) would be valuable if the deceleration history could be determined. Alternatively, accurate measurement of the rate of energy transferral to the wake would reduce uncertainties in the Titan atmosphere properties.

NOTE: The stimulater principle is under study at MMC for surface investigations of bodies with little or no atmosphere.

3. Atmosphere Sampling from Orbit

PURPOSE

To acquire multiple samples of atmosphere constituents (including complex molecules) in condition for subsequent chemical analysis.

APPLICATIONS

Determine upper atmosphere variations with latitude and time-of-day. Search for organic and pre-organic molecules.

CONCEPT DESCRIPTION

For shallow penetration of atmosphere, apply ΔV at apoapsis to control periapsis altitude. For deeper penetration of atmosphere, use ΔV and/or aerodynamic lift to convert impacting trajectory to safe exit trajectory. Collector cups pre-chilled by prolonged isolation from heat sources while radiating to deep space. Atmosphere gases condensed or frozen on contact and particulate matter entrapped. Moved to closed space for heating and/or washing specimen from collector cup prepatory to chemical analysis. Multiple collector cups with each limited to a single usage.

SUPPORT REQUIREMENTS

On-board navigation for prompt orbit determination after passage through atmosphere.
Chemical analysis laboratory on-board Titan orbiter.
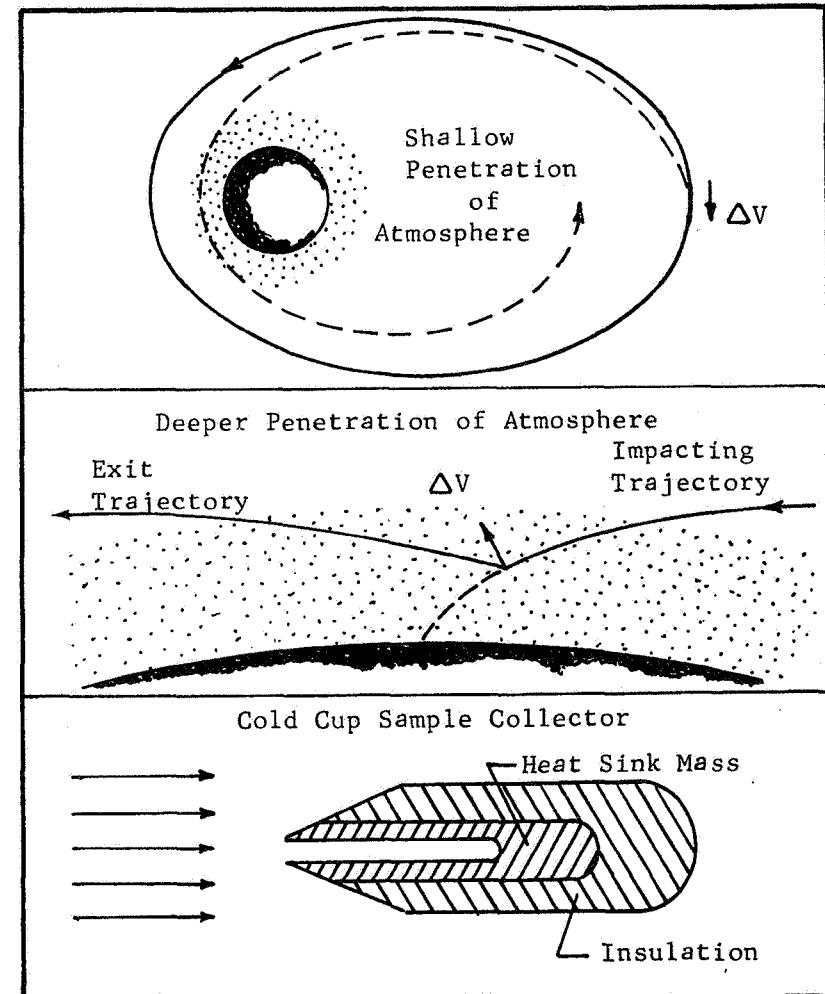
Fig. III-23   Atmosphere Sampling From Orbit

Atmosphere Sampling from Orbit

The best methods of obtaining Titan atmosphere data involve use of specially designed atmospheric probes and surface lander vehicles incorporating comparable instrumentation. In these cases, the entire depth of the atmosphere can be sampled for a limited number of specific descent profiles. Other options for in-situ measurements include post-landing launch of balloon-borne instruments for the lower and intermediate altitudes and repetitive flythrough of the upper atmosphere with a Titan-orbiting spacecraft.

Lowering periapsis of a Titan orbit to skim the Titan atmosphere results in energy loss to aerodynamic drag but the trajectory can be controlled to avoid surface impact. In the case of unpowered flythrough, orbit apoapsis will be lowered and a velocity maneuver will be required at or near apoapsis to control altitude of the next pass-through periapsis. Repeated flythrough of the upper atmosphere will eventually produce a near circular orbit for a modest total velocity budget depending on the depth of penetration into the atmosphere. By these means, atmosphere constituents can be sampled at various high altitudes and for a variety of conditions (phase in the diurnal cycle, etc.).

For deeper penetration into the atmosphere, drag will be sufficient to produce aerodynamic capture and subsequent surface impact. In this case, a velocity maneuver will be required while in the atmosphere to limit the minimum altitude and accelerate the spacecraft to a safe exit trajectory. Magnitude of the maneuver will depend on depth of penetration and a following apoapsis maneuver will be required to control the next periapsis pass.

Providing the orbiter spacecraft with aerodynamic lift characteristics (e.g., carbon cloth Rogallo wing), could significantly defer or reduce propulsion requirements for atmosphere exit. However, total performance gains would probably not result unless the increased mass of a lifting configuration could be partially justified by advantages for other applications such as large orbit plane change maneuvers.

To fully exploit the opportunities for atmosphere analysis from Titan orbit, new technologies will be required. In particular, sample collection techniques compatible with preservation of complex molecules (organic or pre-organic) would be valuable for Titan exploration. The same capabilities may be desirable for delayed analysis of atmosphere constituents (including particulates) collected during descent of entry probes and surface landers.

A method of obtaining undamaged atmosphere specimens at high relative velocity could be based on extreme pre-chilling of the collector device. For example, prolonged shading from heat sources while permitting radiation to deep space could lower temperature to a few degrees Kelvin if adequate insulation from the carrier spacecraft is provided. Such a cold collector may be capable of condensing or freezing gas samples on contact with coincident entrappment of any particulate matter present.

Collector efficiency would be enhanced by high heat capacity and high conductivity to absorb and distribute the heat of impact. Contact surface may be increased by such means as fins or baffles. For subsequent retrieval of the specimen for chemical analysis, heating and/or washing of the collector cup would be conducted in a closed container. In view of the long chilldown time required, an individual cup would probably be limited to a single use. Multiple sample acquisitions would imply a large number of collector units properly isolated until needed.

4. Adaptively Controlled Science Measurements

Adaptively Controlled Science Measurements

PURPOSE

To make on-board decisions about which data are interesting and should be transmitted to Earth and which are redundant.

APPLICATION

Titan landers, penetrators and orbiters that may be recording data during periods when no Earth communications link exists.

CONCEPT DESCRIPTION

Science instruments and data management systems controlled by on-board executive controller and decision-making logic. Permissable decisions controlled from Earth as mission progresses.

ESTIMATED CHARACTERISTICS

Computer Volume - 125 cc

Wt - 0.5 Kg

Power - 0.5 W

SUPPORT REQUIREMENTS

Access to science instruments, housekeeping sensors, telecommunications sytem and command system.

Detect Unusual Light Levels for a Given Time of Day

Detect Changes in Cloud Patterns

Imager "Learns" Where Horizon Is

Coarsely Sampled Image

Detailed Image

Detect Changes in:
Temperature
Seismic Activity
Bio Sample Gas Evolution
XRFS Composition Spectrum

Detect Changes in Surface Brightness for a Given Time of Day and Light Level
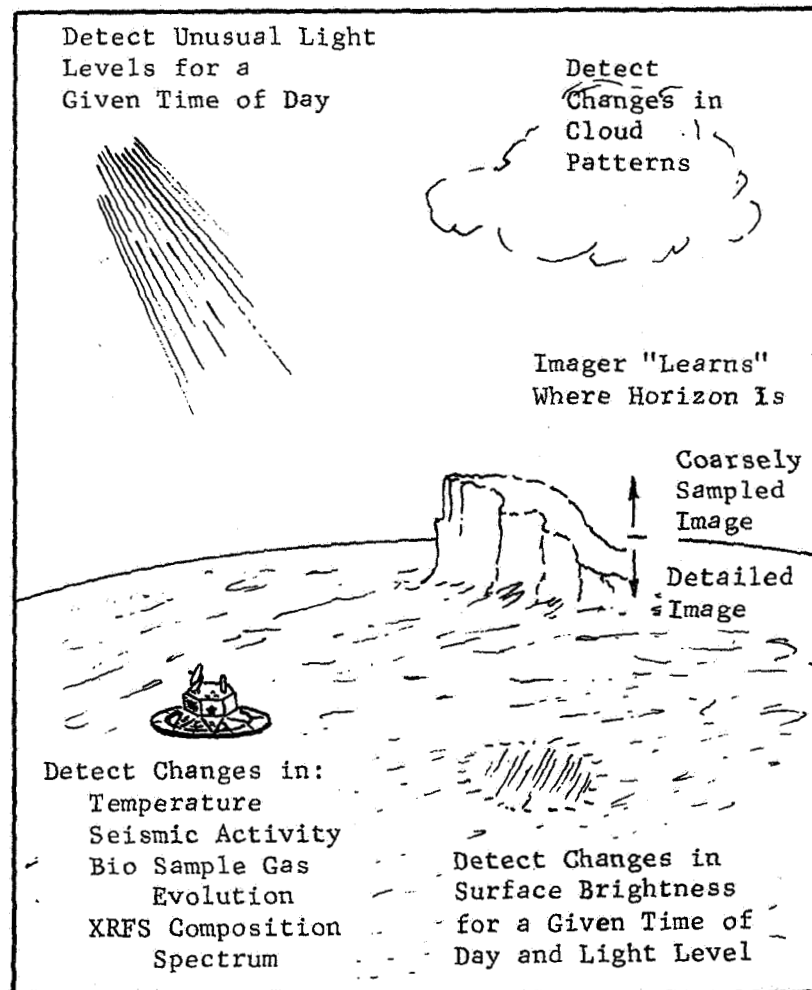
Fig. III-24   Typical Adaptive Science Decisions

Adaptively Controlled Science Measurements

Introduction

Titan exploration, due to its timing (1985-1990+) and communication delays (hours) offers an excellent opportunity to exploit advanced controls technology that will or could become available in the intervening years. Both adaptive and autonomous (artificially intelligent) control concepts are discussed in the following material. Specific applications and the corresponding control developments required are identified.

The goals of advanced controls utilization are two-fold. First, these controls should enhance the probability of successfully completing a mission. Examples of this are controlling orbit insertion, deorbit, entry, descent, and landing at bodies such as Titan where significant uncertainties exist (ephemeris, atmosphere, surface) and communication delays preclude real-time control from Earth. In some cases, these mission operations will be impossible without advanced controls technology.

The second goal is to enhance the scientific return of missions by controlling instruments and processing data from them. Instrument utilization and useful data returned can thereby be increased.

Advanced Controls Categories

The two types of advanced controls under consideration here, adaptive and autonomous, are separated by the complexity and capability of the control hardware and software. It is very difficult to draw a definite line between the two that can be agreed upon by those working in the field. It is easier to describe rudimentary adaptive and "far-out" autonomous examples and see the difference.

A simple adaptive system receives sensed data, processes it, and adjusts the spacecraft's operations according to a preprogrammed set of rules. As an example, consider a lander with delicate camera optics on a planet with an atmosphere and a dusty surface. The adaptive controls monitor the wind velocity and when it reaches a preset level, the controls would retract and shield the optics from potential dust damage, even if the mission controllers had commanded an imaging sequence at that time.

This same lander, equipped with an autonomous, artificial intelligence (AI) control system, would behave quite differently. First, it would use its cameras as a scientist uses his eyes, scanning the surroundings continuously and observing and recording temporal changes. After sending documentary images of the scene around the lander to Earth, the lander would reduce its imaging data transmissions to those images containing unusual phenomena. The AI controls, having an understanding of atmospheric dynamics and their interactions with surface materials and features, would decide by itself what constitutes an unusual phenomenon. An approaching dust storm would be observed. If unusual, the AI controls would record the storm's appearance for later transmission to Earth. If the storm reaches the lander, it will "shut its eyes" until the storm passes. During the storm's passage over the lander, the AI controls might elect to record meteorological data and collect and analyze airborne particulate matter.

The important differences between these two control concepts are that only the autonomous, or AI, system 1) studies and learns about its environment; 2) builds a model of that environment in its memory; 3) identifies new phenomena or features; 4) directs its attention to these and makes observations with appropriate instruments, and 5) records and relays pertinent data to Earth, all without intervention by Earth-based controllers. In its most ambitious embodiment, the AI control system makes decisions like a skilled scientist/technician, well-versed in all disciplines related to the mission including routine spacecraft operations (e.g., thermal control, power management, etc.). While this level of AI control will not be available for several years, significant research efforts are underway worldwide and at least interim results will be available in some form in time for inclusion in Titan exploration missions. The greatest challenge lies in understanding and building hardware and software that duplicate human vision capabilities including collection, assimulation, recall, and imagination of imaging data.

Scientists' Roles in Mission Incorporating Advanced Control Technology

While discussing adaptive science operations with members of the science community, we found that a typical initial reaction is skepticism regarding the ability of a computer to make scientific decisions. Generally, scientists are concerned that by attempting to make a smart system, we may get one that makes bad decisions and ends up with less good data than would have been obtained with a preprogrammed set of actions. We have evolved an adaptive control concept that is more readily understood and accepted by the scientist/user because it does not put scientific judgment into the on-board computer. Rather, the concept gives the scientists a tool that enables them to automate simple decisions so that they can be made on the spacecraft and appropriate commands will be executed with much less delay. This will produce a larger quantity of higher quality scientific results. A first principle therefore, is to put the adaptive system as directly as possible under the control of the scientific teams and to make the adaptive programming readily modifiable.

A second principle that should be followed on any mission of long enough duration is to start with a minimum of autonomy and increase it as confidence is gained. For a Titan lander, typical action on the first day or two after landing will include exercising systems to verify their condition. During this phase, few decisions will be made on Titan. As confidence increases, more decisions will be made by the on-board controller. The fixed schedule of actions and measurements will be replaced by a flexible one based on priorities, these being calculated using preprogrammed algorithms established and tested on Earth. The priorities will be influenced by real-time observations so that recording of transients and unusual phenomena can defer or replace less valuable activities.

If the system is designed with flexibility, great advances in adaptability can be made in a single mission, but if it is attempted to foresee exactly how the system should react, a long series of missions will be required for the same progress.

Figure III-25 shows the interface between the on-board hardware and software for typical adaptive science operations in a Titan exploration mission. A status array which is accessible by both the landed or orbital hardware and by the various computer subroutines forms a major part of the interface. The status array contains numeric values which have one or more of the following functions: 1) constants; 2) input parameters used by operating routines to control associated hardware; 3) outputs of the lander hardware used in decisions of the executive controller; and 4) values indicating the status of various engineering subsystems.

An equally important portion of the hardware/software interface is the equation cache which holds the equations by which the executive controller determines the priorities (How important is it to do the particular action?) and the feasibilities (Is the particular action safe to do at this time?) for any decision.

Interface with the human ground controllers and scientists is provided through the ground commands by which both the status array and the equation cache can be changed.
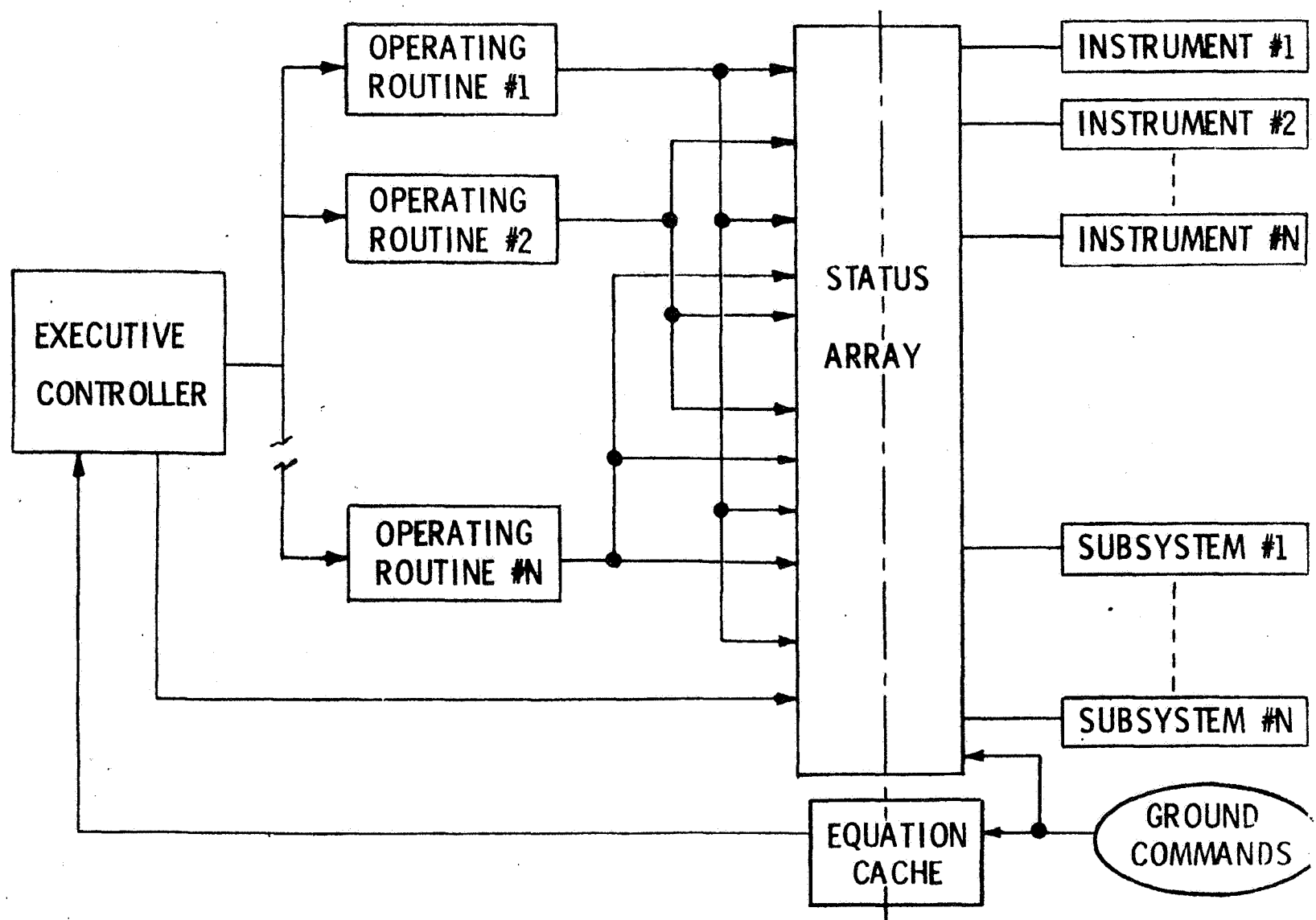
Fig. III-25   Hardware/Software Interface for Adaptive Science Decisions

5. Fixed ΔV Solid Rocket Landing System

PURPOSE

To provide a lander with a fixed-impulse
solid rocket deceleration system that can
adapt to large variations in descent velocity.

APPLICATION

Can be used with a soft lander or penetrator.

CONCEPT DESCRIPTION

By use of a radar altimeter to obtain altitude
and descent rate, an altitude can be calcu-
lated to fire a ΔV that will place the
lander on a predetermined vacuum-free-fall
curve for a large spread of initial terminal
descent velocities. The ΔV is sized for the
worst case "Thin" atmosphere. For the slow
descent cases (Thick atmosphere) the excess
ΔV energy temporarily increases altitude
(negative velocity) but impact velocity
remains constant. Atmospheric drag tends to
further slow the vehicles relative to the
vacuum free-fall curve.
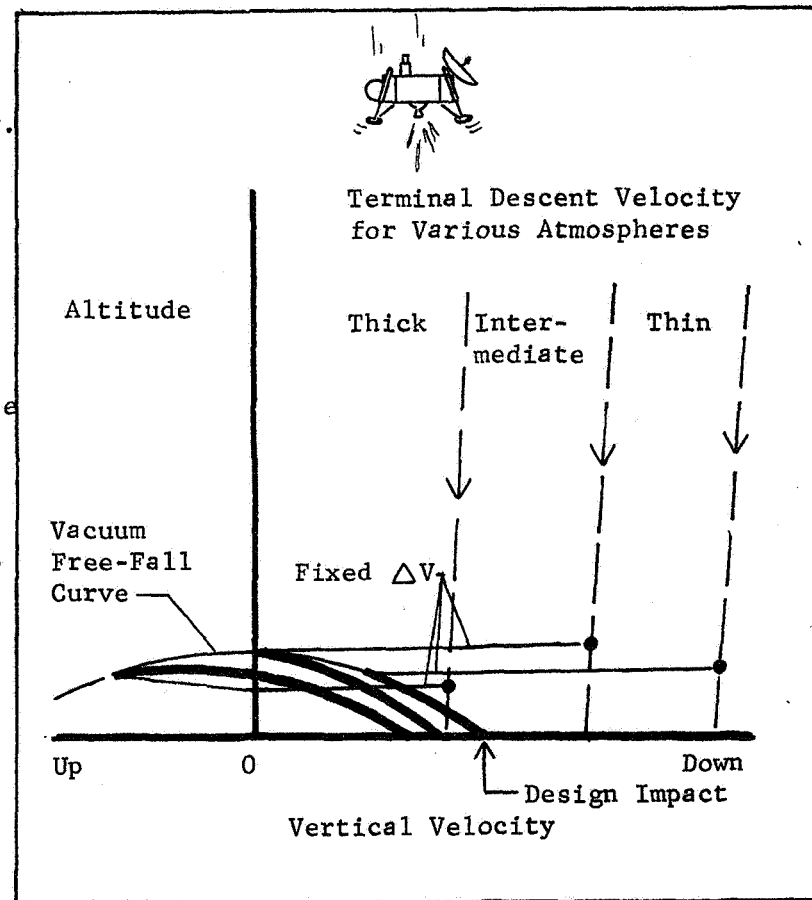
Fig. III-26   Fixed ΔV Landing System

Fixed ΔV Solid Rocket Landing System

A fixed ΔV solid rocket landing system has been proposed to replace the conventional liquid-thrust control and shutdown system. The solid rocket system was originally conceived for landing on airless bodies such as Mercury; however, it appears that it can be applied to Titan with only minor modifications to the control logic.

The concept is most easily explained for an airless body. The effects of an atmosphere such at Titan's are then discussed. The basic technique uses a fixed ΔV impulse for all descent velocities (better control can be obtained with two fixed ΔV impulses). The magnitude of the ΔV is set by the maximum descent velocity anticipated. For cases where the descent velocity is lower, the excess ΔV energy is dissipated through gravity losses. In some cases, the altitude is temporarily increased (negative velocity). Figure III-27 illustrates the altitude (H) and vertical velocity (V_Z) space that the lander has entered for an airless Titan. The family of curves moving down to the right are lines followed by a lander falling freely to the surface under the influence of a gravitational field without an atmosphere. For example, a lander that arrived at any point A, B or C at, say, the end of a major retro burn would follow this free-fall line and impact at about 100 m/s.

Figure III-28 illustrates the case where the lander descends from a large uncertainty space and approaches the altitude/velocity line X-Y-Z. The lander must have the capability of measuring altitude and descent velocity (Doppler radar) and when it reaches any point on line X-Y-Z it fires a fixed ΔV of 88 m/s (in this illustrative case).

This ΔV places the lander on the free-fall line which will result in an impact velocity of 35 m/s for all cases. The 88 m/s was sized to accommodate the worst case (X) and the surplus ΔV for less demanding cases (e.g,, Y and Z) was consumed in gravity losses.

Larger spreads in uncertainties or reduced final impact velocity can be easily accommodated using two separate solid motors. Each ΔV burn reduces the uncertainties and places the lander on a predetermined descent and impact path using only range (altitude) and range rate information. Figure III-29 depicts the effects of atmospheric drag on this descent technique. The initial uncertainty is now represented by terminal descent velocity trajectories which are shown for thick, intermediate, and thin

atmospheres (the nominal atmosphere is very close to the thick model near the surface). Also, these terminal descent velocities are nearly constant as shown for the last 4 to 5 km above the surface. Again the vehicle must measure altitude and descent velocity and when its computer calculates that it has reached line X-Y-Z it fires a predetermined ΔV. This impulse is sized to accommodate the highest velocity case, X. Case Y is omitted for clarity. This first impulse places the vehicle on a predetermined vacuum free-fall trajectory (appropriately chosen to account for drag effects). As the vehicle begins to fall along this trajectory, atmospheric drag will slow it to varying degrees depending on the atmospheric density as illustrated by the heavy lines. The thin atmosphere case will more closely follow the vacuum free-fall lines and a second fixed ΔV may be required as shown to bring the vehicle down to the design impact velocity. The intermediate cases will also require this second ΔV; however, the on-board computer may choose not to use this if it estimates an impact velocity equal to or less than the design value as in case Z for the thick atmosphere in this illustration.

In summary, by the use of a radar altimeter to provide altitude and descent velocity and by developing a microprocessor computer program to calculate estimated trajectory and drag parameters, it is possible to limit impact velocity to any specified design value with the use of two fixed impulse solid rocket motors over a broad range of atmospheric uncertainties.
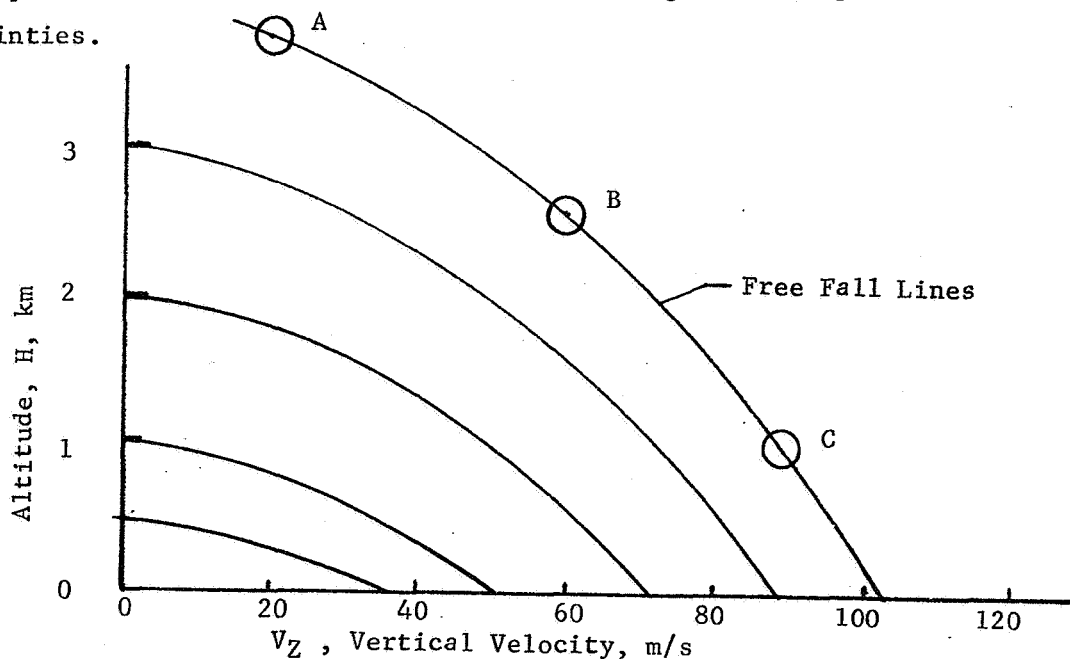
Fig. III-27 Free-Fall Profiles (Altitude vs Descent Velocity) for an Airless Titan

III-65

Altitude, H, km

Initial Uncertainty
Space

Free Fall Lines

88 m/s ΔV

Z   Y   X

V_Z, Vertical Velocity, m/s

Fig. III-28 35 m/s Impact Velocity Obtained Using a Single 88m/s ΔV

Terminal Descent Velocity for
Various Atmosphere Models

Altitude, H, km

Thick   Intermediate   Thin

Vacuum Free-Fall
Trajectories

Fixed ΔV

Y   X

Z

ΔV

Up   0   Design Impact Velocity   Down

V_Z, Vertical Velocity, m/s
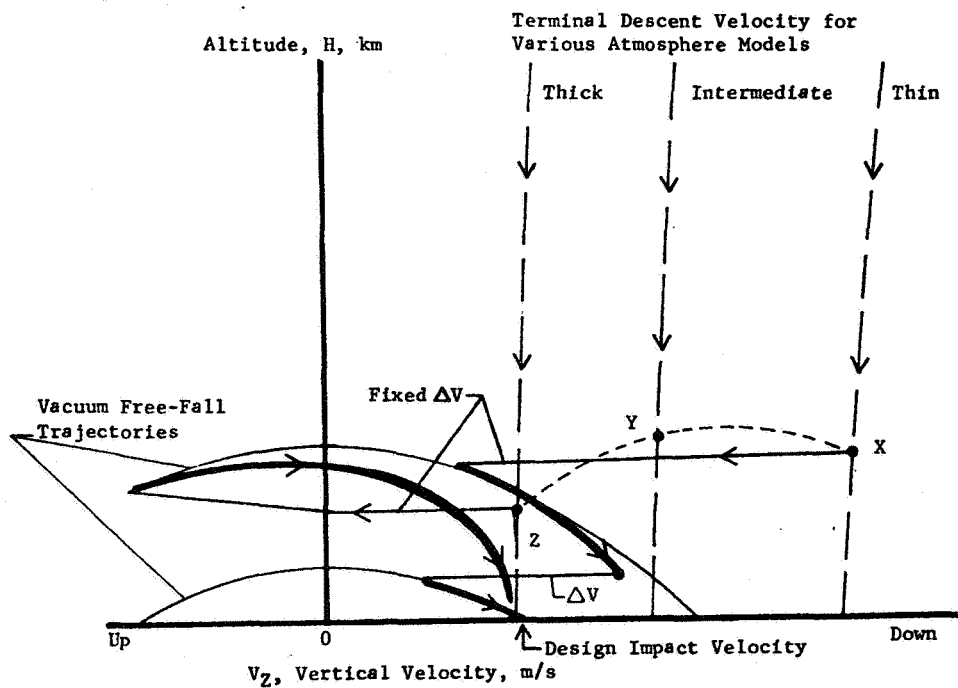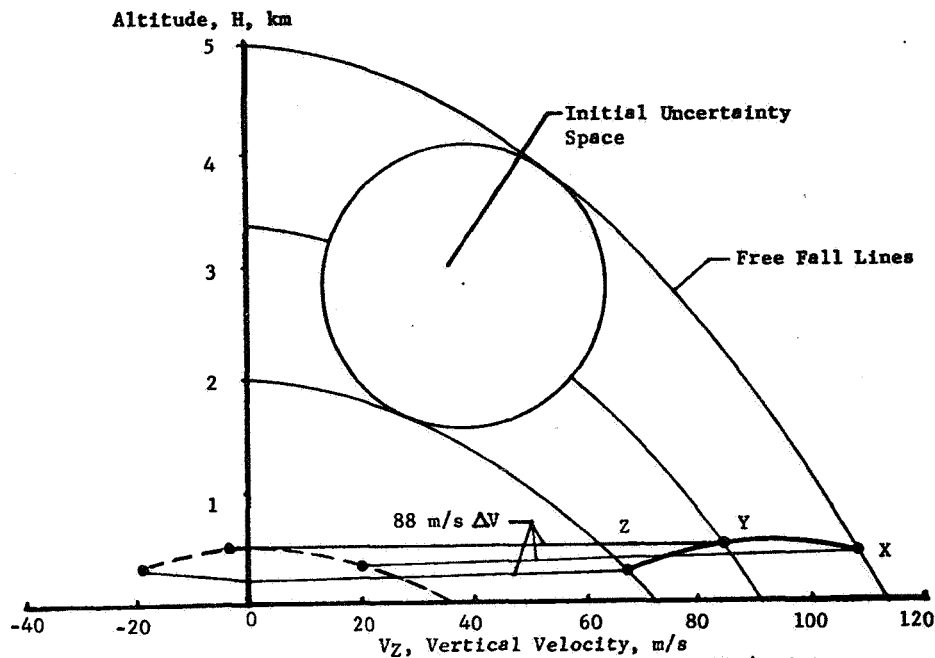
Fig. III-29 Atmospheric Drag Effects on Terminal Descent Concept

III-66

6. Tractor Braking for Surface Landers

PURPOSE

Provide terminal propulsive deceleration for soft landers

APPLICATIONS

Bodies with thin atmospheres
Bodies without atmospheres

CONCEPT DESCRIPTION

Soviet technique reportedly employs solid rocket mounted at yoke of final stage parachute. Canted nozzles and blast shield protect lander from exhaust impingement. Jettison of rocket motor terminates lander deceleration and removes debris from landing site.

Alternate technique supports tractor rocket and stabilizing fins on rigid tower. Options for multi-purpose use of tower structure include mounting of systems benefitted by post-landing elevation (e.g. TV communication antenna) and systems incompatible with permanent internal installation (e.g. RTG)

SUPPORT REQUIREMENTS

Communication Relay
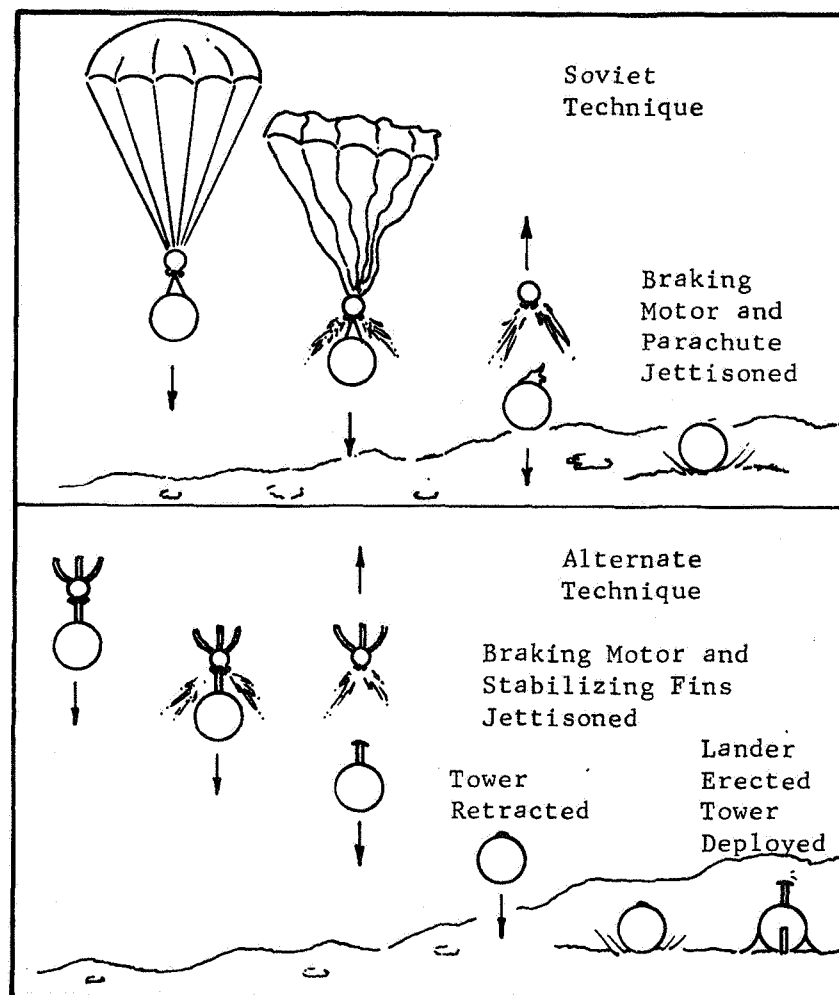
Fig. III-30 Tractor Braking for Surface Landers

For the nominal and thick models of the Titan atmosphere, landers would probably not require a terminal phase of braking propulsion. However, in the case of the thin model atmosphere, parachutes alone will probably be inadequate.

Conventional unmanned landing systems (e.g., Surveyor and Viking) involve complex liquid propulsion systems and sophisticated guidance sensors and control logic. In the case of the performance-limited Titan lander mission, it would be advantageous if simpler systems could be employed while retaining adaptive features to accommodate uncertainties in the atmosphere.

Use of a solid rocket for final propulsion would represent a simple propulsion option compatible with the environment and the long mission time. However, thrust termination and thrust vector control are not readily designed into a small solid rocket. As an alternative, the lander can be configured to employ a solid motor in the tractor propulsion mode; i.e., aft-firing but forward-mounted. In this case, thrust can be effectively terminated by jettisoning the motor when deceleration requirements are satisfied. Rocket nozzles must be canted outward and a blast shield provided to protect the lander from exhaust impingement.

The Soviets reportedly used a version of this technique in conjunction with parachutes for their Mars lander vehicles. A solid rocket was suspended above the lander at the parachute yoke and oriented to aft-firing attitude by the parachute and gravity. The motor was ignited at a pre-determined altitude and released just prior to touchdown to remove the unwanted debris from the landing site.

A variation of the technique could be based on mounting the solid motor on an extensible forward tower. In this case, a simple drag brake could provide vehicle orientation to the descent trajectory and to the Titan surface. When the motor is jettisoned to terminate deceleration, residual propellant must be sufficient to deflect the motor case and the drag brake assembly away from the lander. The motor mount structure could remain with the lander to serve post-landing functions. Temporary retraction of the tower would permit rollover after landing if consistent systems are provided for subsequent recovery and erection.

The tower structure could be integrated with the lander design to serve a variety of purposes after landing. Some of the potential uses of such a movable tower are listed below.

1. Lander systems requiring or benefiting from elevation above the surface (TV, antenna, etc.) could be mounted in the tower. To protect critical elements of such systems from rocket exhaust, a blast shield would be required. In addition, to avoid contamination by the exhaust plume, a jettisonable protective fairing may be necessary.

2. The RTG could be tower-mounted to reduce neutron interference with science instruments. Also, if the tower position is controllable from fully extended to fully retracted, the RTG heat output could be employed as an active thermal control device for the entire lander.

The tractor braking lander configuration is compatible with use on bodies without atmosphere by providing an attitude reference and reaction control system. Such an application is currently under consideration for Mercury as part of a MMC contract with JPL (Ref III-8).

7. Dual Penetrator Concept

PURPOSE

To provide a method of measuring heat flow by placing two penetrators close together at different depths.

APPLICATION

Penetrators can enter the Titan atmosphere directly or be staged from a lander or probe vehicle.

CONCEPT DESCRIPTION

Two conventional penetrators are coupled so that they will impact close together. Upon impact the coupling is destroyed and one penetrator, with a soil drag brake, is retarded more than the other. The penetrators come to rest at different depths and can therefore measure temperature differences with depth.

ESTIMATED CHARACTERISTICS

Conventional penetrator, mass $\cong$ 30 kg each of two. Or a specialized design at about 15 kg each of two.

PERFORMANCE

1 to 15 meter depth

SUPPORT REQUIREMENTS

Requires orbiter to relay data

Dual Penetrators Coupled Together

Soil Drag Brake

Higher Terradynamic Ballistic Coefficient Provides Greater Depth of Penetration
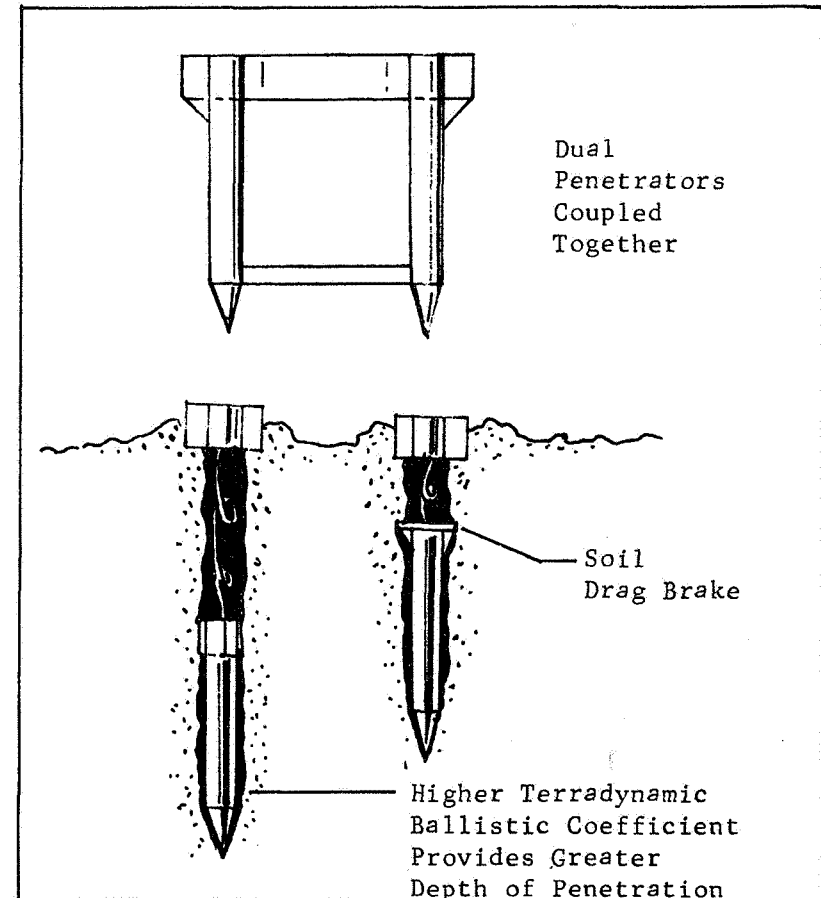
Fig. III-31   Dual Penetrator Configuration

Dual Penetrator Concept

Dual Penetrators - Since a penetrator comes to rest at a significant depth below the surface, it is in a unique position to measure the planetary heat flow. This measurement is important to the understanding of the core and structure of the planet. However, it appears very difficult to obtain an accurate measurement of heat flow because the penetrator internal heat sources and the RTG when used produce temperature gradients of the same order of magnitude or greater than those that are being measured.

Therefore, the dual penetrator concept is suggested as a possible solution to the heat flow measurement problem. Two conventional penetrators are linked together with about a one meter separation distance. The rigid linkage is aerodynamically configured to provide longitudinal stability during descent to impact. At impact the linkage between the penetrators is sheared off and each continues into the ground independently. One penetrator is provided with a terradynamic drag ring which retards its depth to something less than the other will reach.

Although each penetrator still affects the local thermal environment, the effects are very similar around each one. And, since they are at different depths, the difference in temperature is an accurate measurement of the variation of the thermal environment as a function of depth.

The importance of the heat flow measurement may warrant a dual penetrator system designed only for this experiment. If that were the case, then smaller and lighter penetrators compared to the conventional Mars design could be used. The dual penetrators could be optimized for the heat flow experiment in terms of structure, maximum deceleration, overall size and weight reduction, and reduced power requirements. A much greater range of impact velocity uncertainties might be accommodated for a specialized design.

Other solutions to making accurate measurements of the heat flow were considered. In the conventional single penetrator, not only do the on-board electronic equipment and RTG affect the thermal environment,

but also the cavity or hole above the penetrator tends to modify the environment by means of conduction and convection in the atmospheric gases. Figure III-32 shows a technique wherein temperature sensors are projected horizontally into the soil a distance sufficient to reduce the thermal effects from the main penetrator body. A trailing wire is necessary to transmit the temperature signal back to the main penetrator.

A variation of this technique, consists of a pair of drills which are substituted for the projectiles. A telescoping drill shaft would provide directional stability and the shaft could be retracted after placing the thermal sensor at the extreme position away from the main body. Again, two sensors are required to provide a difference in temperature with depth.
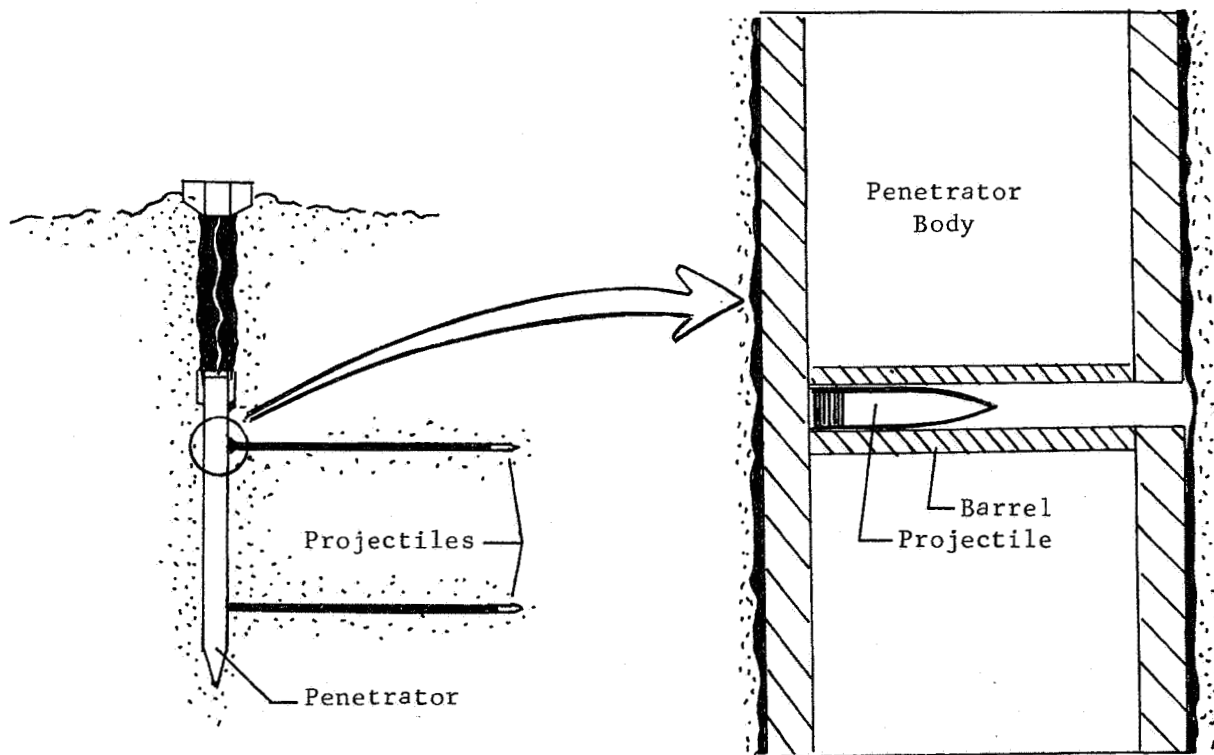
Fig. III-32 Temperature Sensor Projectiles

8. High Peak Power Source Using Titan Atmospheric Methane

PURPOSE

To provide high peak power source for short duration.

APPLICATION

High peak power could operate surface drills, sample heating, laser power, rapid data return, sonar power (if liquid surface), mobility systems, etc.

CONCEPT DESCRIPTION

Atmospheric methane is burned with an oxidizer (i.e., O_2) and the combustion gases drive a turbine powered generator.

ESTIMATED CHARACTERISTICS

    Size: 20 cm x 20 cm x 30 cm

    Weight: 20 Kg

PERFORMANCE

    Output - 12 KW
    Oxidizer Flow Rate - 0.6 Kg/min.
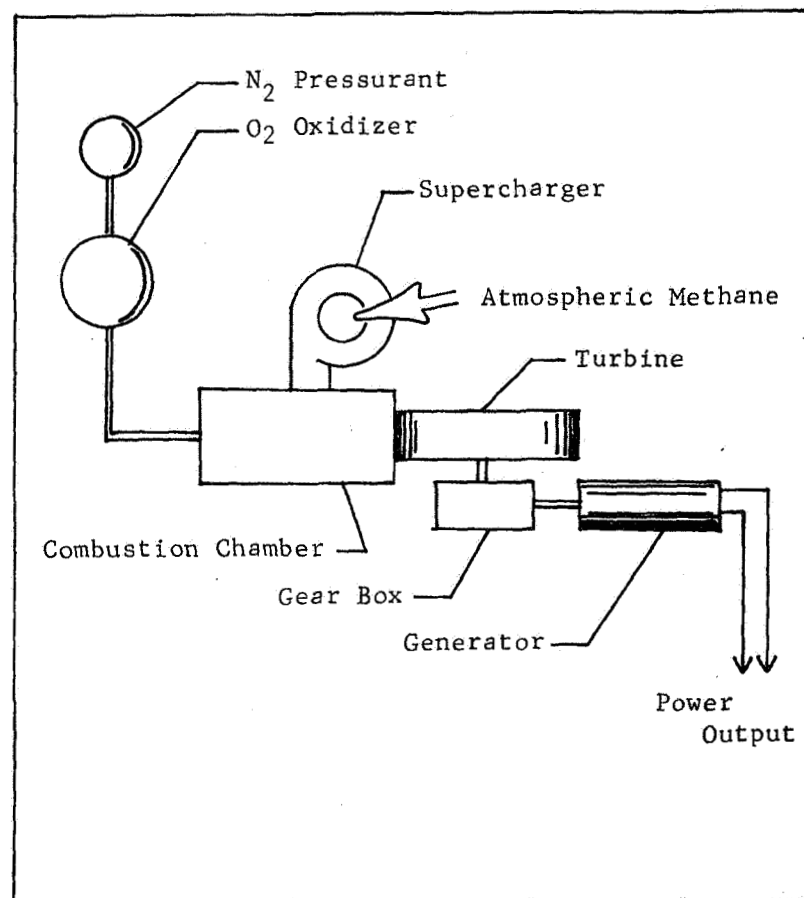
Fig. III-33   Methane Powered Turbine for High Peak Power

High Peak Power Operations

In considering various engineering and scientific technologies which would enhance the Titan mission, the requirement for high peak power was identified. Although some of the functions can be done at lower powers over larger time spans, many of the operations can best be accomplished in a short period at high peak power. These possible applications for high peak power are:

Deep Drilling Operations on Surface for the purpose of:

    Core Sample Acquisition

    Heat Flow Experiment Installation

    Implantation of Explosive Sources for Active Seismic Experiment

Sample Processing Operations

    Heating

    Crushing

Laser Power Supply

    Vaporization of Distant Objects for Spectral Analysis

    Long Distance Illumination

    Atmosphere Occultation (Using Orbiter)

    Laser Communications

Very Rapid Data Return

    Kilobit/Sec Imaging System

    Data Return to Preclude Loss if Lander is Shortlived

Sonar Power Supply (if Liquid Surface)

Mobility System Peak Loads

Various power sources were briefly considered, and the choice of the optimum device would be dependent on the specific application. Candidates include high performance batteries, thermal batteries, and auxiliary power units. Thermal batteries use a molten eutectic salt and are usually applied to very short time applications from seconds to a few minutes. This brief analysis was primarily concerned with the auxiliary power unit which appears to meet the requirements of the above list.

Titan provides a unique opportunity for use of its atmospheric methane as a fuel supply for a power unit and the lander is only required to carry the oxidizer. The auxiliary power unit is based on the aircraft type device and it consists of a turbine driven by hot gases from either an atmosphere methane/oxidizer propellant or a hydrazine-water monopropellant that is decomposed through a catalyst.

The gear box output shaft can be used to drive either an electrical generator or a hydraulic pump depending on the application. For energy/ performance comparison only, the Isp of methane/oxygen is 263 sec and of hydrazine monopropellant is 208 sec. However, the oxygen/methane system may require some additional hardware such as a small turbo-supercharger to control intake of atmospheric methane.

The weight per power output of these devices is about 3.5 lbs/kw or 1.6 kg/kw excluding the propellant system.

9. "Hot Atmosphere" Balloon

PURPOSE

To provide data on atmospheric circulation and atmosphere and cloud composition.

APPLICATION

Can be released from lander or deployed directly from entry.

CONCEPT DESCRIPTION

Balloon can be inflated with either hot atmospheric methane with N_2O_4 oxidizer or with helium Balloon is tracked to obtain circulation data and carries science instruments.

ESTIMATED CHARACTERISTICS

Payload Weight   - 7 Kg

N_2O_4 Weight   - 9 Kg

Floated Weight   - 29 Kg

Balloon Diameter   - 9.7 m

Balloon Volume   482 m^3

PERFORMANCE (NOMINAL ATM)

Flight time with N_2O_4 2.5 Hours

Design Altitude   -42 Km

SUPPORT REQUIREMENTS

Tracked from either Lander or Orbiter

Balloon

Atmospheric Methane

Burner

N_2O_4 Tank

Science and Engineering Payload
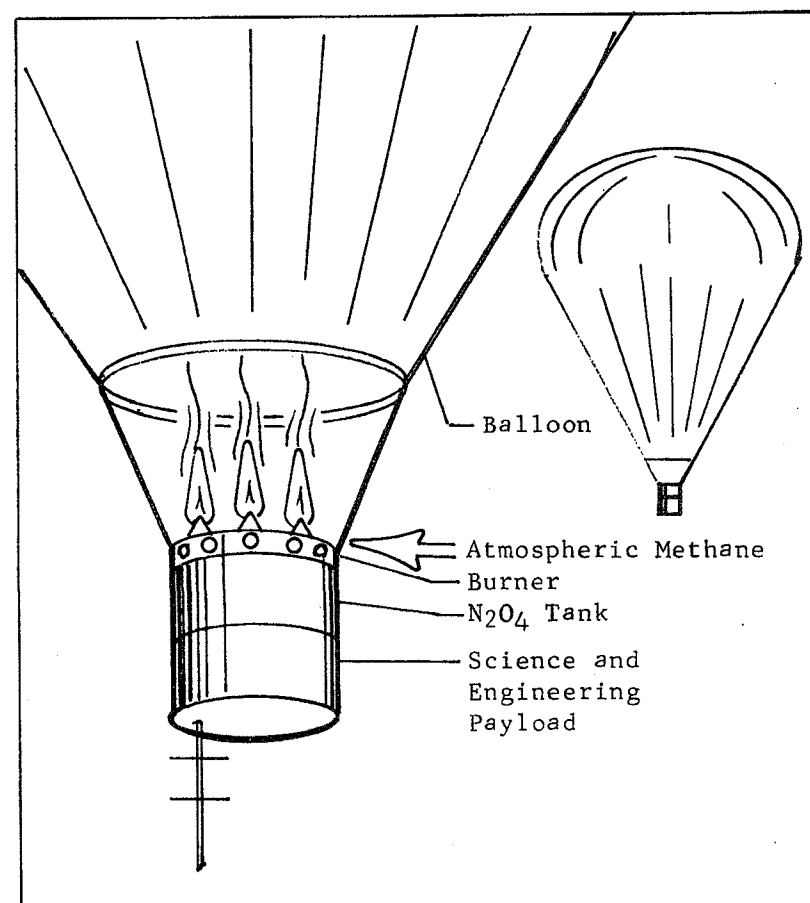
Fig. III-34   "Hot Atmosphere" Balloon Concept

10. Tethered Balloon for Elevated Science Platform

PURPOSE

To provide an elevated platform for imaging cameras so that images can be obtained beyond local obstacles and stereo images can be obtained in various altitudes.

APPLICATION

Can be used with a soft or hard lander

CONCEPT DESCRIPTION

The small balloon is inflated with helium and is released to rise on a tether to various desired altitudes. Tether provides power from the lander and data from the imaging camera.

ESTIMATED CHARACTERISTICS

Camera mass, 6.0 Kg, Balloon Diameter, 2.2 m Balloon and Helium mass, 3.1 Kg

PERFORMANCE

Variable altitude, indefinite duration

SUPPORT REQUIREMENTS

Lander relays data to orbiter, provides power.
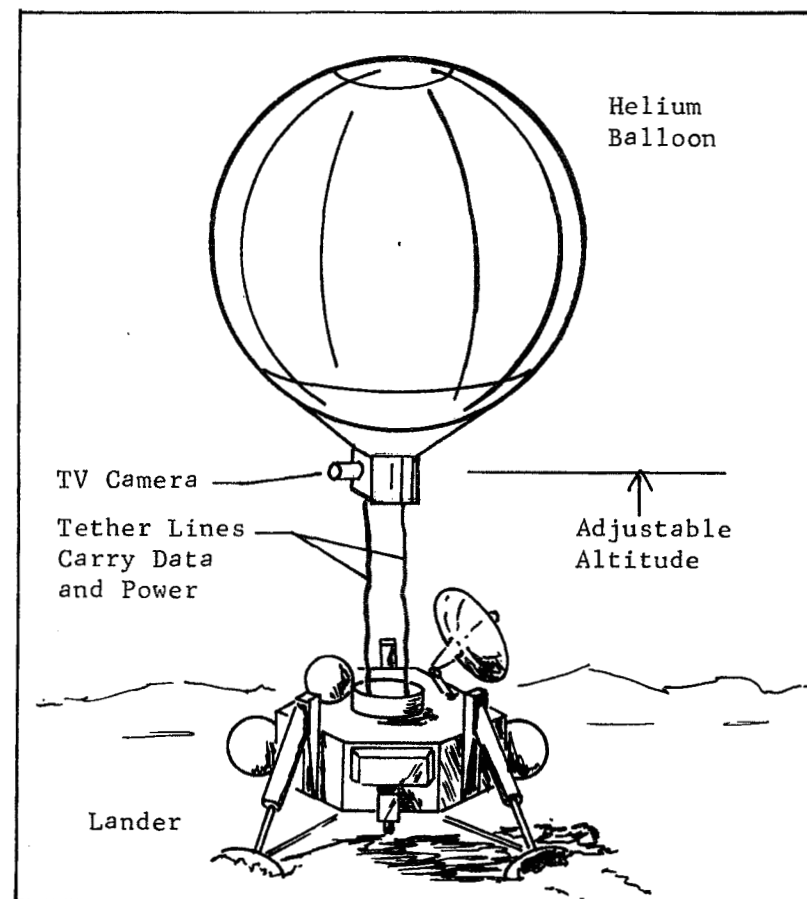
Fig. III-35 Tethered Balloon Elevated Science Platform

11. "Thin" Model Atmosphere Helium Balloon

PURPOSE

To provide more detailed measurements of composition in the clouds and Thin atmosphere where a lander may have descended too rapidly for sufficient measurements.

APPLICATION

Released from lander to obtain vertical profile atmospheric data.

CONCEPT DESCRIPTION

Balloon is inflated with helium or hydrogen gas and relays its data to the lander.

ESTIMATED CHARACTERISTICS

  Payload Weight   - 7 Kg

  Floated Weight   - 27 Kg

  Balloon Diameter - 14.8 m

PERFORMANCE

  Flight Time - 1 hour ascent

  Design Altitude - 25 Km

  Ambient Pressure - 8.2 mb ("Thin" model atm.)

SUPPORT REQUIREMENTS

Relays-data to either lander or orbiter.

Zero Pressure
Helium Balloon

Balloon

Volume   1700 m^3
Diameter   14.8 m

To Lander
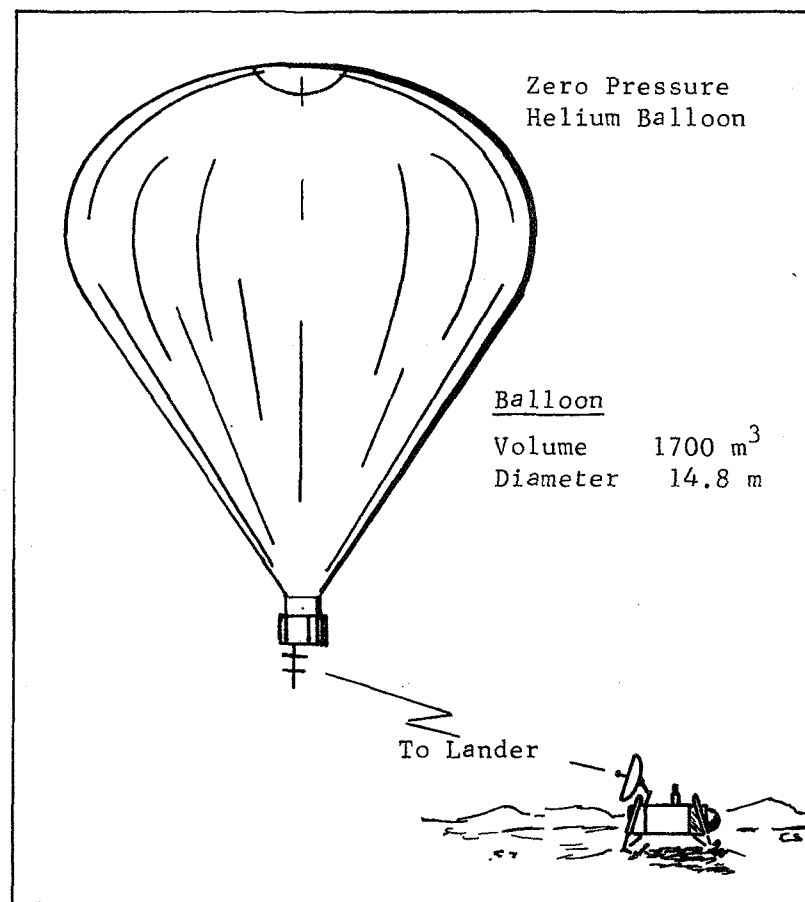
Fig. III-36 Helium Balloon Sonde

Balloon System Applications to Titan Missions

Balloon systems are useful in obtaining atmospheric data and providing long duration platforms for particular experiments. A unique aspect of balloon applications at Titan is the possible use of the atmospheric methane as a fuel for a "hot atmosphere" balloon. In this case, only the oxidizer needs to be carried along in the form of N_2O_4 or liquid oxygen. Also, a monopropellant could be used.

If the "thin" atmosphere model is a strong possibility during the system design phase, then a very lightweight balloon would be useful in providing a detailed vertical profile since a lander would descend through this atmosphere at a very high rate. These balloon applications are discussed in more detail below:

1) A vertical profile balloon carrying a gas chromatograph to obtain more detailed composition measurements through the clouds and lower atmosphere. This might be especially valuable in the "Thin" model atmosphere in which a lander might descend too rapidly to allow sufficient time for measurements.

2) A balloon with pressure, temperature, altimeter, and a transceiver for tracking to obtain data on atmospheric circulation. This design could use either helium gas or burn the atmospheric methane with N_2O_4 to provide a "hot atmosphere" balloon.

3) A tethered balloon could provide an elevated platform for an imaging experiment.

The vertical profile balloon, for the "thin" atmosphere, can be designed as a zero pressure type balloon for the lightest possible weight. This allows a very thin film and scrim balloon material since the pressure inside the balloon is essentially equal to the atmospheric ambient pressure. However, a zero pressure balloon is not very stable and will descend if it encounters a reduced temperature (crossing the terminator to the dark side) or an upward gust which will vent some of the helium.

Figure III-37 presents a summary of characteristics for this balloon design. The science and engineering payload weighs 6.9 kg including battery power for a one-hour ascent and level flight. This provides ample time to make numerous gas chromatograph readings through the lower atmsophere to an altitude of 25 km. Because of the extremely low pressure and density of the "thin" atmosphere, it is difficult to design a balloon for altitudes much greater than 25 km. Some gain is possible through use of hydrogen as the inflation gas; however, high pressure storage of hydrogen is not feasible in titanium tanks due to hydrogen embrittlement. Filament wrapped tank technology would be required.

For determining atmospheric circulation, it is desirable to extend the lifetime of the balloon. This can be done by use of a superpressure type balloon or by an active resupply of lost lift. One method for resupplying lost lift is to use a "hot atmosphere" balloon which may obtain heat by burning the atmospheric methane (nominal atmosphere), with N_2O_4 or other oxidizer carried on-board the balloon gondola. This balloon design is summarized in Figure III-38. The payload includes pressure, temperature, altimeter and a transceiver for tracking and sufficient battery power and oxidizer for a 2.5-hour total mission at an altitude of 42 km. The limiting constraint on lifetime is the amount of oxidizer required to offset the heat loss from the balloon to the surrounding atmosphere.

For a "hot atmosphere" balloon, the initial deployment and inflation can be accomplished by the technique shown in Figure III-39. The balloon is packaged directly over the methane/N_2O_4 burner in a toroidal canister. When the burner is ignited, the initial hot gas only has to lift that small portion of balloon that is directly over the burner. When completely extended, the balloon pulls the gondola away from the lander body and continues to ascend to its design altitude. The burner is then cycled to maintain some preset altitude range.

For comparison, a helium gas balloon was designed using the super-pressure concept to maintain the desired altitude. Although a much stronger balloon wall is required, the balloon volume can be much smaller for the

same lift and the payload weight can be reduced since no oxidizer is required. However, heavy, high pressure helium tanks are required on the lander and therefore the total system weights are somewhat heavier than the "hot atmosphere" balloon system weights. Figure III-40 summarizes this helium balloon design for the nominal atmosphere model.

¼ x ¼ MIL BILAMINATE (KEVLAR)

"ZERO" PRESSURE
TYPE BALLOON

h = 25km
P_A = 8.2 mb
T_A + 94°K
ρ_A = .0157 kg/m³

VOLUME   1700 m³
DIAM.   14.8 m
(FULLY EXPANDED)
LIFT   26.7 kg

PAYLOAD MASS   6.9 kg
BALLOON MASS   12.6 kg
HELIUM MASS   7.2 kg
    TOTAL   26.7 kg

h = 0 km
P_A = 17 mb
T_A = 78°K
ρ_A = .042 kg/m³

DATA RELAY

LANDER

INFLATION TANK
• EPOXY WRAP MASS = 68 kg
• TITANIUM, MASS   = 92 kg

LANDER
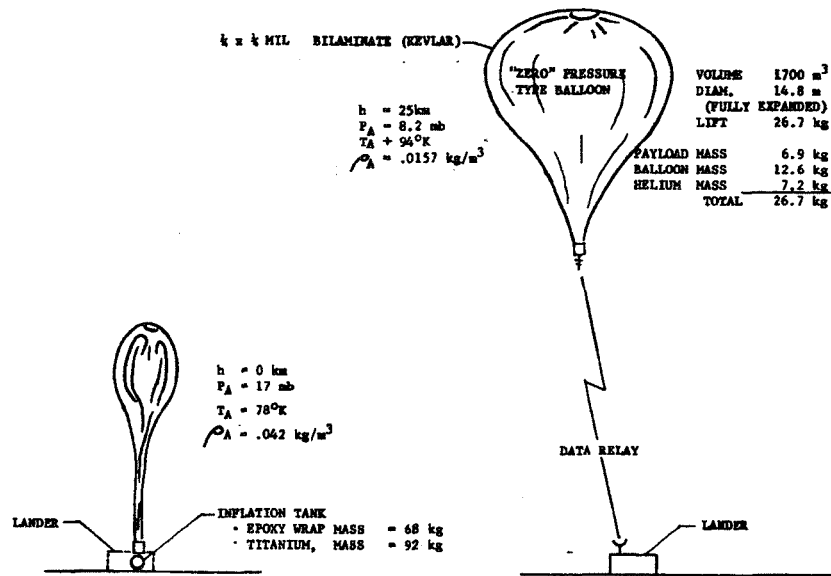
Fig. III-37 "Thin Atmosphere" Zeropressure Helium Balloon

DESIGN CONDITIONS
NOMINAL ATMOSPHERE
h = 42 km
P_A = 50 mb
T_A = 103°K
ρ_A = 0.16 kg/m³

TOTAL FLIGHT DURATION > 2.5 HOURS

"ZERO" PRESSURE
"HOT ATMOSPHERE"
TYPE BALLOON

VOLUME = 482 m³
DIAM. = 9.7 m

	MASS, kg
PAYLOAD	= 7.0
BALLOON	= 11.5
N_2O_4 TANK	= 1.5
N_2O_4	= 9.0
TOTAL	29.0

BURNER
N_2O_4 TANK
PAYLOAD

DATA RELAY

LANDER
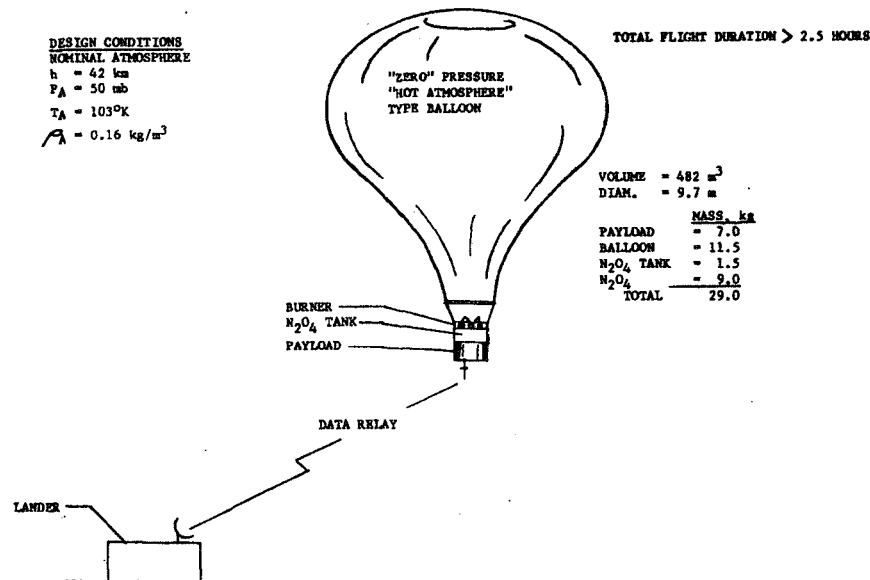
Fig. III-38 "Hot Atmosphere" Balloon Using Atmospheric
Methane and N_2O_4 Oxidizer

III-81

BALLOON FULLY INFLATED
AT DESIGN ALTITUDE

BURNER
N_2O_4 TANK
PAYLOAD

LANDER

1. BALLOON PACKAGED   2. INITIAL HEATING   3. BALLOON DEPLOYED
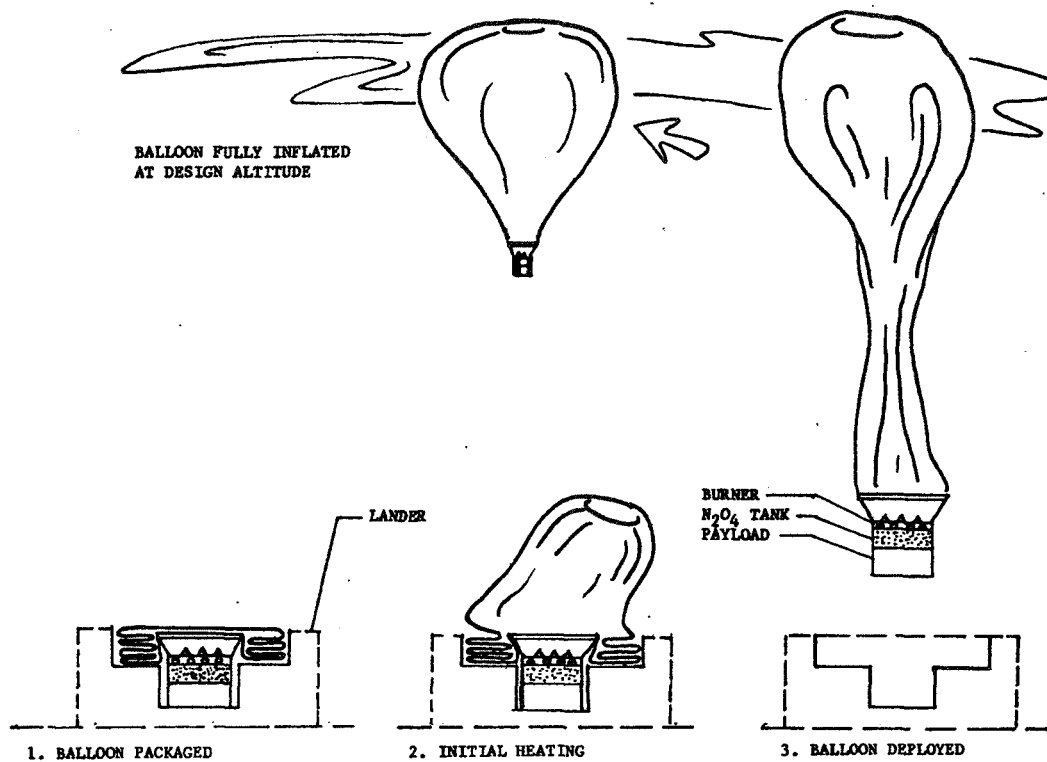
Fig. III-39 "Hot Atmosphere" Balloon Deployment Technique

DESIGN CONDITIONS

NOMINAL ATMOSPHERE
h = 42 km
P_A = 50 mb
T_A = 103°K
ρ_A = 0.16 kg/m³

MYLAR + DACRON

FLIGHT DURATION,
INDEFINITE

"SUPER" PRESSURE
HELIUM
TYPE BALLOON
$\Delta P = 0.2P_A$

VOLUME = 72.6 m³
DIAMETER = 5.2 m

	MASS, kg
PAYLOAD	7.0
BALLOON	2.8
HELIUM	2.1
FLOATED	11.9

DATA RELAY

INFLATION SYSTEM
EPOXY WRAPPED TANK, MASS = 24.3 kg
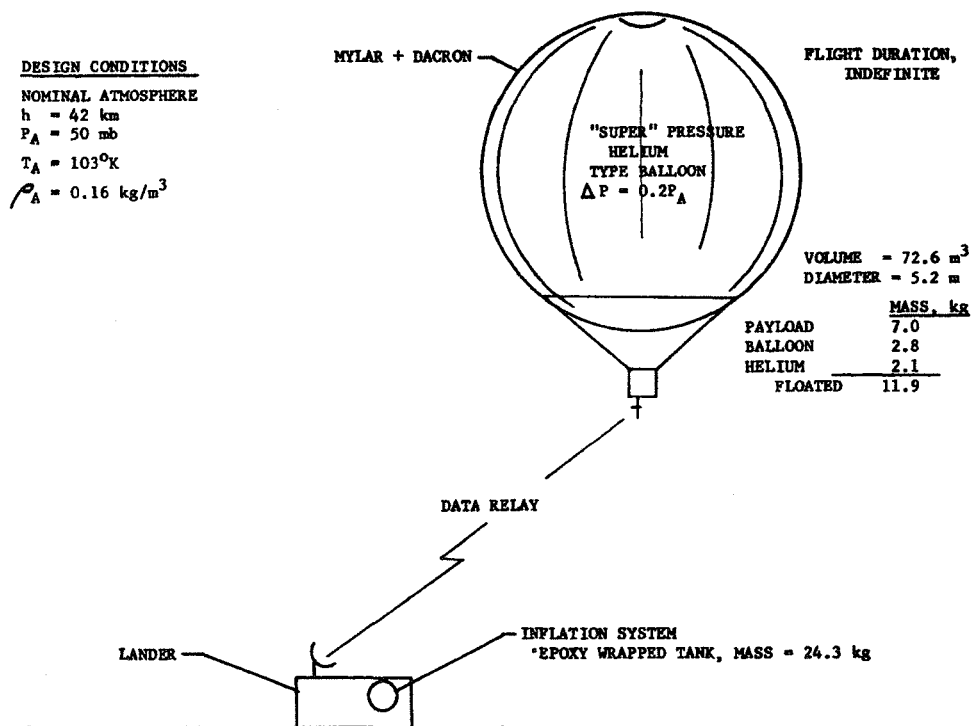
LANDER

Fig. III-40 Helium Superpressure Balloon Design

III-82

12. Two-Wheel Crawler

PURPOSE

To provide mobility for small landers to
extend science exploration or recover from
undesirable lander location

APPLICATIONS

Solid surface bodies with terrain characteristics
of sand, snow or ice.
Titan surface model involving possibility of
partial or complete coverage with liquid or
slush methane.

CONCEPT DESCRIPTION

Spherical landing configuration with net
positive buoyancy. Post-landing lateral
separation of protective hemispheres to
provide wheel base for parallel two-wheel
drive system. Independent, reversible motors
for each wheel. Drive torque reaction force
from offset center-of-gravity relative to
wheel rotation axis. Large footprint wheel
treads designed into body-cover hemispheres
or extended from lander body.

PERFORMANCE

Range and rate of progress dependent on power
availability and autonomous course control
capabilities.

SUPPORT REQUIREMENTS

Communication relay
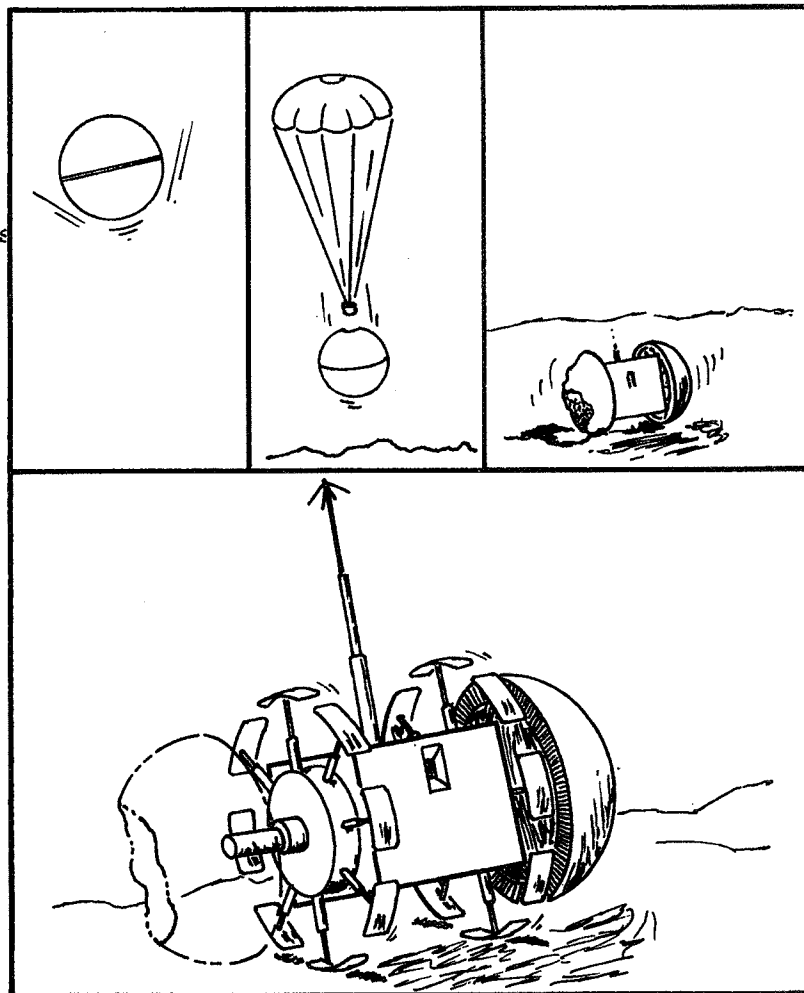
Fig. III-41   Two-Wheel Crawler

Two-Wheel Crawler

Post-landing mobility for a Titan lander would offer the usual advantages quoted for surface operations on terrestial bodies. In addition, the possibility of a Titan surface consisting partially or entirely of liquid methane may provide further impetus.

Of the many mobility concepts which have been studied at MMC, one which may be particularly applicable to Titan involves two side-by-side wheels with independent drive. For this configuration, differential wheel speed would control direction and an option for free-wheeling roll down slopes could be incorporated.

A basic spherical shape with self-righting capability could be separated on an equatorial plane after landing. The two hemispheres would be comprised of shock attenuation material with insulating and flotation properties. Also, they could be employed directly as large-footprint tires after lateral separation by reverse telescoping the enclosed lander body. This option depends on minimizing damage to the tread surfaces by orienting the touchdown attitude to impact on the wheel axis. As an alternative, if such damage cannot be avoided, stowed segmented wheels could be deployed from the protected lander body.

Motive torque for the 2-wheel configuration can be provided by one of two basic methods. If the lander center-of-gravity is offset from the wheel rotation axis, Titan gravity will provide a force for reacting with wheel drive torque. Vehicle speed and slope climbing ability (without roll-over of the lander body) will be limited by the amount of c.g. offset. Alternatively, a drag device could be extended from the lander body to contact the surface at a position providing advantageous leverage. In this case, reversal of the lander direction would require the drag device (and lander body) to rotate up and over to the opposite position thus misaligning forward directed lander sensors. To avoid this result, it would be preferable to turn 180° rather than attempt reversing.

Mobility while floating in liquid can be readily accomplished by wheel rotation if the c.g. is offset. A substitute "drag" device would require buoyancy.

Tire tread design could include consideration of sand and "snow". Even ice could be accommodated with implanted metal studs. Finally, traction in liquid could be incorporated in the design.

III-84

Reclosure of the hemispheres could be required for such purposes as thermal control. Also, such a capability would provide protection from uncontrolled roll arising from improper mobility maneuvers. In such cases, self righting features would be needed to resume operations.

13. Deployable Mass Spectrometer

PURPOSE

Obtain composition of surface material without sophisticated soft lander.

APPLICATION

Survivable entry probe or small hard lander.

DESCRIPTION

Mass spectrometer sensor equipped with heat source is deployed from probe after touchdown Surface material vaporized by heat source is analyzed by mass spectrometer and data transmitted back through probe telemetry system.

CHARACTERISTICS

   Mass   6 kg Mass Spectrometer
          .5 kg Heat Source

SUPPORTING REQUIREMENTS

Probe systems capable of surface impact survival.

Landed Probe

Sensor and
Heat Source
Deployed
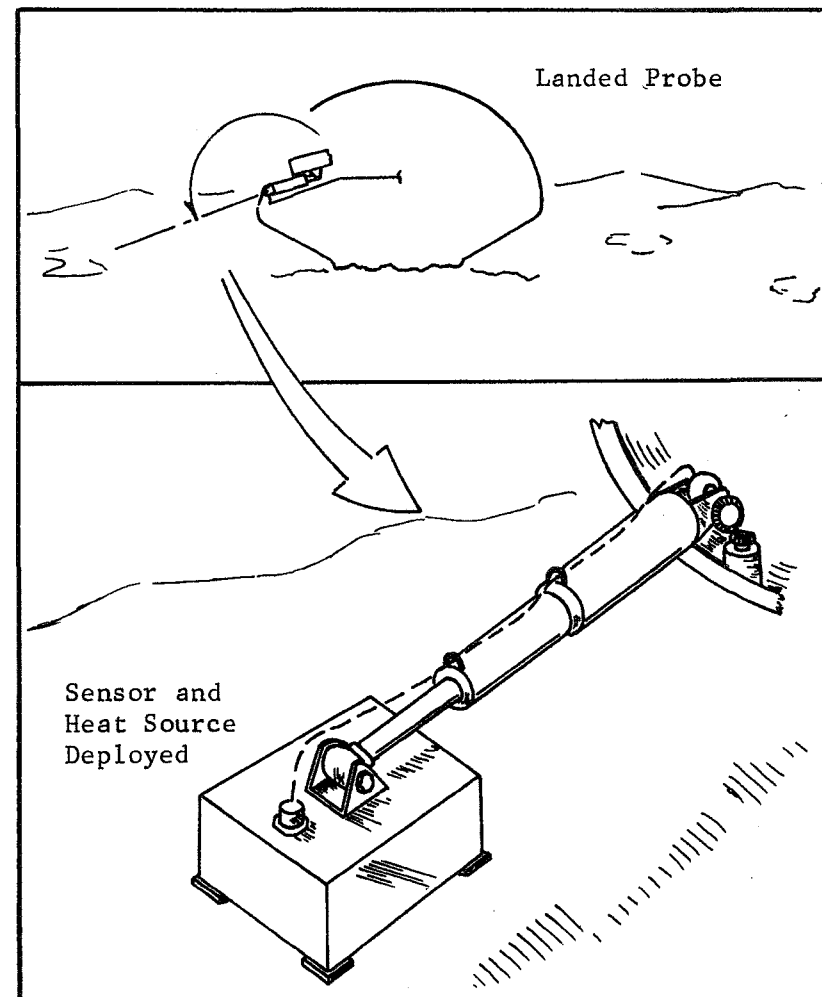
Fig. III-42   Deployable Mass Spectrometer Concep

Deployable Mass Spectrometer

One of the major questions about Titan's surface is whether its surface is made up of hydrocarbons that have condensed out of the atmosphere. A sophisticated soft lander would determine this composition through detailed analyses of samples brought on-board. However, a less complex lander, or a probe designed to survive impact, could obtain a significant amount of information about the surface composition with a mass spectrometer and a heat source for vaporizing the surface material. In the case of the survivable probe, the normal location for the mass spectrometer inlet will probably be damaged on impact, therefore a separate deployable device is envisioned. Use of a mechanism, such as the telescoping arm shown in the illustration, for deploying the mass spectrometer/heat source unit provides a way of positioning the unit so that its heat source and mass spectrometer inlet port are facing downward. (A version in which the unit is catapulted away from the probe would have to have bi-directional capability.)

The data from the mass spectrometer is transmitted via the probe antenna (to the relay spacecraft) unless enough damage is anticipated to occur on probe systems on impact to warrant building a telemetry package into the deployed sensor unit.

If practical, the deployable instrument should also be utilized during probe descent phase measurements so that dual systems are avoided. Integration problems are anticipated in isolating the heat source until required if it consists of an isotope heater type, and alternatives that could be remotely activated should be explored.

14. Drill-Augmented Penetrator

PURPOSE

Improve performance and operating characteristics
of penetrators

APPLICATIONS

Sub-surface emplacement of science instruments,
seismic charges, etc.

CONCEPT DESCRIPTION

High-speed rotating drill head at forward end
of penetrator stores angular kinetic energy
derived from spacecraft power supply. Linear
kinetic energy associated with impact velocity
can be reduced for same penetration depth.
Energy exchange factor requires empirical testing.
If efficient exchange can be achieved, advantages
would include: reduced peak deceleration levels,
reduced sensitivity to impact conditions, control
of instrument placement depth by jettison of the
drill head. Design complications result from
descent through an atmosphere. A fairing around
the drill head required to avoid severe windage
losses. Movable fins and active nutation control
necessary to manage the angular momentum vector.

SUPPORT REQUIREMENTS

Communication relay
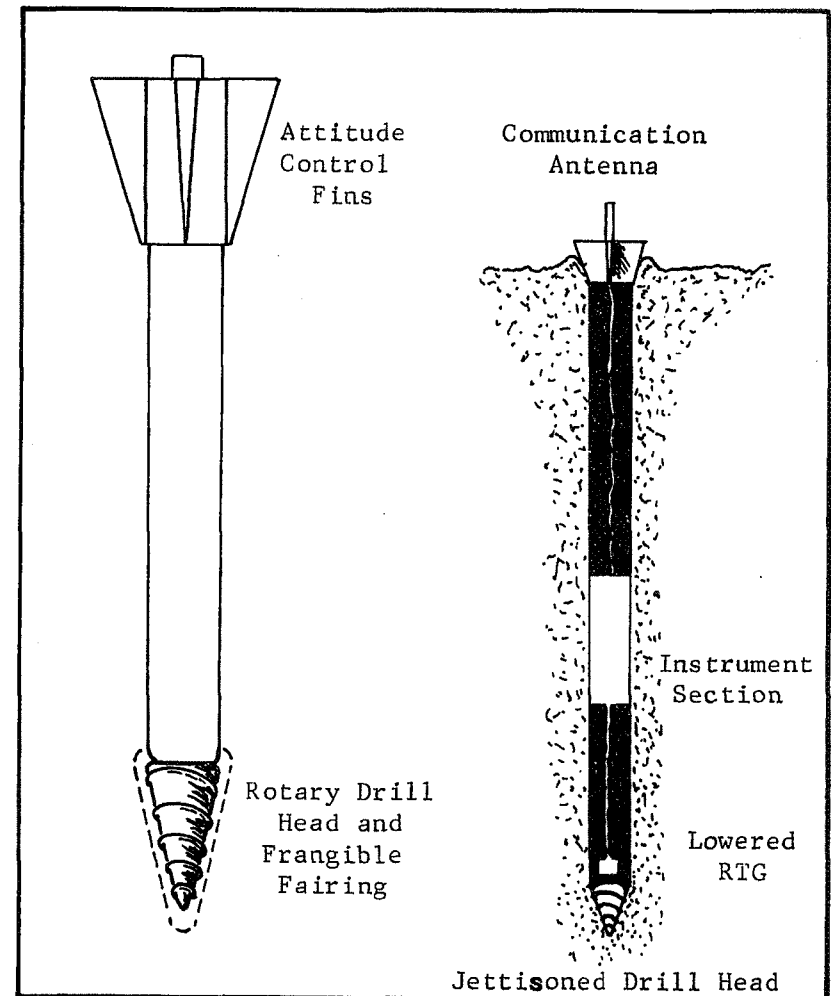
Fig. III-43   Drill-Augmented Penetrator

Drill-Augmented Penetrator

Conventional penetrators depend on linear energy proportional to surface contact velocity. Penetration capabilities and decelerations imposed on vehicle subsystems are affected by the nature of the surface and subsurface material encountered. As a consequence, over-design is necessary for some conditions and over-performance results for other conditions. Also, alignments of the vehicle attitude to the velocity vector and to the surface terrain normal are of major concern.

It may be possible to augment penetrator performance and reduce sensitivities to primary variables by providing a high speed rotating drill head at the forward end. If substantial angular energy is imparted to the rotary drill by orbiter spacecraft power and preserved through surface contact, depth of penetration for a fixed impact velocity should be increased. Conversely, for fixed depth of penetration, a reduction of impact velocity should be permissable.

If a practical design could be developed, the augmented penetrator would offer the following potential advantages for subsurface emplacement of payload (instruments, seismic charges, etc.).

1. Reduced sensitivity to impact velocity variations associated with atmosphere uncertainties.

2. Reduced g-levels imposed on vehicle systems and payload instruments for a given depth of penetration.

3. Increased tolerances for off-perpendicular surface contact and for aerodynamic angle of attack at surface contact.

4. Opportunities to tailor the drill characteristics to the expected subsurface material (e.g., ice versus pulverized rock).

5. Option to avoid excessive penetration by jettisoning the drill head after achieving a desired depth.

6. Decreased inert mass for emplacement of a given payload.

7. Decreased penalties for accommodating large diameter science instruments.

Design complications are introduced by operation of such a vehicle in a sensible atmosphere. For instance, to avoid excessive losses of angular energy to windage, a frangible or jettisonable fairing would be required to enclose the drill head. The clearance space could be evacuated or filled with a low density, low viscosity gas. A more serious problem could be that of management of the angular momentum vector during descent. Dependence on simple aerodynamic stability (normally an advantage for penetrators) may not be sufficient. It may

be necessary to provide active nutation control with control forces derived from movable aerodynamic surfaces.

Technology requirements include high strength materials to permit extremely high spin rates and to maintain sharp cutting edges in abrasive material. Design of drill flutes and determination of proper ratios of linear and angular energies would require empirical testing.

15. Autonomous Landing Site Selection and Hazard Avoidance Guidance System

PURPOSE

To improve landing reliability in unknown terrain.

APPLICATION

Appropriate to "conventional" Titan lander, other planetary body landers, and the proposed combined Titan Orbiter/Probe/Lander vehicle (TOPL).

CONCEPT DESCRIPTION

Video sensors scan potential landing sites and process light intensity received in various frequency bands to determine contrast and thus the relative smoothness of various sites.

ESTIMATED CHARACTERISTICS

  Mass - 6 Kg

  Power - 12 W

  Data Storage - 4×10^7 bits

PERFORMANCE

Detection and avoidance of obstacles down to a fraction of a lander dimension.

Scanned Field-of-View
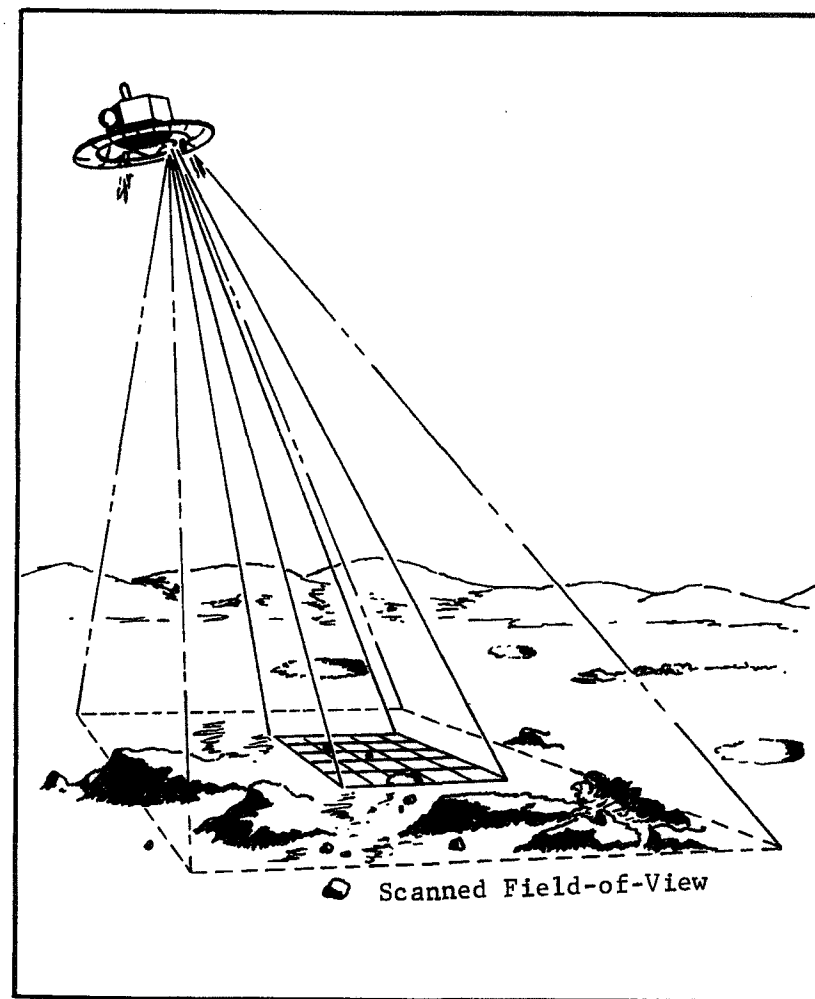
Fig. III-44 Autonomous Landing Site Selection

Autonomous Landing Site Selection and Hazard Avoidance Guidance Systems

For a lander entering an unknown environment, it is desirable to provide navigation during entry and scientific site selection and obstacle avoidance during the terminal descent phase of flight by way of autonomous real-time observation and decision making. The basic technology (required) has been investigated with regard to advanced Mars landers and successfully demonstrated in the laboratory, see Ref. III-4. It therefore appears appropriate to extend this technology to Titan Lander missions. Also, application of developments in the area of Earth resources satellites involving tracking a particular surface feature would have application to Titan lander guidance systems.

Advanced Video Guidance System

A brief description of the landing guidance system suggested in Ref III-4 is given in the following paragraphs.

The guidance system begins its function during terminal descent. At approximately 1000 meters, the system is activated and dynamically scans the area surrounding the impact point predicted by the lander computer. The video data are then processed, resulting in a steering command to the lander computer and, consequently, to the propulsion subsystem to avoid areas containing rocks, craters, and major slopes. Use of electronic beam positioning obviates the need for extensive data processing of the entire area, and the need for mechanical gimbals or for reorienting the vehicle to observe the area about the Predicted Impact Point (PIP). The scanned field of view is a fixed angle, i.e., the surface area scanned diminishes as a function of altitude while resolution improves. After the guidance system scans the surface, the video data are processed and a new impact point is selected (the area with the least contrast). A bias steering command to the lander computer initiates maneuvering to the preferred landing site. The sequence is repeated at intervals until an altitude of about 15 meters from the surface is reached.

The site selection algorithm is implemented as follows. Receiving a positioning command from the lander computer, the scanned field of view is centered about this point, and a matrix of areas is scanned, as shown in Figure III-45
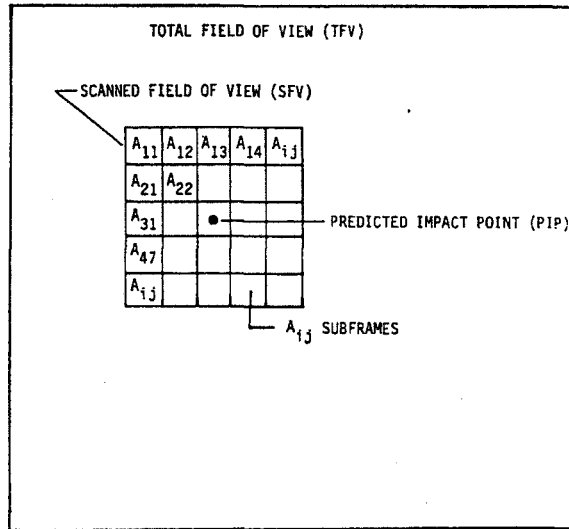
Fig. III-45   Scan Format

The video signal is then processed by the appropriate filters, as shown in Figure III-46

```
VIDEO     ┌─────────────────┐         ┌──────────────┐
INPUT     │ LOW-PASS NOISE  │         │ LOW-PASS     │
          │ FILTER          │    ┌───▶│ FILTER       │
   o─────▶│ (f  ≈ RESOLUTION│    │    │ (f    < FRAME│───▶ V
          │   c             │────┤    │   c          │      L
          │ LIMIT)          │    │    │ RATE)        │
          │          30 kHz │    │    │         20 Hz│
          └─────────────────┘    │    └──────────────┘
                                 │
                                 │    ┌──────────────┐
                                 │    │ BANDPASS     │
                                 ├───▶│ FILTER       │───▶ V
                                 │    │ 30 HZ TO 9 kHz│     M
                                 │    └──────────────┘
                                 │
                                 │    ┌──────────────┐
                                 │    │ HIGH-PASS    │
                                 └───▶│ FILTER       │───▶ V
                                      │ 1 k to 30 kHz│      H
                                      └──────────────┘
```
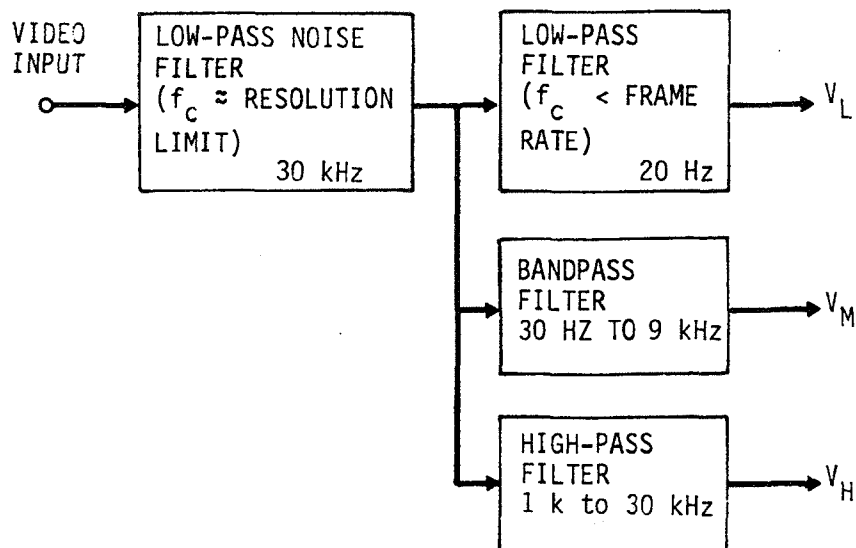
Fig. III-46 Video Signal Processor

The ratios of the outputs in the various frequency bands are thus a quantitative measure of the degree of "contrast" existing in a given area. The best landing site, the smoothest area, is the one with the least "contrast" and is the one selected by the system as the new impact point.

Future Work

The significance of the work accomplished to date is that the output of a scanning sensor system such as a TV camera can be operated on by conventional filtering techniques and simple processing algorithms to arrive at an adaptive and autonomous sensor system capable of making intelligent decisions. In other words, computational and hardware complexity is not required to provide an adequate degree of intelligence

for the proposed applications. Further experimental work, however, is required to provide a more comprehensive definition and selection of the observables, and to optimize the algorithms and data formatting electronics for a particular mission. The future activity needed to make video guidance systems available for Titan and other planetary body landers are summarized below;

(1) An imaging sensor tradeoff study is required to select the most suitable camera for the time frame of interest. Advanced technology cameras, such as charge-coupled devices, should be considered as well as IR and Laser devices in view of uncertain light levels at the surface.

(2) A laboratory test program should be conducted to evaluate proto-type system performance against scaled target models with the anticipated albedo, geomorphological, and illumination characteristics.

(3) Continued digital simulation is necessary in order to estimate advanced video guidance system's impact of fuel, stability, and maneuvering capability for specific trajectories.

(4) Ultimately, a helicopter flight test would provide an excellent performance evaluation check.

Also, the techniques developed for acquisition, pointing, and tracking from orbit for Earth resources purposes show promise for recognizing and tracking objects of interest on the Titan surface for navigation and scientific site selection purposes.

16. Self Propelled Penetrator Concept

PURPOSE

To produce a controlled penetrator velocity at impact regardless of atmospheric density

APPLICATION

Parachute penetrators, penetrobe or lander carried penetrators

DESCRIPTION

Penetrator afterbody is equipped with solid rocket motor to augment kinetic energy of free fall, or to provide entire ΔV in the case of lander carried penetrators

CHARACTERISTICS

Mass - 2 to 4 kg for solid rocket

SUPPORTING REQUIREMENTS

Radar altimeter and descent rate sensor (Doppler radar) and micro controller for impulse selection
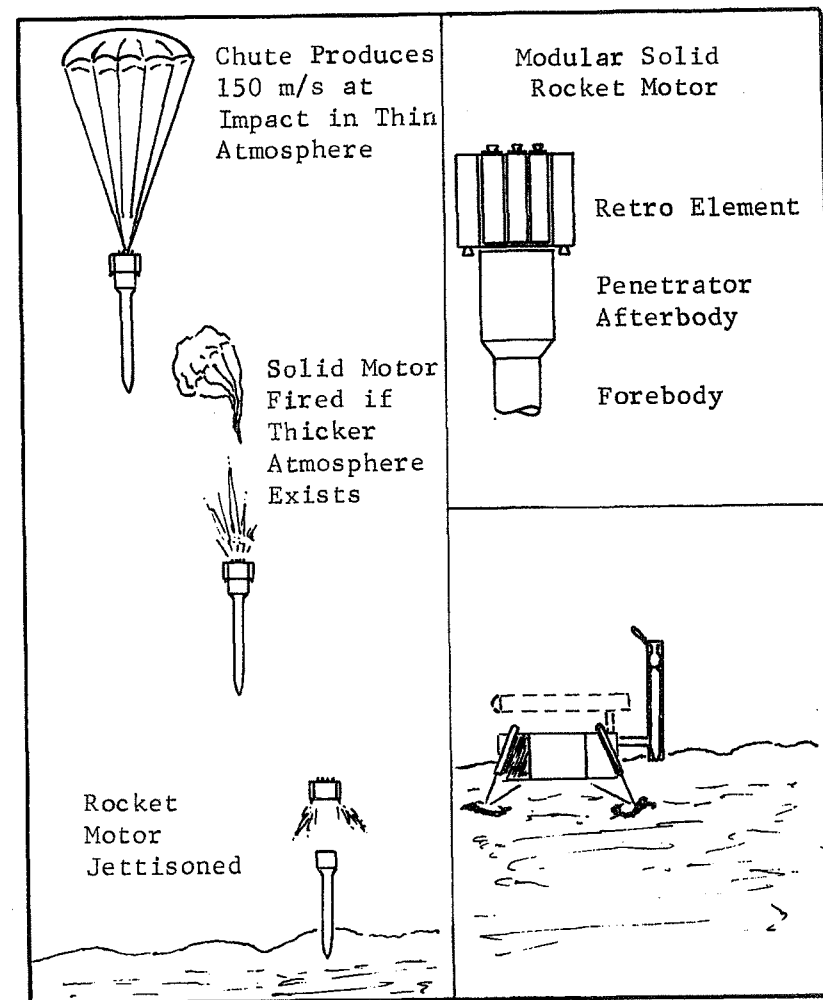
(a) Parachute Descent/
Multi-Impulse Motor
Version

(b) Lander Mounted Version

Fig. III-47 Self Propelled Penetrator Configurations

<u>Self Propelled Penetrator Concept</u> - Penetrators provide subsurface data that is difficult to obtain with any of the other exploration modes, e.g., heat flow, "soil" structure and layering, and subsurface chemical composition. However, controlling the impact velocity purely by ballistic coefficient variation is difficult. The idea of adding variable impulse-level propulsion was discussed in conjunction with the Penetrobe concept (See Page III-41) and it is also appropriate for an individual penetrator mission.

After staging from its entry housing, the penetrator would descend on a parachute sized so that in the thinnest atmosphere anticipated, the impact velocity would be 150 m/s. If at a few meters above the surface the velocity is determined to be less than 150 m/s, due to a denser atmosphere having been encountered, a solid rocket motor is fired to make up the ΔV required. The rocket motor is envisioned as a modular unit made up of about 7 small cylindrical solids in a circular pattern with built-in aft facing nozzles and 2 or 3 with forward facing nozzles for separation. Separation is required to avoid blocking the afterbody antenna deployment. This type of system is also appropriate for the deployment of decoys in weapons systems applications. The decision as to whether to fire one or more units is based on stored information of velocity-vs-number-of-units contained in a small memory.

In the case of a lander carried penetrator, the trade-off is between use of a drill, which would probably be more efficient, and a powered penetrator which might already be developed and thus cost less. The penetrator transmitter and antenna functions could be performed onboard the lander. Another option for a lander mounted device is the drill augmented penetrator discussed in a separate paragraph (See Pg III-88).

17. On-Board Trajectory Prediction

PURPOSE

To provide on-board trajectory prediction for
adaptive control of descent rate.

APPLICATION

For use with landers, atmospheric probes, and
penetrators.

CONCEPT DESCRIPTION

A microcomputer provides electronic memories
which contain programs for predicting the
atmospheric characteristics, initially using
deceleration data from a 3-axis accelerometer
and estimated initial conditions. Using these
real time atmospheric predictions, an estimate
of the time to deploy drag devices can then be
made. After the entry heat pulse, measurements
of pressure and temperature can be made allowing
more exact atmospheric structure predictions
to be made.

ESTIMATED CHARACTERISTICS

Based on recent technology forecasting data the
size, weight and power of this electronic
equipment can be made small enough to be
readily compatible with the proposed spacecraft.
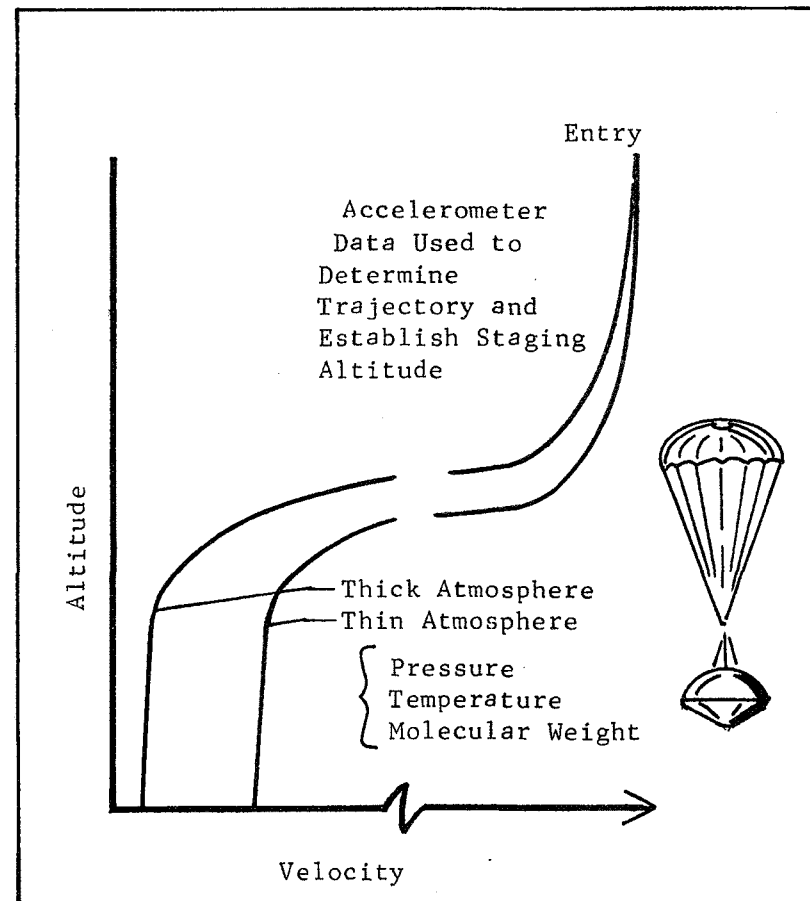
Fig. III-48   On-Board Trajectory Determination

On-Board Trajectory Prediction

In order to efficiently design exploratory vehicles which must enter, descend through an atmosphere, and in some cases land, it is desirable to know the atmospheric characteristics very accurately. If large uncertainties exist in the atmospheric model, the vehicle must incorporate large design margins in order to accommodate the uncertainties. However, it may be possible, using advanced technology concepts to design a highly adaptive system which can evaluate the environment and adapt the vehicle response to fit the situation. The current Titan model has a very large uncertainty in the atmospheric density at the surface. The density varies by a factor of 64. In the very thin model atmosphere, a high ballistic coefficient vehicle such as a penetrator, which has been slowed to a low velocity while in its entry housing, will not reach terminal velocity after staging and the penetration depth will be very unpredictable.

By the use of on-board trajectory prediction, the entering penetrator or probe can use measurements obtained during entry and later during descent to constantly estimate the atmospheric structure below the probe altitude. Then by using the estimated atmospheric characteristics, the probe microprocessor computer can predict the descent rate time history and impact time. With this information the probe can adapt or modify its drag configuration by deploying or releasing drag devices. In this way the descent time history can be modified to better accomplish the mission objectives such as controlled impact velocity or prescribed descent rate for measurement acquisition.

For the thin atmosphere model any effective changes in drag, such as parachute deployment, may have to be done early in the entry because of the short time to impact. Therefore, the on-board trajectory prediction program must be able to make early predictions based on only deceleration data at initial entry. By providing real time estimates, continually updating them by continuous recalculation, and using Kalman filtering techniques to smooth the results, it should be possible to fairly accurately predict the deployment time, if deployment is required. Initially the calculations will use the measured deceleration and estimated values for the critical unknowns such as entry velocity, flight path angle, gravity field, radius, and molecular weight. The vehicle drag, mass, and area would be accurately known. After entry, additional data can be obtained from pressure, temperature and even composition for a further refinement of the trajectory prediction.

18. Synthentic Aperture Side Looking Radar Imager

PURPOSE

To provide high resolution images of the surface from orbit independent of the opacity of the atmosphere.

APPLICATION

Can be used for mapping Titan surface or obtaining local images of proposed landing site as part of an adaptive landing control scheme.

CONCEPT DESCRIPTION

A long, linear array is synthesized analytically to get very high resolution by processing the output data from one relatively small antenna. Multifrequency radar is used to guarantee imaging of the surface through an unknown atmosphere.

ESTIMATED CHARACTERISTICS

Weight: 5.0 Kg (Excluding Antennas)
Size: 0.107 m^3 (Excluding Antennas)
Radar Power Required   9-155 Watts
Telemetry Power   400-500 Watts

PERFORMANCE

Range   1000 km to 100,000 km
Resolution   1.5 meters
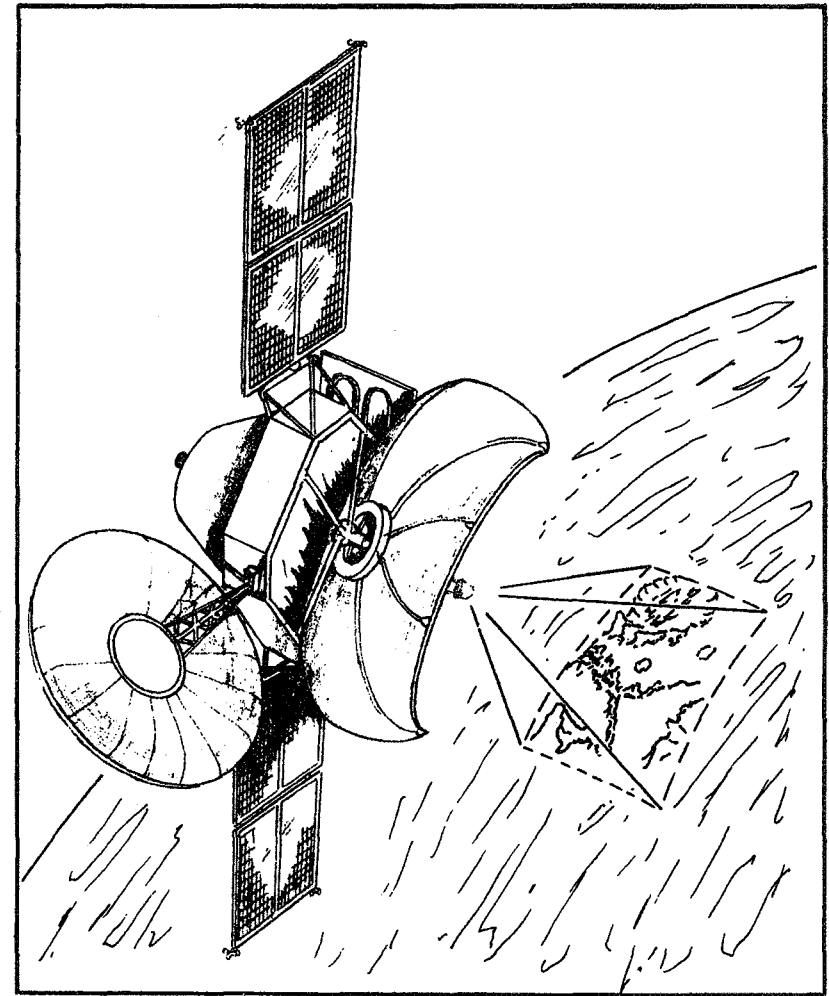
Fig. III-49   Synthetic Aperture Side Looking Radar Imager

Synthetic Aperture Radar Imaging System

The synthetic aperture (SA) radar is an excellent method for imaging a planetary body with an unknown atmosphere, since the frequency or frequencies can be selected to reduce the risks of not penetrating to the surface. Also, synthetic aperture side looking radar resolution does not have to be a function of altitude, so it's an ideal device to use in elliptical orbits. Very high resolution, down to a meter, is obtainable. This kind of resolution is not obtainable with state-of-the-art orbital TV systems and is almost equivalent to the resolution possible with lander TV systems.

The radar imaging systems accumulate data very fast and capability is therefore necessary for sending large volumes of data to Earth in real time or for buffering it until it can be sent. The synthetic aperture radar in fact generates much more data than a TV system unless its output is processed onboard.

For Titan applications, it would thus be desirable for complete image processing to be done onboard. However, to produce onboard-processed images that achieve the image reconstruction quality compared with those done on the ground requires an advance in processing technology.

Figure III-50 shows the azimuth resolution capability obtainable with side looking radars where their outputs are processed to get either real or synthetic apertures. The azimuth resolution is the resolution obtainable parallel to the direction that the S/C is moving-- parallel to the S/C velocity vector. The range resoltuion which is perpendicular to the velocity vector, is a function only of the transmitted pulse width.

In the real aperture implementation, the radar is operated like a conventional radar. When operated like this, the image resolution is a function of range similar to a TV system. The real aperture radar resolution is also a function of the azimuth dimension of the antenna and
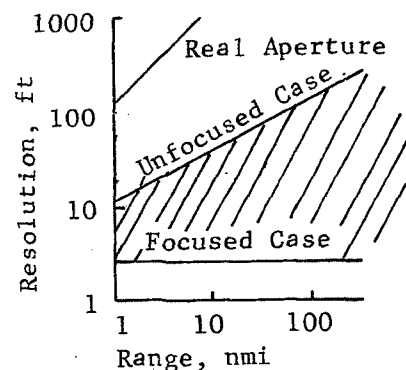
Fig. III-50 Resolution Possible with Side Looking Radar

the operating frequency of the radar. The synthetic aperture radar operated either in a focused or unfocused mode differs from the real aperture radar in the processing that is done on the radar output data, and in the constraints on the size of the antenna that can be used.

The principle of the synthetic aperture radar is based on the generation of an effective long antenna by signal processing means rather than the actual use of a physical long antenna. In fact, only a single relatively small antenna is needed. The synthetic aperture radar uses the microwave returns from the antenna at different positions along its flight path to analytically synthesize a long linear array.

If each element in the synthesized antenna is corrected for phase then a focused SA radar is obtained. The resolution now is only a function of the azimuth dimension of the antenna and is equal to one-half this dimension. In fact, the radar can operate anywhere between the focused and unfocused cases as indicated by the cross hatched areas of Fig. III-50. The only difference in the implementation is the amount of processing to develop the final image. When the SA is implemented to operate in the cross-hatched area, it is called a partially focused synthetic aperture.

To determine its applicability to Titan missions, two SA radar designs were examined. In case 1 the radar is mounted on a Saturn orbiter that is in an orbit inclined to Titan's such that its period is approximately equal to Titan's and its path stays within 100,000 km of Titan(See Page III-23). Case 2 involves a Titan orbiter in a circular orbit with an altitude of 1000 km. Designs are based on data from the Venus Orbital Imaging Radar (VOIR) study, Ref. III-5. The resulting systems are summarized in Table III-6.

Based on these designs it appears that SA radar imaging of Titan would be best accomplished from a Saturn orbiter which has the size (300 kg) consistent with the large radar antenna and telemetry antennas and the power capability needed (for telemetry).

Also, further technology development in onboard image processing is needed to keep data return rates to the levels consistent with telemetry capability (or telemetry capability has to be improved).

III-102

Table III-6 SA Radar Systems for Titan

Item	Saturn Orbiter (Case 1)	Titan Orbiter (Case 2)
Velocity Relative to Titan's Surface (m/s)	11	1640
Range (Km)	100,000	1000
Resolution (Meters)	15	2.25[(1)]
Antenna Size (Meters)	3 x 4.1 (Truncated)	4.5 x 4.1 (Truncated)
Peak Output Power	3.2 KW	0.9 Watts
Average Output Power (W)	31.0	1.8
Input Power (W)	155	$\approx$ 9
Additional Power for Processing etc., (W)	100	100
Frequency	S-Band, 3 GHZ	S-Band, 3 GHZ
Swath Width (Km)	5000 (4)	22.5
Data Rate to Earth [(2)] (Megabits)	3.0	3.6
Power Required for Telemetry[(3)] (Watts)	426	510

    (1) In fully focused mode

    (2) Complete on-board data processing assumed

    (3) Based on data transmission to mapping time ratio of 1 to 10, and a 3 meter dish antenna for telemetry (power can be reduced by decreasing resolution).

    (4) To fully illuminate Titan Surface.

19. Adaptive Thermal Control Concepts for Titan Landers

PURPOSE

Afford a lighter weight means for tempera-
ture control of a Titan Lander than current
technology permits

APPLICATION

Titan or Other Outer Planetary Body
Landers

CONCEPT DESCRIPTION

Various techniques, see sketch, are proposed
for controlling the heat flow from the
Lander equipment compartment to the environ-
ment,and between the RTG waste heat source
and the equipment compartment.

Removable Insulation Window

Canopy with Heat Pipes and Variable Direction Reflector

Varying Insulation Thickness

Snap Action Thermal Switch
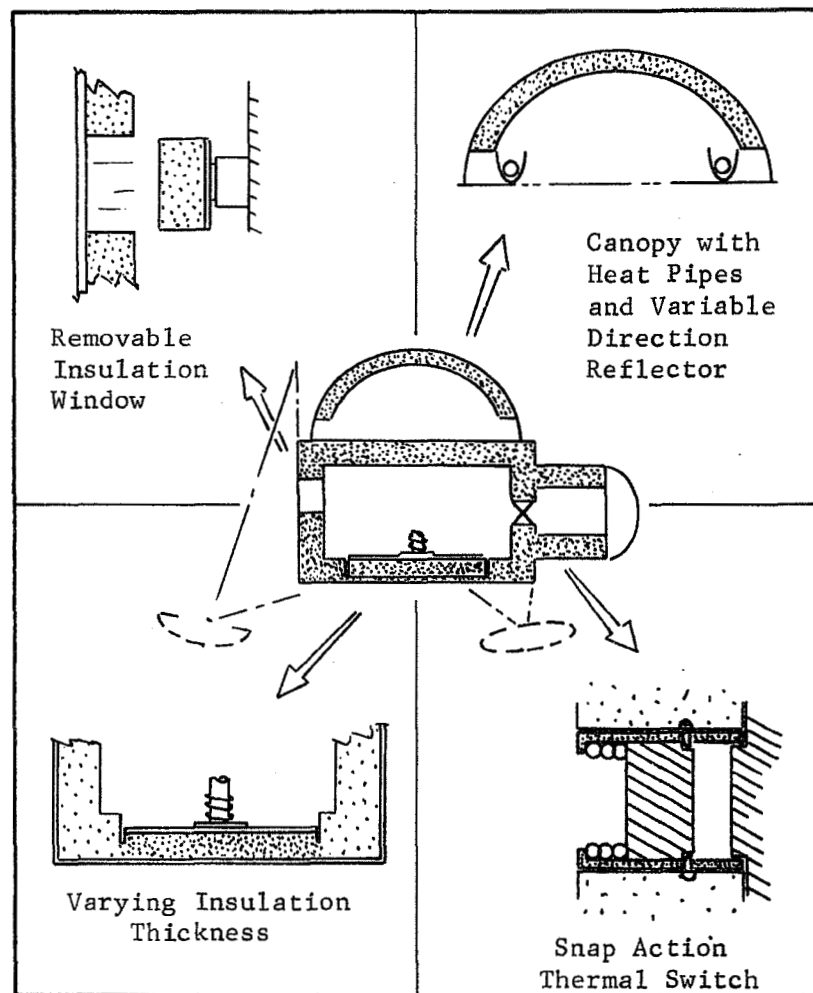
Fig. III-51   Adaptive Thermal Control Concepts

Adaptive Thermal Control Concepts

The major thermal control problem for a Titan lander is balancing the waste heat from the RTG and the heat generated by on-board equipment operation with heat lost through insulation, science instrument penetrations, and structure. The problem is complicated by the markedly different boundary conditions during cruise, when the lander is inside the aeroshell attached to the delivery spacecraft, and after landing, when the exposed lander is subjected to significant convective and conductive heat losses. Current technology (Viking 75) utilizes a bimetallic-strip operated thermal switch that controls a conduction path between the externally mounted RTGs and the insulated lander equipment compartment. The thermal switch *hardware is heavy since considerable force is required to maintain good thermal coupling.* Consequently, improved ways of managing the heat balance should be sought for the very weight-critical Titan and outer planet's missions. Several such ideas are depicted in Figure III-51

Two of these are aimed at controlling the heat lost from the compartment as an alternative to controlling the RTG heat with a thermal switch. A system of sliding or hinging insulation plugs or windows, or one which compresses sections of insulation to variable wall thicknesses might require less weight than the switch. Also, since for Titan only a low temperature environment must be dealt with (as opposed to Mars with its large night and day temperature variation), the switch might need to be operated only once. Therefore a light weight, snap-action switch might be adequate in combination with one of the insulation control schemes.

Finally, an adaptation of the thermal canopy concept proposed for protecting the ascent vehicle in Mars Sample Return Mission, Ref. III-6, might be appropriate. This device has heat pipes connected to the RTG and IR reflectors that either reflect heat to the insulated canopy walls or to a non-insulated "window" in the wall which allows it to be rejected to the atmosphere.

20. Advanced Optical Guidance Sensor

PURPOSE

To enable the optical navigation techniques required in performing Titan encounter maneuvers.

APPLICATION

Determination of Titan's position from the approach trajectory at a range from Titan compatible with performing Probe/Lander deflection maneuvering and/or Titan swingby maneuvers.

DESCRIPTION

Modified CCD camera with increased dynamic range to pick up faint star field when Titan appears as a very bright object.

PERFORMANCE

Dynamic Range = 10 orders of Magnitude

Life time = 5-7 years
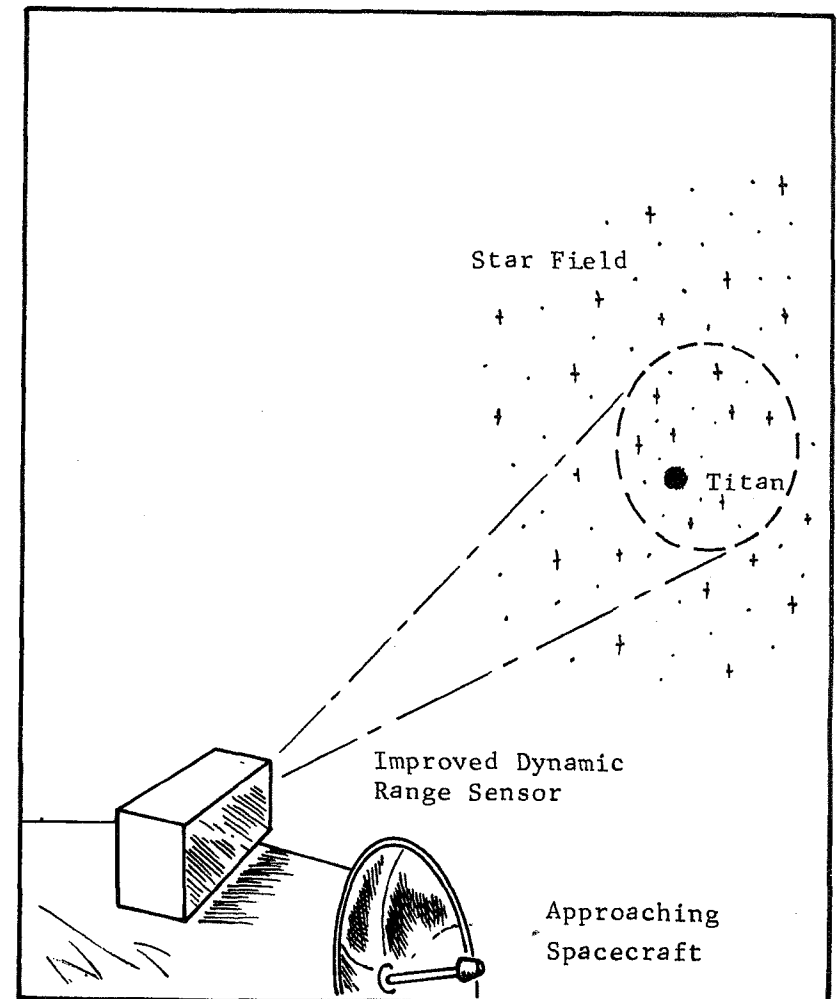
Fig. III-52   Advanced Optical Guidance Sensor

Advanced Optical Guidance Sensor

The requirement for optical navigation arises from the large (500-5000 km) uncertainty in the position of Titan. The limiting accuracy with radio navigation is the ephemeris uncertainty. Clearly it is not possible to impact the surface of Titan for these large levels of ephemeris uncertainties.

Two interplanetary missions have been flown (M'71 and MVM) which incorporate optical navigation. The specifications of the existing optical systems have been compared against the requirements desired at Titan. The conclusion is that today's technology is not adequate for the Titan missions.

Titan is a bright object at the distances approximating reasonable deflection radii (10M km) and to detect stars of magnitude six (6) or greater requires a dynamic range, for the sensor, of 10 orders of magnitude. The conventional vidicons cannot accommodate this range. Sensor lifetime is also a problem area. Missions to Titan have flight times from 5 to 7 years. There is a degradation in the high voltage filament performance with time that decreases instrument sensitivity.

The CCD camera is a new technology development that can alleviate many of the problems associated with conventional vidicon technology. A comparison of the MJS vidicon with a projected CCD equivalent is shown in Table III-7. In all areas except dynamic range, the CCD camera is expected to meet or exceed the requirements of a Titan mission. The subject of dynamic range can be worked either with electronic filtering, two cameras set at different exposure levels or adaptive data processing.

TABLE III-7   Comparison of MJS Narrow Angle Camera with CCD Equivalent

MJS CAMERA

Weight	22.3 kg(49 lbs)
Power	29 Watts
Volume	61250 cm^3 (3738 in^3)
Detection Sensitivity	MV = 9
Picture Grid	800 x 800 pixels
Resolving Capability	1-2 pixels
Long Life Characteristics	Vidicon High Voltage degrades with time
Dynamic Range	$< 10^3$

CCD Equivalent

Weight	9.1 kg(20 lbs)
Power	5 Watts
Volume	21000 cm^3 (1281 in^3)
Detection Sensitivity	Better than Vidicon
Picture Grid	200 x 200 element
Resolving Capability	.1 element
Long Life Characteristics	No High Voltage Degradation Consistent Optical Response
Dynamic Range	10^3

D. EVALUATION AND RECOMMENDATIONS

Any of the three new types of mission modes for Titan exploration identified in this chapter could be employed in a first mission. If the enthusiasm among planetary scientists for investigating the organic chemistry at Titan is sustained or increases, then the TOPL mission mode should be given high priority for an early flight. TOPL allows the widest range of science experiments to be carried out from orbit, in the atmosphere and on the surface with only a modest commitment in terms of spacecraft cost and complexity.

If planetary scientists are willing to delay the performance of the more sophisticated surface science experiments, then the Penetrobe concept may be the preferred choice for the first mission. The Penetrobe can adapt to a wide spread in atmospheric density while conducting atmospheric and rudimentary surface science.

An advanced remote sensing orbiter would be the most conservative first mission to Titan but depending on the sophistication of the sensor system, could meet many of the high priority science objectives.

It is recommended that all three mission modes be studied in more detail.

Implementation of these new mission modes which provide more effective and timely means of learning about Titan, will require only slightly greater launch vehicle performance than conventional lander, probe or penetrator systems that are delivered to Titan before the cruise vehicle goes into orbit (see Fig. III-53). However, with either the conventional or advanced systems, a lighter-weight 3-axis version of the cruise vehicle (Saturn orbiter) is seen to be needed to enable missions to be flown with the Shuttle launch vehicle at any time during the 1980's and 1990's. Use of space storable propellants for orbit insertion maneuvers would reduce the required injected weight for the Mariner class missions by about 200 Kg from the values shown in Fig. III-53. An additional reduction in the dry weight of the Mariner vehicle of about 200-400 kg would still be required to keep the injected weights within the performance limits of the Shuttle-Tug.
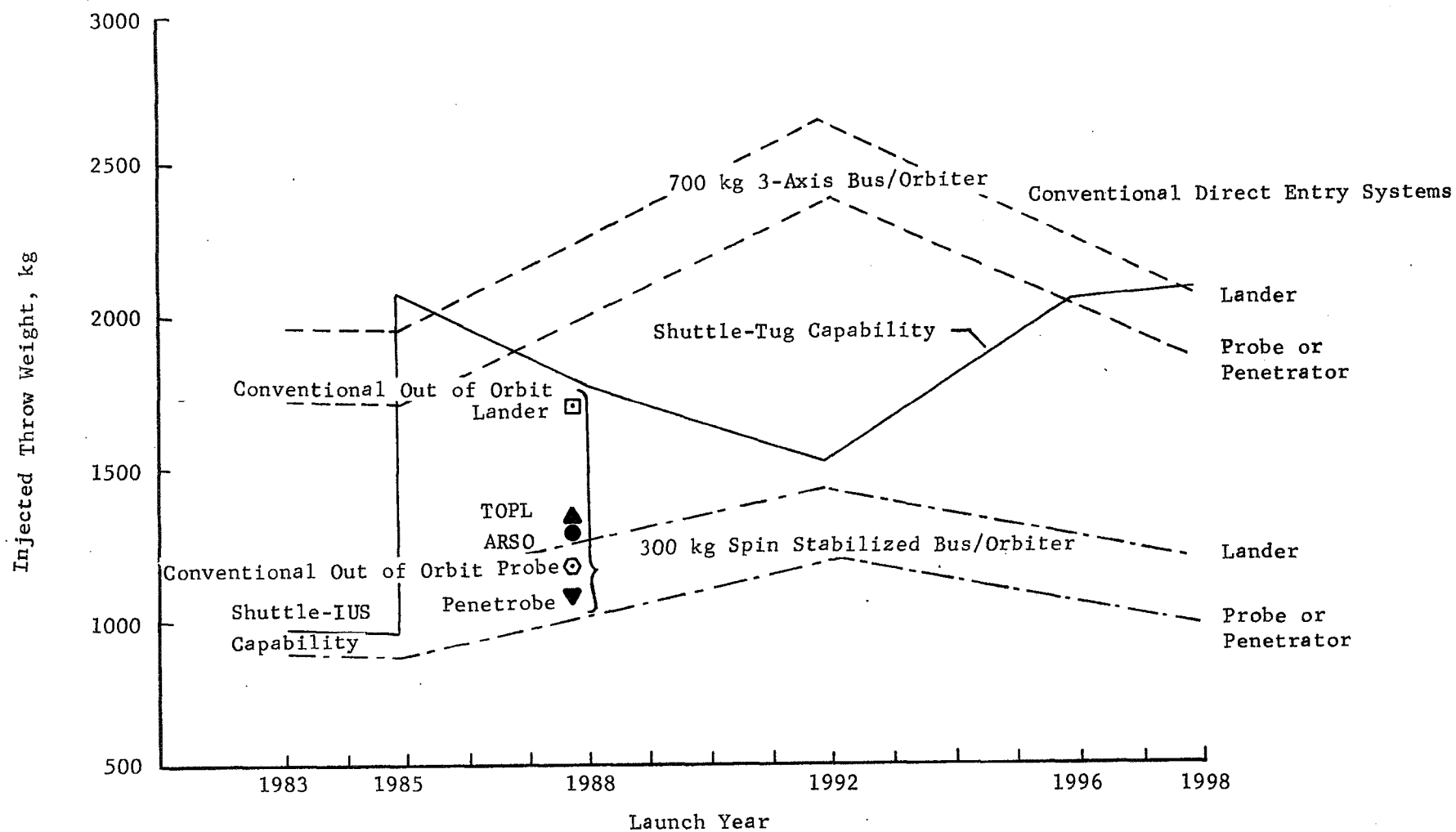
Fig. III-53 Comparison of Launch Vehicle Requirements for Conventional and Advanced Concept Systems

Alternatively, if all of the projected advances in materials and subsystem technologies forecast in the outlook for Space Study, Ref. III-7 are fully realized it is possible that Titan vehicle weights could be reduced sufficiently to allow use of current Mariner class spacecraft for Titan missions. Another possibility is increasing launch vehicle capability, e.g., development of the "Heavy Lift System" (Ref. III-7).

Tradeoffs between these elements, i.e., spin-stabilized spacecraft versus new development 3-axis spacecraft versus increased capacity launch vehicle systems versus lighter-weight Titan vehicles requires development cost data and performance information not currently available. The specialized techniques identified will require various amounts of time and development funding to make them available for application to Titan missions. Certain items, such as the laser stimulated remote material composition device, need long lead times for development since they will involve much basic experimental work and also require the supporting development of a large but light weight power source. Others involve relatively straightforward extrapolation of previously used techniques and are thus fairly predictable.

A logical next step would then be to take the new approaches and techniques identified in this chapter, along with the conventional approaches defined in the trial mission exercises, and establish several specific Titan mission options. The technology development span times and costs could be thus ascertained and compared to science value obtained from the given mission.

In parallel with such a study it would also appear appropriate to initiate development of some of the technology areas identified in view of their either being essential to any of the possible mission modes, or having broad enough application to warrant pursuing at this time. Items falling in this category would include development of improved optical guidance techniques, adaptive control systems, remote sensing instruments, and landing techniques, including site selection and hazard avoidance devices.

D. REFERENCES

III-1   Paul R. Weissman, "Titan Exploration Study - Final Report",
        JPL 760-132, Jet Propulsion Lab, Pasadena, CA, Oct. 1975.

III-2   "Mars Penetrator Subsurface Science Mission", SAND-74-0130,
        Sandia Laboratories, Albuquerque, New Mexico, August 1974.

III-3   J. Bekey, et al., "Study of the Commonality of Space Vehicle
        Applications to Future National Needs (Unclassified Portion)",
        Aerospace Report No. ATR-75 (7365)-2, Prepared under NASA
        Contract No. NASW 2727, March 1975.

III-4   R.T. Schappel, et al., "Video Guidance, Landing, and
        Imaging Systems for Space Missions", Prepared for NASA Under
        Contract NAS1-13558, Martin Marietta Corporation, Denver,
        Colorado.

III-5   W. T. Scofield and D. B. Cross, "Venus Orbital Imaging
        Radar (VOIR) - Final Report", JPL Contract 953766, Martin
        Marietta Aerospace, Denver, Colorado, August 1974.

III-6   W. T. Scofield, "A Feasibility Study of Umanned Rendezvous
        and Docking in Mars Orbit-Final Report", Contract JPL 953746,
        Martin Marietta Corporation, July 1974.

III-7   "A Forecast of Space Technology", JPL Under Contract to
        the National Aeronautics and Space Administration, Pasadena,
        California, Feb. 1975.

III-8   "Advanced Conceptual Study of an Alternate Hard Lander, JPL Study
        Contract No. 954486, Final Report due to be published July
        15, 1976, Martin Marietta Corp, Denver, Coloado.

APPENDIX A
MISSION ANALYSIS FOR TITAN EXPLORATION

This appendix summarizes the analytical results of the performance and navigation analyses done in support of the launch, encounter, orbit, and entry phases of Titan exploration missions. Because no Titan mission studies had been conducted previously, it was necessary to perform these basic analyses to identify where performance and navigation problems exist. The existence of such problems then point the way to applications of new technology.

To give perspective to the subjects discussed in the following sections, it is useful to examine the general profiles of typical orbiter, probe, penetrator and lander missions to Titan. Figure A-1 diagrams the basic sequence. The missions begin with a launch from the Eastern Test Range (ETR). The Shuttle/Tug combination is the prime launch vehicle under consideration, with the Shuttle/IUS combination considered for launches in the 1980 to 1985 time interval. Spacecraft bus configurations considered included applications of the Pioneer and Mariner class designs. The basic Pioneer spacecraft bus is spin-stabilized and weighs 300 kg. The Mariner-type vehicle is three-axis stabilized and weighs approximately 700 kg.

The spacecraft/tug/Shuttle combination is initially launched into a 150 nautical-mile circular parking orbit. This combination may orbit earth up to five revolutions while spacecraft/tug checkout proceeds. The shuttle bay is opened and the tug/spacecraft combination ejected. After a short coast period, during which checkout and attitude maneuvers are performed the spacecraft is injected onto the interplanetary trajectory.

After the interplanetary cruise, which may last as long as eight years, the spacecraft approaches Saturn. Tracking is initiated for the final midcourse maneuver. Due to the large ephemeris uncertainty of Titan, optical tracking is used in conjunction with conventional Earth based radio tracking. The final midcourse maneuver refines the spacecraft

Saturn

Titan

4

3

Earth

1   Launch from Earth Orbit

2   Final Mid-course Maneuver

3   Deflection Maneuver

4   Saturn Orbit Insertion
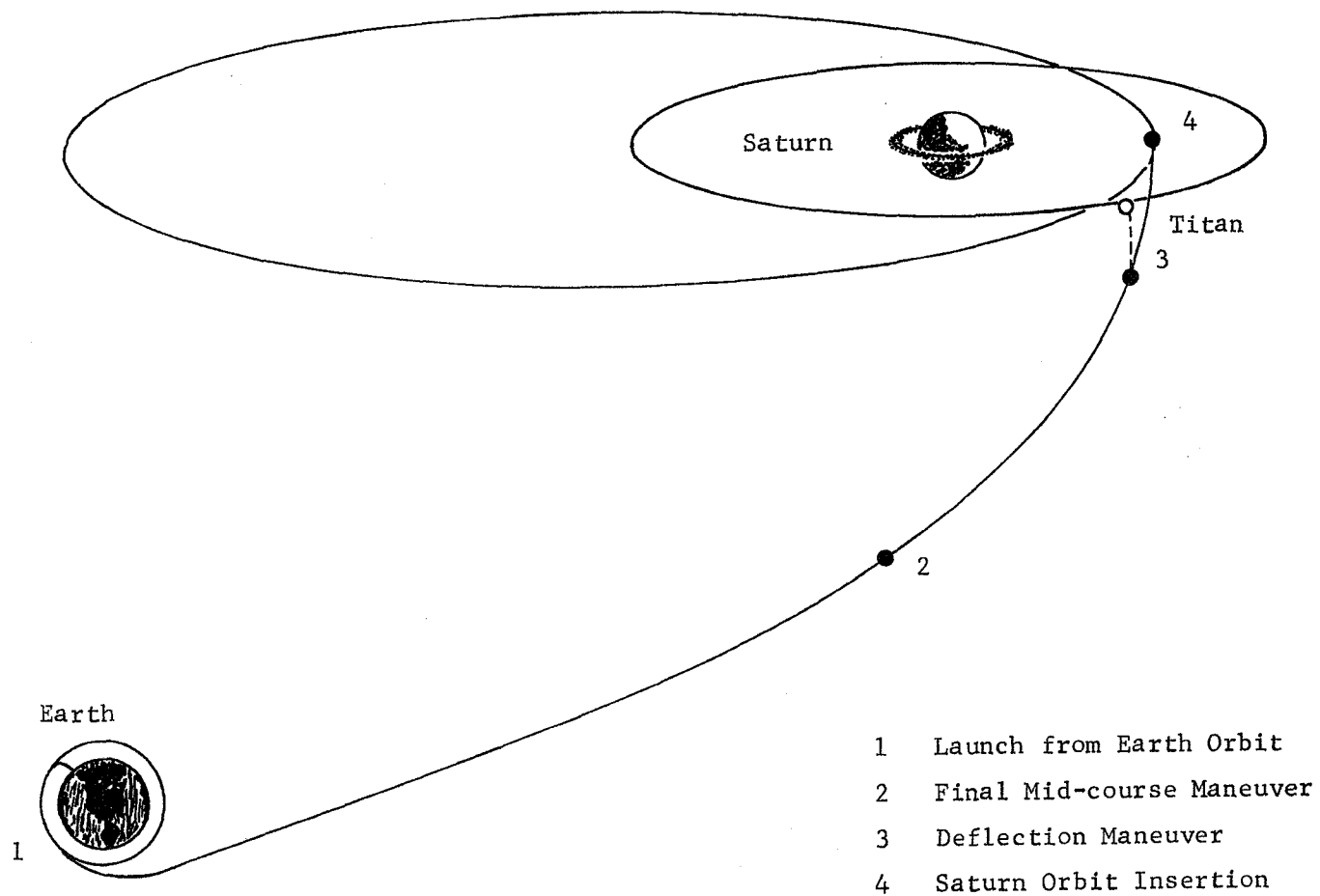
Fig. A-1 Typical Titan Mission Sequence

trajectory to the desired encounter conditions with Titan.

The deflection maneuver separates the probe, penetrator or lander from the spacecraft bus and places it on the desired Titan entry trajectory. Because most of the mission options considered in this study were performance limited, deflection of the probe, penetrator or lander was usually accomplished on the initial encounter with Titan and before the Spacecraft bus is inserted into Saturn orbit.

At this point the mission scenario becomes a strong function of the mission type.

For the probe mission, engineering data on the status of the probe and instruments are transmitted back to the bus. The probe then enters Titan's atmosphere, and transmission is terminated at the initiation of blackout. The probe signal is reacquired and atmosphere measurements are taken and transmitted to the spacecraft for relay back to earth. Data transmission lasts nominally for 42 minutes and ends when the probe makes contact with the surface of Titan.

In the case of the surface penetrator, after it is deployed from the spacecraft there is no further communication until contact is made with the surface of Titan. The spacecraft bus is targeted to be directly overhead at impact and receives the signal transmitted from the penetrator. Typical penetrator lifetime and spacecraft viewing geometry constraints indicate that data can be transmitted up to one hour after impact.

The lander mission combines the communications requirements of both the probe and penetrator missions. Engineering data is transmitted prior to entry. Atmospheric data is transmitted during entry. Surface data is transmitted after touchdown. The life detection experiment as currently understood requires an incubation period of at least 16 days. Therefore multiple passes of the spacecraft over the lander are required. Initial communication with the lander is sustained for 60 minutes. Approximately forty hours later the spacecraft bus is inserted into a loose capture orbit about Saturn. Reencounter with Titan may not occur

for another 128 days. During this and subsequent passes lander data is transmitted to the spacecraft for relay to earth.

The following sections discuss the detailed performance and navigation requirements, constraints and options for these basic Titan mission phases: 1) Earth to Saturn trajectories; 2) deflection maneuvers; 3) Titan entry; and, 4) Saturn orbit strategies.

A. EARTH TO SATURN TRAJECTORY OPTIONS

Several trajectory types are available for delivery of a Saturn orbiter, probe, penetrator or lander to explore Titan. The direct ballistic transfer, Jupiter swingby and the ΔVEGA are three trajectory techniques investigated during the study. The following three sections describe each technique, delineate their advantages and disadvantages, and present typical performance data for each during the 1983-1999 period of interest.

1. *Direct Ballistic Trajectories to Saturn* - Earth to Saturn ballistic trajectories can be characterized by a point to point conic. Fixing the launch and arrival dates essentially determines the Earth-Saturn transfer. By Lambert's theorem, those two vectors and the time interval required to traverse them determine the heliocentric conic that closely approximates the actual flight path of the mission.

Ballistic opportunities to Saturn occur every 13 months and are characterized by flight times ranging from 4 to 9 years. Minimum energy transfers correspond to a node-to-node Hohman transfer and occur at approximately twice Saturn's orbital period of 30 years. The launch years of 1983 and 1998 are the minimum energy Earth-Saturn transfers that occur within the period of interest for this study. The Direct Mode consists of a single maneuver for Earth departure and a single retro maneuver to brake at Saturn for orbital capture. The Earth departure ΔV is the Lambert solution for the prescribed flight time. Launch/encounter windows were first established by optimizing weight-in-orbit for a 15 day launch period with the Shuttle/4 Stage IUS launch vehicle. Once this

was accomplished the dependence of weight-in-orbit on launch vehicle was determined. Three Shuttle Tug candidates and one Interim Upper Stage (IUS) candidate were studied. The Shuttle/2 stage IUS was not considered because of its poor high energy payload characteristics. The throw weight versus C_3 curves for these vehicles with 3-axis and spin-stabilized payloads were furnished by ARC (Ref. A-1). Because of the similarity in performance curves for the payload types (varying by at most 50 Kg out of at least several hundred) only the 3-axis set was analyzed. When the orbiter work was complete the windows were redefined for a flyby mission. In this case the injected weight was maximized over a 15-day launch period. For each of the launch years considered between 1983 and 2000 additional mission parameters and constraints were also output for use in later studies.

a. Launch/Encounter Windows for Single Launch Missions in 1983 - 2000

Every other year from 1984 to 2000 along with the years 1983, 1985 and 1997 were scanned in 5-day launch intervals and 30 day arrival intervals to find the largest minimum orbited payload for a 15-day Shuttle/4 Stage IUS launch period. The spacecraft bus is assumed inserted in a 32 day Saturn orbit (2:1 commensurability with Titan) with periapsis radius equal to 5 Saturn radii*. The resultant launch/ encounter windows along with the minimum and maximum injected weight, weight-in-orbit, C_3, VHP, orbital insertion ΔV, flight time and declination of launch asympote (DLA) are shown in Tables A-1 and A-2. Note that data is presented for trajectory types I (transfer <180) and II (transfers >180). The largest minimum inserted weight is achieved with a Type II transfer in 1983 (516 kg). This is primarily due to the relatively large throw weight (895 Kg). The years 1984, 1985 and 1986 are also good years with only slightly less orbited payload capability. The situation worsens through much of the remaining century until the year 1997. Here a Type 1 transfer yields a 15-day launch window with a

---

*Impulsive SOI burn, I_{SP} = 280 sec.

TABLE A-1 - PERFORMANCE DATA FOR 15-DAY LAUNCH PERIOD FOR SHUTTLE/4 STAGE IUS LAUNCH VEHICLE

LAUNCH YEAR	LAUNCH DATES	ENCOUNTER DATE	INJECTED WEIGHT (KG)	WEIGHT IN ORBIT (KG)	C_3 (Km^2/Sec^2)	VHP (Km/Sec)
1983 TYPE I	01/14/83 01/29/83	06/17/90	940. 575.	547 (Max)* 332 (Min)*	112 136	5.30 5.36
1983 TYPE II	12/30/82 01/14/83	09/09/90	1060 895	612 (Max) 516 (Min)	105 114	5.37 5.39
1984 TYPE I	01/11/84 01/26/84	12/27/89	988. 730.	577 (Max) 425 (Min)	109 124	5.27 5.29
1984 TYPE II	12/27/83 01/11/84	06/25/90	988. 700.	582 (Max) 411 (Min)	109 126	5.20 5.23
1985 TYPE I	01/13/85 01/28/85	06/08/90	1055. 915.	594 (Max) 514 (Min)	106 113	5.59 5.61
1985 TYPE II	01/03/85 01/18/85	04/04/91	915. 620.	536 (Max) 362 (Min)	113 132	5.24 5.28
1986 TYPE I	01/25/86 02/09/86	04/30/91	1006. 845.	554 (Max) 464 (Min)	108 117	5.76 5.79
1986 TYPE II	01/20/86 02/04/86	03/19/93	755. 565.	437 (Max) 326 (Min)	123 137	5.34 5.37
1988 TYPE I	02/21/88 03/07/88	03/08/93	845. 685.	449 (Max) 364 (Min)	117 127	6.04 6.04
1988 TYPE II	02/16/88 03/02/88	11/18/95	575. 450.	319 (Max) 249 (Min)	136 149	5.70 5.72
1990 TYPE I	03/16/90 03/31/90	12/17/94	715. 585.	362 (Max) 295 (Min)	125 135	6.40 6.43
1990 TYPE II	04/05/90 04/20/90	11/21/99	635. 520.	300 (Max) 245 (Min)	131 141	6.89 6.91
1992 TYPE I	04/09/92 04/24/92	10/28/96	635. 520.	313 (Max) 254 (Min)	131 141	6.61 6.66
1992 TYPE II	05/14/92 05/29/92	07/29/02	790. 685.	344 (Max) 298 (Min)	120 127	7.44 7.45
1994 TYPE I	05/08/94 05/23/94	01/15/99	585. 475.	300 (Max) 242 (Min)	135 146	6.31 6.35
1994 TYPE II	06/17/94 07/02/94	08/16/04	915. 845.	392 (Max) 361 (Min)	113 117	7.55 7.56
1996 TYPE I	06/06/96 06/21/96	05/13/01	635. 500.	340 (Max) 267 (Min)	131 143	5.99 6.00

*For Launch Period

LAUNCH YEAR	LAUNCH DATES	ENCOUNTER DATE	INJECTED WEIGHT (KG)	WEIGHT IN ORBIT (KG)		C_3 (Km^2/Sec^2)	VHP (Km/Sec)
1996 TYPE II	06/21/96 07/06/96	08/25/04	988. 895.	483 436	(Max) (Min)	109 114	6.67 6.69
1997 TYPE I	06/18/97 07/03/97	04/29/02	685. 575.	366 306	(Max) (Min)	127 136	6.00 6.02
1997 TYPE II	06/28/97 07/13/97	12/14/04	1006. 915.	515 467	(Max) (Min)	108 113	6.33 6.35
1998 TYPE I	06/25/98 07/10/98	09/27/02	805. 685.	396 336	(Max) (Min)	119 127	6.61 6.63
1998 TYPE II	06/30/98 07/15/98	01/14/05	1024. 860.	552 463	(Max) (Min)	107 116	5.93 5.95
2000 TYPE I	07/19/2000 08/03/2000	02/17/05	1006. 895.	530 470	(Max) (Min)	108 114	6.11 6.14
2000 TYPE II	07/19/2000 08/03/2000	10/10/2006	790. 620.	435 339	(Max) (Min)	120 132	5.77 5.81

LAUNCH	ORBIT INSERTION DV (Km/S)		FLIGHT TIME (YRS)	DLA (DEGS)
	$5R_s$ x 32d	$3.5R_s$ x 112d		
1983 TYPE I	1.482 1.501	.947 .964	7.4	-19.5 -12.7
1983 TYPE II	1.504 1.511	.966 .972	7.6	-11.5 10.1
1984 TYPE I	1.473 1.479	.939 .945	5.9	15.8 3.6
1984 TYPE II	1.451 1.460	.921 .929	6.5	-7.9 12.7
1985 TYPE I	1.576 1.582	1.027 1.033	5.4	4.1 -6.5
1985 TYPE II	1.463 1.476	.931 .942	6.3	-12.9 9.6
1986 TYPE I	1.633 1.643	1.076 1.084	5.3	-33.4 * -15.1
1986 TYPE II	1.495 1.504	.958 .966	7.1	-10.2 13.2
1988 TYPE I	1.730 1.730	1.159 1.159	5.0	-45.7 * -27.3
1988 TYPE II	1.613 1.619	1.058 1.064	7.7	-46.5 * -36.0
1990 TYPE I	1.861 1.873	1.270 1.280	4.8	-54.3 * -36.1
1990 TYPE II	2.050 2.058	1.432 1.439	9.6	-1.3 12.4
1992 TYPE I	1.940 1.960	1.338 1.355	4.6	-56.4 * -40.0
1992 TYPE II	2.275 2.280	1.625 1.629	10.2	3.7 11.2
1994 TYPE I	1.828 1.843	1.242 1.254	4.7	-52.3 * -37.1
1994 TYPE II	2.322 2.327	1.666 1.669	10.2	5.4 4.6

LAUNCH	ORBIT INSERTION DV (km/s)		FLIGHT TIME (YRS)	DLA (DEGS)
	$5R_s$ x 32d	$3.5R_s$ x 112d		
1996	1.713	1.144	4.9	-40.7*
TYPE I	1.716	1.147		-26.4
1996	1.963	1.358	8.2	7.9
TYPE II	1.972	1.365		10.6
1997	1.716	1.147	4.9	-32.4*
TYPE I	1.723	1.152		-20.8
1997	1.835	1.248	7.5	8.5
TYPE II	1.843	1.254		7.5
1998	1.940	1.338	4.3	-22.5
TYPE I	1.948	1.345		-12.7
1998	1.691	1.126	6.6	10.4
TYPE II	1.699	1.132		6.0
2000	1.755	1.180	4.6	11.1
TYPE I	1.766	1.189		9.3
2000	1.637	1.079	6.2	11.9
TYPE II	1.650	1.090		-.5

* These year/types violate the DLA constraint of $|DLA| \leq 32^{\circ}$.

minimum inserted weight of 306 Kg. The geometric nature of the payload
dependence on launch year will be explained later. Note from TABLE A-2
that the ΔV values for insertion into the 32 day orbit are rather large
and vary between 1.451 Km/s and 2.327 Km/s. For comparison purposes
the ΔV values for insertion into a loose 3.5 Rs x 112 day orbit are
displayed in the column beside the 5.0 Rs x 32 day results, they range
from .921 km/sec to 1.669 km/sec. If launch declination is constrained
between $\pm$ 32° there would be a violation for the starred years/trajec-
tory types. These occur primarily for the fast Type I trajectories
which would not be flown anyway because of the poor inserted weights.

Figures A-2 and A-3 show the C_3 and VHP dependence on launch
year for the optimized Type I and II windows. The values plotted
correspond to the minimum weights-in-orbit. Note the classic Type II
behavior (C_3 large when VHP small and vice-versa) whereas the Type I
variation is more in phase. The corresponding weights in orbit for
the Type I and II trajectory classes is shown in Figure A-4. The
presence of the Type I peak in 1985 follows from Figure A-2. Both
C_3 and VHP are relatively small in this region. Type I dominates
through 1990 where Type II becomes more favorable. The major payload
peaks occur for 1985/Type I and 1997/Type II. The injected weights
for the 15-day windows optimized on weight-in-orbit are shown in
Figure A-5. Again the peaks occur for 1985/Type I and 1997/Type II.
The peaks follow the C_3 behavior of Figure A-2. This is an indication
that windows optimized for flyby missions will not differ appreciably
from the orbiter cases.

In order to better understand the significance of the superiority
of launch in 1985 and 1997, the one day launch window data of Table A-3
was used to construct Figure A-6. In Figure A-6, Saturn's perihelion vector
is denoted by p. The position of Saturn at arrival is shown for each
optimized launch year-trajectory type with the weight-in-orbit in

Fig. A-2 Type I Tranfer Energies for 15 Day Window

A-11
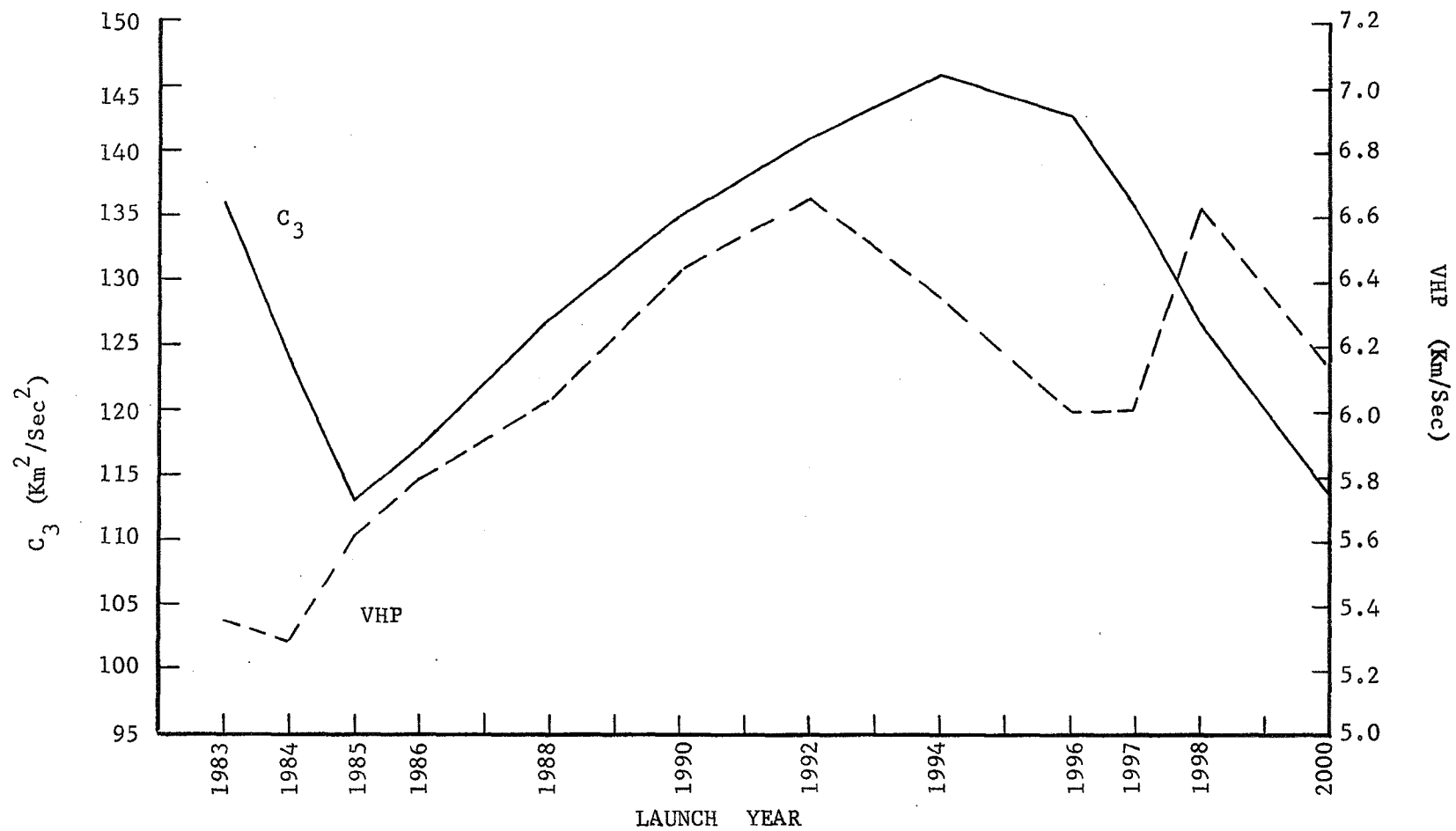
Fig. A-3 Type II Transfer Energies for 15 Day Window

A-12
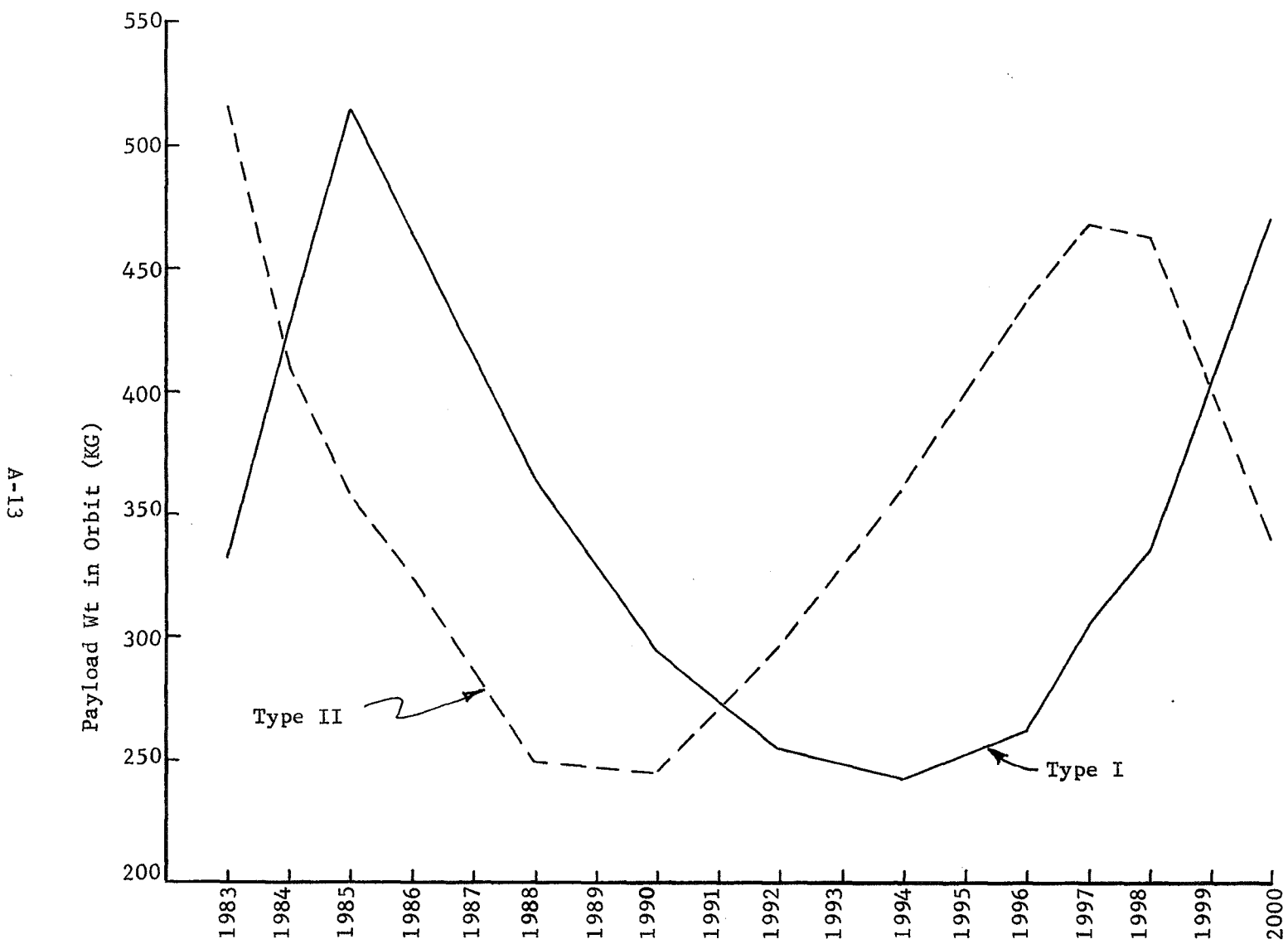
Fig. A-4   Weight-in-Orbit for 15 Day Launch Window

4 Stage IUS Launch Vehicle
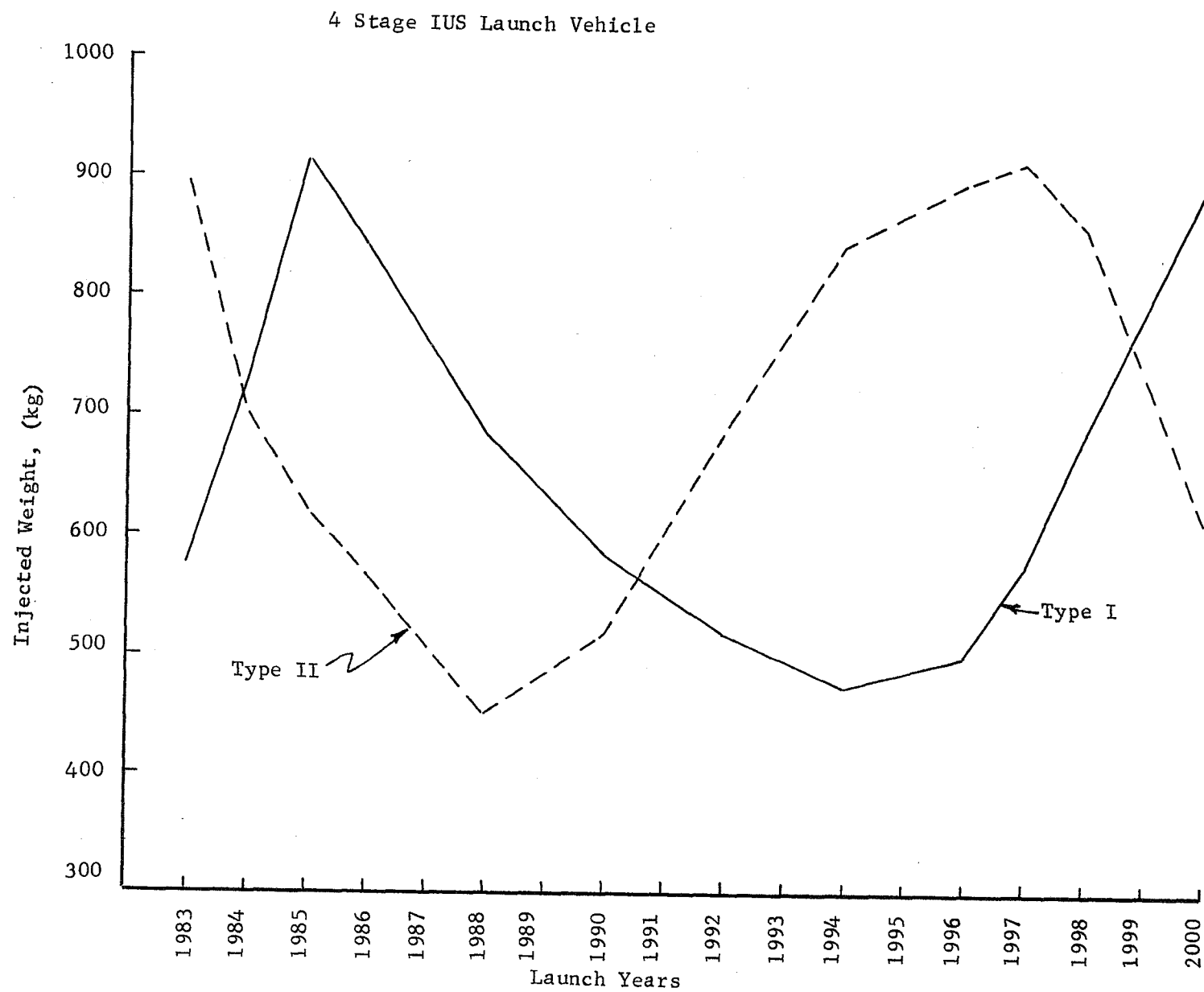
Fig. A-5 Injected Weight for 15-Day Launch Period

Fig. A-6 Launch/Arrival Geometry

1994-II (392)

1996-II (483)

1997-II (515)

1998-II (552)

2000-I (530)

1992-II Max Weight
in Orbit (344 kg)**

Saturn's Orbit

1983-II

Earth's Orbit*

1990-I

1992-II

2000-I

1990-I (362)

1988-I (449)

1986-I (554)

1983-II (612)
1984-I (577)
1985-I (594)
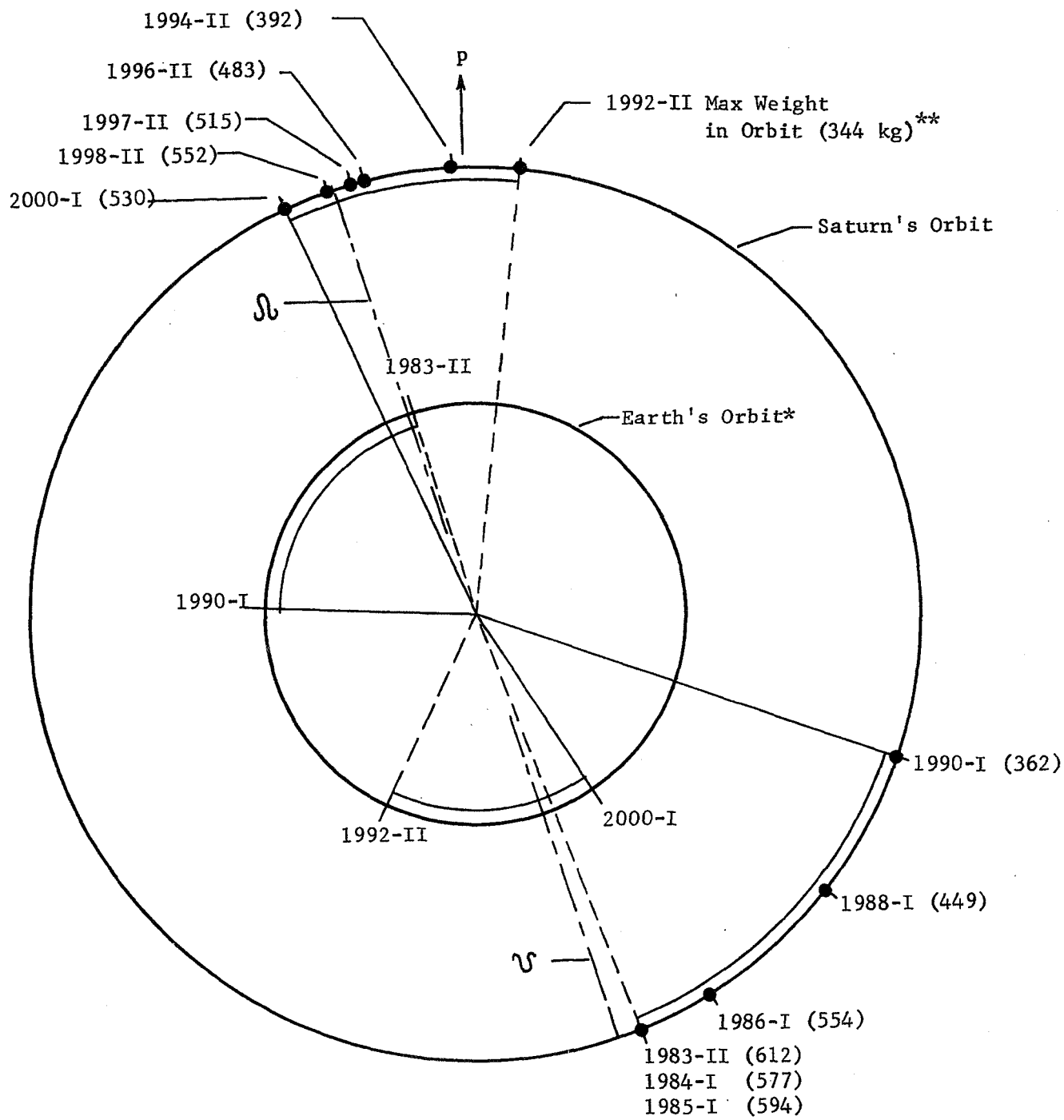
*Not to Scale
**- For 15 Day Launch Period

A-15

parenthesis. The ascending node of Saturn's orbit in the ecliptic is denoted by Ω and the descending node by $\mho$. Type I trajectories generally intercept Saturn at the descending node while Type II trajectories go to the ascending node. When the trajectories intercept Saturn at the node the transfer plane lies in the ecliptic and hence C_3 is kept small. Note that in Figures A-2 and A-3 the minimum C_3 for Type I occurs in 1985 and for Type II in 1997. Also note from Figure A-6 that the maximum weight in orbit occurs for Saturn intercepts nearest the nodes (1998-II and 1983-II). Missions to the descending node deliver more payload in orbit becuase of smaller VHP's at Saturn. These are reduced because the descending node is near aphelion where Saturn's heliocentric velocity is smaller.

Table A-3 One Day Launch Period

LAUNCH YEAR	TRAJEC- TORY TYPE	SATURN TRUE- ANOMALY AT ARRIVAL(DEGS)	TRANSFER ANGLE (DEGS)	FLIGHT TIME (DAYS) (YEARS)		C_3 (Km^2/s^2)	VHP (Km/S)
1983	II	-160	184.3	2746	(7.52)	105	5.33
1984	I	-160	178.7	2418	(6.62)	105	5.19
1985	I	-160	173.7	2141	(5.90)	106	5.34
1986	I	-150	169.9	2031	(5.60)	109	5.53
1988	I	-130	165.4	1837	(5.00)	117	6.04
1990	I	-110	162.5	1732	(4.70)	125	6.40
1992	II	7.2	198.4	3866	(10.60)	118	7.63
1994	II	1.6	194.3	3358	(9.20)	114	7.11
1996	II	13	192.1	2922	(8.00)	110	6.59
1997	II	15	187.6	2601	(7.10)	108	6.19
1998	II	18	184.5	2320	(6.40)	107	5.88
2000	I	24	171.7	1724	(4.70)	108	5.98

b. <u>Dependence of Weight-In-Orbit on Launch Vehicle</u> - The launch/ encounter windows of Section (a) were optimized with orbital payloads corresponding to a Shuttle/four-stage IUS launch vehicle (L/V). This section reports on the orbited payload capability of other L/V in the same launch/ encounter windows. Figure A-7 shows the throw weight (or launch payload) versus C_3 performance curves for five launch vehicles. The three upper curves assume maximum use is made of the Space Tug Earth orbital capability.
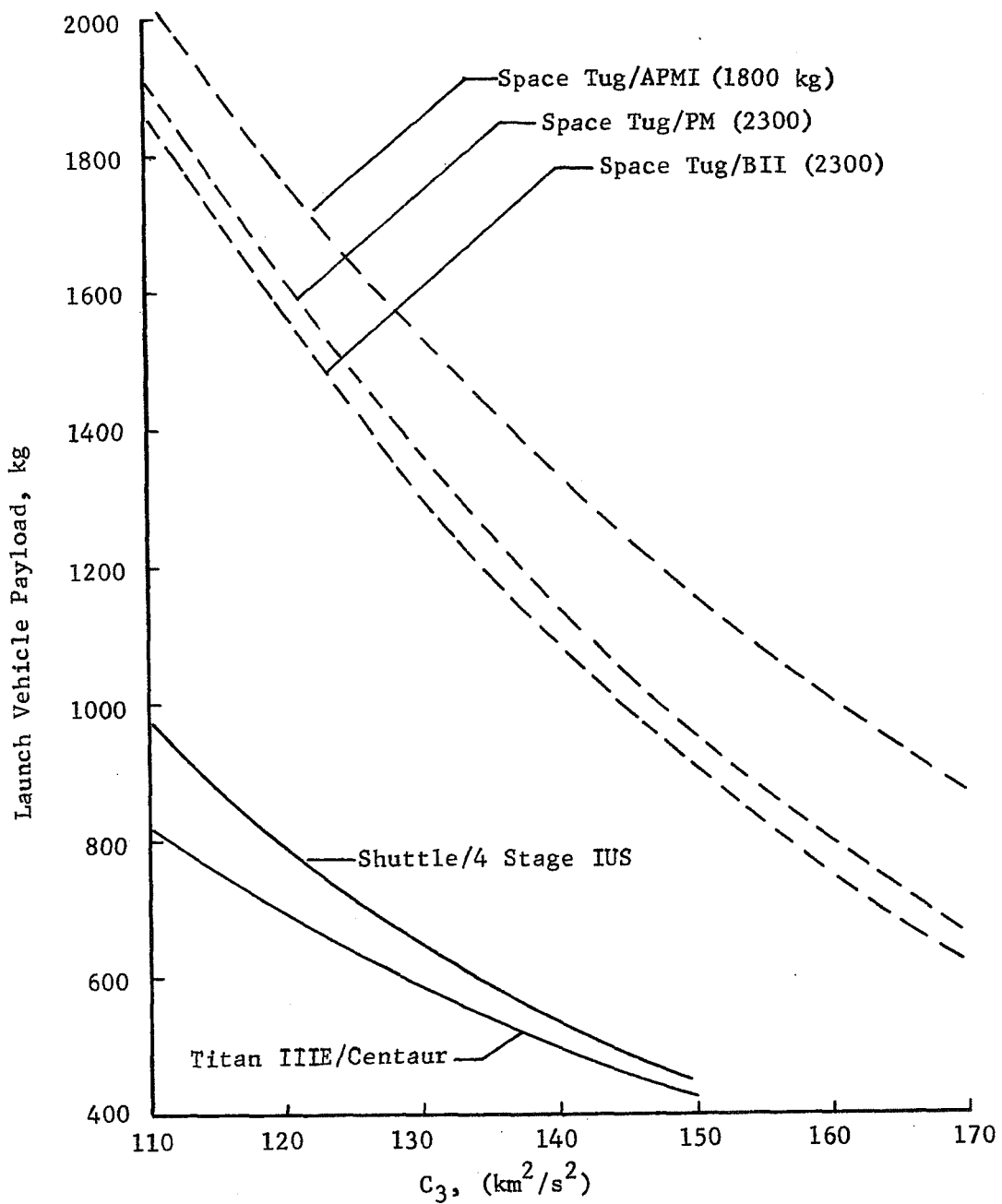
Fig. A-7   Launch Vehicle Performance

A-17

The upper, solid line is for the Shuttle/four-stage IUS. The Titan 3E/ Centaur capability is shown for reference. Only 3-axis stabilized payload performance was considered. Modified kick-stages for spin-established payloads degrade the TUG and IUS performance only slightly. These curves were fit with quadratic functions for interpolation at various values of C_3.

Tables A-4 and A-5 present injected weight and weight-in-orbit for the 15-day launch windows of Section a. Orbited weight vs. launch year data is shown graphically in Figure A-8 for the highest performing TUG and IUS candidates. The TUG can insert 50% more weight in orbit than the IUS to a maximum of 1118 kg in 1983. These weights are somewhat optimistic since no S/C-L/V adapter weight was assumed and allowance was not made for in-orbit maneuvers. However, 100 m/s was budgeted for midcourse ΔV propellant and 100 m/s for finite-burn loss in orbital insertion. Orbited payloads for the other TUG vehicles were computed from the throw-weight ratios displayed in Figure A-9. The ratios may be used to obtain weights-in-orbit for the specific L/V by multiplying the ratio times the corresponding reference L/V payload (i.e., the Space Tug with the PM (2300) stage is capable of inserting 85% of the APMI payload in 1992. The performance ratios as well as the reference L/V performances are optimal for 1985 and 1997 launches.

Table A-4 INJECTED WEIGHT (KG)

(15 Day Window)

LAUNCH YEAR	SPACE TUG APMI	SPACE TUG PM	SPACE TUG B II	SHUTTLE 4-STAGE IUS
1983 (I)	1410.	1230.	1180.	575.
1983 (II)	1940.	1800.	1750.	895.
1984 (I)	1680.	1520.	1470.	730.
1984 (II)	1630.	1470.	1410.	700.
1985 (I)	1970.	1830.	1780.	915.
1985 (II)	1490.	1310.	1260.	620.
1986 (I)	1860.	1710.	1670.	845.
1986 (II)	1390.	1200.	1150.	565.
1988 (I)	1600.	1440.	1390.	685.
1988 (II)	1170.	970.	920.	450.
1990 (I)	1430	1250.	1200.	585.
1990 (II)	1310.	1120.	1070.	520.
1992 (I)	1310	1120.	1070.	520.
1992 (II)	1600.	1440.	1390.	685.
1994 (I)	1230.	1030.	980.	475.
1994 (II)	1860.	1710.	1670.	845.
1996 (I)	1270.	1080.	1030.	500.
1996 (II)	1940.	1800.	1750.	895.
1997 (I)	1410.	1230.	1180.	575.
1997 (II)	1970.	1830.	1780.	915.
1998 (I)	1600.	1440.	1390.	685.
1998 (II)	1880.	1740.	1690.	860.
2000 (I)	1940.	1800.	1750.	895.
2000 (II)	1490.	1310.	1260.	620.

Table A-5 WEIGHT IN SATURN ORBIT (kg)

(15-Day Window)

LAUNCH YEAR	SPACE TUG APMI	SPACE TUG PM	SPACE TUG B II	SHUTTLE 4-STAGE IUS
1983 (I)	816.	712.	683.	332.
1983 (II)	1118.	1038.	1009.	516.
1984 (I)	980.	887.	858.	425.
1984 (II)	957.	863.	828.	411
1985 (I)	1107.	1028.	1000.	514
1985 (II)	870.	765.	736.	362
1986 (I)	1022.	940.	918.	464.
1986 (II)	804.	694.	665.	326.
1988 (I)	852.	767.	740.	364.
1988 (II)	649.	538.	510.	249.
1990 (I)	723.	632.	606.	295.
1990 (II)	619.	529.	505.	245.
1992 (I)	641.	548.	524.	245.
1992 (II)	697.	627.	606.	298.
1994 (I)	628.	526.	501.	242.
1994 (II)	797.	732.	715.	361.
1996 (I)	680.	578.	551.	267.
1996 (II)	946.	877.	853.	436.
1997 (I)	753.	657.	630.	306.
1997 (II)	1006.	935.	909.	467
1998 (I)	787.	708.	683.	336.
1998 (II)	1012.	937.	910.	463.
2000 (I)	1019.	946.	919.	470.
2000 (II)	817.	718.	691.	339.
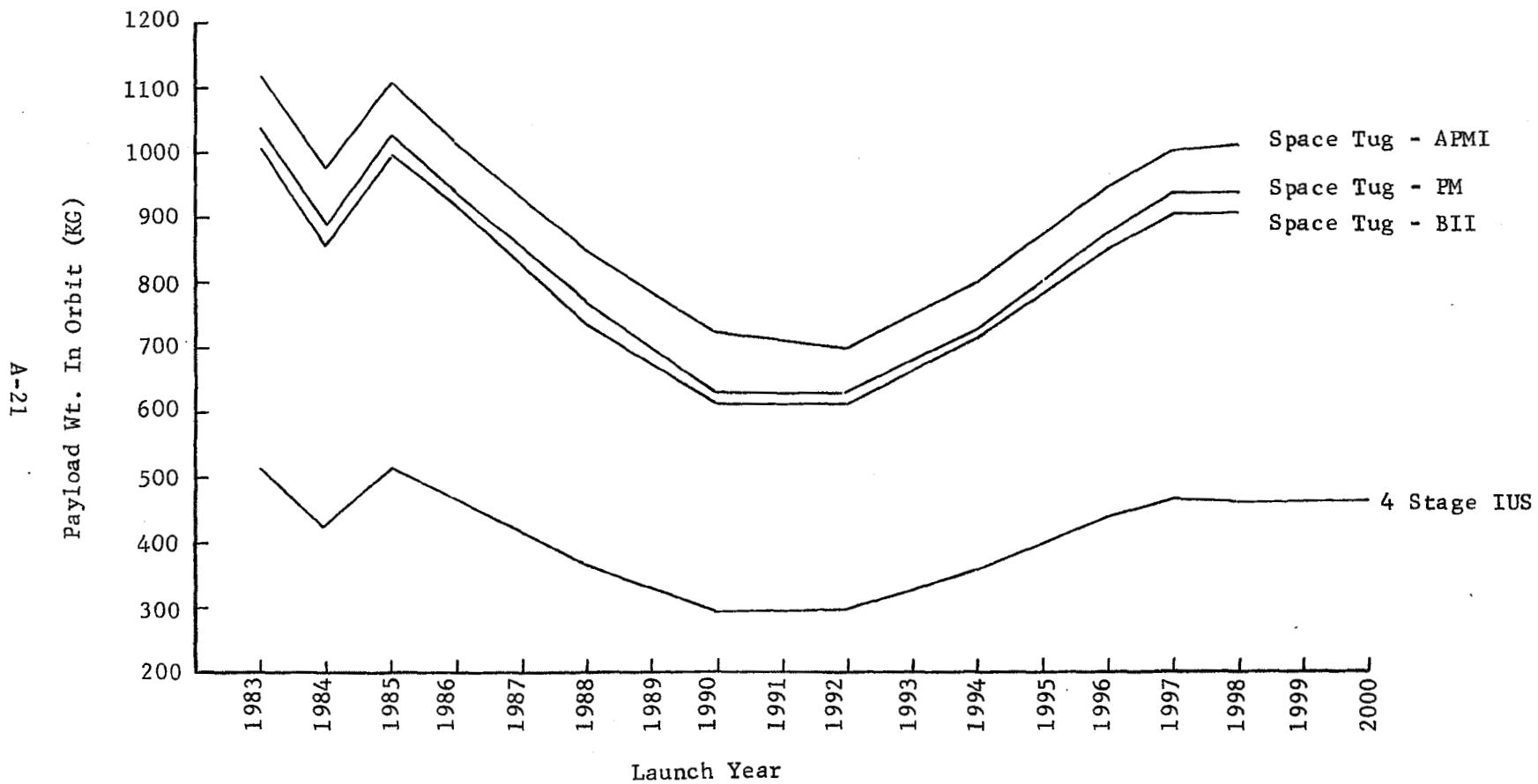
Fig. A-8 Orbited Payload for Tug vs. IUS (15-Day Window)
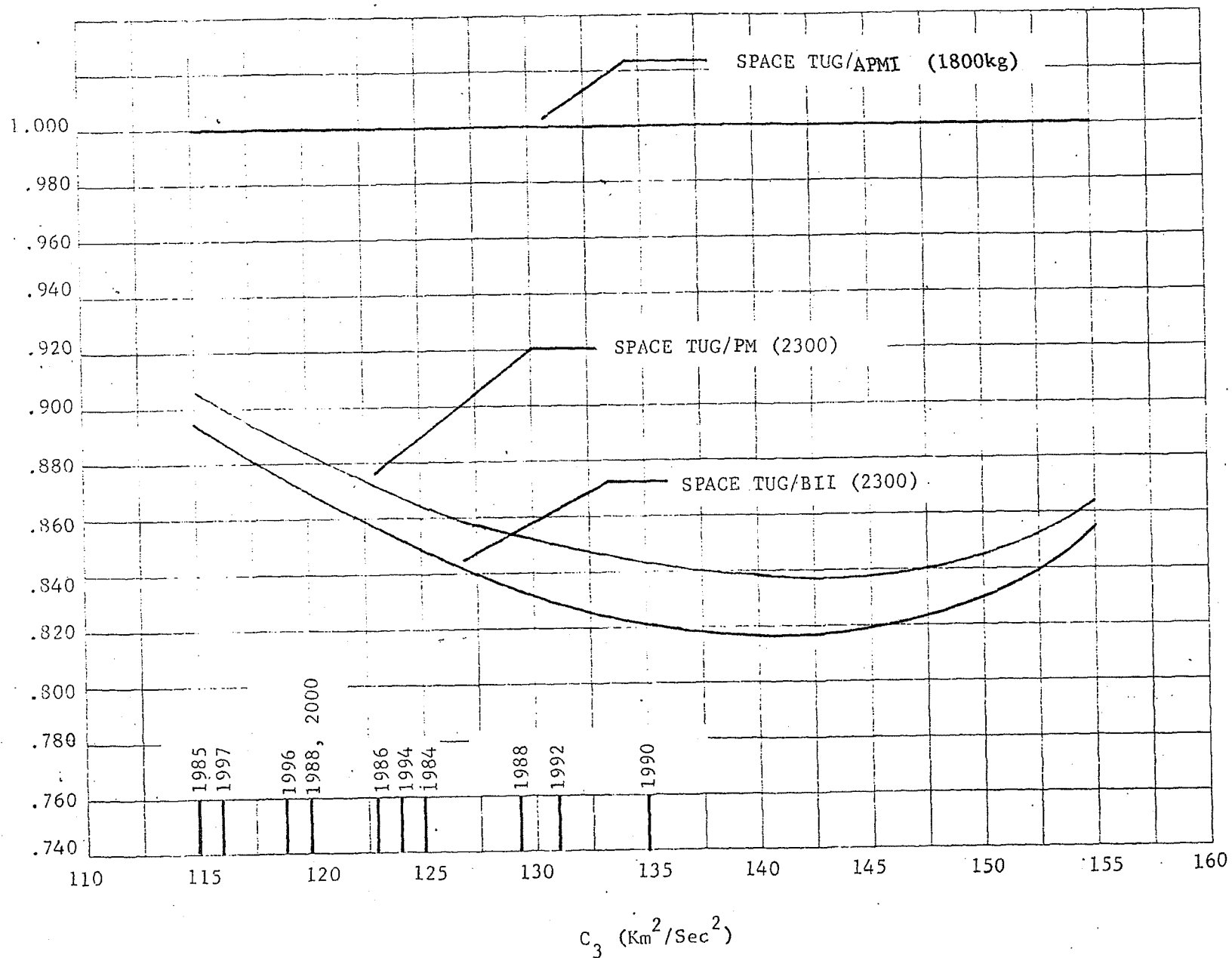
Fig. A-9 Space Tug Performance Ratio

A-22

c. <u>Performance for Mariner and Pioneer Class Spacecraft</u> - To better understand the launch vehicle requirements for Titan missions it was decided to examine several launch years and determine the throw weights required to fly an optimized Mariner or Pioneer class probe penetrator or lander mission. The direct ballistic missions chosen are shown on Table A-6. These are representative of windows defined previously in Table A-1, Section a. Spacecraft component weights are given in Table A-7.(The total S/C propellant weight is denoted by W_p). Orbit insertion ΔV's are taken from Table A-37, Section D of this report. These ΔV's are minimum performance requirements for orbiter missions which make use of Titan pumping and cranking maneuvers. Using these ΔV's the orbited payload (bus + lander/penetrator/probe or just bus) was "backed up" to pre-SOI (where any pre - SOI deflection was accounted for) and then to Earth (to include 100 m/s for mid-course correction).

1) <u>Mariner Based Missions</u> - Required throw weights are shown in Table A-8 and Figure A-10 for lander, probe and penetrator missions flown with a 700 kg Mariner-based orbiter spacecraft in the years 1983, 1985, 1988, 1992, 1996 and 1998. (A typical throw weight derivation is shown in Table A-9). These are to be compared with the Shuttle/IUS and Shuttle/Tug capabilities. The orbiter ΔV budget is .3 km/s plus the required powered swingby or multiple burn insertion ΔV for the particular year. Open symbols are for lander, probe and penetrator deployment before SOI. Solid symbols (in 1988) are for lander and probe deployment from Saturn orbit. All the latter are for an Earth storable retro propulsion system (Isp = 295). The improvement expected with space storable (SS) propellants (Isp = 375) is also shown. Note that the probe (and therefore penetrator) mission is possible in 1983, 1985, 1996 and 1998 with the Tug, and in 1988 with the Tug and SS propellants. The same missions are marginal in 1983 and 1985 with SS propellants and the IUS. Lander missions in 1983, 1985 and 1998 require the Space Tug, and those in 1988, 1992 and 1996 exceed the capability of even the Space Tug.

A-23

Table A-6   Representative Direct Ballistic Missions

Year	Launch Date	Arrival Date	Flight Time	VHS	RA	DEC	C_3
1983 (II)	01/06/83	05/12/90	7.4 years	5.31	75.91	- 4.16	108.5
1985 (I)	01/23/85	02/03/91	6.0 years	5.30	94.84	-14.81	108.5
1988 (I)	02/28/88	05/07/93	5.2 years	5.88	112.15	-21.90	119.0
1992 (I)	04/16/92	11/27/96	4.6 years	6.50	124.88	-14.34	131.0
1996 (II)	06/24/96	03/27/04	7.8 years	6.48	62.59	- 6.83	110.5
1998 (II)	07/07/98	10/16/04	6.3 years	5.86	74.95	4.02	107.5

Table A-7 Spacecraft Weight Summary

	Pioneer Based (kg)	Mariner Based (kg)
Orbiter at Launch	300	700
Retro Unit	$.2\ W_p + 50$	$.2\ W_p + 50$
Probe	100	100
Orbiter Support Structure for Probe	10	10
Probe Bioshield	25	25
Lander	280	280
Orbiter Support Structure for Lander	28	28
Lander Bioshield	60	60
Penetrator	92	92
Penetrator Launcher	8	8
Orbiter Support Structure for Penetrator	10	10
Spacecraft to Launch Vehicle Adaptor	36	60

Table A-8
Throw Weight Requirements for MSO: Pre-SOI Deployment

LAUNCH YEAR	LANDER	PROBE	PENETRATOR
1983	1953.1	1712.6	1687.1
1985	1946.4	1705.8	1680.4
1988	2241.0	2000.4	1975.0
1992	2620.9	2380.4	2354.9
1996	2237.4	1996.8	1971.4
1998	1992.2	1841.7	1816.2

Table A-9
Throw Weight Derivation for Probe Mission in 1985

	MSO	PSO
Orbit Insertion ΔV (Km/sec)	1.267	1.267
Total ΔV (Km/sec)	1.567	1.567
$W_{Propellant\ Inerts}$	176.1	108.8
Usable Payload	700.0	300.0
Gross Payload	876.1	408.8
Wp, In-Orbit Trims	15.3	7.1
Inserted Orbiter	891.4	415.9
Wp, SOI	538.9	251.4
Pre-SOI Orbiter	1430.3	667.3
Wp, Deflection	25.0	11.6
Probe	100.0	100.0
Bioshield	12.5	12.5
Orbiter/Probe Struct.	10.0	10.0
S/C Pre-Sep.	1577.8	801.4
Wp, MCC	55.5	28.2
S/C Pre-MCC	1633.3	829.6
L/V Adapter	60.0	36.0
Bioshield Cover	12.5	12.5
Throw Weight	1705.8	878.1
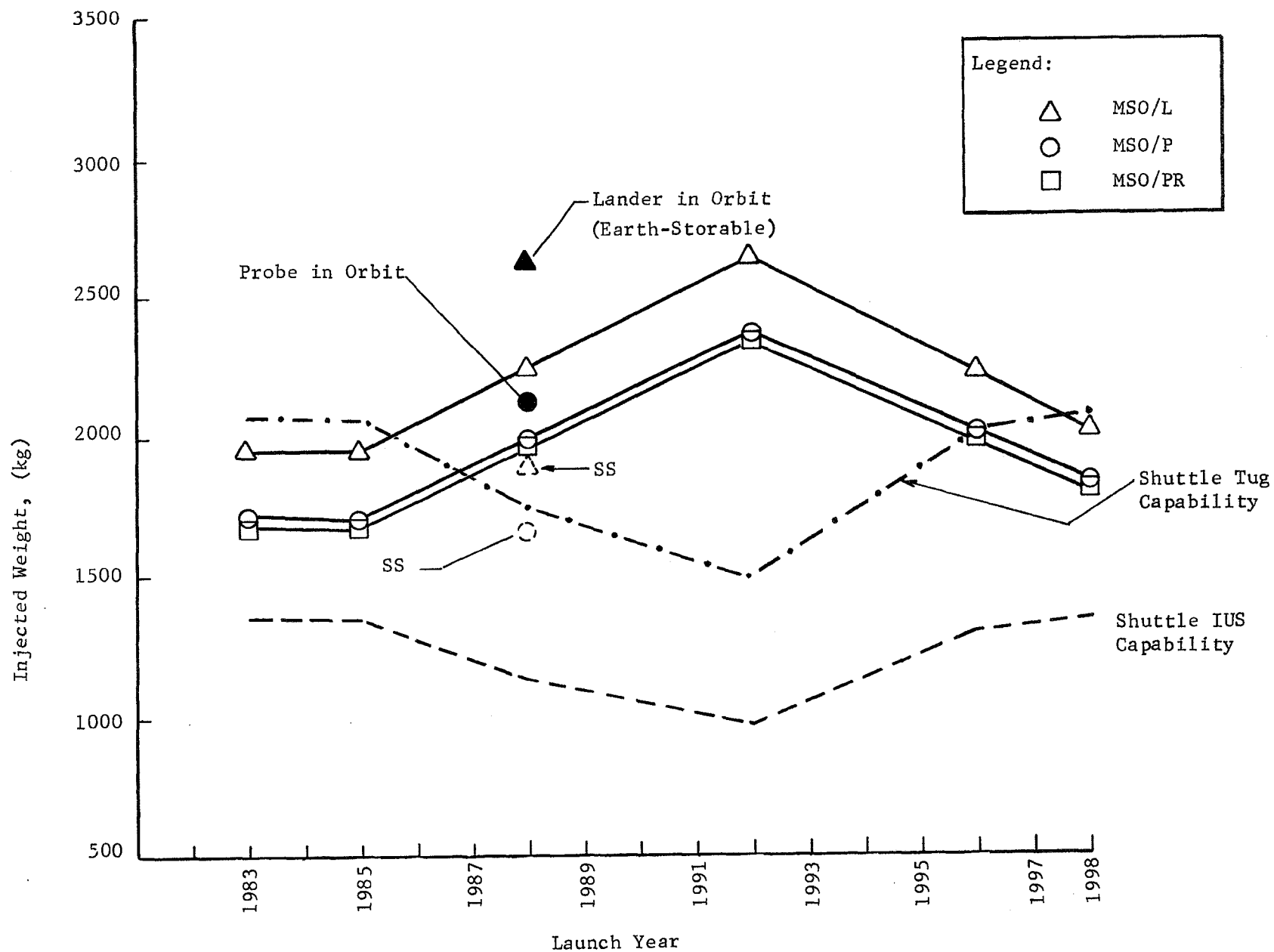
Fig. A-10 Mariner-Based Missions

2) <u>Pioneer Based Missions</u> - Table A-10 and Figure A-11
point out that all Pioneer-class lander, probe and penetrator missions
are possible with the Shuttle/Tug. The tug will also allow Titan
landings from Saturn orbit for all years but 1992 (solid symbols).
Probe and/or penetrator missions are possible with the IUS in all years
but 1992. Lander missions on the other hand can be flown with the
IUS in only 1983, 1985, 1996 and 1998 utilizing Earth storable propellants.
With SS propellants, IUS/lander missions can also be flown in 1988.

Table A-10
Throw Weight Requirements for PSO: Pre-SOI Deployment

LAUNCH YEAR	LANDER	PROBE	PENETRATOR
1983	1122.2	882.1	856.2
1985	1118.7	878.6	852.7
1988	1256.5	1016.4	990.5
1992	1433.7	1193.6	1167.7
1996	1254.7	1014.1	988.7
1998	1182.3	941.7	916.2

2. <u>Jupiter Swingby Trajectories to Saturn</u> - The Jupiter swingby
technique takes advantage of the relative alignments between Earth,
Jupiter and Saturn to allow trajectories to Saturn to be flown with
launch energies equivalent to Jupiter trajectories. The swingby or
gravity assist technique is well known and was used in the Mariner-
Venus-Mercury mission and is being planned for the MJS 1977 mission.
Jupiter-Saturn alignments that permit swingby missions occur once every
22 years and the next opportunity of interest is not until the late
1990's period. Analysis has shown considerable increase in both throw
weight capability and inserted payload capability as well as a reduction
in flight time for swingby trajectories compared with ballistic flights.
The only difficulty is the relatively small number of launch opportunities
in the interval of interest.

A-28
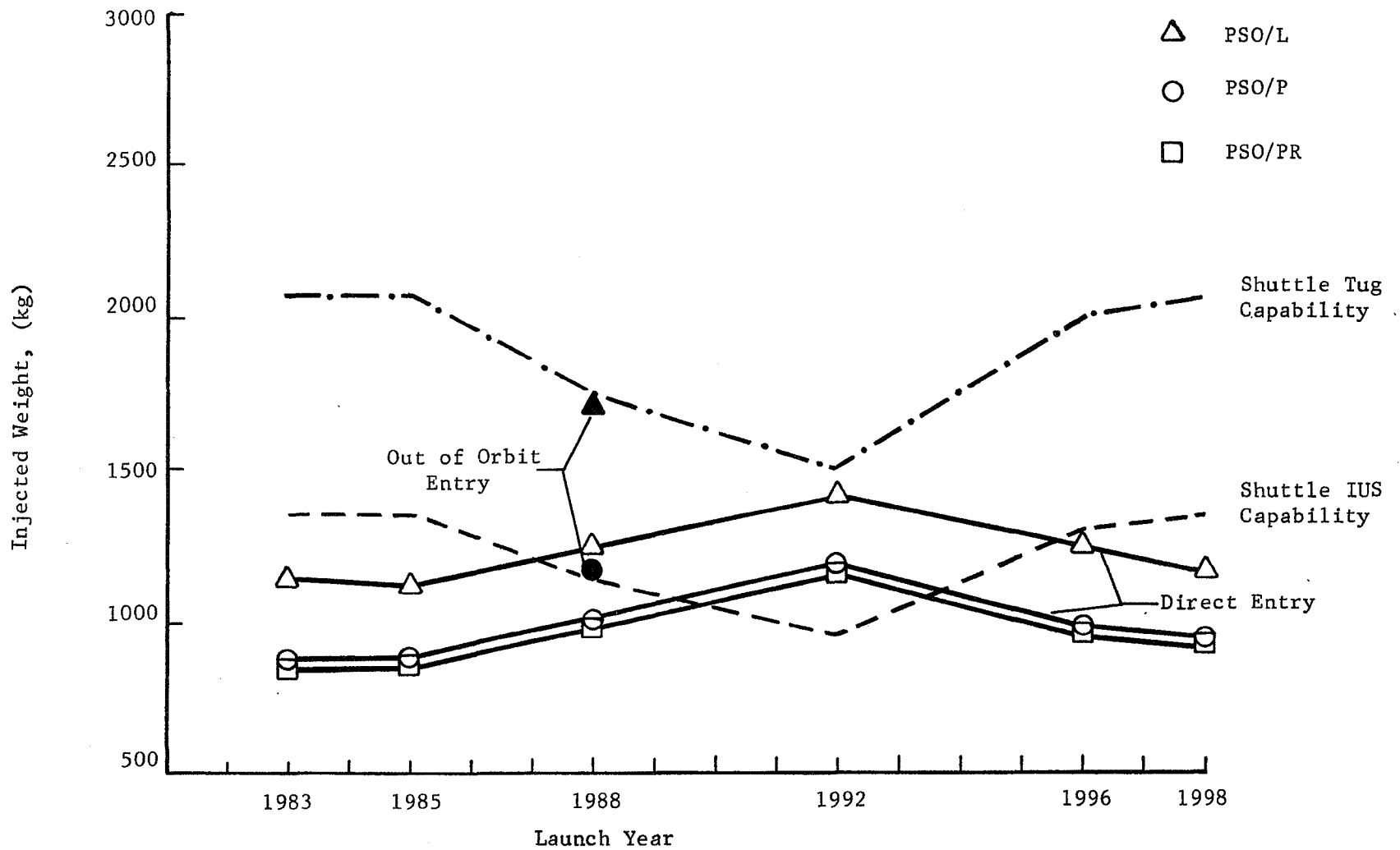
Fig. A-11 Pioneer-Based Missions

a. <u>Jupiter Swingby Performance Capabilities</u> - In this study
the years 1996 through 2000 were analyzed to ascertain performance
advantages over non-swingby years for Titan missions involving a Saturn
orbiter. These analyses were done early in the study when Shuttle IUS
and Shuttle Tug performance projections were in a considerable state of
flux. For that reason the basic comparison of ballistic and swingby
trajectory capabilities was made on the bases of Titan IIIE/Centaur
performance. Later, comparative data were developed for IUS and Tug
launch systems. It was found that the best swingby year is 1998 with
1999 a close second. In 1998 a Titan IIIE/Centaur launch vehicle is
capable of inserting 710 kg of payload into an elliptical orbit about
Saturn with a period of 32 days and periapsis radius equal to five
Saturn radii ($5R_s$). This orbit is used so that a direct comparison with
non-swingby results can be made. The flight time corresponding to the
710 kg inserted weight is $5\frac{1}{2}$ years. The best non-swingby Titan IIIE/
Centaur result is 478 Kgms in 1985 - also with a $5\frac{1}{2}$ year flight time.
Utilizing the Jupiter swingby opportunity with the Titan IIIE/Centaur
affords a larger orbiter payload (710 kg) than the IUS is capable of
yielding with the best 1985 direct trajectory (594 kg). The space tug
performance with non-swingby trajectories, however, exceeds the Titan
IIIE/Cenatur swingby value by as much as 200 kg. The additional space
tug launch performance may be used in conjunction with the Jupiter
swingby trajectory mode to reduce the flight time to Saturn, i.e., a
S/C mass of 710 kg can be placed in Saturn orbit with a flight time of
only $3\frac{1}{2}$ years.

In the data presented here, Jupiter swingby trajectories to
Saturn were targeted for the years 1996 through 2000. Flight times as
high as $6\frac{1}{2}$ years were considered with launch and arrival dates separated
by 15 days and 60 days respectively. The minimum allowable closest
approach distance to Jupiter was 2 R_j. The launch energy (C_3) and hyper-
bolic excess speed at Saturn (VHP) were used to compute an injected weight
from Earth and an orbited payload mass in Saturn orbit. A Saturn orbit

of 32 day period and periapsis radius equal to 5 R_s was selected so that an orbited weight comparison could be made with the direct ballistic results of Reference A-3. In addition to the insertion ΔV, the total maneuver budget allowed 100 m/s for midcourse maneuvers and 100 m/s for finite burn loss in SOI. The orbiter engine I_{sp} was taken to be 280.

The inserted weight results were output in tabular format on a launch/encounter grid and then converted to weight-in-orbit vs. launch date with fixed flight time contours. (See Figures A-12 and A-13). Figure A-12, for 1998, shows the maximum inserted weight for each flight time contour increasing with flight time to a maximum of 780 Kgms for a 6½ year time-of-flight. The requirement for a 15 day launch period reduces this to 736 Kgm. Successively shorter flight times correspond to ever widening reductions in the maximum orbited weight. The curves of Figure A-12 and A-13 along with similar type data for injected weight can be used to obtain the weight-in-orbit vs. flight time results of Figures A-14 and A-15. The C_3 values are shown on the injected weight profile (WINJ) and VHP's on the orbited weight curve (WINORB). The C_3 and VHP magnitudes are considerably smaller than those for the direct ballistic trajectories. (The latter being at best in the 105 Km^2/sec^2 and 5.2 Km/sec range respectively.) Figures A-14 and A-15 are for single launch dates (6/3/98 and 7/4/99 respectively). Injected weights of the order of 1200 Kgm far exceed the non-swingby capability of 900 Kgm.

When the launch periods are opened up to 10 days and 15 days the maximum weight in orbit decreased by at most 6%. (Figure A-16) Figure A-17 summarizes the swingby results for each of the launch years - 1996 through 2000. The peak year is 1998 with 1999 yielding only 40 Kgms or so less inserted payload. Figure A-18 illustrates how the swingby and direct missions compare during the years 1996 to 2000. Note that in 1997, a very favorable year for the direct
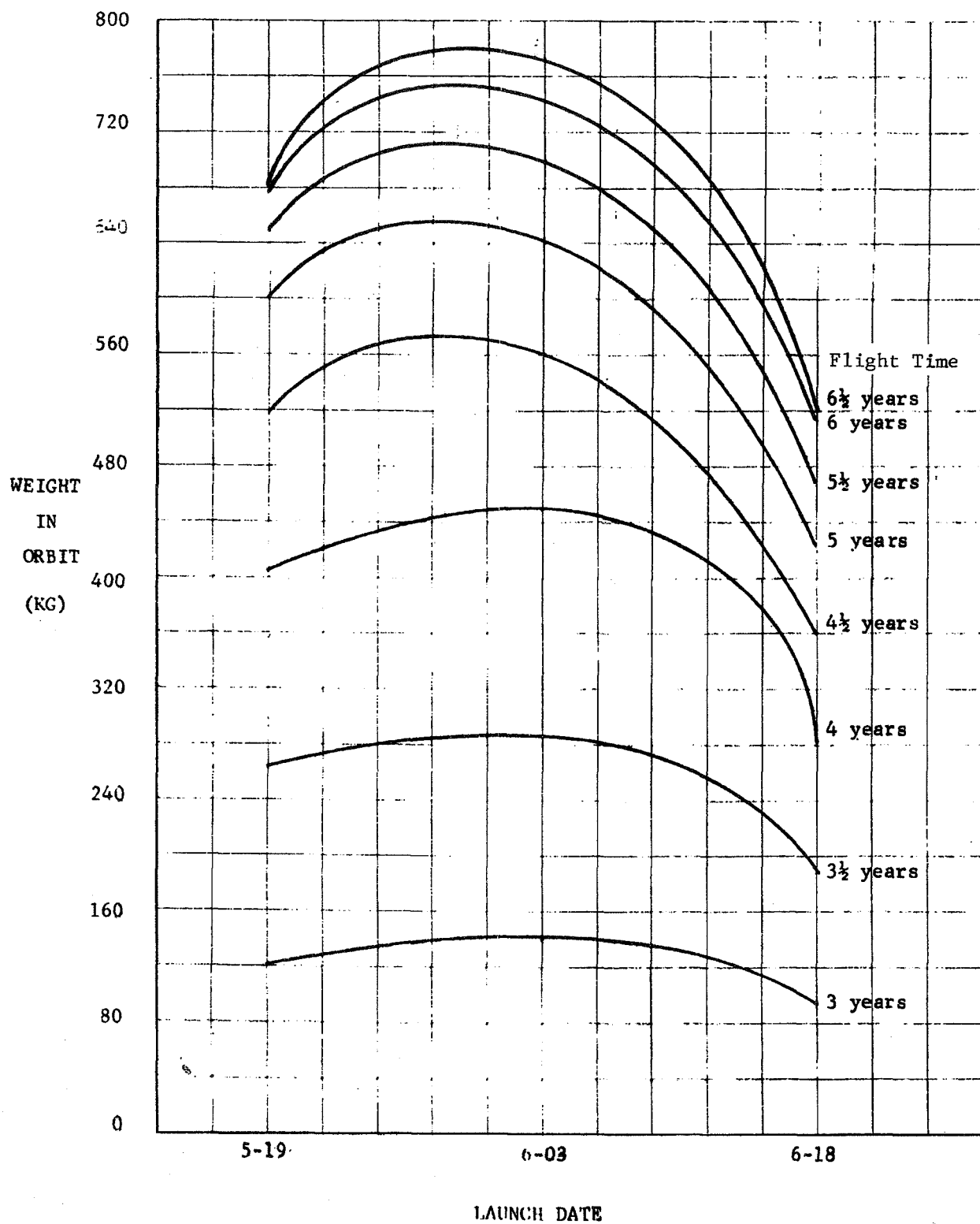
Fig. A-12 1998 Jupiter Swingby To Saturn

A-32
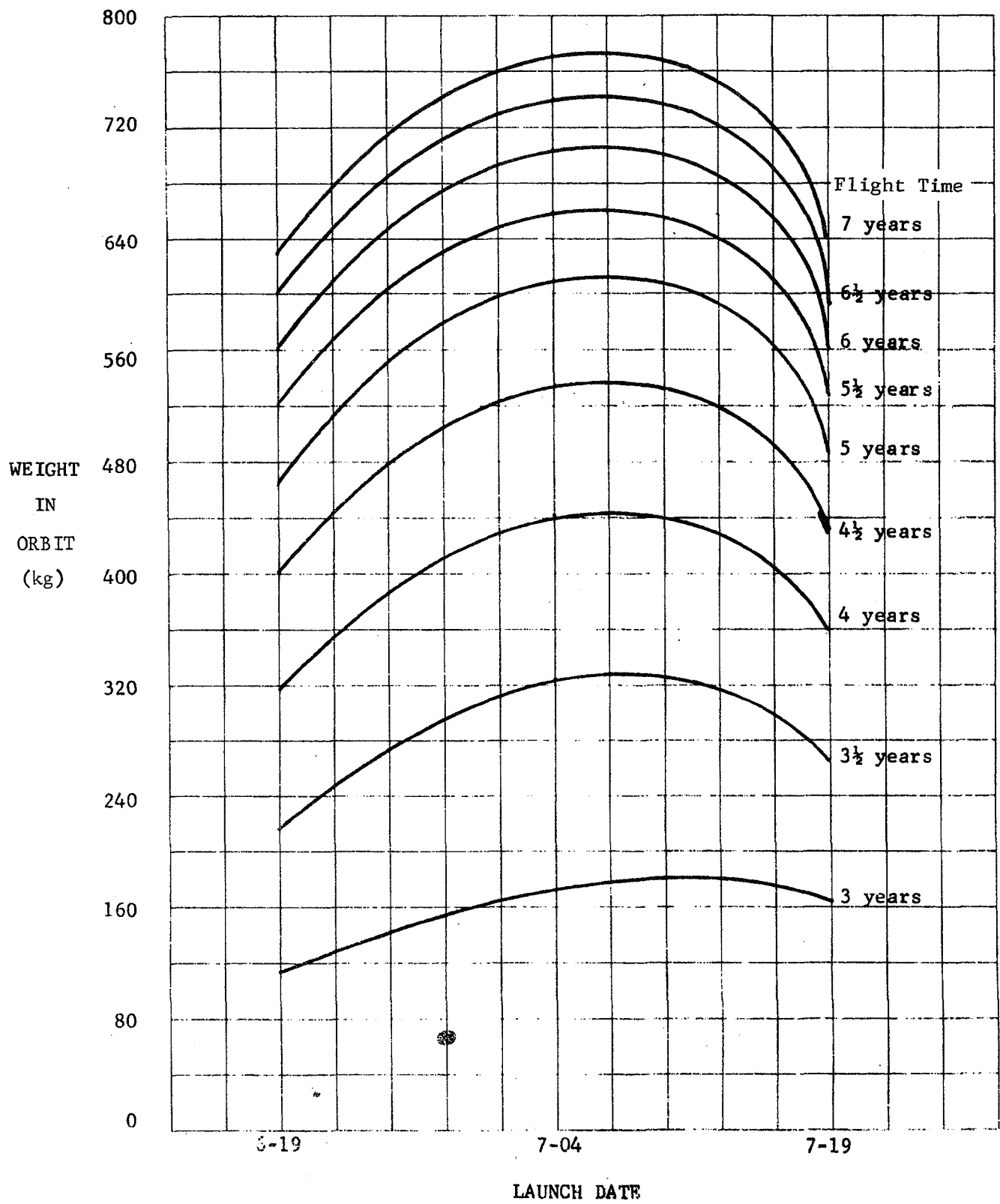
Fig. A-13 1999 Jupiter Swingby To Saturn

A-33
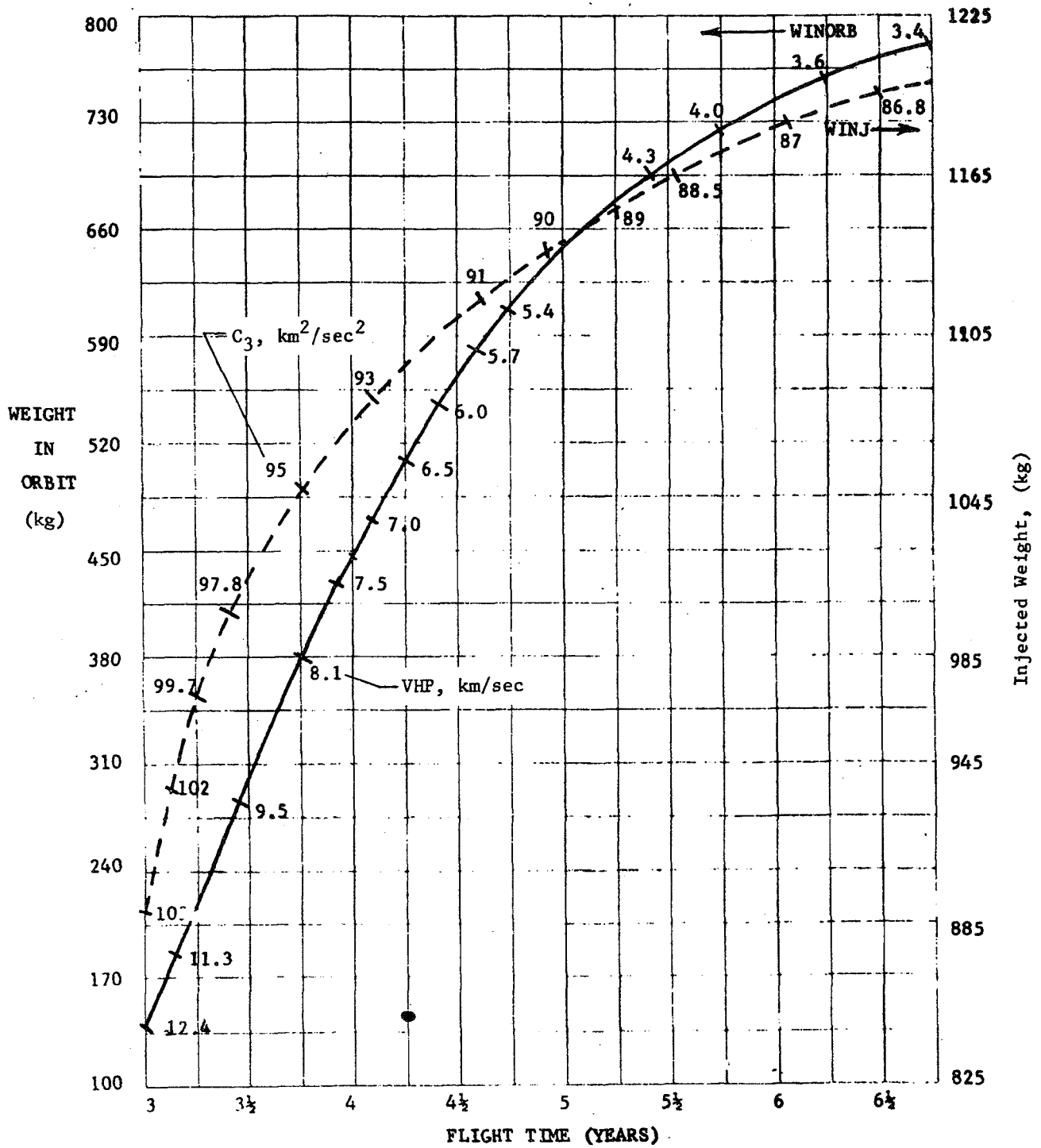
Fig. A-14 1998 Jupiter Swingby
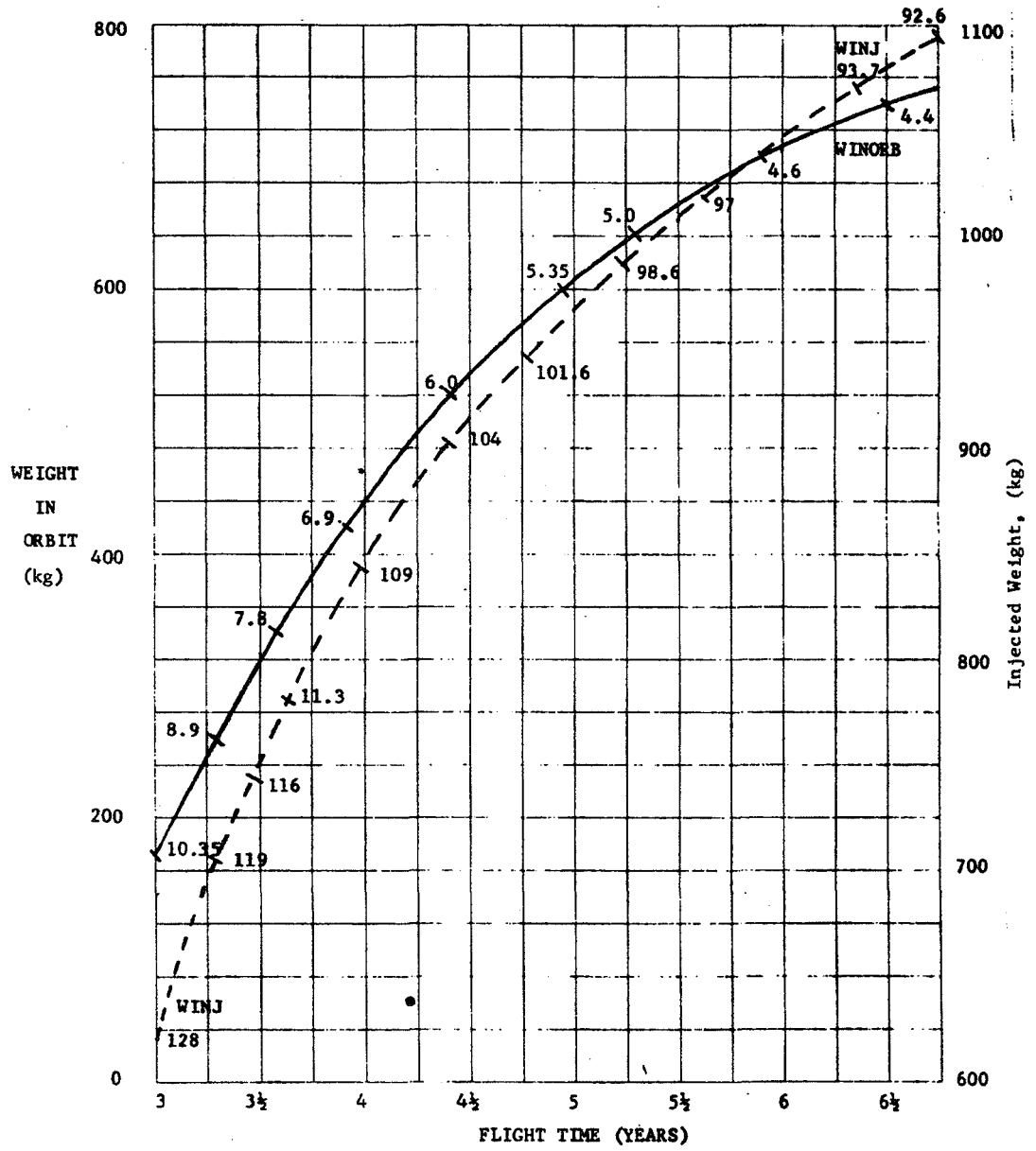
Fig. A-15 1999 Jupiter Swingby

A-35
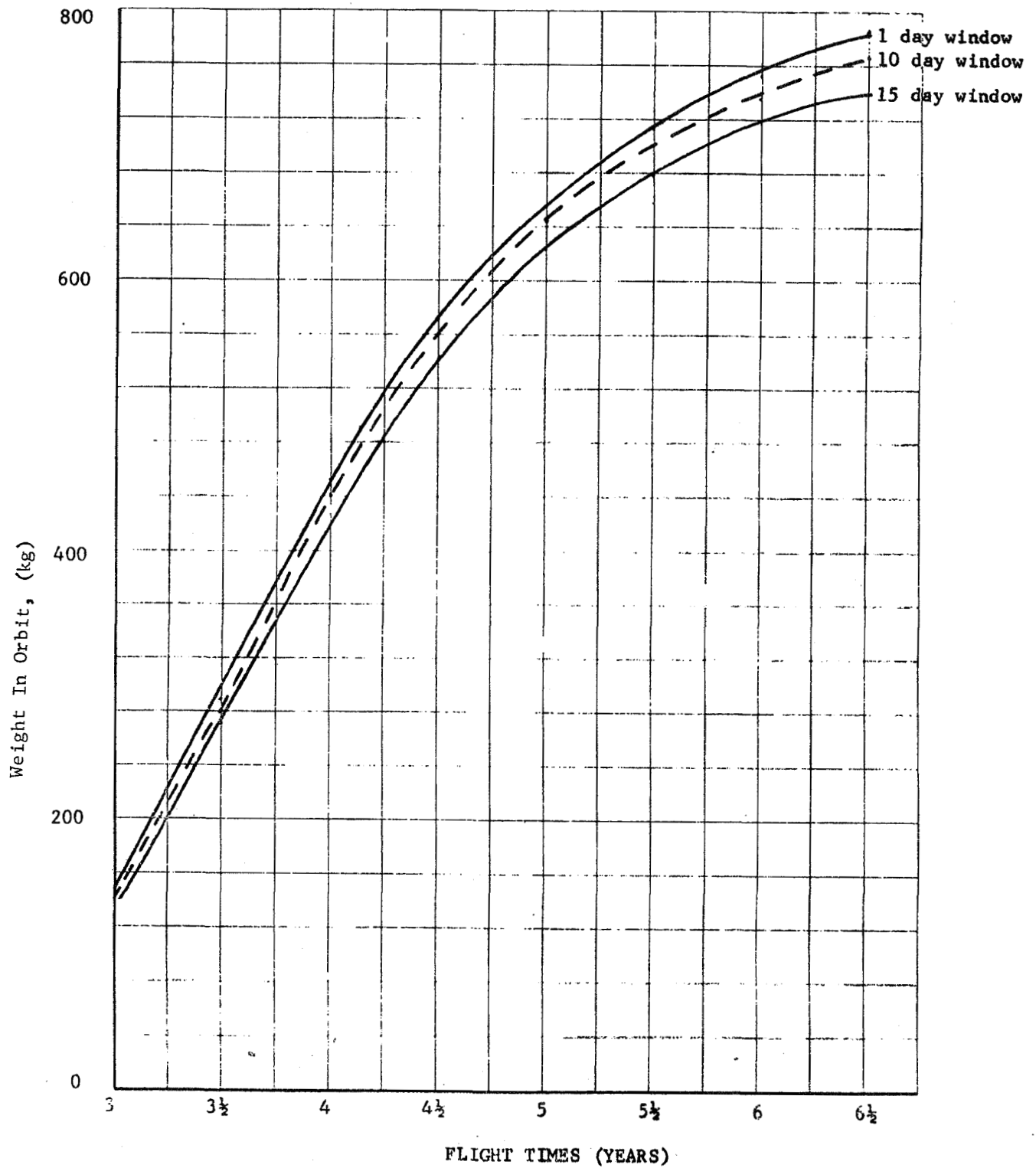
Fig. A-16 Effect of Varying Launch Window Duration - 1998 Jupiter Swingby

A-36

15 DAY WINDOW   JUPITER SWINGBY
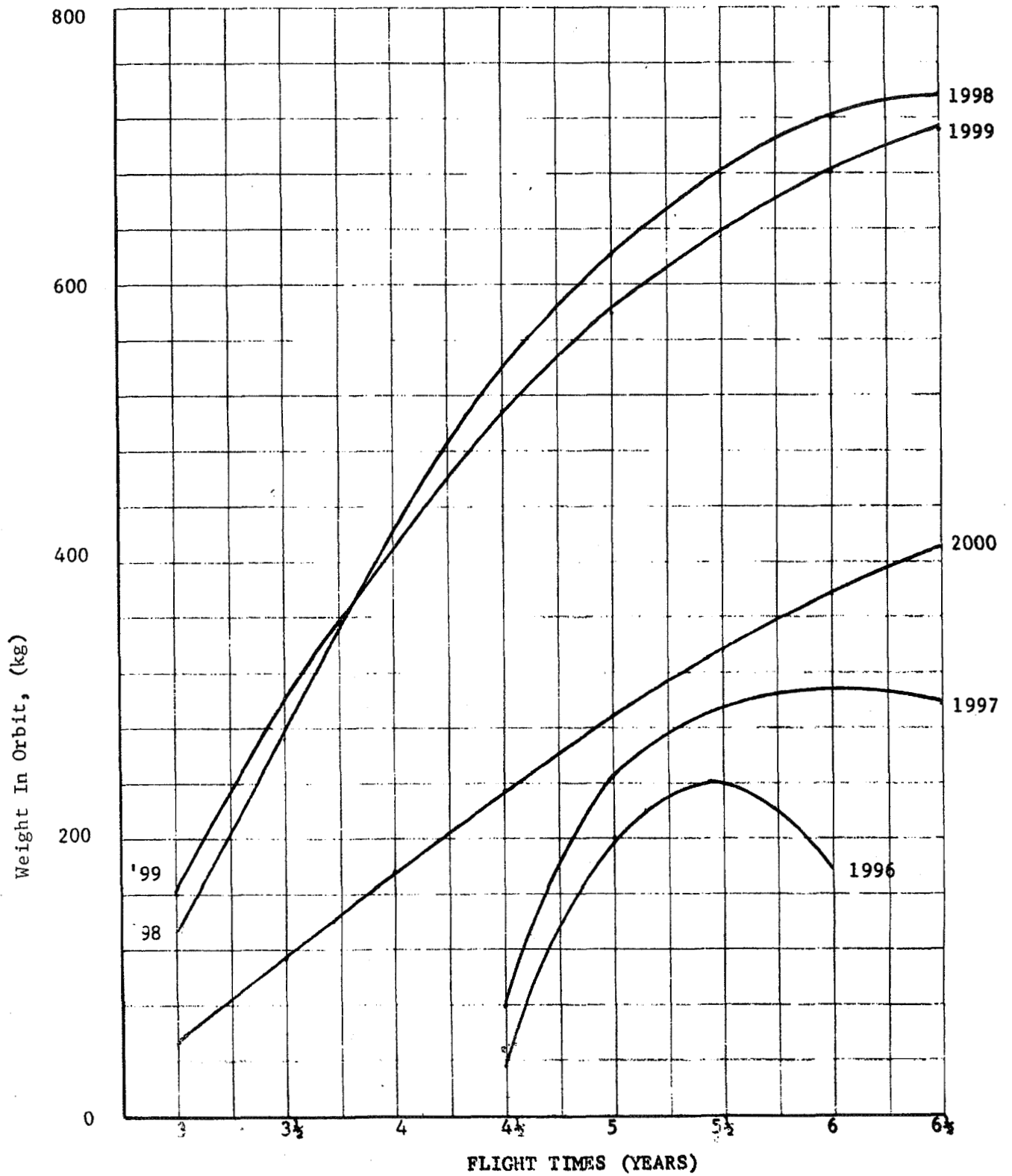
Fig. A-17 Jupiter Swingby
A-37
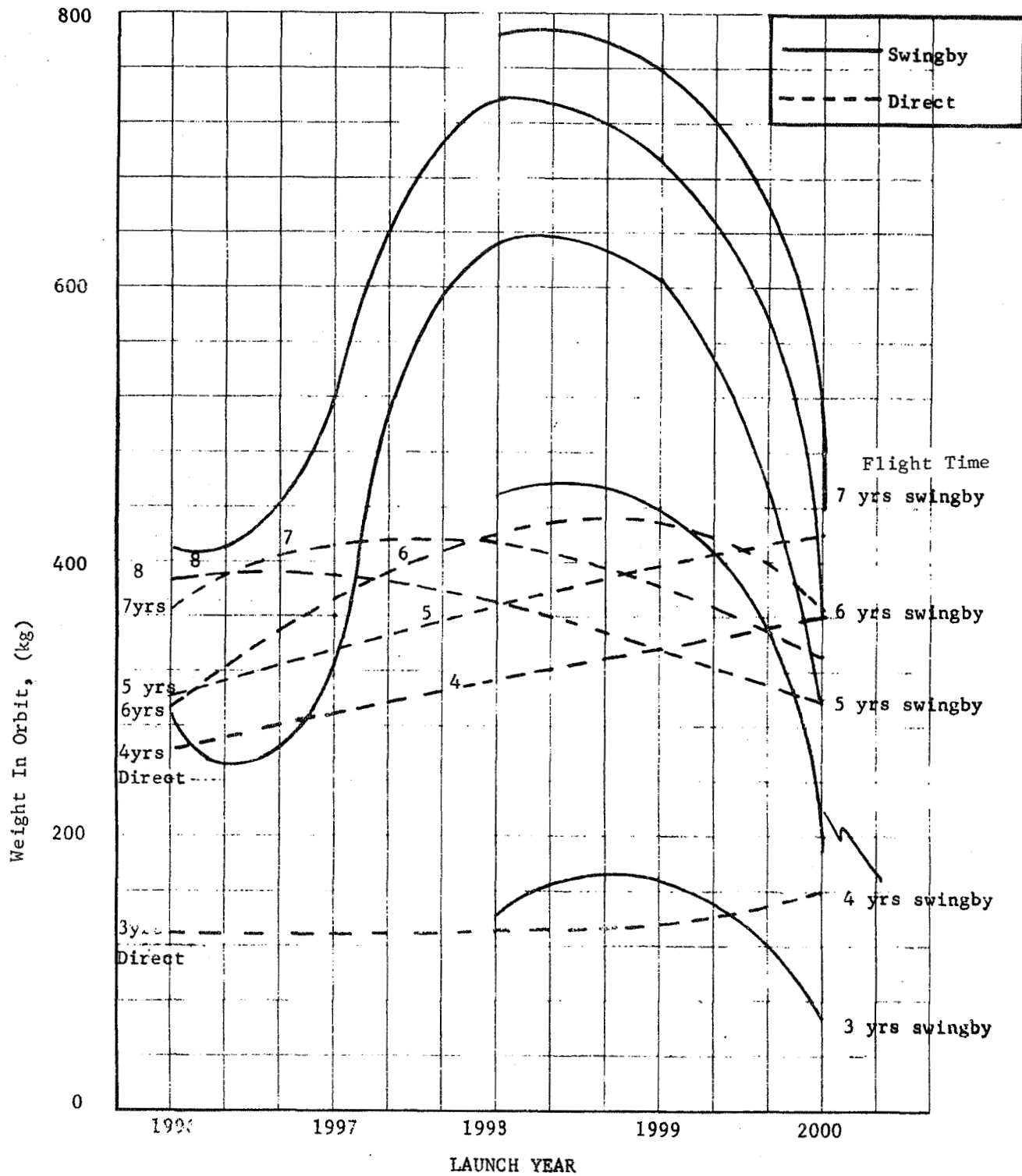
Fig. A-18 1996 to 2000 Jupiter Swingbys

trajectory mode, the 5, 6, 7 and 8 year missions have larger inserted payloads than the 5 year swingby. The 6 year swingby, however, achieves much higher levels of performance. Finally, Figures A-19 and A-20 demonstrate the added injected weight and inserted payload capability available with the IUS and space tug. The IUS is good for 500 Kgm more injected weight than the Titan IIIE/Centaur but the tug injects 1000 Kgm more than the IUS. The inserted weight picture is not as dramatic because of the small inserted period. The tug can be used to achieve more inserted payload (almost 1700 Kgms) or it can be used to shorten the flight time to Saturn with reduced payloads.

3. Δ VEGA Trajectories to Saturn - The Δ VEGA trajectory mode is a new flight technique developed at Martin Marietta, which utilizes the gravity field of Earth in a swingby mode to reduce the energy requirements for missions to Saturn. The basic technique as diagrammed in Figure A-21 launches from earth (E_L) with a low C_3 ($\approx 27 \frac{km^2}{sec^2}$) into heliocentric trajectory with aphelion selected to produce an orbit with period near 2 or 3 years. A retro maneuver (ΔV_a) is performed near aphelion, targeted to produce an Earth swingby (ESB) either before or after completion of the orbit. The possibility exists that an Earth swingby maneuver (ΔV_{ESB}) will be required to reach specific target objectives. This need depends on the period of the ΔVEGA orbit (2 or 3 years) designated in this report as 2^- or 3^- and the target planet heliocentric radius. An Earth swingby ΔV is required for Saturn trajectories with 2 year phasing orbits.

The significant advantages of this technique are increased payload, approximately triple that of a ballistic trajectory, and launch opportunities every year. Although phasing periods of two or three years are required to achieve the necessary planetary alignments for optimum performance, significant performance advantages can be realized without increasing total flight time(see Page A-46).

a. ΔVEGA Performance Capabilities - A comparison of the direct ballistic and ΔVEGA techniques was made for a 1983 Titan mission. The

1998 JUPITER SWINGBY 15 DAY WINDOW

INJECTED WEIGHT - DEPENDENCE ON LAUNCH VEHICLE
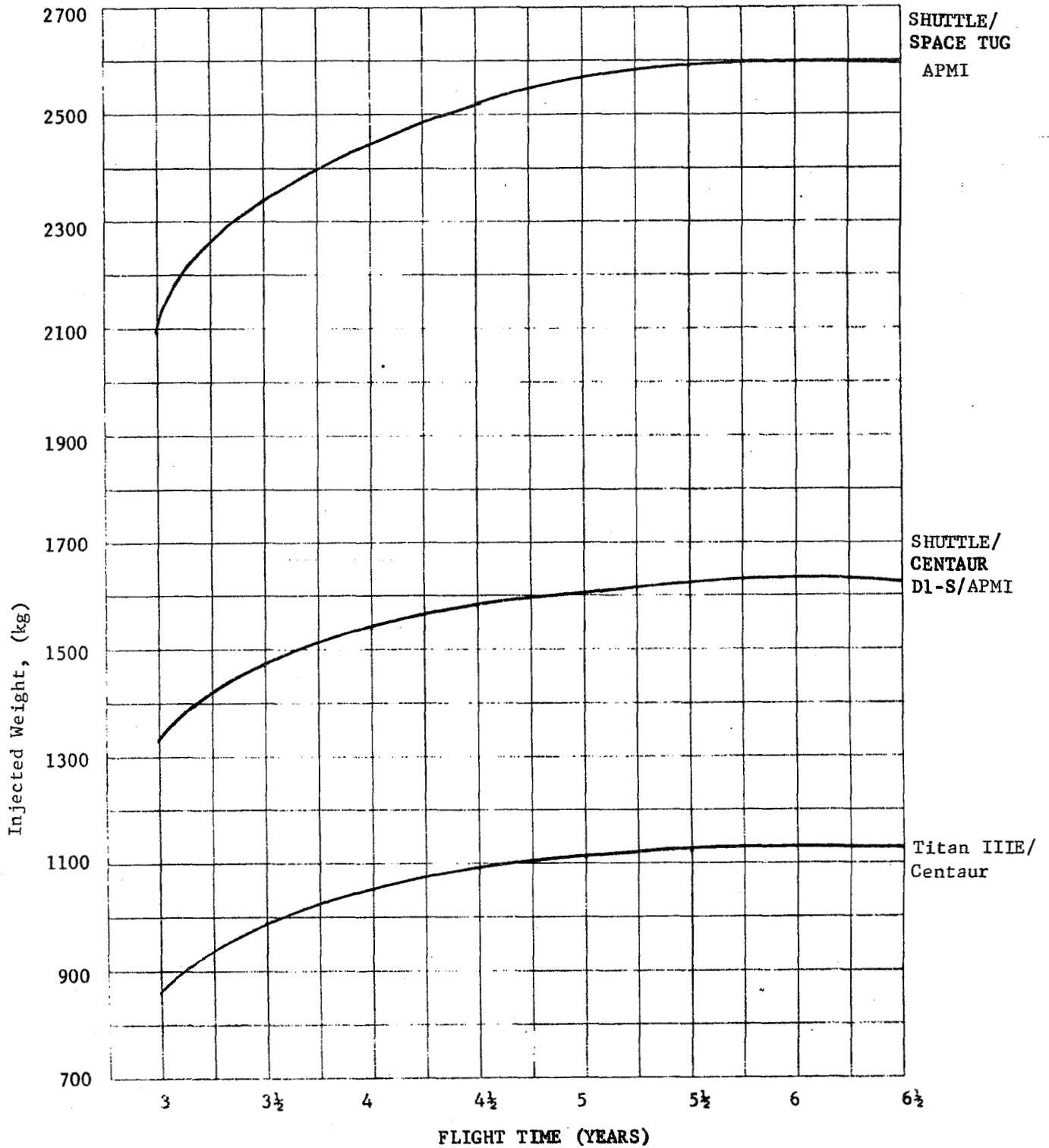
Fig. A-19 1998 Jupiter Swingby- Injected Weight

WEIGHT IN ORBIT DEPENDENCE ON LAUNCH VEHICLE
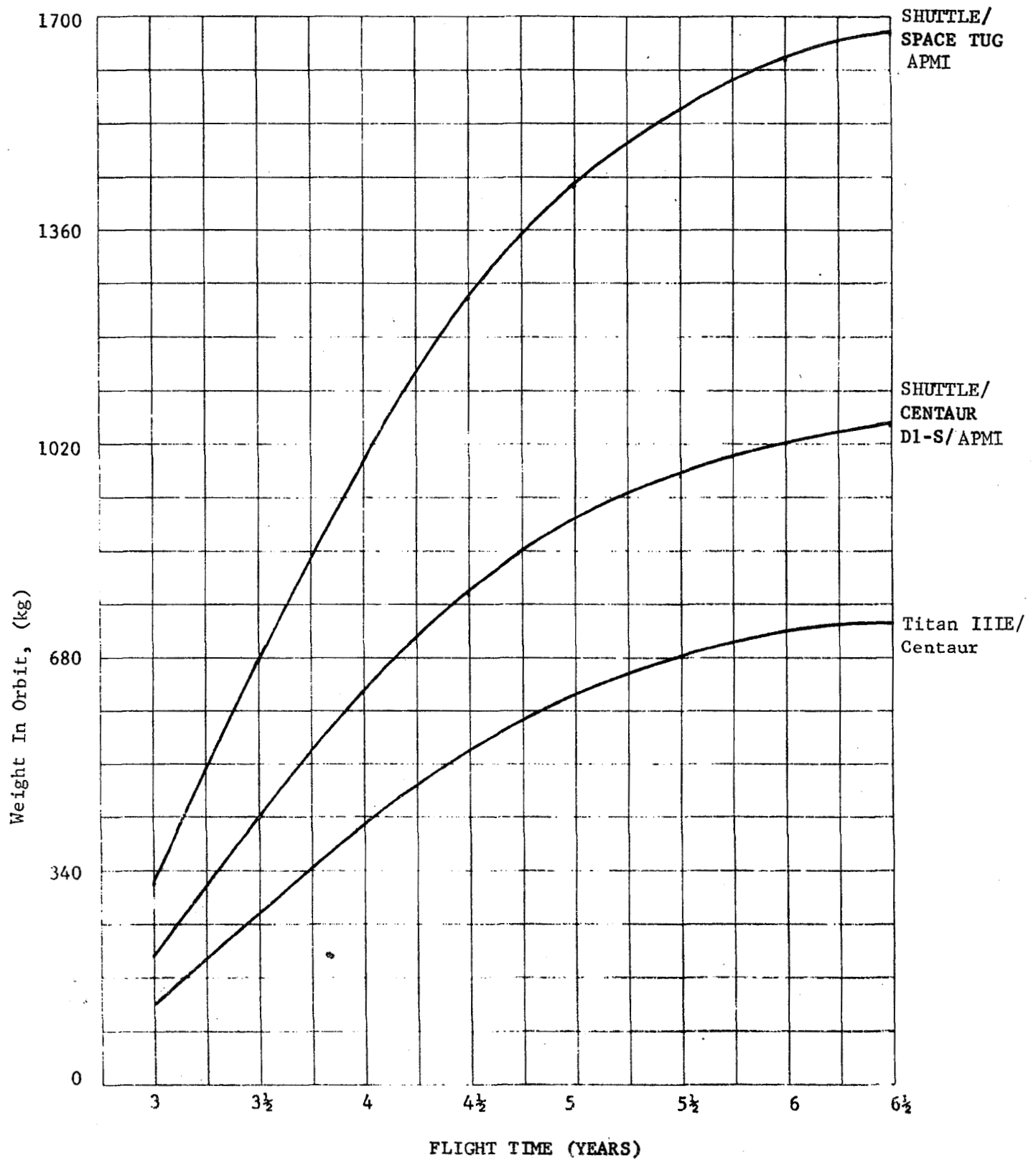
Fig. A-20 1998 Jupiter Swingby- Weight in Orbit

ΔV_a

ΔV_{SB}

E_{2_a}

E_L

E_{2_b}

ΔV_{SB}

To Saturn
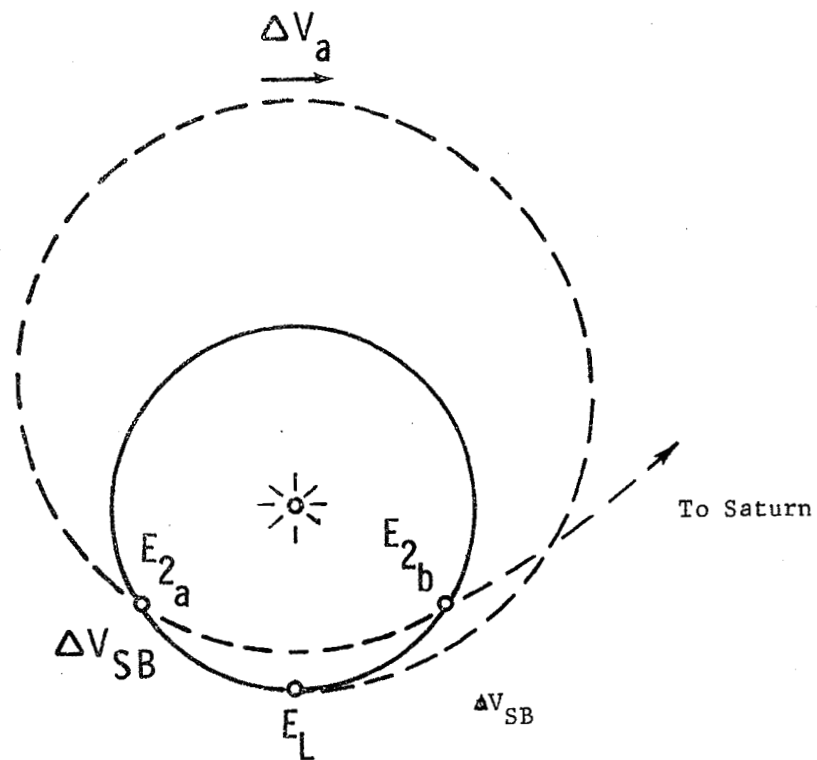
E_L = Earth Launch

E_{2_a} = Earth Re-encounter Option, n^- years after Launch

E_{2_b} = Earth Re-encounter Option, n^+ years after Launch

Fig. A-21 ΔVEGA Flight Techique

Δ VEGA optimization program was used to determine the Earth launch date which minimizes the total maneuver ΔV ($C_3 + \Delta V_a + \Delta V_{SB}$) for a prescribed flight time to Saturn. By varying flight time, Tables A-11 (for 2^-) and A-12 (for 3^-) were developed. Weights are presented for the Titan IIIE/ Centaur (TE364-4) launch vehicle. The final payload is placed in a 4 R_S x 32 day orbit about Saturn with a retro motor Isp of 295. In the tables,

Flt Time	=	Total flight time (years) from Earth launch to Saturn encounter
C_3	=	Earth launch energy (km^2/sec^2)
W_{INJ}	=	Weight injected at Earth launch (kg)
$\Delta V_a + \Delta V_{SB}$	=	Aphelion + swingby velocity change (km/sec)
W_{ENC}	=	Weight at encounter with Saturn (kg)
VHS	=	hyperbolic excess speed at Saturn (km/sec)
ΔV_{SOI}	=	velocity change to achieve Saturn orbit (km/sec)
W_{ORB}	=	orbited payload (kg)
DLA	=	declination (equatorial) of launch asymptote (degrees)

For the 7 year 3^- case, ΔV_{SB} did indeed go to zero but the minimum total of $\Delta V_a + \Delta V_{SB}$ occurred for the 2/24 launch date which happens to have a non-zero ΔV_{SB}.

Several trajectory related quantities from Tables A-11 and A-12 are presented graphically in Figure A-22. It is noted that C_3 varies slowly with flight time and is primarily a function of the period of the ΔVEGA orbit, being larger for the 3^- type because of the higher aphelion radius. While C_3 is larger, the sum of $\Delta V_a + \Delta V_{SB}$ (essentially only ΔV_a for the 3^- case) is smaller. As will be seen later, the 2^- and 3^- performance for the 1983 mission is very similar. The VHS at Saturn does minimize to very reasonable levels near 5.3 km/sec.

Figure A-23 compares the weights from Tables A-11 and A-12 with the direct ballistic weights. Type I and II performance curves are shown for weight at encounter (solid line) and weight in-orbit (broken line).

Table A-11 2⁻ ΔVEGA: Weight Computations

Flt Time	Launch Date	C_3	W_{INJ}	$\Delta V_a + \Delta V_{SB}$	W_{ENC}	VHS	ΔV_{SOI}	W_{ORB}	DLA
6	02/19/83	26.16	3350	1.234 1.300 2.534	1394	7.55	2.090	676.5	−20.9°
7	02/24/83	26.34	3350	0.933 0.828 1.761	1822	5.87	1.498	1085.0	−21.8°
8	03/01/83	26.43	3350	0.898 0.753 1.651	1892	5.29	1.325	1196.0	−22.6°
9	03/06/83	26.30	3350	0.955 0.810 1.765	1819	5.33	1.336	1146.0	−23.0°
10	03/16/83	26.93	3350	0.977 0.867 1.844	1770	5.64	1.428	1080.0	−23.4°

Table A-12 3⁻ ΔVEGA: Weight Computations

Flt Time	Launch Date	C_3	W_{INJ}	$\Delta V_a + \Delta V_{SB}$	W_{ENC}	VHS	ΔV_{SOI}	W_{ORB}	DLA
7	02/24/83	47.82	2200	0.425 0.352 0.777	1681	7.67	2.137	802.7	−21.7°
8	02/24/83	47.73	2200	0.469 0.0 0.469	1870	5.92	1.514	1107.7	−21.7°
9	03/01/83	47.85	2200	0.467 0.0 0.467	1871	5.31	1.331	1180.7	−22.4°
10	03/06/83	47.95	2200	0.527 0.0 0.527	1833	5.35	1.342	1152.3	−23.0°
11	03/16/83	48.58	2200	0.533 0.0 0.533	1829	5.67	1.437	1112.6	−23.4°
12	03/21/83	48.19	2200	0.754 0.0 0.754	1694	6.16	1.591	977.0	−23.4°
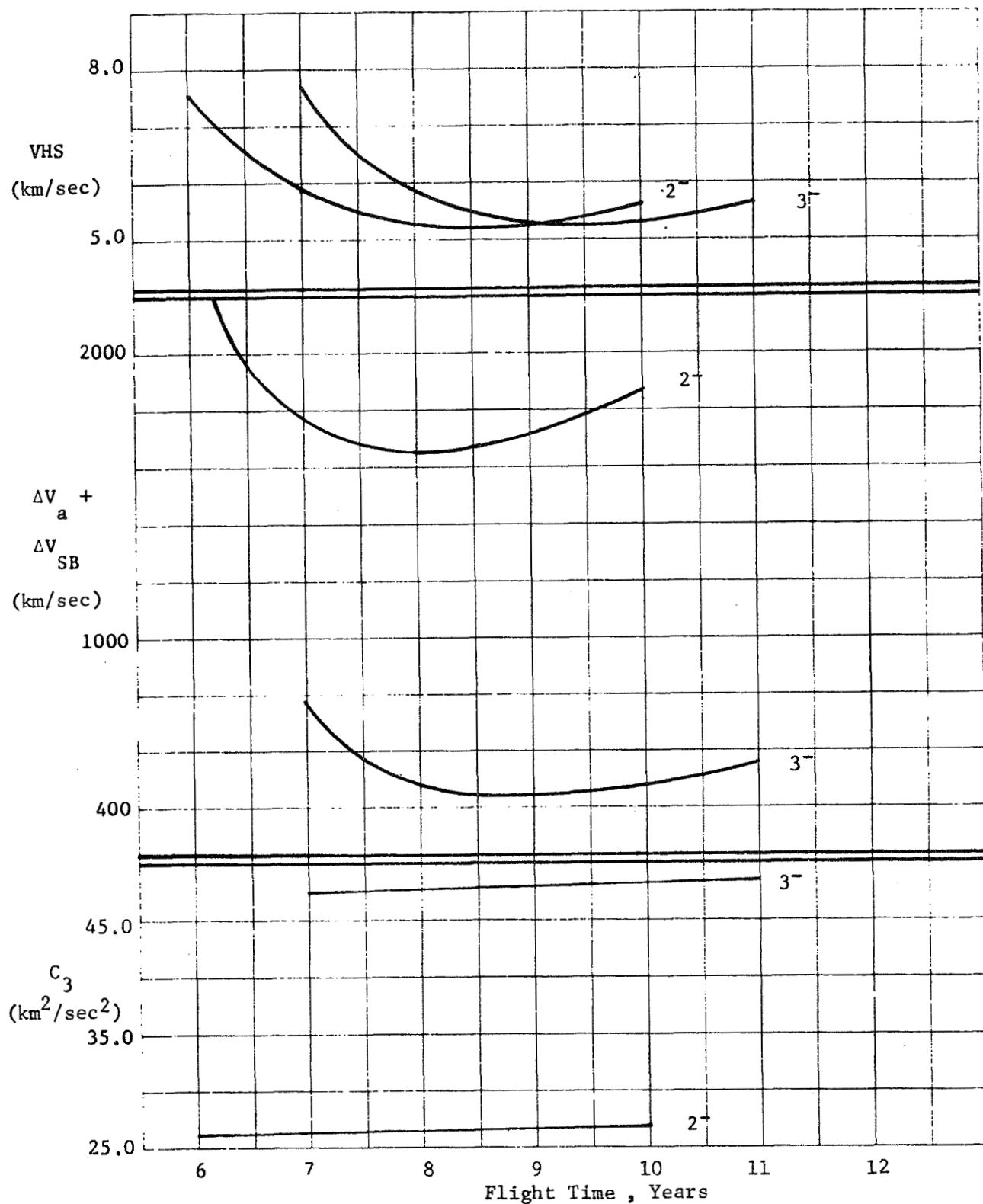
Fig. A-22 ΔVEGA/Saturn/1983 Launch Period = 1 Day

Weight, kg

ΔVega, $3-$

ΔVega, $2-$

1500

Legend:
——— Weight at Encounter
– – – Weight in Orbit

Retro $I_{sp} = 295$
T3E/Centaur/TE364-4

ΔVega, $3-$

ΔVega, $2-$

1000

Direct Type II

Direct, Type I

500

Direct, Type II

Direct, Type I

6   7   8   9   10   11
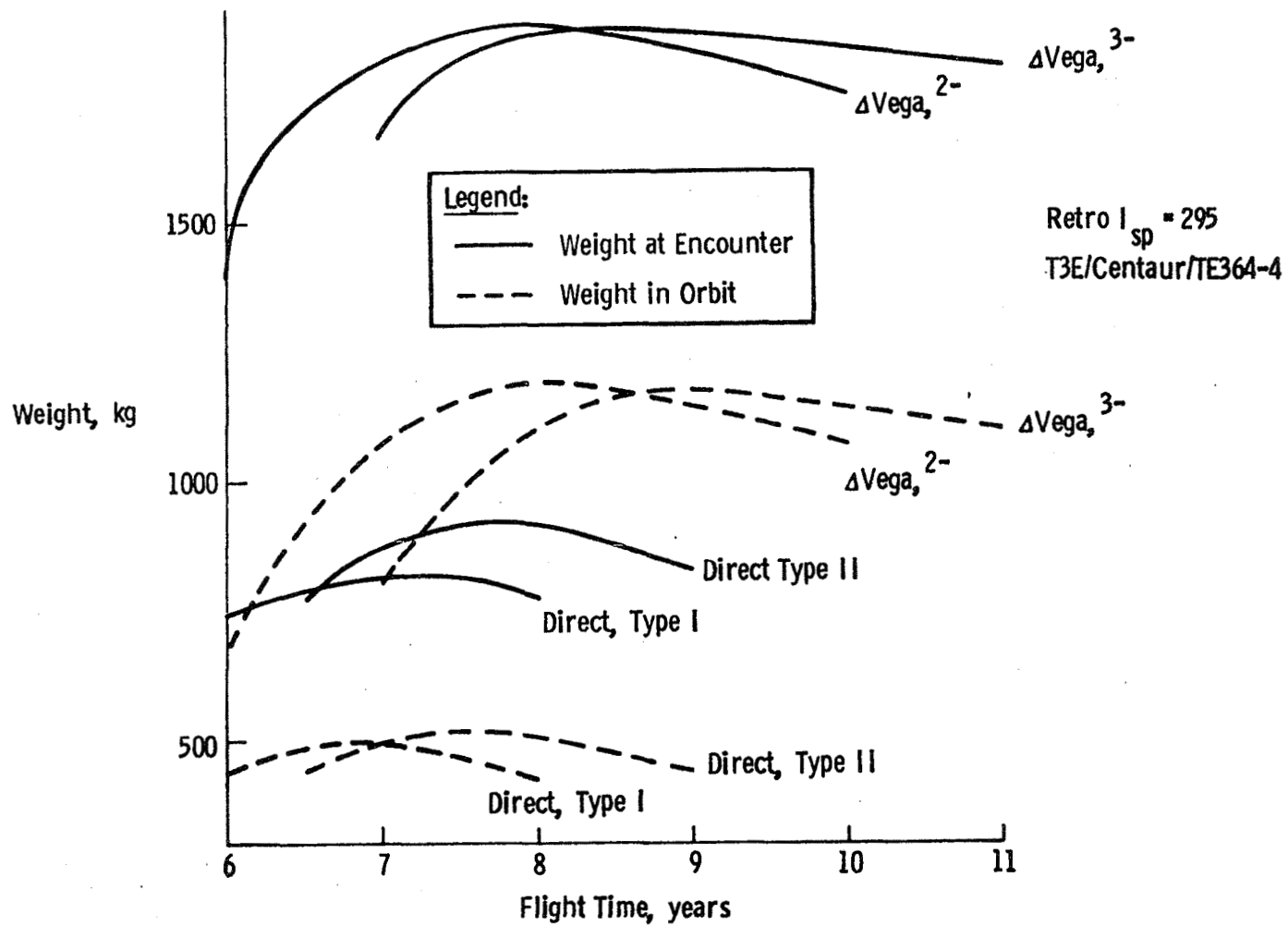
Flight Time, years

Fig. A-23 Comparison of ΔVEGA and Direct Performance

In the vicinity of 7 years flight time where the direct Type I orbited weight is ~500 kg, the 2⁻ ΔVEGA orbited weight is over 1000 kg, more than twice the orbited weight! An orbited weight of ~1200 kg can be obtained if an additional year of flight time can be tolerated. The ΔVEGA weight curves drop off for short flight times but there is still an advantage to be gained even at 6 year and shorter flight times. Weights at encounter, of course, should have the same behavior. It is important to note that at least for the 1983 opportunity there is nothing to be gained by going to the 3⁻ type ΔVEGA.

Performance data are also presented for the 1983 2⁻ ΔVEGA case flown with a Shuttle/IUS launch vehicle. These are shown in Table A-13 and Figure A-24. Orbited payload curves are presented for the suggested range of high (H.P.) and low (L.P.) performance IUS candidates. The low performance IUS provides an additional 200 kg of payload over the Titan IIIE. The higher performing IUSs can more than double the Titan IIIE orbited mass to the 2600 kg range.

These results show ΔVEGA to be a most attractive flight technique for Titan missions. One which can increase delivered payload without costing additional flight time, and one certainly deserving of more study.

Table A-13 2⁻ ΔVEGA IUS Performance

Flight Time	High Performance IUS				Low Performance IUS		
	W INJ	W ENC	W ORB		W INJ	W ENC	W ORB
6	7400	3080	1495		3900	1623	788
7	7400	4024	2397		3900	2121	1263
8	7400	4180	2643		3900	2203	1393
9	7400	4019	2532		3900	2118	1334
10	7300	3858	2354		3800	2008	1225

b. ΔVEGA Performance for Mariner and Pioneer Class
Missions - All the Mariner and Pioneer missions considered can be
flown with the IUS using the ΔVEGA technique in 1983 (Table A-14).
Deployment can take place from Saturn orbit and probably from an orbit
around Titan. Required throw weights are very similar to those for the
1988 direct mission (VHS's similar). The main advantage is in the
additional L/V throw weight resulting from lower "effective" C_3.
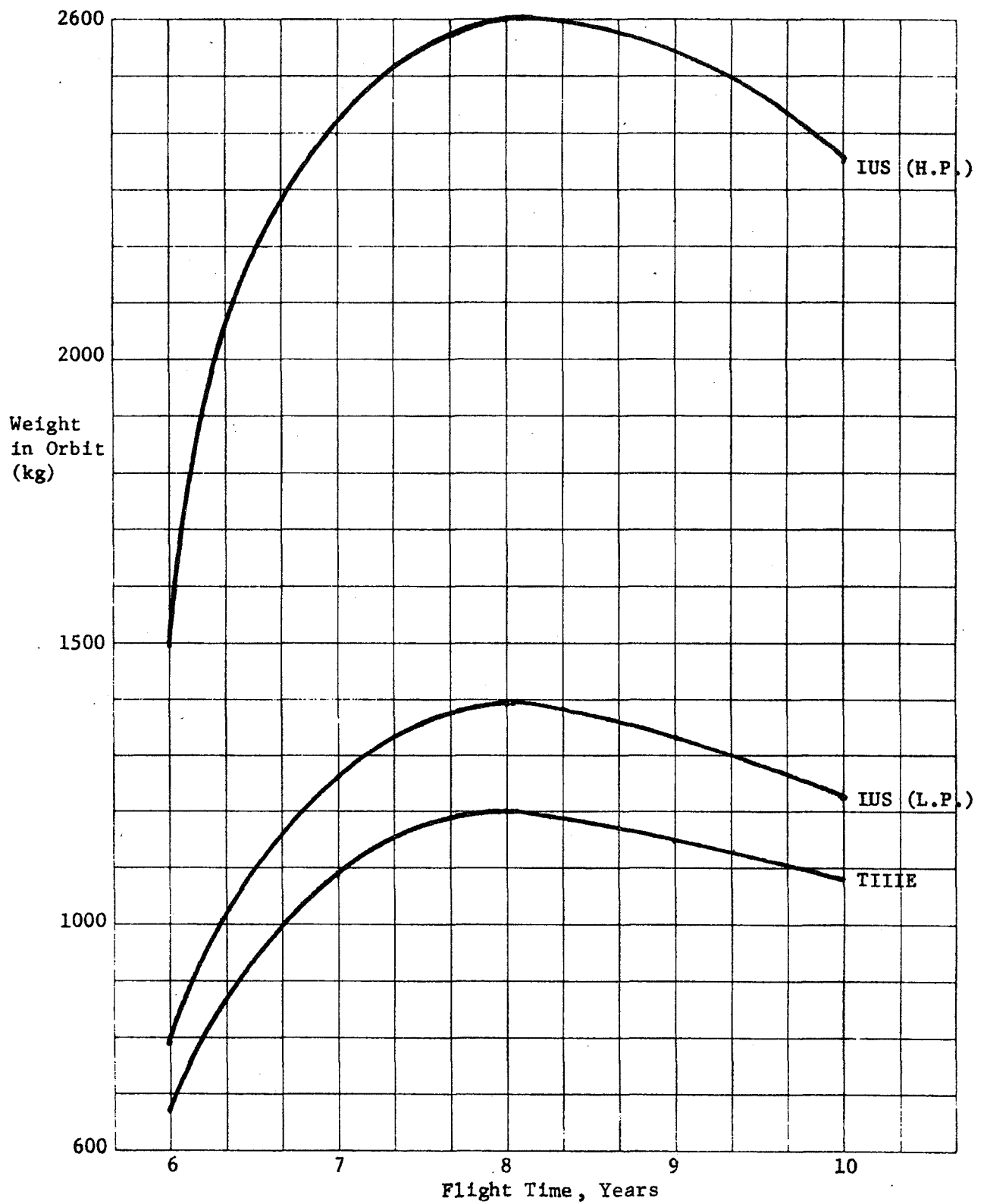
Fig. A-24 Orbiter Payload Using Shuttle/IUS and 2⁻ΔVEGA Trajectories to Saturn

A-49

Mission	Required Throw Weight	IUS Throw Weight Capability
MSO/L	2241	3480
MSO/P	2000	3480
MSO/PR	1975	3480
PSO/L	1257	3480
PSO/P	1016	3480
PSO/PR	991	3480
MSO/L (in orbit)	2636	3480
MSO/P (in orbit)	2131	3480
PSO/L (in orbit)	1700	3480
PSO/P (in orbit)	1178	3480

B. DEFLECTION MANEUVER

The successful implementation of the deflection maneuver is essential to achieve the science objectives of the mission modes under consideration. We have analyzed three deflection maneuvers and have determined the advantages and disadvantages of each. These will be given below. For purposes of a concise description of the deflection event we will discuss the maneuver as if applied only to the probe mission when in fact the same comments apply equally to each mission mode. Since this study was performed under the assumption that planetary quarantine restrictions equivalent to those met by the Viking Mars mission would be imposed, the deflection maneuver becomes more complex and critical.

1. Probe Deflection

Probe deflection imposes minimum requirements on the spacecraft design. The spacecraft probe combination is targeted for the desired Titan flyby conditions. The probe is ejected from the spacecraft by a simple technique, possibly springs, and orients itself in the desired attitude for the deflection propulsive maneuver that will produce acquisition of the desired entry site. Upon completion of this burn the probe orients its attitude to enter at a 0° angle of attack. Probe deflection is most demanding upon the probe systems design requiring both a propulsion and attitude control system. The primary advantage of probe deflection is the minimal planetary quarantine impact upon the spacecraft since at no time during the deflection maneuver is the spacecraft targeted to a Titan impacting trajectory.

2. Spacecraft Deflection

The spacecraft probe combination, for the spacecraft deflection mode, is initially targeted to impact Titan at the desired entry location. The probe is released from the spacecraft in the desired entry attitude. The spacecraft then is deflected away from Titan to establish communication geometry and the required flyby radius. Thus, the spacecraft performs all the maneuvers, and the probe is kept as simple as possible. Because of the planetary quarantine requirement at Titan either the spacecraft must be sterilized or an ultrareliable propulsion subsystem is required to satisfy the P.Q. constraints.

3. Shared Deflection

The spacecraft probe combination is targeted to the desired Titan flyby conditions. In this mode the probe ΔV is constrained to the direction required to acquire the desired entry location. The spacecraft must then be accelerated to establish the required communications geometry.

The implementation sequence for this mode follows:

a. The spacecraft rotates away from the earth pointing attitude to the deflection maneuver attitude and releases the probe.

b. The probe then fires its axial thruster for its deflection.

c. The spacecraft is then rotated to the attitude required to establish the desired communications geometry.

Thus, the probe is only required to generate the axial thrust and the planetary quarantine implications of the spacecraft deflection mode are bypassed. One disadvantage of the shared deflection mode is that the probe must enter at the same attitude established for the deflection propulsive maneuver which implies a non-zero angle of attack at entry. However, for all cases investigated for the 1985 opportunity, the entry angle of attack was less than 30°.

A-52

4. Deflection Radius Selection

The distance from Titan that the deflection maneuver is performed, or the deflection radius, is plotted against a wide range of parameters as shown in Figure A-25. The important trends will be summarized here.

Deflection ΔV - The ΔV requirements are reduced drastically as deflection radius is increased. This is apparent from the downward slope of all the curves in Figure A-25(a).

Spacecraft Periapsis - The ΔV requirements for three different periapsis radii as a function of a deflection radius is shown in Figure A-25(a) Note that the ΔV requirements are about linearly proportional to spacecraft periapsis radius at Saturn: doubling the periapsis radius about doubles the ΔV requirement for fixed deflection radius.

Coast Time - The relationship between coast time and deflection radius is shown in Figure A-25(b) It is seen that coast time and deflection radius are linearly related: doubling the deflection radius doubles the coast time.

Dispersions - Dispersions in probe aspect angle (PAA), entry flight path angle (γ_E) and range are shown for four different deflection radii in Figure A-25(c) The spacecraft uncertainty with respect to Titan was assumed to be 250 km spherical (1 σ). Dispersions, while increasing with deflection radius, do not increase in proportion to the change in deflection radius. Therefore, for the assumed spacecraft uncertainty, the dispersions shown in Figure A-25(c) are not a strong function of deflection radius.

(a)

$\gamma_E = 60°$

Targets

$Range_E = 30$ Kkm

$RCA = 3700$ km

$R_P = 18 R_S$

$R_P = 10 R_S$

$R_P = 1.8 R_S$

Deflection ΔV, m/sec

Deflection Radius, 10^6 km

(b)

$V_{HP} = 5.5$ km/sec

Coast Time, days

Deflection Radius, 10^6 km

(c)

Assumed S/C Uncertainty
= 250 km (1σ)

PAA, deg

3
5
10
20

3σ Dispersions, deg

γ_E, deg

Defl Radius
in Mkm

3
5
10
20

3σ Dispersions, deg

Range, km

3
5
10
20

3σ Dispersions, km
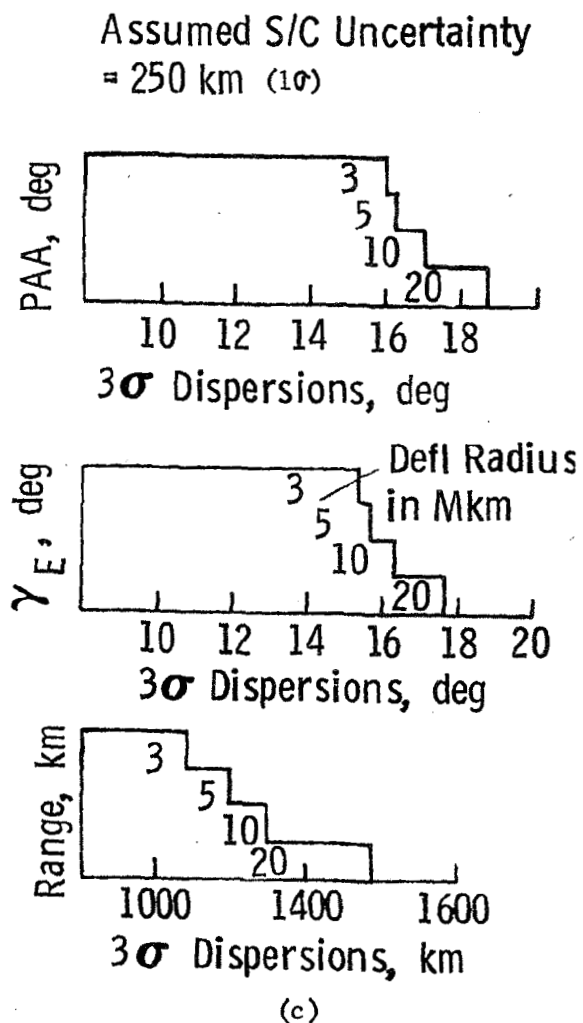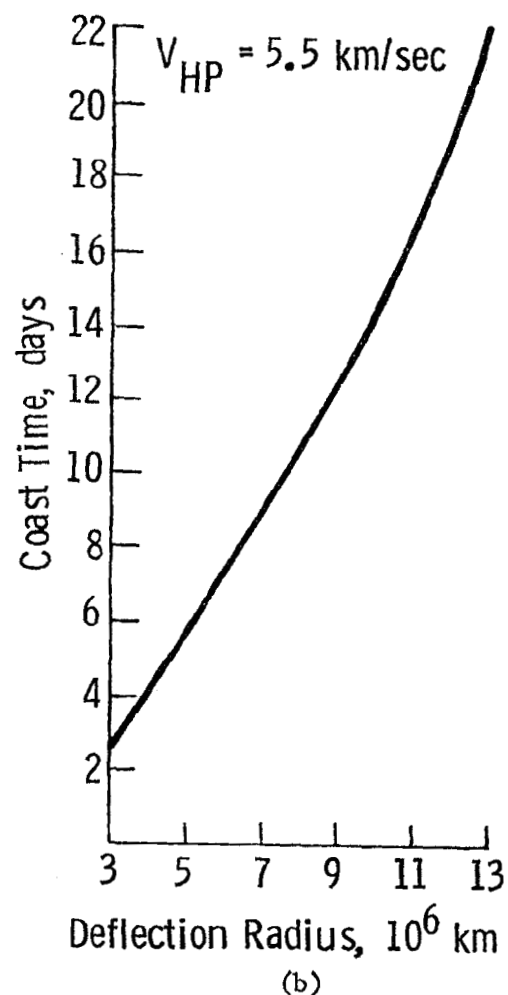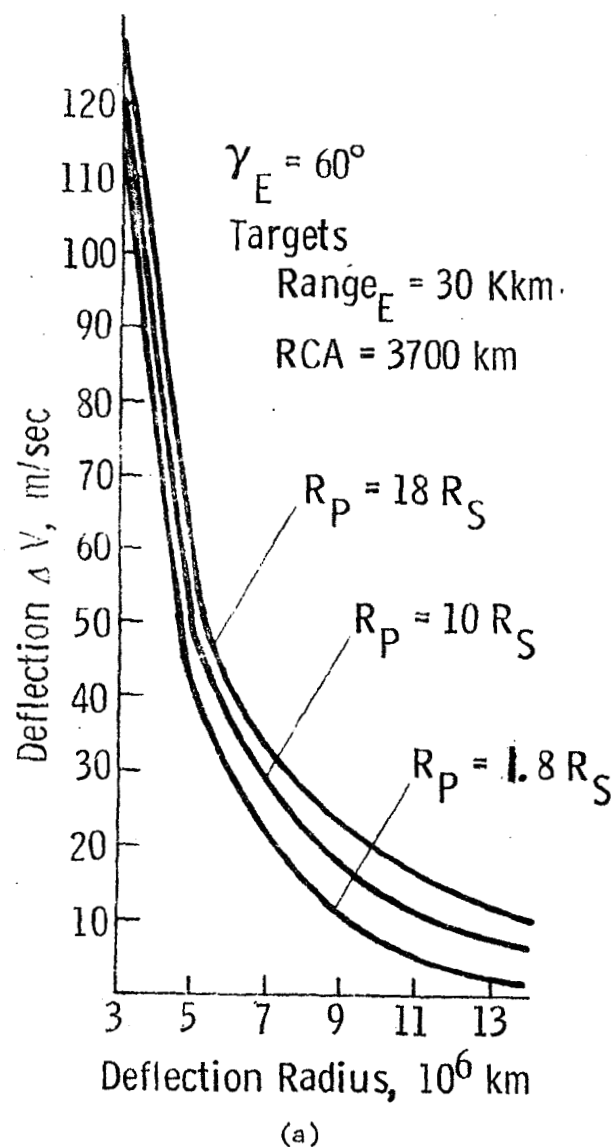
Fig. A-25   Deflection Radius Selection

5. Dispersion Analysis

Unavoidable errors in navigation and guidance processes lead to uncertainties in spacecraft state at the deflection point. Execution errors in the deflection maneuver itself cannot be escaped. These errors and their resulting dispersions must be considered in mission design.

Parameters whose dispersions are critical fall naturally into two classes -- entry parameters and communications parameters. Entry parameters are variables associated with probe entry, such as entry site, flight path angle, angle of attack, or time of entry. Dispersions in these parameters can affect the science return of the mission. Communication parameters are quantities describing the communications link between the probe and space-craft such as probe aspect angle, communications range, range rate and range direction. Dispersions in communication parameters must be accounted for in the design of the link to insure that science data can be returned to Earth.

Deflection Dispersion Trends - A quantitative discussion of the deflection dispersion trends is given in this section. For each individual study, the variations in the dispersion (3σ) of the critical mission parameters are presented.

Entry Angle - The variations in dispersions as a function of entry angle are illustrated in Table A-15. The missions assume a spacecraft deflection mode with execution errors of 1% proportionality, 0.5° ΔV pointing, and 0.5° probe tipoff, all 3σ. The trajectories are all deflected 5 million km from Titan for entry angles of -60°, -70°, and -80°. The navigation errors are assumed to be spherical 500 km (1σ). With perfect radio tracking this is the smallest navigational uncertainty possible and corresponds to the smallest assumed ephemeris uncertainty of Titan.

TABLE A-15 - Entry Dispersions as Functions of Entry Angle

ENTRY ANGLE deg	DEFL ΔV m/sec	ENTRY TIME (3σ) min	ENTRY ANGLE (3σ) deg	PAA ENTRY (3σ) deg	RANGE ENTRY (3σ) km	ANGLE OF ATTACK (3σ) deg	ENTRY DR* (3σ) deg	SITE XR* (3σ) deg	SPACECRAFT-PROBE DIRECTION CA* (3σ) deg	CLA* (3σ) deg
-60	53.2	2.6	34.6	36.1	2352	.634	5.8	4.2	4.4	1.8
-70	53.2	2.6	29.1	30.0	2376	.58	5.6	3.3	4.3	1.7
-80	53.2	2.6	27.5	25.3	2393	.56	5.2	1.4	4.3	1.6

NOTE: The nominal mission from which the above dispersions were generated was targeted to have a range at entry of 30K km and a closest approach altitude of Titan of 1000 km.

* DR - Down Range

XR - Cross Range

CA - Cone Angle

CLA - Clock Angle

The general trend is predictable: the shallower the entry angle the larger the entry parameter dispersions.

Deflection Radius Effects - The selection of the deflection radius must consider the impact of dispersions. Since the deflection ΔV magnitude decreases as deflection radius is increased, the contribution due to execution errors also decreases. However, this is compensated for by the effect that increases in coast time from deflection to entry increases the time interval over which the dispersions will grow. Table A-16 illustrates the trades in deflection radius. The missions considered assumed a spacecraft deflection mode with the same execution errors as used for the entry angle study. The navigational errors are assumed to be spherical 250 km (1σ). This magnitude had to be reduced from 500 km since several probes missed Titan for the 10×10^6 km deflection radius. The general trend illustrated in Table A-16 is increasing dispersions with deflection radius.

Periapsis Radius - The velocity of the probe at entry is largely a function of the hyperbola periapsis radius with respect to Saturn. When intercept occurs at a point tangent to Titan's orbit, V_{HP} is minimized. The approach velocity then increases with decreasing periapsis radius. Dispersions were analyzed as a function of periapsis radius. The results are displayed in Table A-17. Three values of periapsis radius were considered, 2.8 R_s, 10 R_s, and 18 R_s. Other assumptions are deflection radius, 5×10^6 km, and navigational uncertainties 500 km (1σ).

TABLE A-16 Entry Dispersions as Functions of Deflection Radius

DEFL RADIUS 10^6 km	ENTRY ANGLE deg	DEFL ΔV m/sec	ENTRY TIME (3σ) min	ENTRY ANGLE (3σ) deg	PAA ENTRY (3σ) km	RANGE ENTRY (3σ) km	ANGLE OF ATTACK deg	ENTRY DR (3σ) deg	SITE XR (3σ) deg	SPACECRAFT PROBE DIRECTION CA (3σ) deg	CLA (3σ) deg
3	-60	128	1.3	15.3	16.0	1093	.522	3.3	4.5	1.8	.62
5	-60	53	1.34	15.5	16.2	1198	.524	3.44	4.65	1.9	.79
10	-60	19	1.38	16.1	17.0	1369	.527	3.6	4.75	2.0	.9
20	-60	8	1.50	17.6	18.6	1582	.531	4.6	4.9	2.0	1.0

TABLE A-17   Entry Dispersions as Functions of Periapsis Radius

PERIAPSIS RADIUS R_s	DEFL RADIUS 10^6 km	ENTRY ANGLE deg	DEFL ΔV deg	ENTRY ANGLE (3σ) deg	PAA ENTRY (3σ) deg	RANGE ENTRY (3σ) km	ANGLE OF ATTACK deg	ENTRY DR (3σ) deg	SITE XR (3σ) deg	SPACECRAFT PROBE DIRECTION CA (3σ) deg	CLA (3σ) deg
2.8	5	-60	53.2	34.6	36.1	2352	.634	5.8	4.2	4.4	1.8
10	5	-60	47.7	31.1	33.1	2588	.815	7.7	5.2	3.7	1.24
18	5	-60	40.9	26.0	27.6	2910	1.135	10.7	7.6	3.3	.94

By referring to Table A-17, we see the dispersions generally decrease

with increasing periapsis radius. Note, however, the behavior of

the entry site dispersions: here the trend is reversed and down-

range and crossrange dispersions increase with increasing periapsis

radius. One possible explanation is that for the large periapsis

case the relative probe velocity is minimized so that any uncertainty

in the entry velocity translates into a larger percentage error and

hence results in increasing entry site dispersions.

Optical Navigation - In order to simulate the orbit determination

uncertainties associated with an optical navigation sensor, we made

certain simplifying assumptions. The limiting accuracy in any

optical device be it vidicon or CCD is the ability to accurately

locate the center of Titan. Current projections indicate that an

accuracy of 1% of the target radius is possible. One percent of

Titan's radius is 27 km. Using a spherical navigation uncertainty

of 27 km (1σ) resulted in the dispersions illustrated in Table

A-18. Deflection radius was parameterized at 5M km, 10M km and 20M km

and the entry angle and periapsis radius were -60° and $2.8 R_s$

respectively.

Table A-19 illustrates the comparison between three different levels

of navigational errors: 27 km, 250 km and 500 km. As expected, the

dispersions are about linearly related to navigational uncertainty.

The question to be answered by this analysis is whether or not

optical navigation is required at Titan. Reference to Table A-19

gives a partial answer. Optical navigation gives an order of magnitude

improvement in dispersions over the very best that radio guidance can

TABLE A-18 Entry Dispersions for Simulated Optical Tracking

DEFL RADIUS 10⁶ km	PERIAPSIS RADIUS R_s	ENTRY ANGLE deg	DEFL ΔV m/sec	ENTRY ANGLE (3σ) deg	PAA ENTRY (3σ) deg	RANGE ENTRY (3σ) km	ANGLE OF ATTACK (3σ) deg	ENTRY DR (3σ) deg	SITE XR (3σ) deg	SPACECRAFT PROBE DIRECTION CA (3σ) deg	CLA (3σ) deg
5	2.8	-60	53.2	3.2	3.4	385	.516	2.3	1.1	.48	.78
10	2.8	-60	19.4	4.1	4.3	439	.517	2.5	1.5	.48	.73
20	2.8	-60	7.9	6.8	7.2	649	.519	3.8	2.5	.73	.95

Navigation uncertainty = 27 km(1σ)

TABLE A-19 Entry Dispersions as Functions of Navigation Uncertainty

NAV UNCERTAINTY (1σ)	DEFL RADIUS 10^6 km	PERIAPSIS RADIUS R_s	ENTRY ANGLE deg	DEFL ΔV m/sec	ENTRY ANGLE (3σ) deg	PAA ENTRY (3σ) deg	RANGE ENTRY (3σ) km	ANGLE OF ATTACK (3σ) km
27	5	2.8	-60	53.2	3.2	3.4	385	.516
250	5	2.8	-60	53.2	15.5	16.2	1198	.524
500	5	2.8	-60	53.2	34.6	36.1	2352	.634

achieve. If the radio guidance can indeed result in spacecraft uncertainties which approach the underlying ephemeris error assumptions, then the Titan mission is probably possible using radio tracking if the ephemeris uncertainty is no more than 500 km (1σ). Clearly higher levels of ephemeris uncertainty require optical guidance. However, previous studies (e.g., JPL contract 953311) have indicated that reduction of the control uncertainties at Saturn to the levels of the Titan ephemeris uncertainty is an optimistic objective. The results with respect to Saturn are summarized in Table A-20. The DSN equivalent station location errors are $\sigma_{RS} = 1.5$ meters, $\sigma_{LONG} = 3.0$ meters and $\sigma_{Z} = 2.0$ meters and the Saturn ephemeris errors are assumed to be 750 km spherical (1σ). Note that even with QVLBI tracking, the control uncertainty with respect to Saturn is 1100 km.

TABLE A-20   Navigation Uncertainties at
              Saturn for DSN Tracking

PLANET & DATA TYPE	SMAA km	x	SMIA km	x	TOF sec
Saturn					
range/range rate	2178	x	760	x	40
with QVLBI	1100	x	759	x	40

C. TITAN ENTRY

1. Atmosphere Definition

The atmosphere models used in the analysis presented in this section are based on a technical memorandum by Neil Divine of JPL. The document is a revised or updated version of Divine's "Titan Atmosphere Models (1973)". The changes primarily reflect a heavier atmosphere model which has a surface pressure of 17 mb, 400 mb and 1000 mb for the Thin, Nominal and Thick models. The other significant change is the increase in radius from 2500 km to 2700 km. For completeness, Tables A-21, A-22 and A-23 are reproductions of the three Titan atmospheres: Thick, Nominal and Thin. Table A-24 contains the compositions of each model atmosphere.

2. Probe Mission

Entry and descent for the probe mission is primarily determined by the atmosphere model, aerodynamic characteristics of the probe, entry velocity and entry angle.

The Thin and Thick atmospheres previously defined are considered to be the bounding atmospheres, while the Nominal is considered most likely. Science payload primarily determines the aerodynamic configuration. Details concerning the trial mission probe configuration are given in Appendix B. Entry velocity was treated parametrically, with three values considered: 10.4 km/sec, 7.9 km/sec and 5.8 km/sec.

Figure A-26 illustrates the entry deceleration as a function of time for the three model atmospheres and two entry velocities. The peak decelerations range from 23 "gs" for entry into the Thick atmosphere to 7 "gs" for entry into the Thin atmosphere. The magnitude of peak deceleration is seen to be linearly proportional to entry velocity as illustrated in Figure A-26. Figure A-27 shows deceleration dependences on entry angle.

TABLE A-21   Thin Model Atmosphere of Titan

P (bars)	T ($^\circ$K)	ρ (g/cm^3)	R (km)
10^{-7}	160	1.2 (-10)	3673
10^{-6}	160	1.2 (-9)	3421
10^{-5}	160	1.2 (-8)	3201
2×10^{-5}	160	2.4 (-8)	3141
5×10^{-5}	160	6.0 (-8)	3064
1×10^{-4}	160	1.2 (-7)	3008
2×10^{-4}	160	2.4 (-7)	2954
5×10^{-4}	160	6.0 (-7)	2886
1.1×10^{-3}	160	1.3 (-6)	2830
2×10^{-3}	137	2.8 (-6)	2792
5×10^{-3}	108	9.0 (-6)	2745
10×10^{-3}	90	2.1 (-5)	2718
17×10^{-3}	78	4.2 (-5)	2700

TABLE A-22   Nominal Model Atmosphere of Titan

P (bars)	T (°K)	ρ (g/cm^3)	R (km)
1×10^{-7}	160	2.1 (−10)	3309
2×10^{-7}	160	4.2 (−10)	3272
5×10^{-7}	160	1.1 (−9)	3223
1×10^{-6}	160	2.1 (−9)	3188
2×10^{-6}	160	4.2 (−9)	3153
5×10^{-6}	160	1.1 (−8)	3108
1×10^{-5}	160	2.1 (−8)	3075
2×10^{-5}	160	4.2 (−8)	3043
5×10^{-5}	160	1.1 (−7)	3001
1×10^{-4}	160	2.1 (−7)	2971
2×10^{-4}	160	4.2 (−7)	2940
5×10^{-4}	160	1.1 (−6)	2901
1×10^{-3}	160	2.1 (−6)	2873
1.9×10^{-3}	160	4.0 (−6)	2846
2×10^{-3}	159	4.3 (−6)	2844
5×10^{-3}	141	1.2 (−5)	2810
1×10^{-2}	128	2.6 (−5)	2787
2×10^{-2}	117	5.8 (−5)	2767
5×10^{-2}	103	1.6 (−4)	2743
1×10^{-1}	94	3.6 (−4)	2727
2×10^{-1}	86	7.9 (−4)	2713
4×10^{-1}	78	1.7 (−3)	2700

TABLE A-23   Thick Model Atmosphere of Titan

P (bars)	T (°K)	ρ (g/cm³)	R (km)
1×10^{-7}	113	3.0 (-10)	3213
3×10^{-7}	121	8.4 (-10)	3172
1×10^{-6}	132	6.6 (-9)	3125
3×10^{-6}	142	7.2 (-9)	3080
1×10^{-5}	154	2.2 (-8)	3028
1.8×10^{-5}	160	3.7 (-8)	3003
2×10^{-5}	160	4.2 (-8)	2997
5×10^{-5}	160	1.1 (-7)	2957
1×10^{-4}	160	2.1 (-7)	2927
1.8×10^{-4}	160	3.7 (-7)	2903
2×10^{-4}	153	4.4 (-7)	2898
5×10^{-4}	114	1.5 (-6)	2866
1×10^{-3}	91	3.7 (-6)	2848
1.8×10^{-3}	76	7.8 (-6)	2837
2×10^{-3}	76	8.9 (-6)	2834
5×10^{-3}	76	2.2 (-5)	2817
1×10^{-2}	76	4.5 (-5)	2804
1.8×10^{-2}	76	7.8 (-5)	2794
3×10^{-2}	81	1.3 (-4)	2783
1×10^{-1}	94	3.6 (-4)	2758
3×10^{-1}	108	9.4 (-4)	2732
1×10^{0}	125	2.7 (-3)	2700

TABLE A-24   Titan Model Atmosphere Compositions

	Thin	Nominal	Thick
Composition CH_4	100%	2%	0
N_2	0	60%	100%
N_e	0	38%	0
Ratio of S_p Heats	1.31	1.52	1.47
Mean Molecular Wt	16	24.7	28
Turbopause Radius	3673	3309	3213
Surface Pressure	17mb	400mb	1 bar
Surface Temperature	78	78	125

Fig. A-26 Entry Time Function Dependence on Model Atmosphere
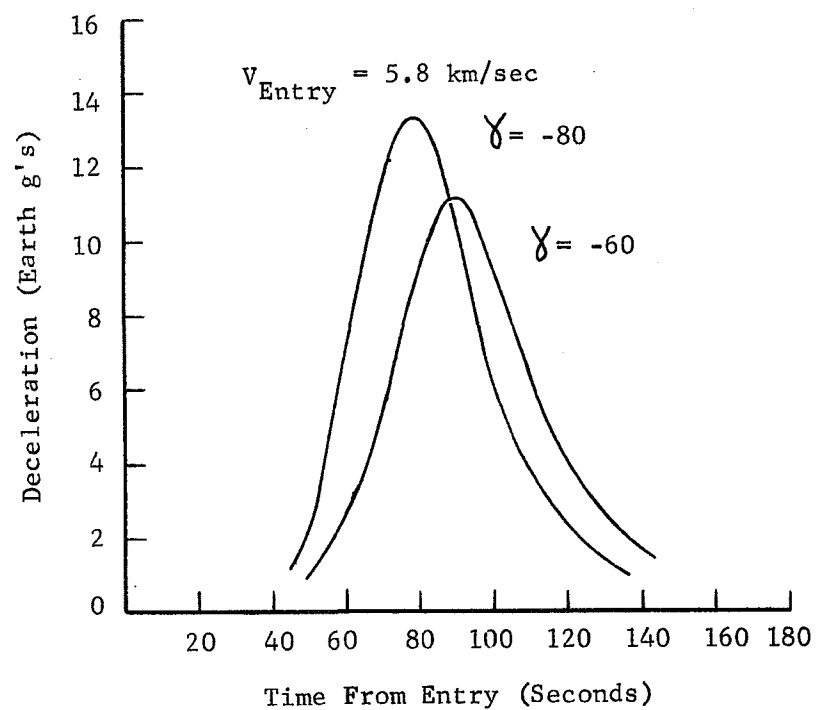
Fig. A-27 Entry Time Function Dependence on Entry Angle (Nominal Atmosphere)

As expected peak deceleration increases with increasing entry angle. The significant probe entry parameters are summarized in Table A-25. Of particular interest is the strong dependence of mission duration on model atmosphere. As shown, the total mission time varies from 6.2 minutes for the thin atmosphere to 74 minutes for the thick atmosphere.

Table A-25 Probe Entry Analysis Summary

	THIN	NOM	THICK
Entry Angle, deg	-60	-60	-60
Entry Altitude, km	973	609	513
Entry B, Slugs/ft^2	0.5	0.5	0.5
kg/m^2	78	78	78
Max Deceleration, g's	7	11.3	23.
Touchdown Velocity, m/sec	114.8	14.8	11.1
Total Mission Time, min	6.2	42	74

3. Penetrator Mission

For the selected candidate penetrator design, atmospheric entry analysis was performed for all three (i.e., Thick, Nominal and Thin) model atmospheres. For these analyses the initial entry velocity and flight path angle were 5.84 km/sec and -60 degrees, respectively.

Initially the penetrator is enclosed in a protective capsule, which is staged at a predetermined altitude for final penetrator descent. The ballistic coefficient of the initial entry configuration is 62.84 kg/m^2 (.4 $slugs/ft^2$), and the ballistic coefficient of the bare-body penetrator, after staging, is 13000 kg/m^2 (82.75 $slugs/ft^2$).

Table A-26 summarizes the results of these studies and indicates that even for staging at 10 millibars freestream pressure in all three atmospheric models, the spread in impact velocities is still unacceptably large. Figure A-28 illustrates the deceleration time histories for the cases depicted in Table A-26. Note in Figure A-28 that the deceleration time histories are presented only in the region of peak deceleration, in each case.

Further attempts to minimize impact velocity spread by varying the staging altitude to altitudes corresponding to ambient pressures as low as 3 millibars did not significantly decrease the spread in impact velocity. In all such cases the impact velocity for entry into the Thin atmosphere model was larger by at least a factor of two than those for entry into the Nominal and Thick atmosphere models.

TABLE A-26   Summary of Results of Penetrator Entry into Titan's Model
Atmospheres with Fairings staged at 10mb Ambient Atmospheric
Pressure

V_E = 5.84 km/sec, γ_E = -60°, B_E = 62.84 $\frac{kg}{m^2}$, B_{Staged} = 13000 $\frac{kg}{m^2}$

Atmosphere Model	Entry Altitude (km)	Staging Altitude (km)	Impact Velocity (km/sec)
Nominal	609	90	.138
Thick	513	105	.110
Thin	973	18	.879
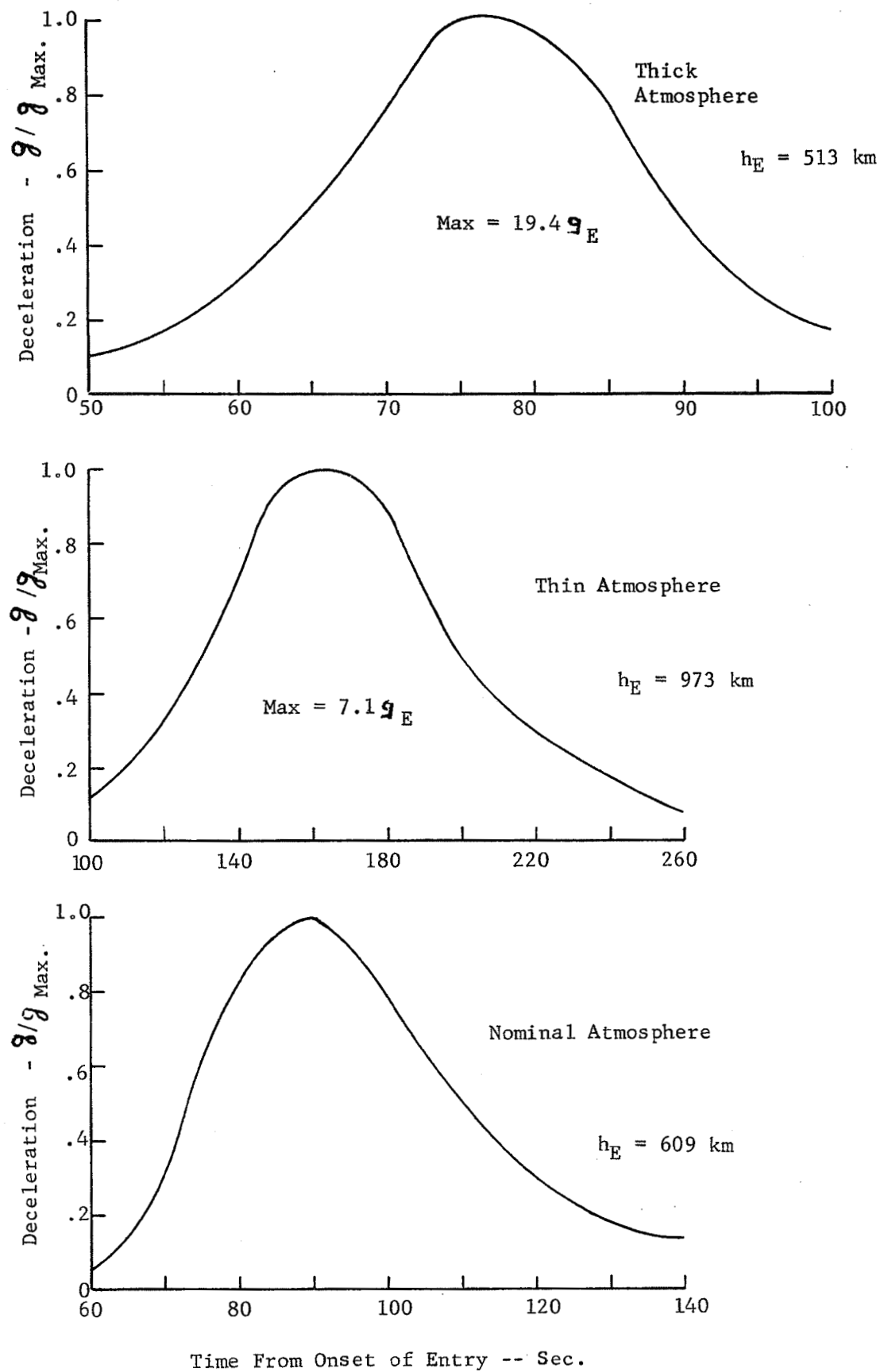
Fig. A-28 Deceleration Time Histories for Penetrator Entry Into Titan's Atmospheres

The conclusion to be inferred from these results is that no single penetrator design would be adequate for entry into all three of the proposed atmosphere models of Titan. This implies that if penetrators are to be utilized during the first mission to Titan, they would require some way of adaptively changing ballistic coefficient depending upon the atmosphere encountered. On the other hand, if more certainty regarding composition and structure of Titan's atmosphere were to become available from earlier missions involving flyby spacecraft, orbiters, or entry probes, the utility of a single-design penetrator for future missions would be greatly enhanced.

4. Lander

The entry portion of the lander trajectory is identical to the probe mission. Entry angle, entry velocity, peak "gs" and dynamic pressure are all similar. The key difference between the two trajectories is the design of the staging event. Touchdown velocity of the lander is desired to be below 4m/sec while there is no corresponding requirement for the probe mission. A parametric analysis of staging altitude indicated that 2 km was a good value. Again the large variations in model atmospheres are difficult to accommodate with a single design. A summary of the lander entry parameters is illustrated in Table A-27. The final ballistic coefficient was designed for a touchdown velocity of 3 m/sec in the nominal atmosphere.

TABLE A-27 Lander Entry Analysis Summary

Entry Angle, deg   -60

Entry Altitude, km   . 609

Entry B, slugs/ft^2 .5

     kg/m^2 78

Final B slugs/ft^2 .035

     kg/m^2 5.5

Max Deceleration, g   11.3

	Thin	Nom.	Thick
Staging Altitude, km	2	2	2
Touchdown Velocity, m/sec	23.7	3	2.2
Total Mission Time, minutes	7.5	51	85

Using this same parachute (B_{chute} = 5.5 kg/m^2) in the Thin and Thick atmospheres results in touchdown velocities of 23.7 m/sec and 2.2 m/sec respectively. Clearly 23.7 m/sec is not acceptable. One possible approach to atmosphere accomodation is an active descent system. However, a more reasonable approach is to assume that by the time the lander mission flies, the bounds in atmosphere uncertainty will be sufficiently reduced to accommodate a passive landing system.

D. SATURN ORBIT INSERTION AND IN-ORBIT MANEUVER STRATEGIES

An orbit around Saturn provides an opportunity for multiple encounters of Titan either for the purpose of probe/lander/penetrator (P/L/P) deployment or to support a P/L/P deployed at Saturn encounter. The orbit period should be commensurate with Titan's and small enough so that encounters occur frequently. Tight Saturn orbits can be realized most efficiently by using Titan swingbys to "pump down" (Ref. A-3) an initial capture orbit of large period. The large initial orbit can be accomplished with minimal propulsive ΔV by a maneuver performed at periapsis on an approach hyperbola with low periapsis altitude. The resultant low periapsis altitude capture orbit maneuver however is not compatible with an efficient pump maneuver because it produces high Titan relative velocity magnitudes at swingby. Another maneuver is required (at apoapsis on the loose capture orbit) to increase the periapsis radius to something near Titan's orbital radius. These maneuvers constitute the Multiple Burn Insertion mode. An alternate insertion mode utilizes a Titan powered swingby. In this case, the approach hyperbola is designed to allow a Titan swingby before periapsis. By judicious choice of swingby orbital parameters, the required post-swingby velocity vector (corresponding to a prescribed Saturn orbit period) can be obtained with minimal retro propulsion. Both these modes are discussed in conjunction with two P/L/P deployment options: pre-SOI and post-SOI. For the pre-SOI case, the approach hyperbola is constrained to intercept Titan and the maneuver strategy is to produce a Titan re-encounter. For post-SOI deployment, the strategy is to freely choose the approach hyperbola which allows in-orbit

Titan encounter with the least total ΔV expenditure.

1. Multiple Burn Insertion

Figure A-29 shows the ΔV required to insert into Saturn orbit with a single maneuver as a function of periapsis radius. Direct insertion at large radii (near 20 R_s) requires more than 2 Km/sec even for large orbital periods (144 days). Insertion at 3 R_s, beyond Saturns rings, requires a ΔV of about .850 Km/sec for a final period of 144 days. A large final periapsis radius (required for an efficient pump maneuver) may be obtained by a posigrade maneuver at apoapsis on the initial capture orbit. Since the final orbit must be commensurate with Titan's, the initial apoapsis altitude is chosen so that after the periapsis adjust maneuver the orbital period is commensurate. Figure A-30 shows the total ΔV cost associated with injecting at 3 R_s and then increasing the periapsis radius to various values. A total ΔV of 1.450 Km/sec for instance, is required to establish an orbit with a periapsis radius of 20 R_s and period of 144 days. Direct insertion into this orbit, on the other hand, takes 2.075 Km/sec. The two maneuver sequence saves .625 Km/sec - a considerable amount.

a. Final Orbit Selection/ΔV Cost

An orbit of 144 day period and 15 R_s periapsis radius can be pumped down to 32 days with a single Titan swingby at 1000 km altitude (Ref. A-3). The post-pump periapsis radius is 12 R_s. Higher period capture orbits may also be pumped down to 32 days but not much additional ΔV is saved, as can be seen from the bunching up of curves for high periods in Fig. A-30 . Pumping to 16 days is not possible with a single pump from
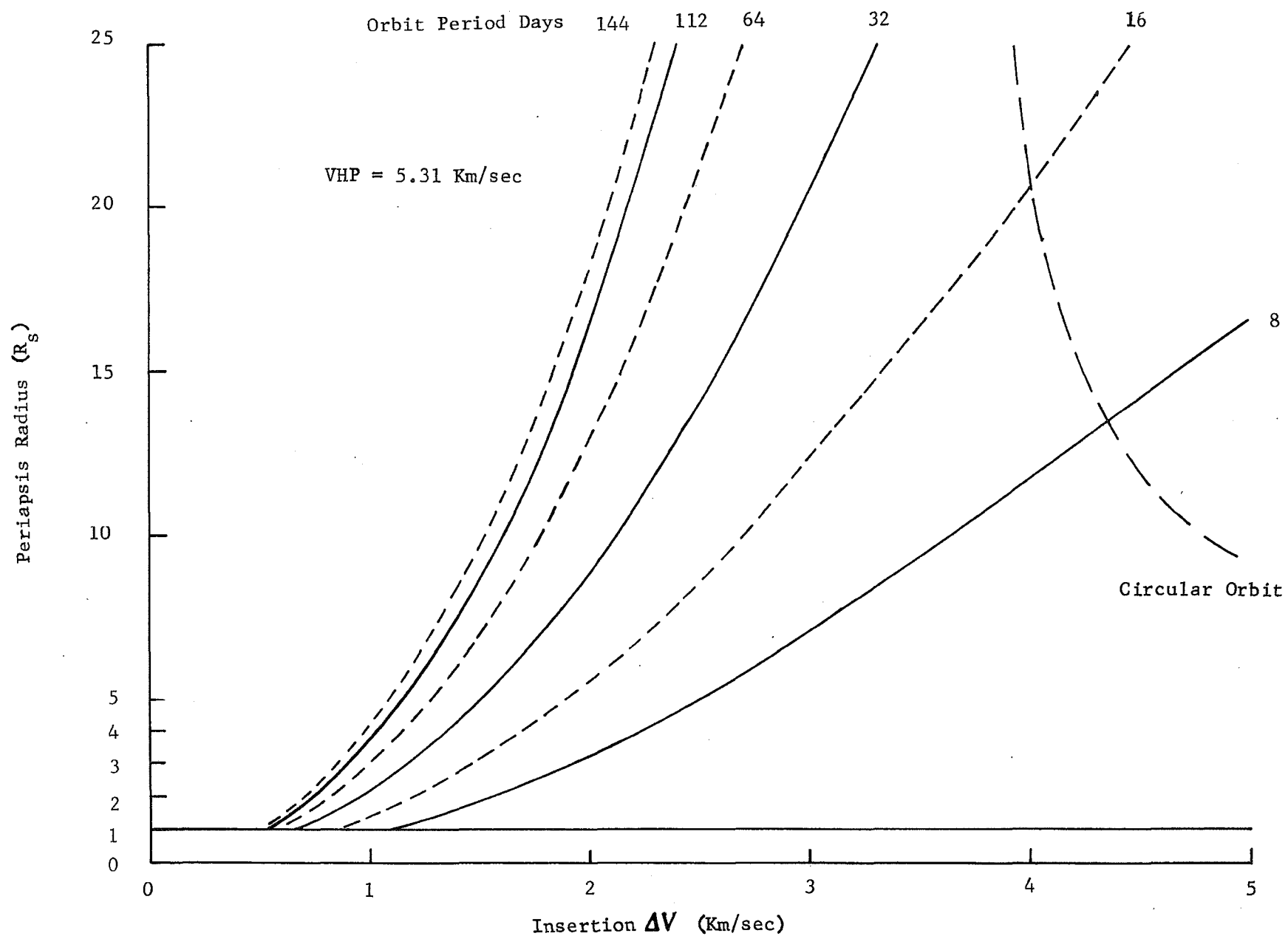
Fig. A-29 Single Maneuver Orbit Insertion ΔV

A-80
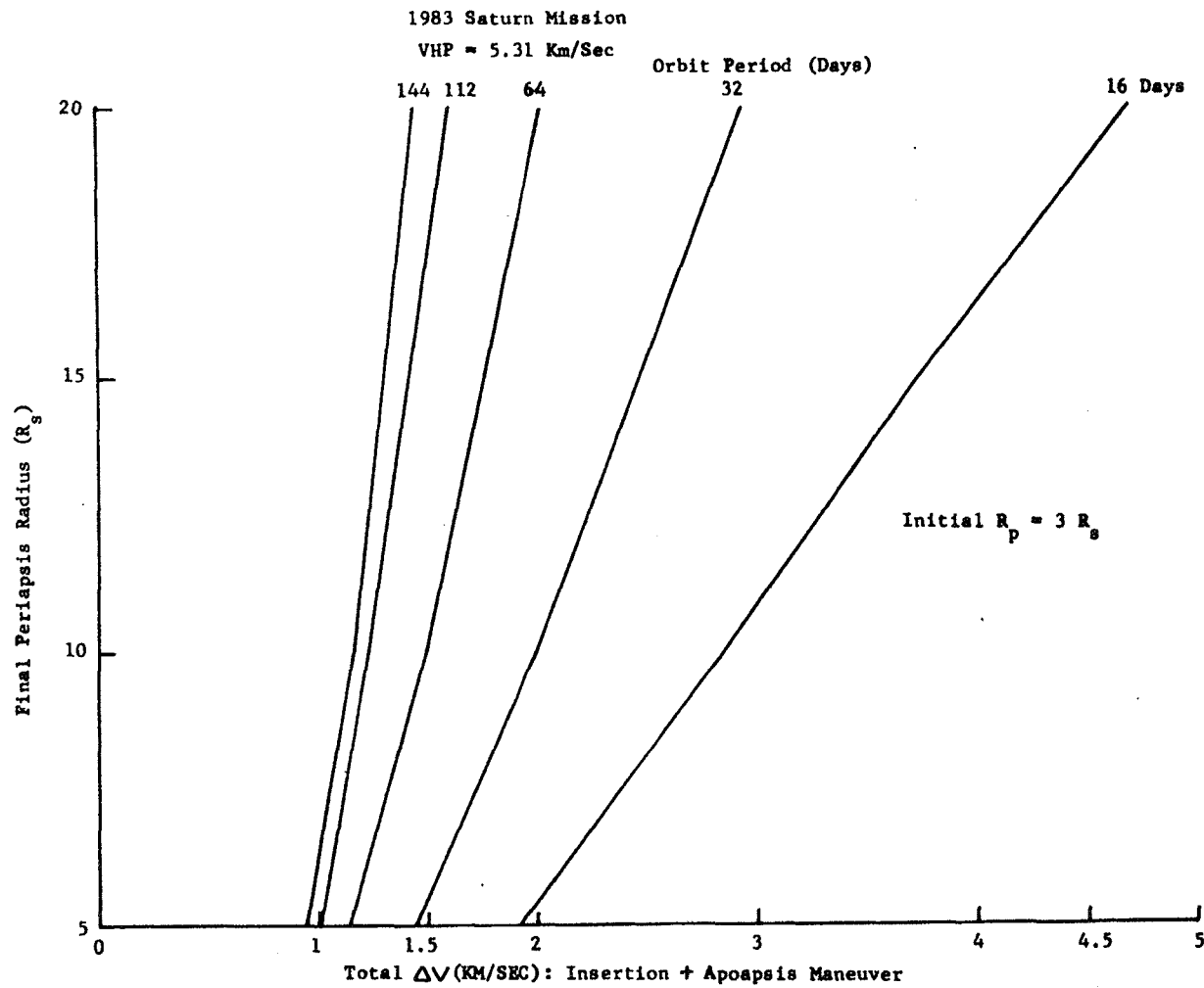
Fig. A-30 Total ΔV Required for Insertion into R_p = 3 Rs Orbit and Raise Periapsis

an orbit of period greater than 50 days. The 15 R_s X 144 day orbit is a good representative case for comparison with the Titan powered swingby mode to be discussed next. Table A-28 presents the capture maneuver velocity change (ΔV_{CAPT}), the periapsis adjust velocity change (ΔV_{r_p}) and the total velocity change (ΔV_T) required to establish the 15 R_s x 144 day Saturn in the designated years. The VHE values for the 15 day windows which provide maximum orbited weight are also shown.

Table A-28 ΔV Components & Total ΔV for 15 R_s X 144 Day Orbit

YR	VHE (Km/Sec)	ΔV_{CAPT} (Km/Sec)	ΔV_{r_p} (Km/Sec)	ΔV_T (Km/Sec)
1983	5.31	.862	.436	1.298
1985	5.30	.860	.436	1.296
1988	5.88	1.012	.436	1.448
1992	6.50	1.190	.436	1.626
1996	6.48	1.184	.436	1.620
1998	5.86	1.006	.436	1.442

The discussion thus far has assumed that the approach hyperbola, the capture orbit and the final orbit (15 R_s X 144 day) are all co-planar with Titan's orbit. If this were the case, a Titan encounter could easily be produced on either the approach hyperbola or in the final capture orbit by proper timing of the Saturn encounter date. An in-plane approach, however, is only possible if the equatorial declination of the Saturn relative hyperbolic excess velocity vector (VHS) is zero. In general, the two classes of missions, i.e., pre-SOI deployment (inter-cept) followed by in-orbit re-encounter and post-SOI deployment (intercept),
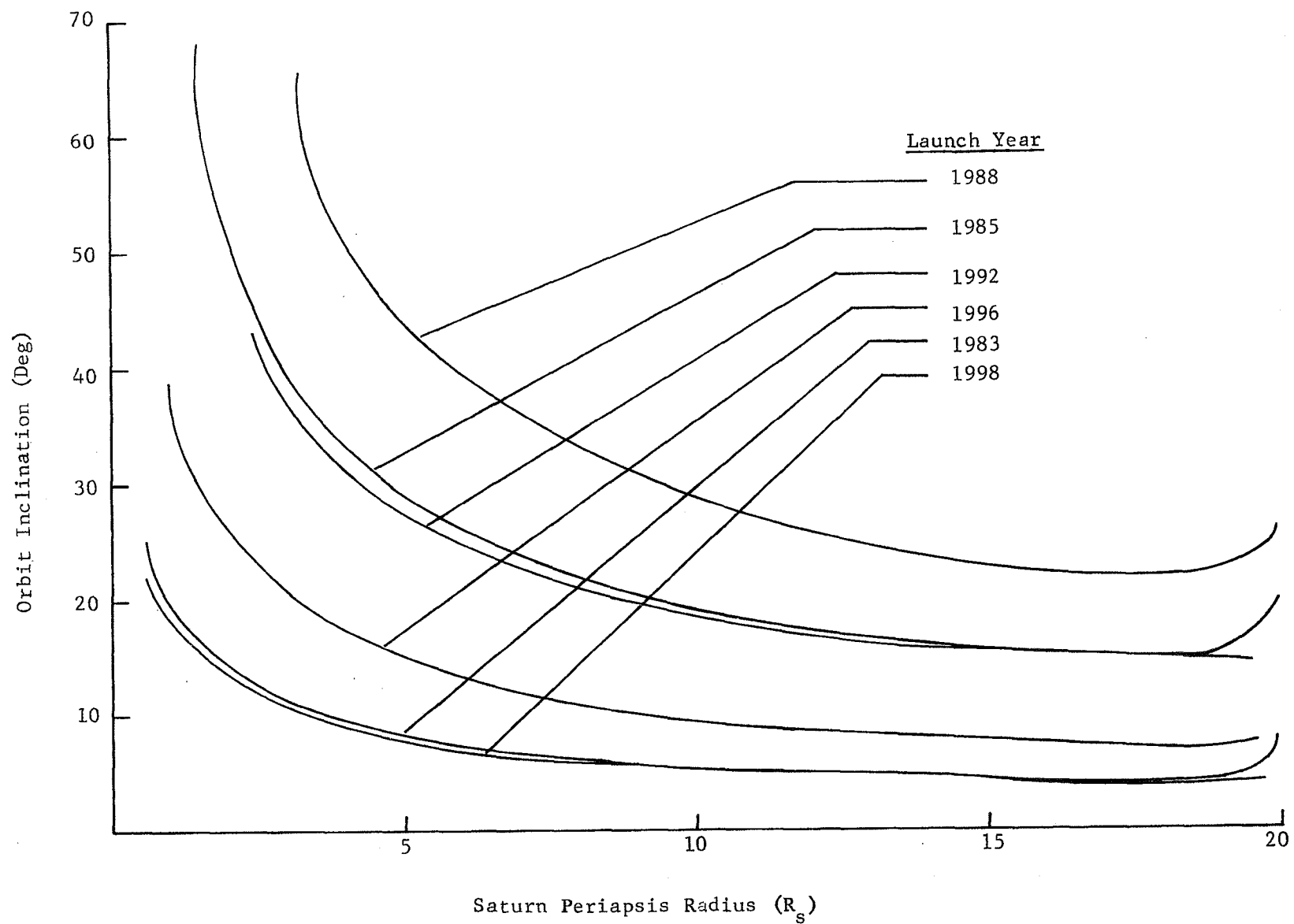
Fig. A-31 R_p vs i for Titan Intercept Trajectories

will require additional spacecraft maneuvers to cause the final Saturn
orbit to intersect Titan. The pre-SOI interception is accomplished
merely by choosing an approach hyperbola with any of a number of
acceptable combinations of periapsis radius and inclination. A typical
plot of R_p and inclination for various launch dates is shown in Figure
A-31. The relationship indicated is that high inclinations generally
correspond to low periapsis radii and low inclinations to high periapsis
radii.

b. <u>Maneuver Strategies for Post-SOI Deployment</u>

When no pre-SOI interception must occur the periapsis
radius and inclination of the approach hyperbola may be selected in-
dependently. For the multiple insertion mode, however, r_p is set to
3 R_s so that only i (or Θ_{AIM}) is adjustable. Two strategies are sug-
gested for this class of missions. One utilizes a plane change maneuver
to produce an equatorial intercept orbit, while the other produces inter-
cept with no additional maneuver.

1) Intercept with Plane Change Maneuver

If the turn angle (Υ- Tau) of the Saturn approach
hyperbola is larger than the VHS declination, then there exists an
approach inclination (Θ_{AIM}) for which the line-of-apsides lies in the
equatorial plane. The corresponding B-vector is achieved at the last
midcourse correction maneuver before SOI. The resultant capture orbit
orientation allows for a plane change maneuver at apoapsis where the
orbital velocity is at a minimum. Table A-29 shows the equatorial
declination (δ_i), hyperbolic eccentricity (e), turn angle (Υ), and

inclination (i) for orbits with periapsis in the equator.

Table A-29 Hyperbolic Approach Parameters with Periapsis
in Saturn's Equator

	δ	e	τ	i
1983	-4.16°	1.13328	28.07°	8.87°
1985	-14.81°	1.13278	28.02°	32.96°
1988	-21.90°	1.16343	30.74°	46.86°
1992	-14.34°	1.19971	33.54°	26.63°
1996	-6.83°	1.19848	33.45°	12.46°
1998	4.02	1.16232	30.64°	7.91°

The plane change maneuver at apoapsis drives the inclinations illustrated in Table A-29 to zero. This maneuver can be integrated in with the periapsis adjust maneuver of the Multiple Burn Insertion Mode. Figure A-32 shows how the required ΔV is computed:
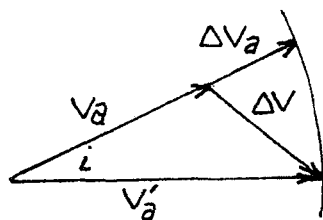
V_a = .377 Km/Sec

ΔV_a = .436 Km/Sec

Figure A-32 Vector Plot

The initial apoapsis velocity V_a requires a magnitude increase ΔV_a to raise periapsis. At the same time, however, it must be rotated through i degrees. The final velocity V_a is obtained by adding ΔV to V_a. The magnitude of ΔV is computed from the law of cosines. Table A-30 shows the ΔV maneuver magnitudes required to establish the equatorial intercept orbit in each launch year. Again, the final orbits are 15 R_s x 144 days. Comparing Table A-30 with Table A-28 shows that an average

of 3 m/s is spent per degree of plane change.

Table A-30 Summary of ΔV's to Establish Equatorial Intercept Orbits

YEAR	ΔV_{CAPT} (Km/Sec)	ΔV_a (Km/Sec)	ΔV (Km/Sec)	ΔV_T Km/Sec)
1983	.862	.436	.444	1.306
1985	.860	.436	.537	1.397
1988	1.012	.436	.620	1.632
1992	1.190	.436	.505	1.695
1996	1.184	.436	.452	1.636
1998	1.006	.436	.443	1.449

2) Intercept with No Additional Maneuver

Table A-31 shows orbital parameters for 15 R_s X 144 day ellipses which intersect Titan's orbit. The parameter θ is the true anomaly of the intersect point. The hyperbolic turn angle τ was computed for a periapsis radius of 3 R_s. The approach hyperbola inclinations shown (i_h) guarantee Titan orbital intersection after the 3 R_s periapsis has been raised to 15 R_s. Again, timing of the encounter can be adjusted so that Titan arrives at the intersection point at the same time the S/C does. This intercept strategy works best when the VHS declination (δ) is small, i.e., more efficient orbital pumping is possible. Note that the "intercept inclinations" are all nearly equal to the VHS declinations. This is because $\theta + \tau$ is near 90°.

Table A-31 Parameters for Saturn Ellipses
(15 R_s x 144 days) Which Intersect Titan's Orbit

YEAR	δ	θ	VHE	τ	i_h
1983	-4.16	68.3	5.31	28.1	4.19°
1985	-14.81	68.3	5.30	28.0	14.9°
1988	-21.90	68.3	5.88	30.7	22.2°
1992	-14.34	68.3	6.50	33.5	14.7°
1996	-6.83	68.3	6.48	33.4	7.0°
1998	4.02	68.3	5.86	30.6	4.1°

This intercept concept appears to be more desirable than the previous one since it achieves essentially the same final orbit without the plane change component.

c. Maneuver Strategies for Pre-SOI Deployment and Post-SOI Re-encounter

The orbital characteristics of approach hyperbola which intersect Titan before periapsis passage with r_{p_h} = 3 R_s are shown in Table A-32. For a given r_{p_h} only one orbit orientation (specified by inclination and argument of periapsis, w) produces intercept. Figure A-31 illustrates the r_p vs i relationship for each launch year. The inclinations for the 3 R_s hyperbola depend solely on the VHS declination, with higher declinations producing bigger inclinations. The initial inserted orbit period (or apoapsis radius) depends on the particular post-SOI re-encounter strategy. Three of these are discussed.

1) Intercept with a Periapsis Adjust Maneuver

Once the loose capture orbit has been achieved

A-87

(with $r_p = 3 R_s$) it is possible to produce a Titan Intercept by merely increasing the periapsis radius. This is accomplished with a maneuver at apoapsis on the capture orbit. Table A-32 shows the required elliptical periapsis radius (r_{p_e}), maneuver size (ΔV_{AP}) and total ΔV including orbital capture (ΔV_T). The r_{p_E} is for a 144 day orbit. The corresponding apoapsis radius determines the inserted orbital period.

The disadvantage of this technique is that the low r_p intercept orbit is very hard to pump down. The following intercept strategy also leads to the same sort of situation.

2) Intercept by Apsidal Rotation

The capture orbit line of apsides may be rotated during SOI so that the final 3 R_s x 144 day orbit intersects the Titan orbit. The required number of degrees, ΔV cost/degree and total cost are presented in Figure A-33 as a function of r_{p_h} (for a 1985 opportunity). Note that the cost at low r_p is very high. At large r_p the cost goes down but the capture ΔV then becomes prohibitive (insertion ΔV at 10 R_S is 1.5 Km/sec). Apsidal rotation during SOI does not appear to be competitive. Rotation may also be accomplished once the Saturn orbit is closed. Table A-33 shows the total cost for an in-orbit rotation produced by a maneuver at apoapsis. (The apoapsis velocity on the 3 R_s x 144 day orbit is .351 Km/sec.)

3) Intercept by Apoapsis Plane Change

The 15 R_s x 144 day orbit has an apoapsis radius of 162.4 R_s. For this strategy the apoapsis radius of the initial capture orbit is set to 162.4 R_s (the periapsis radius is still 3 R_s). Table A-34

shows the inclination of the approach hyperbola (i_h) and the corresponding inclination of the 15 R_s x 144 day ellipse (i_E) required to produce a Titan intercept at true anomaly $\theta = 68.3°$. The i_E is mainly derived from the declination of the hyperbolic periapsis vector. The inclination change Δi can be accomplished by a plane change maneuver at apoapsis on the initial capture orbit. After the plane change the r_p is raised to 15 R_s. The angle $\Delta \rho$ is the amount of rotation about the periapsis direction. The total apoapsis maneuver magnitude (ΔV_{AP}) is larger than the periapsis raise component (.436) by the amount V_{XS}. This strategy produces intercept with very little ΔV expenditure. The only drawback to this technique is that in 1985, 1988 and 1992 relatively large final orbit inclinations will degrade the orbital pump efficiency.

Table A-32 Orbital Parameters for Pre-SOI Titan Encounter

	i_h	r_{P_h}	w	θ_{INT}	r_{P_e}	ΔV_{AP}	ΔV_T
1983	10.2	3.0	-52.2	-127.8	4.51	.080	.942
1985	38.7	3.0	-52.1	-127.9	4.49	.079	.939
1988	74.0	3.0	-53.6	-126.4	4.73	.092	1.104
1992	42.3	3.0	-55.1	-124.9	4.97	.104	1.294
1996	18.8	3.0	-55.1	-124.9	4.97	.104	1.288
1998	10.4	3.0	-53.5	-126.5	4.71	.091	1.097
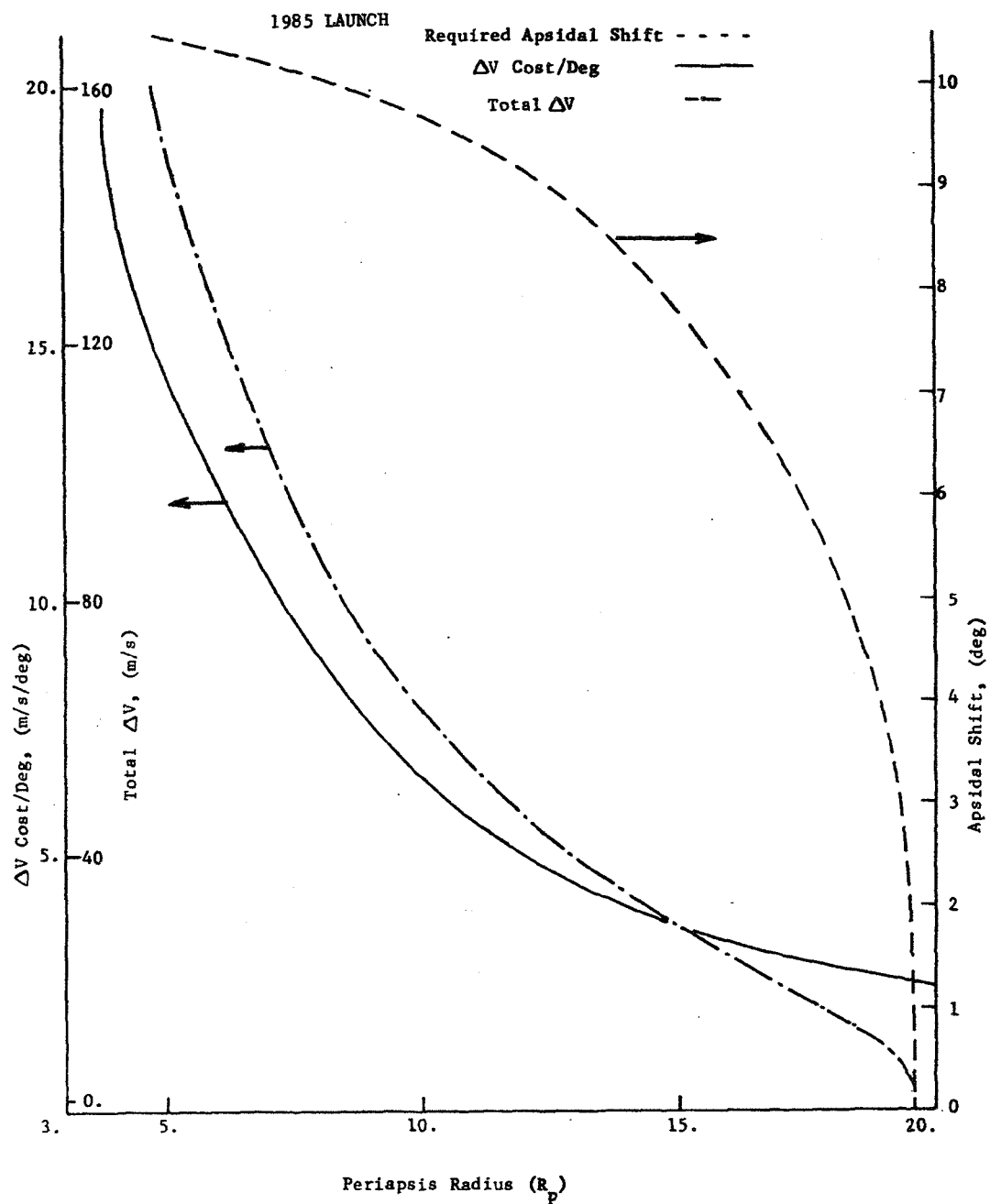
Fig. A-33 Required Apsidal Rotation During SOI, ∆V Cost/Deg and
          Total ∆V Cost vs Periapsis.

A-90
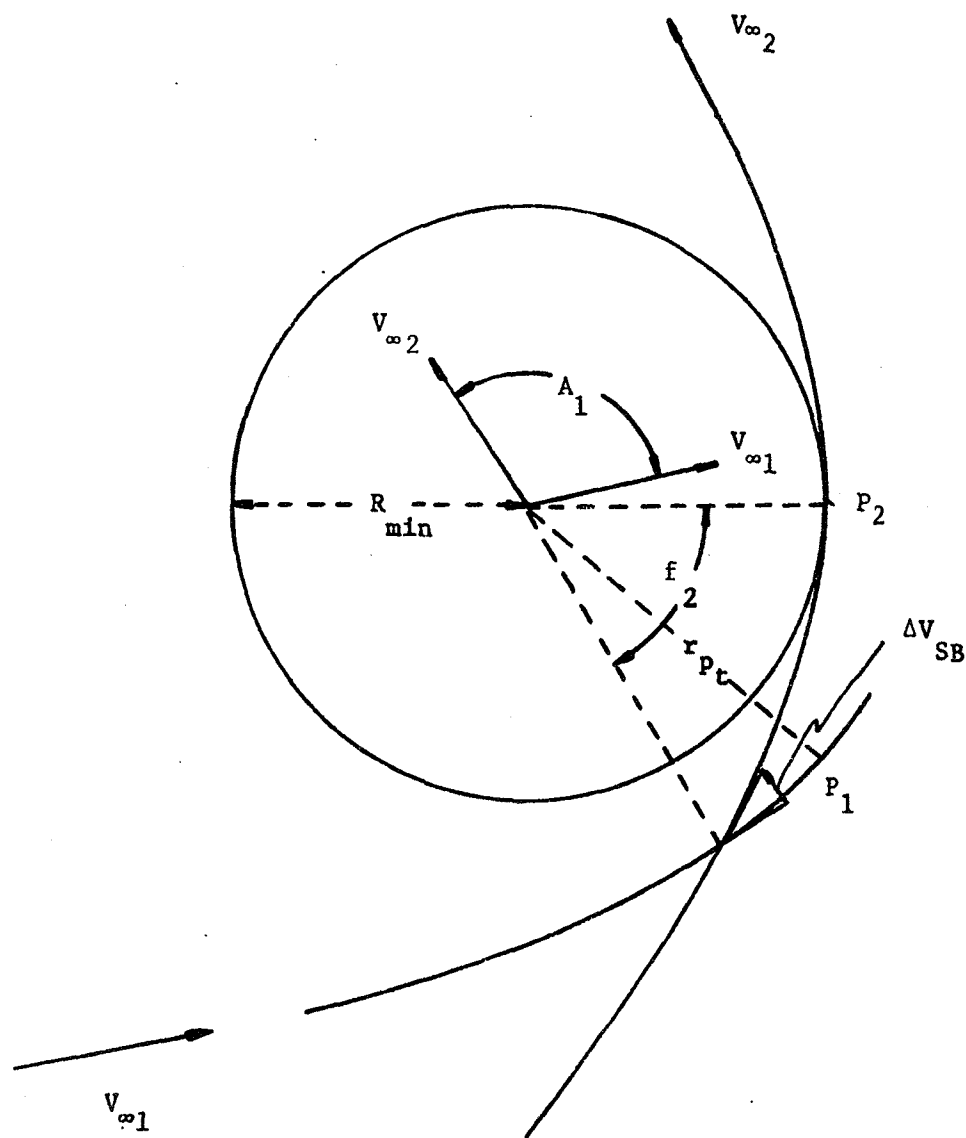
Fig. A-34 Titan Relative Geometry for FR Transfer

Table A-33   Intercept by In-Orbit Rotation of the Line-of-Apsides

YEAR	θ_h	$\theta_E(r_p=3R_s)$	ΔT_{AP}	ΔV_{AP}
1983	-127.8	-138.1	10.3^O	.063
1985	-127.9	-138.1	10.2^O	.062
1988	-126.4	-138.1	11.7^O	.072
1992	-124.9	-138.1	13.2^O	.081
1996	-124.9	-138.1	13.2^O	.081
1998	-126.5	-138.1	11.6^O	.071

2. Powered Swingby Insertion

Saturn orbit insertion at large periapsis radii may be accomplished with the powered swingby maneuver. This is a propulsive ΔV maneuver performed near periapsis passage on a Titan relative hyperbola. Reducing the velocity magnitude within Titan's sphere of influence aids the natural bending of the velocity vector by Titan's gravitational field. By carefully choosing the Saturn approach hyperbola and the direction and shape of the Titan flyby trajectory, it is possible to bend the Titan relative spacecraft velocity vector in such a way as to have the post flyby velocity relative to Saturn correspond to a Saturn orbit with desired period.

Figure A-34 illustrates the swingby geometry for the "FR" type of transfer (Ref. A-4). This transfer is accomplished by a pre-periapsis maneuver which places the spacecraft on an outgoing hyperbola which grazes Titan at the minimum allowed distance of closest approach. It is usually optimal for powered insertions where the magnitude of $V_{\infty 2}$ is less than $V_{\infty 1}$ and when the required turn angle A_1 is larger than the turn angle available with a periapsis-to-periapsis transfer. (The latter is the so-called "optimal deviation transfer" angle).

A-92

Table A-34 Apoapsis Plane Change for Post-SOI Re-encounter After Pre-SOI Deployment

YEAR	VHE	T	δ_{VHE}	θ_h	i_h	ΔV_T	Δi	i_E	ρ_h	ρ_E	$\Delta\rho$	ΔV_{AP}	δ_P	ΔV_{XS}
1983	5.31	28.07°	− 4.16°	−127.84	10.23	1.299	1.55	8.68	83.7	86.8	3.1°	.437	8.06	.001
1985	5.30	28.02°	−14.81°	−127.87	38.74	1.314	6.63	32.11	63.8	76.9	13.1°	.454	29.6	.018
1988	5.88	30.74°	−21.90°	−126.43	74.01	1.562	17.65	56.36	25.7	60.9	35.2°	.550	50.67	.114
1992	6.50	33.54°	−14.34°	−124.86	42.28	1.642	5.82	36.46	62.5	74.7	12.2°	.452	33.51	.016
1996	6.48	33.45°	− 6.83°	−124.91	18.81	1.622	2.28	16.53	79.0	83.8	4.8°	.438	15.33	.002
1998	5.86	30.64°	4.02°	−126.48	10.39	1.443	1.41	8.98	83.8	86.7	2.9°	.437	8.34	.001

In the figure the outgoing hyperbola with periapsis p_2 is "grazing" at the minimum allowable radius R_{min}. The incoming hyperbola has periapsis radius r_{p_t}. The transfer occurs at true anomaly f_2 on the outgoing hyperbola. Note that $V_{\infty 1}$ is rotated by the angle A_1 and is reduced to $V_{\infty 2}$ as a result of the powered swingby maneuver ΔV_{SB}.

a. Final Orbit Selection/ΔV Cost

The final orbit period was again selected to be 144 days. The single impulse powered swingby algorithm of Ref. A-4 was used to compute minimum powered swingby ΔV maneuvers for Titan intercept hyperbolae corresponding to different Saturn arrival times. The Saturn relative hyperbola which allowed the smallest ΔV_{SB} for each year was noted. These are shown in Table A-35. The ΔV savings is computed relative to ΔV cost for direct insertion at the high periapsis radius. The maneuver ΔV's for all years except 1992 and 1996 compare favorably with the Multiple Burn Insertion Mode. High VHS's for these two years degrade the powered swingby performance more than the multiple burn performance.

b. Intercept with Pre-SOI Deployment & Post-SOI Re-Encounter

Pre-SOI deployment is a natural with powered swingby insertion since both require a Titan intercept before Saturn encounter. It must be shown however, that an acceptable probe/bus communication link can be made compatible with the desired Titan flyby altitude (1000 km). Since the post-swingby orbital period is commensurate with Titan's, the re-encounter will occur exactly 144 days later. Since orbital inclinations are low, a pump maneuver in conjunction with the re-encounter will be very efficient. A single flyby can reduce the orbital period from 144 days to 32 days.

Table A-35 Powered Swingby Summary

YEAR	VHS	(1) BEFORE (2) AFTER VHT	ΔV_{SB}	$\Delta V_{SAVINGS}$	INITIAL i	INITIAL r_p	FINAL i	FINAL r_p
1983	5.31	(1) 4.27	1.277	.678	4.4	19.0	6.7	17.7
		(2) 2.38						
1985	5.30	(1) 4.55	1.267	.788	15.8	19.3	23.4	19.8
		(2) 2.73						
1988	5.88	(1) 5.34	1.626	.725	22.8	19.3	27.1	19.1
		(2) 3.36						
1992	6.50	(1) 5.12	1.988	.801	14.9	20.4	19.9	20.2
		(2) 2.58						
1996	6.48	(1) 4.90	1.939	.726	7.0	19.2	10.9	18.3
		(2) 2.33						
1998	5.86	(1) 4.47	1.595	.707	4.0	19.5	6.7	18.4
		(2) 2.21						

c. Conclusions

The smallest ΔV's for Saturn orbit insertion in 1983 and 1985 (1.277 and 1.267 km/sec respectively) are obtained with the powered swingby (PSBY) mode. (Compare Tables A-36 and A-29). This mode should be used whether deployment is pre or post-SOI. Titan re-enounter is guaranteed by the 144 day commensurate capture period (CCP) which can be pumped down to 32 days with a single swingby.

In the remaining years (1988, 1992, 1996, and 1998) insertion and re-encounter, for the post-SOI deployment case, is best accomplished by the Multiple Burn Insertion (MB) mode. Re-encounter is guaranteed by appropriate choice of Saturn approach inclination (i_h) as shown in Table A-37. The total ΔV cost is per Table A-28. Low orbital inclinations will guarantee good orbital pumping capability. For pre-SOI deployment in 1996 and 1998 the Multiple Burn Insertion mode coupled with the Apoapsis Plane Change (APC) Intercept method (Table A-34) should be used. Total ΔV cost is 1.622 Km/sec and 1.443 Km/sec respectively. The large inclinations associated with the intercept hyperbolas in 1988 and 1992 (Table A-34) preclude the use of the Multiple Burn Insertion Mode with pre-SOI deployment. The powered swingby mode must be used - even though ΔV's are large. This results from the requirement that the 144 day capture orbit period be capable of being pumped down to 32 days in a single flyby. Table A-37 summarizes these conclusions.

Table A-36   Summary of Maneuver Strategies & Total ΔV Expenditures

	DEPLOYMENT MODE			
	PRE-SOI		POST-SOI	
YEAR	INSERTION MODE/ INTERCEPT STRATEGY	ΔV INSERTION/ ΔV INTERCEPT	INSERTION MODE/ INTERCEPT STRATEGY	ΔV INSERTION/ ΔV INTERCEPT
1983	PSBY/CCP	1.277/0.	PSBY/CCP	1.277/0.
1985	PSBY/CCP	1.267/0.	PSBY/CCP	1.267/0.
1988	PSBY/CCP	1.626/0.	MB/i_h	1.448/0.
1992	PSBY/CCP	1.988/0.	MB/i_h	1.626/0.
1996	MB/APC	1.620/.002	MB/i_h	1.620/0.
1998	MB/APC	1.442/001	MB/i_h	1.442/0.

3. Orbit Determination Requirements for a Titan Swingby

For maximum utilization of the gravity field of Titan during powered swingby, the closest approach radius should be small. A close approach to Titan is also desirable for probe, penetrator or lander missions. There are certain unavoidable orbit determination errors associated with the spacecraft trajectory. Clearly, large orbit determination errors will restrict the closest approach radius. Additionally, the planetary quarantine requirement associated with Titan missions indicates a minimum probability of contamination. For an unsterilized spacecraft the probability of contamination is identical with the probability of impact. A relationship exists between probability of impact, Titan flyby radius, and the spacecraft orbit determination errors. This section parametrically addresses this relationship, and is used as a guide in determining the smallest permissible flyby distance.

The probability of impacting Titan during hyperbolic approach is a function of the radius of closest approach (r_p), the orbital inclination and the size (σ_B) and orientation of the delivery ellipse in the B-plane. Figure A-35 illustrates the approach geometry. For the preliminary computations presented here, where it is only desired to get a feel for the impact probability for different r_p and σ_B, the B-plane distribution was represented by a density function with circular contours of constant probability density. (The 1σ radius being σ_B.) With this assumption the impact probability is also independent of orbital inclination. The impact radius, B_I, about Titan is computed from

$$B_I = \sqrt{R_T(R_T + 2a)} \quad \text{where}$$
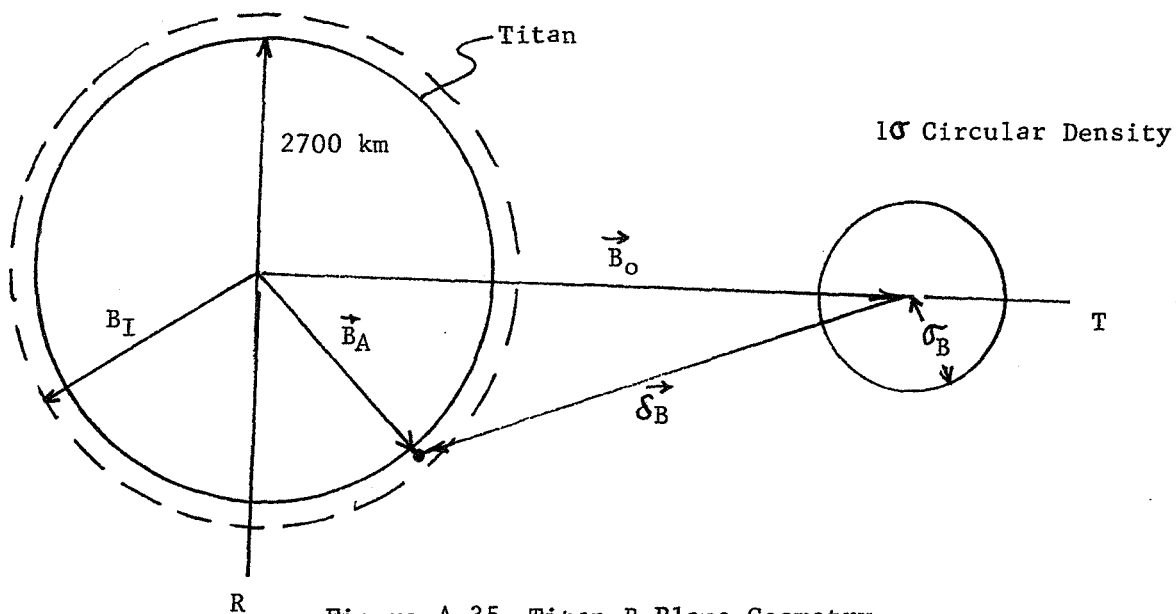
Figure A-35 Titan B-Plane Geometry

R_T is the radius of Titan (2700 km) and a is the hyperbolic semi-major

axis (= 575.2 km in this study for a VHP = 4 km/sec). Any trajectory

with corresponding B vector magnitude less than B_I will impact the

satellite. In general the magnitude of the B_o vector is

$$| \vec{B}_o | = \sqrt{r_p(r_p+2a)} \quad \text{with}$$

$r_p = R_T + h_p$ where h_p is the periapsis altitude of the approach

hyperbola. In the figure the actual B vector, $\vec{B}_A$, is expressed as

$$\vec{B}_A = \vec{B}_o + \vec{\delta B} \quad \text{with } \vec{B}_o \text{ being the nominal vector and } \vec{\delta B} \text{ the normally}$$

dispersed perturbation. Probabilities were computed by integrating the

circular distribution, characterized by σ_B and located at B_o (a function

of h_p), over the circular impact zone of radius B_I. Results are shown

in Table A-37 for a range of σ_Bs from 50 km to 5000 km and h_ps from

500 km to 4000 km. The quoted probabilities are numerically accurate

to one part in 10^7. Any probability computed smaller than 1×10^{-7} was

assumed zero. Note that a σ_B of 50 km or less, obtainable only with

an onboard optical sensor, corresponds to a zero impact probability for

all h_p values. For a σ_B of 500 km, the most optimistic estimate for

radio only tracking, the closest approach altitude would have to be

backed off to 3000 km to satisfy a requirement that the impact probability

be less than 1×10^{-5}. The 5000 km σ_B yields large probabilities for all

h_p's considered. Table A-37 results are graphically illustrated in Figure

A-36. Here probability is plotted vs h_p for contours of

Table A-37 Titan Impact Probabilities - Dependence on h_p and σ_B (VHP = 5.0)

Titan Closest Approach Altitude (h_p)

σ_B	500	1000	2000	3000	4000
50	0.	0.	0.	0.	0.
100	.34003E-6	0.	0.	0.	0.
200	.60997E-2	.26057E-6	0.	0.	0.
300	.44725E-1	.37486E-3	0.	0.	0.
400	.96324E-1	.53104E-2	.21280E-06	0.	0.
500	.14180	.19144E-1	.23492E-4	0.	0.
1000	.25352	.12431	.16241E-1	.88335E-3	.19130E-4
2000	.26971	.20224	.9857E-1	.39313E-1	.12698E-1
3000	.21605	.18425	.12506	.77319E-1	.43478E-1
4000	.15936	.14447	.11388	.84897E-1	.59635E-1
5000	.11732	.10987	.93728E-1	.77044E-1	.61021E-1

constant σ_B. Contours of constant probability are somewhat more interesting
and are presented in Figure A-37. These curves define the σ_B, h_p relation-
ship required to satisfy a particular level of impact probability. For
example, to obtain an impact probability of 1 part in 10^5 or less with an
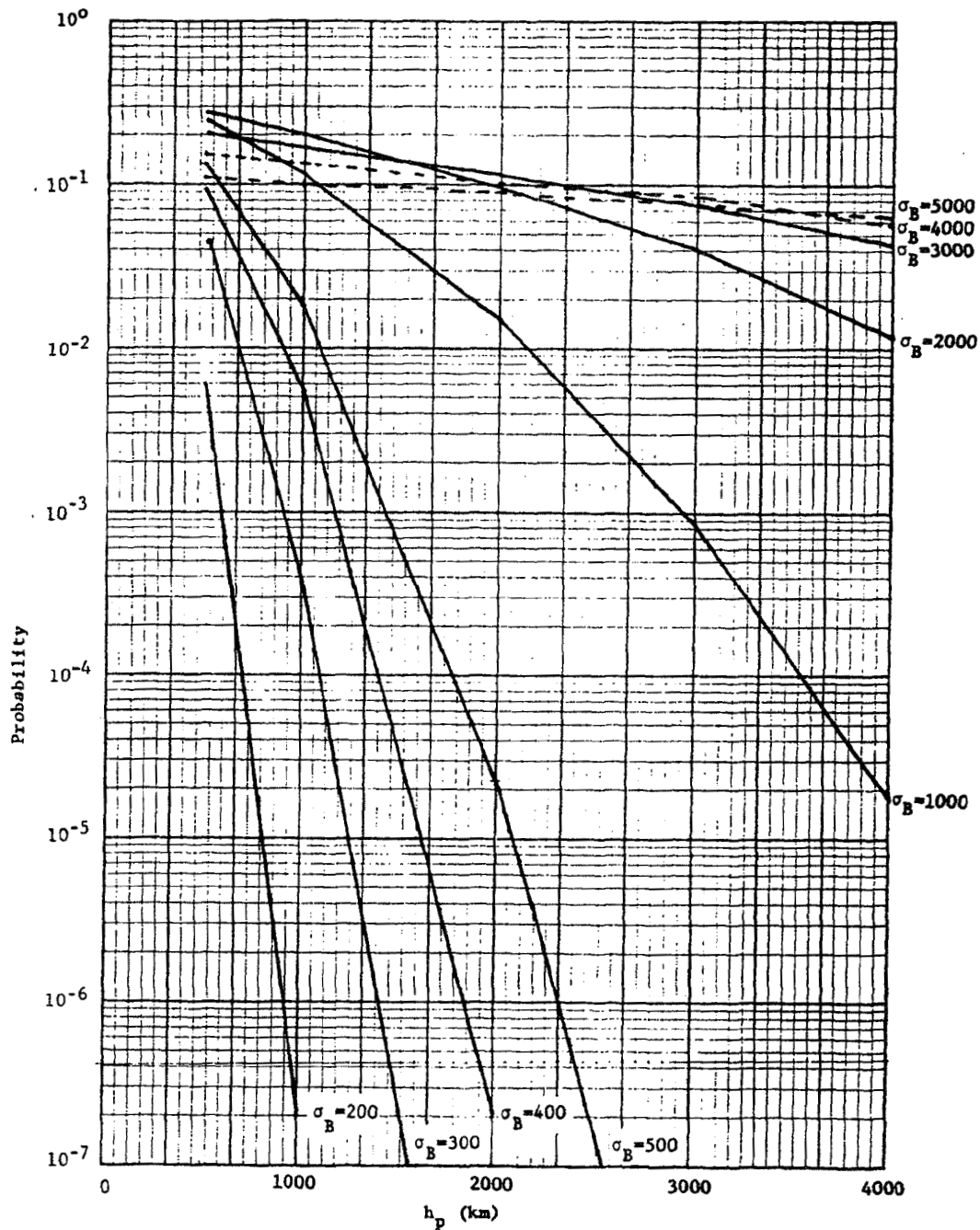
Fig. A-36 Titan Impact Probabilities - Constant σ_B Contours

A-100
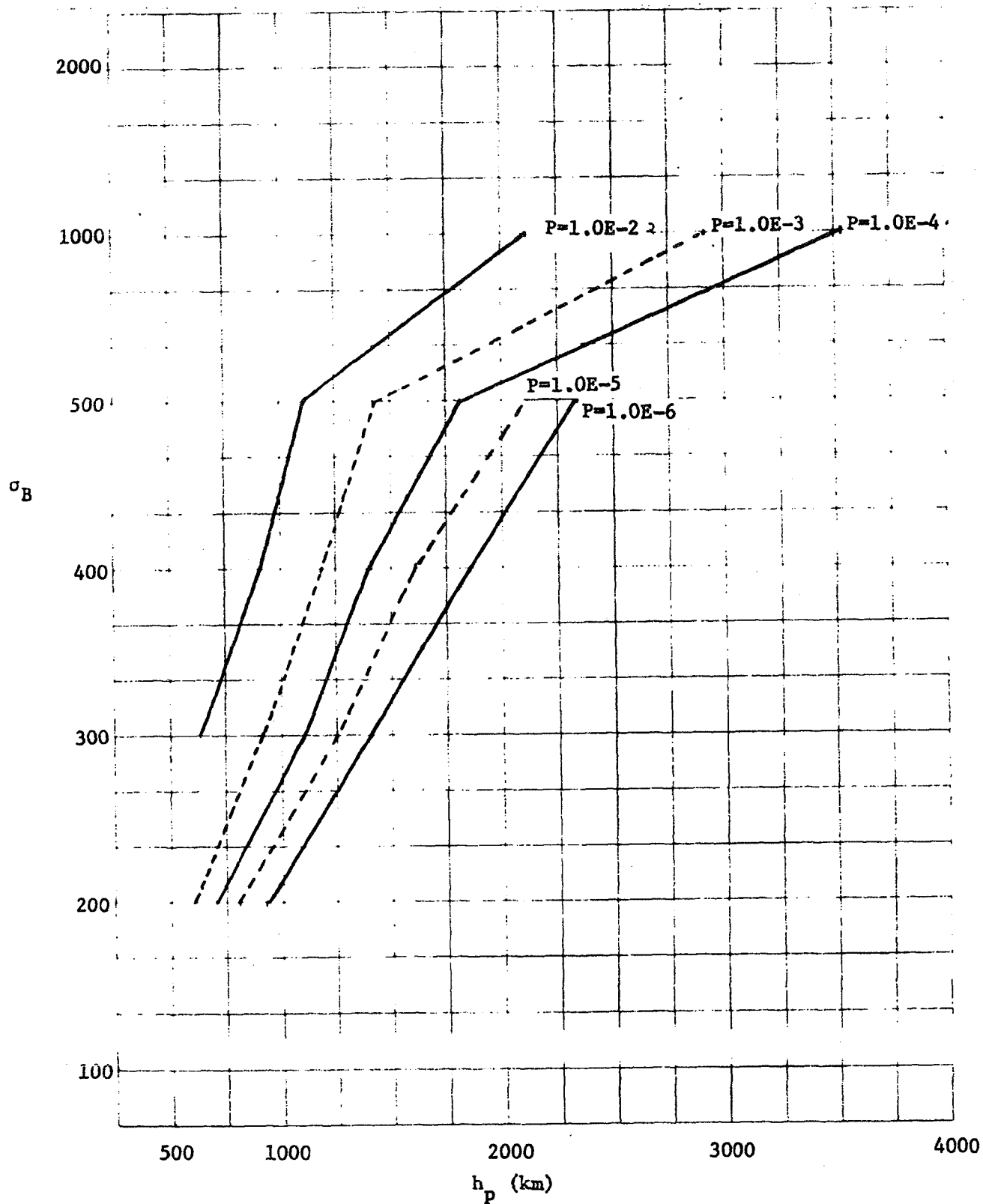
Fig. A-37 Allowable σ_B vs h_p for Various Impact Probability Levels

h_p of 1000 km requires that σ_B be less than 240 km. With h_p = 2000 km σ_B can grow to 430 km. Periapsis altitudes in the range 500 to 3000 km are being considered for Titan powered swingby trajectories which result in Saturn orbit insertion. The closer the passage is to Titan the more effective will Titan's gravity field be for bending the trajectory and producing the desired velocity change. Figure A-38 illustrates the h_p dependence of the maximum effective ΔV obtainable with a free satellite swingby. For typical Titan relative velocities in the 4 to 5 km/s range, doubling the h_p from 1000 km to 2000 km, reduces the maximum obtainable ΔV by 20%. Increasing h_p to 3000 km cuts the ΔV from 1.14 km/s to .76 km/s, a drop which effectively eliminates the usefulness of the technique. Figure A-36 also shows that a powered swingby with h_p = 2125 km and σ_B = 500 km (radio only tracking) might be compatible with an impact probability of 1×10^{-5}.

$$\Delta V = \frac{2V_\infty}{1 + r_p \, V_\infty^2 / \mu}$$

$h_p = 500$ km

$h_p = 1000$ km

$h_p = 2000$ km

$h_p = 3000$ km

Swingby ΔV, (km/sec)

V_∞ (Titan Relative)
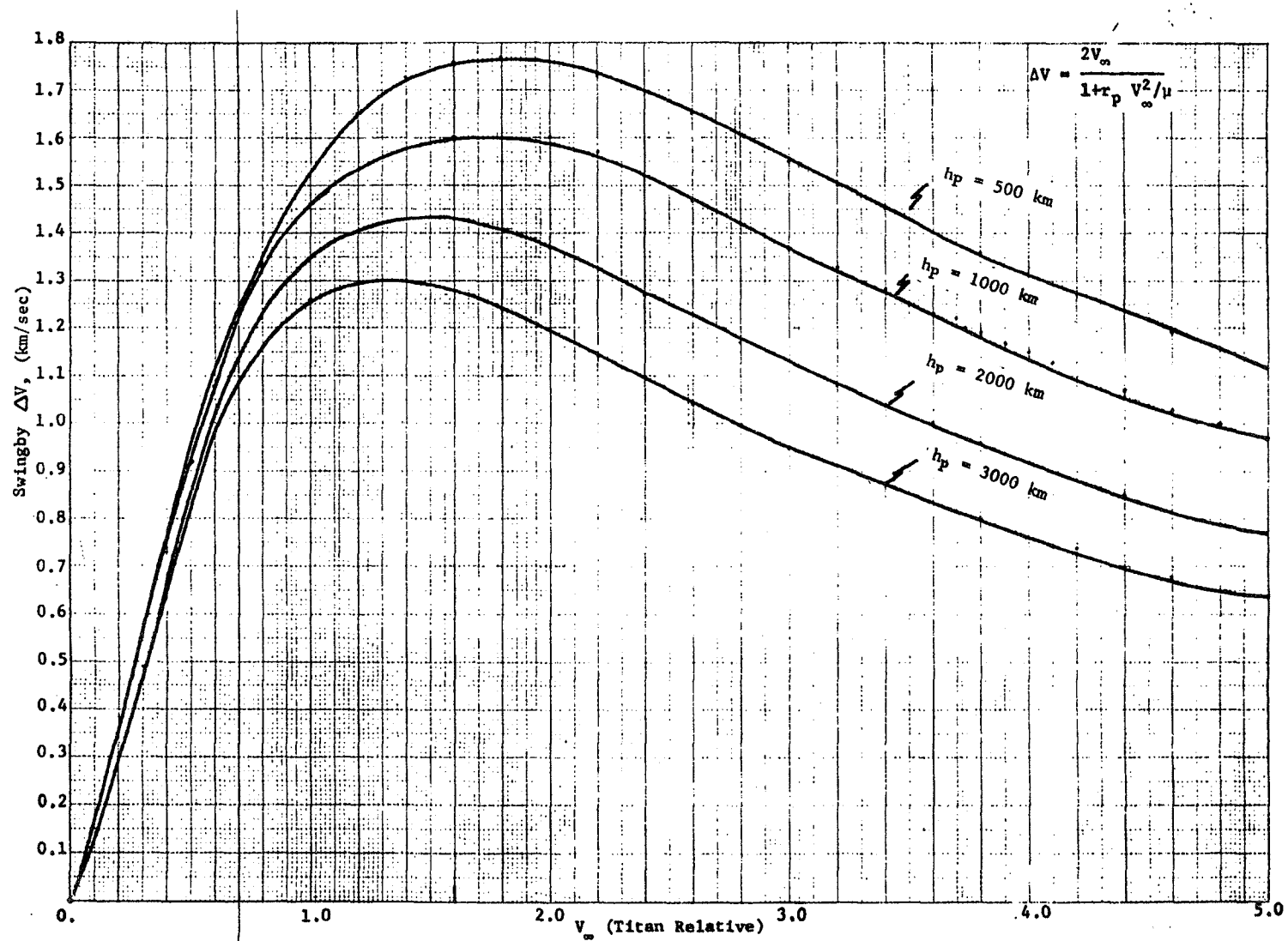
Fig. A-38 Free Swingby ΔV, (km/sec)

E. <u>REFERENCES</u>

A-1 "Design of Multi-Mission Chemical Propulsion Modules for Planetary Orbiters", Volume II Technical Report, NASA CR 137790.

A-2 "Shuttle/IUS Performance for Planetary Missions" Cork and Driver, JPL AAS 21st Annual Meeting, Space Shuttle Missions of the 80's, Denver, Colo., August, 1975

A-3 "The Saturn Orbiter Study Final Report", Dr. P. H. Roberts, July 10, 1975, JPL 760-126.

A-4 "The Powered Swingby and its Application to Jupiter Orbit Mission Design", C. Uphoff, Vector Sciences, Inc., La Canada, Calif. AAS Paper #75-084, AAS/AIAA Astrodynamics Specialists Conference, Nassau, Bahamas, July 28-30, 1975.

APPENDIX B

PRELIMINARY SYSTEMS DESIGN FOR TITAN EXPLORATION

To establish a point of departure from which to develop advanced
technology and mission planning options for Titan exploration, a number
of "trial mission" system and subsystem designs were generated. These
designs include examples of entry probes, surface penetrators and soft
landers. The design concepts for these trial systems are based on
existing designs with modification to account for Titan-peculiar require-
ments. The results therefore reflect current or near term state-of-the-
art technology.

An evaluation of the degree to which these systems accomplish the
scientific objectives reveals some shortcomings which, in conjunction
with problems of an engineering nature stemming from the uncertainties
in Titan conditions, serve as stimuli for the development of more
advanced approaches and techniques. These are discussed in Chapter III.
The following paragraphs contain the descriptions of the "conventional"
trial system designs.

A. TRIAL MISSION ATMOSPHERIC ENTRY PROBE

The science payload selected for the probe is given in Table B-1
along with estimated mass and power requirements. The rationale for
this instrument complement is discussed in Chapter II. Since the
science instruments are quite similar to those identified for the Jupiter
entry probe, the low entry angle, 10 bar probe of Reference B-1, that de-
sign was used as the basis for the Titan trial mission probe design. The
mission profile and system characteristics are summarized in Figure B-1.
Details of the design are contained in the next two sections.

1. Mission Profile

a. Interplanetary Trajectory - The trial mission probe/space-
craft combination can be launched from Earth on the Shuttle launch
vehicle system during any launch opportunity in the period of interest,
1980-1998, provided a 300 kg weight-class spacecraft (Pioneer) is

TABLE B-1 Titan Atmospheric Probe Science Payload

INSTRUMENT	CHARACTERISTICS	MASS (Kg)	POWER (Watts)
Atmospheric MS	1-50 AMU, 3 meas/scale ht.	5.0	10.0
Organic MS	50-250 AMU, 1 meas/scale ht.	5.0	5.0
GC	1-3 analyses, up to 3-carbon	3.0 warmup	20.0
UV Photometer	Solar pointing, 220, 260, 280y bands	2.5 oper.	8.0
Accelerometer	Entry	1.5	-
T, P Transducers	3 meas/scale ht.	1.5	0.5
Impact Transducer	Surface location, penetrability	1.0	-
Expanded Organic Analysis *		19.0 warmup	40.5
		oper.	28.5
IR Radiometer	IR Balance		
Visible Light Monitor	Solar Pointing		
Nephelometer	Pioneer Venus		
Cloud Particle Size Analyzer	Pioneer Venus		
Ion MS	Ionosphere Meas.		
RPA or Plasma Probes	Charged particles in ionosphere		
X-ray Fluorescence Sprectrometer	P, S, Cl, Ar Detection		

*The following instruments are optional

Max g

t = 90 sec
h = 179 km
Decel = 11.3 g_E

Store Entry Data
B = 78.5 kg/m^2

Separate from Spacecraft

t = -5.2 days
ΔV = 52 m/s

Entry

t = 0
h = 594 km
γ_E = -60°
V_E = 5.84 km/s

Activate Deployable Science

Begin Transmission
t = 202 sec
h = 99 km
Data Rate 88 bps
RF Power 7 W

Impact

t = 43 min
h = 0 km (R = 2700 km)
P_A = 400 mb
T_A = 78°K

Weights	kg
Science	19.0
Electronic/ Electrical	24.0
Structural/ Mechanical	27.0
Heat Shield	10.0
Margin	10.0
	90.0

Science
Temperature
Pressure
Accelerometers
Neutral Mass Spectrometer
Organic Mass Spectrometer
Gas Chromatograph
UV Photometer
Impact

Fig. B-1 Typical Titan Atmopsheric Probe Mission in Nominal Atm

selected. For a 1985 launch, a throw weight of 850 kg is required and the Shuttle/IUS can deliver 920 kg (C_3 = 113 km^2/sec^2). The corresponding flight time is 5.7 years. With the Shuttle/Tug combination which has about twice the payload capability, the options exist to either increase the injected weight payload (1500 kg) for the 5.7 year flight time or reduce both injected weight and flight time. The disadvantage of reducing flight time is the corresponding increase in approach velocity (VHP) and insertion ΔV. For the trial mission the 5.7 year flight time is baselined.

b. <u>Titan Approach Trajectory</u> - The Titan approach trajectory for the probe trial mission design resulted from the trade-offs and parametric studies discussed in Appendix A. The approach trajectory is targeted to a Saturn periapsis radius of $18 R_s$. The inclination of the approach hyperbola is selected so that the incoming trajectory crosses that plane of Titan at the radius of Titan. The alignment of the spacecraft relative to Titan is essential both to effect a probe encounter with Titan and to use the gravity field of Titan to reduce the orbit insertion ΔV.

The probe/spacecraft combination is targeted to a closest approach altitude relative to Titan of 1000 km. At 5×10^6 km or 5.2 days from Titan, the spacecraft orients and releases the probe. The probe then performs a ΔV maneuver which acquires the desired entry location. The probe does not have an active attitude control system and enters Titan's atmosphere at the same attitude required to acquire the desired entry site. For all missions studied the resultant angle of attack is less than 25°.

After the spacecraft deploys the probe a small ΔV is required to adjust the phasing between the spacecraft and the probe at entry. Range from the probe to the spacecraft is never more than 30K km and the critical spacecraft and probe aspect angles are within tolerable ranges.

After completion of the probe mission, which nominally lasts

43 minutes, the spacecraft is oriented and a ΔV initiated to produce the powered Titan swingby that results in a 144 day orbit about Saturn.

    c. <u>Entry and Descent Analysis</u> - The critical entry and descent portion of the probe mission begins at the turbopause (10^{-7}bars), continues through peak deceleration and terminates at touchdown 43 minutes later. The -60° entry angle was selected as a compromise between reduced dispersions, maximum entry environment, with the dominate driver being skipout. The skipout angle for entry into the nominal atmosphere is -20°. Reasonable, 500 km (1σ), navigation uncertainties result in an entry angle dispersion of $\pm$ 36° (3σ); therefore to reduce the possibility of skipout requires an entry angle of at least -60°.

    The descent portion of the mission begins when the probe reaches terminal velocity- 202 seconds after entry. The velocity of the probe at this point is entirely a function of the atmospheric density, and ballistic coefficient.

    d. <u>Navigation and Dispersions</u> - Navigation was performed by radio tracking from Earth. The nominal mission design assumes a Titan ephemeris uncertainty of 500 km (1σ). The resulting entry dispersions are illustrated in Table B-2.

<u>Table B-2 Entry Dispersions</u>

Entry Time (3σ) min	Entry Angle (3σ) deg	PAA (3σ) deg	Entry Site		Range (Entry) (3σ) km
			DR (3σ) deg	XR (3σ) deg	
2.6	34.6	36.1	5.8	4.2	2352

While these dispersions are large, they do not preclude the execution of a viable probe mission. For higher levels of ephemeris uncertainty, however, radio tracking would no longer be adaquate and would have to be supplemented with optical navigation.

2. Design

    a. Configuration and Mechanical Subsystems - The blunted cone
forebody and hemispherically domed afterbody configuration selected
for the trial mission design is shown in Figure B-2. The science
instruments as well as their subsystem support equipment are mounted
directly to the aeroshell stiffening frames to assist in maintaining
a c.g. forward of the aeroshell/basecover intersection and also to
minimize the amount of installation hardware required. Since it is
desirable for the gas chromatograph, mass spectrometer, and pressure
sensor all to obtain samples from the stagnation point, a single sampler
is provided which is manifolded to each of these instruments. The
sampler also provides a mount for the accelerometer instrument which is
located at the probe c.g. A segmented toroidal packaging scheme was
used for the remainder of the components. This arrangement is shown
in the photograph of Figure B-3. With this configuration, access to
one component is not dependent upon the removal of any other piece of
equipment. The four elements of the toroid are the gas chromatograph,
mass spectrometer, electrical/electronics module, and the data handling
module. The packaging efficiency of the probe is improved with this
modular concept over that of the Reference B-1 probe in that individual
components of a subsystem may be mounted uncased and hardwired inside
the toroidal container as opposed to mounting each one individually.

    Other differences between this probe and the Reference B-1
outer planets/Jupiter probe design are a lighter weight heat shield and
the incorporation of an orbit deflection motor. Thermal control pro-
visions can be similar to the reference probe.

    The entry heating predictions for the nominal Titan atmospheric
model are shown in Figure B-4 for the low-relative-velocity entries of
the powered swingby missions (V_E = 5.8 km/sec). The peak value of about
50 watts/cm^2 (0.5 mw/m^2) on the cone compares to about 20 w/cm^2 for Viking
'75 Mars entries and 40,000 watts/cm^2 for the proposed low entry angle
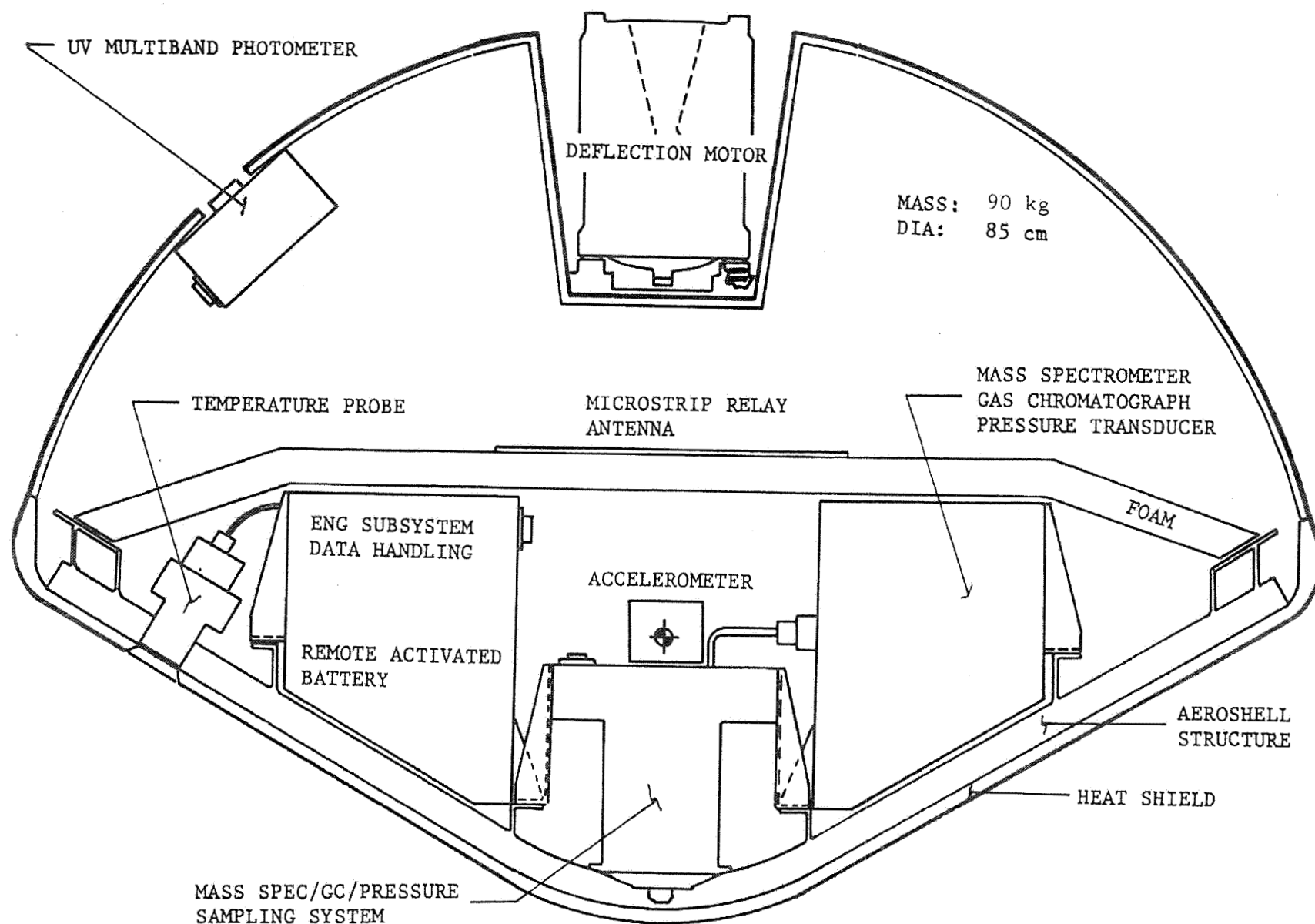
Fig. B-2 Titan Entry Probe – Trial Mission Configuration – Nominal Atmosphere
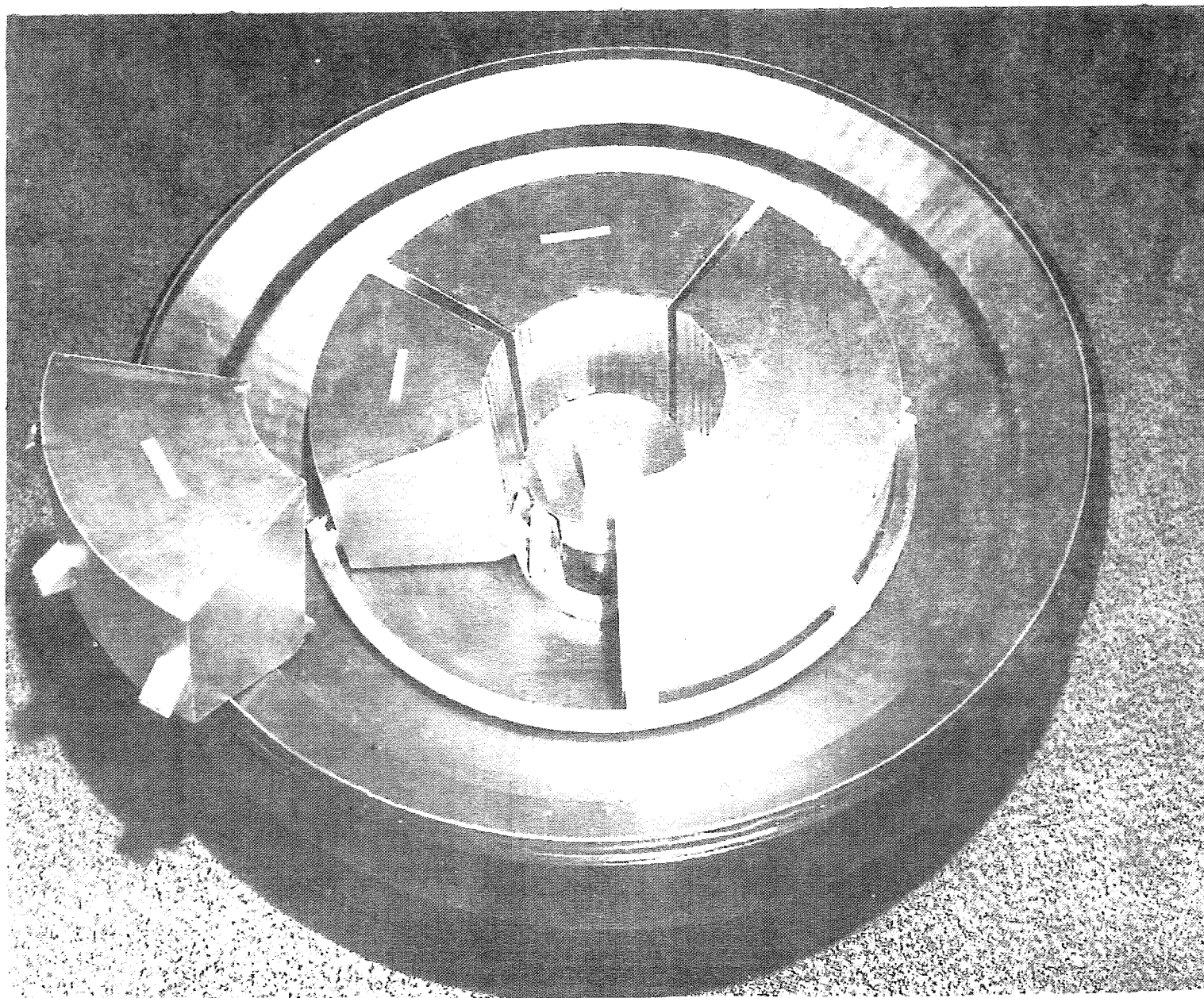
Fig. B-3   Equipment Arrangement Mockup - Titan Entry Probe
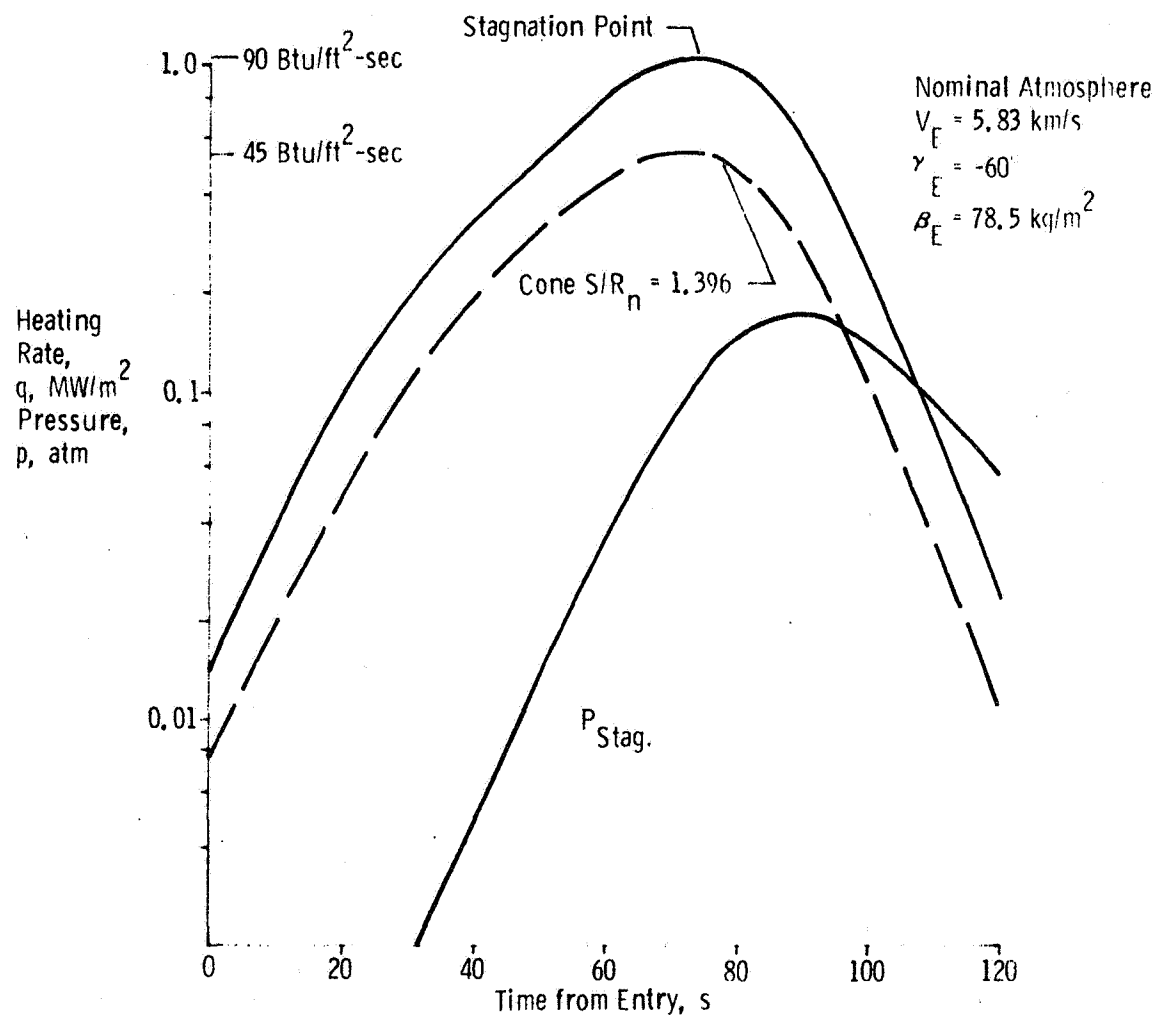
Fig. B-4 Titan Entry Heating

Jupiter entries. For Titan, the heat input is entirely convective.

Due to these moderate heating rates, the Titan heat shield design can be much lighter than the outer planets entry probe designs. If the dense relatively high conductivity carbon phenolic heat shield material planned for Pioneer Venus and also proposed for the outer planets probes is used, a relatively heavy design results even though a greatly reduced thickness will be adequate. 12.2 kg per square meter or 8 kilograms total for the forebody heat shield would be required. The low density 240 kg/m^3 Viking material is considered applicable up to rates of about the 50 $watts/cm^2$ value predicted for Titan . If this material were used it would result in a heat shield weight about one-fifth of that required with carbon phenolic (or a much lower structural temperature) as shown in Figure B-5. If the Viking material proves to be marginal for the Titan rates, the 480 kg/m^3 density elastomeric silicone used on the PAET vehicle could be used instead. Its use permits a heat shield design that is still less than ½ of the mass of a carbon phenolic design and well under 10% of the entry weight.

Figure B-6 shows the descent temperatures for the trial mission probe using the vented probe concept proposed for the outer planets probe. The initial probe temperature of 298°K is achieved by an *isotope heater in balance with the external multilayer insulation* heat loss during the pre-entry coast period. Although the probe is vented, incoming gases cause little cooling of the payload. Also, losses through the 2.5 cm of descent insulation are much less severe than for the outer planets probes due to the considerably lower conductivity of the predominately N_2 atmosphere (postulated in the nominal atmosphere model for Titan) relative to the H_2 atmospheres of the outer planets.

A probe ΔV of approximately 30 m/s is required for the "shared deflection" mode required by planetary quarantine considerations. A solid rocket motor the size of the Marc 61A motor shown in Figure B-7
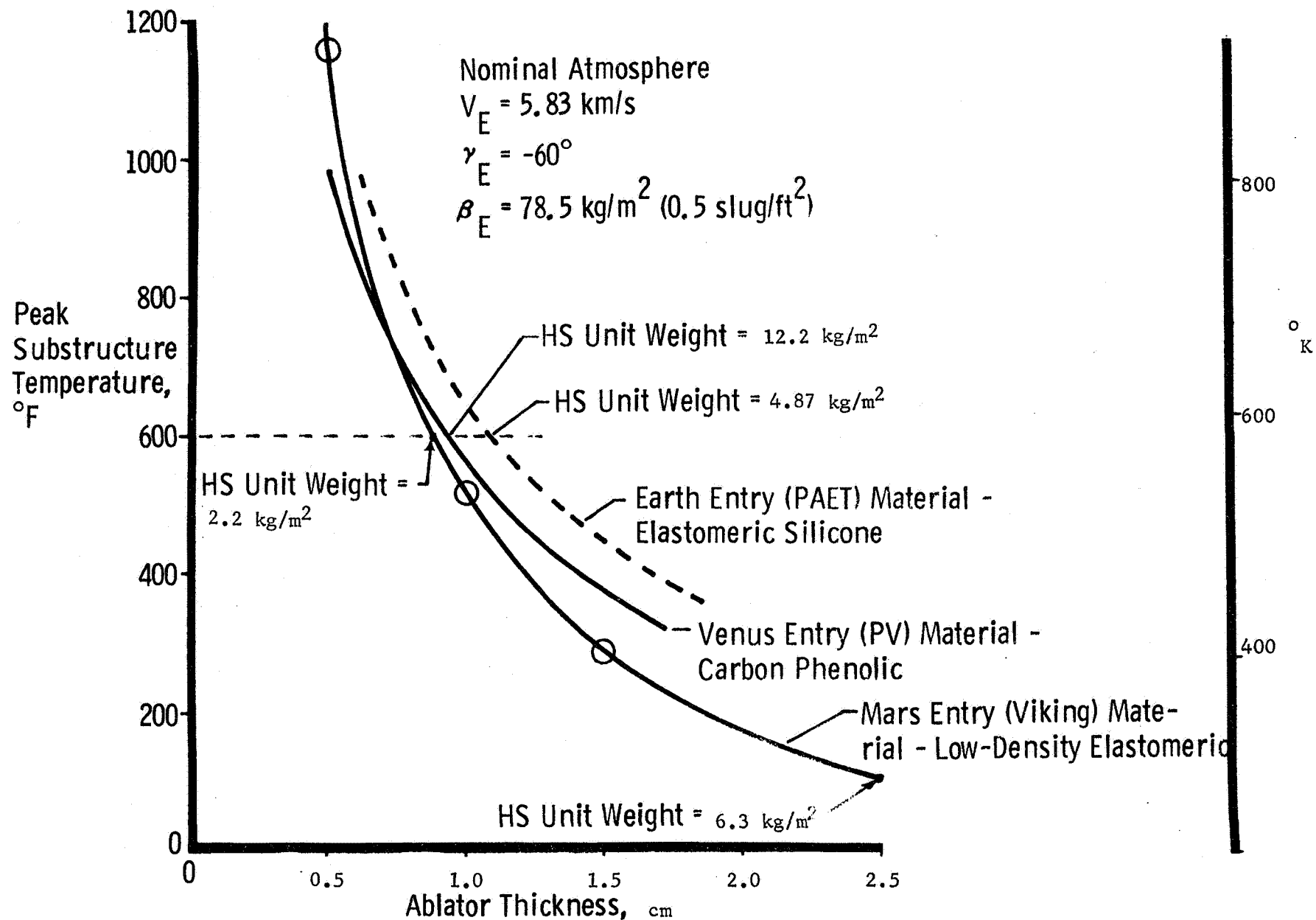
Fig. B-5 Titan Probe Heat Shield Design Options

Probe Mass, 60 kg
Power
   Isotope Heaters, 5 W
   Science & Data, 53 W
   Communications, 28 W
Insulation, 2.5 cm Fibrous
Vented Equipment Compartment
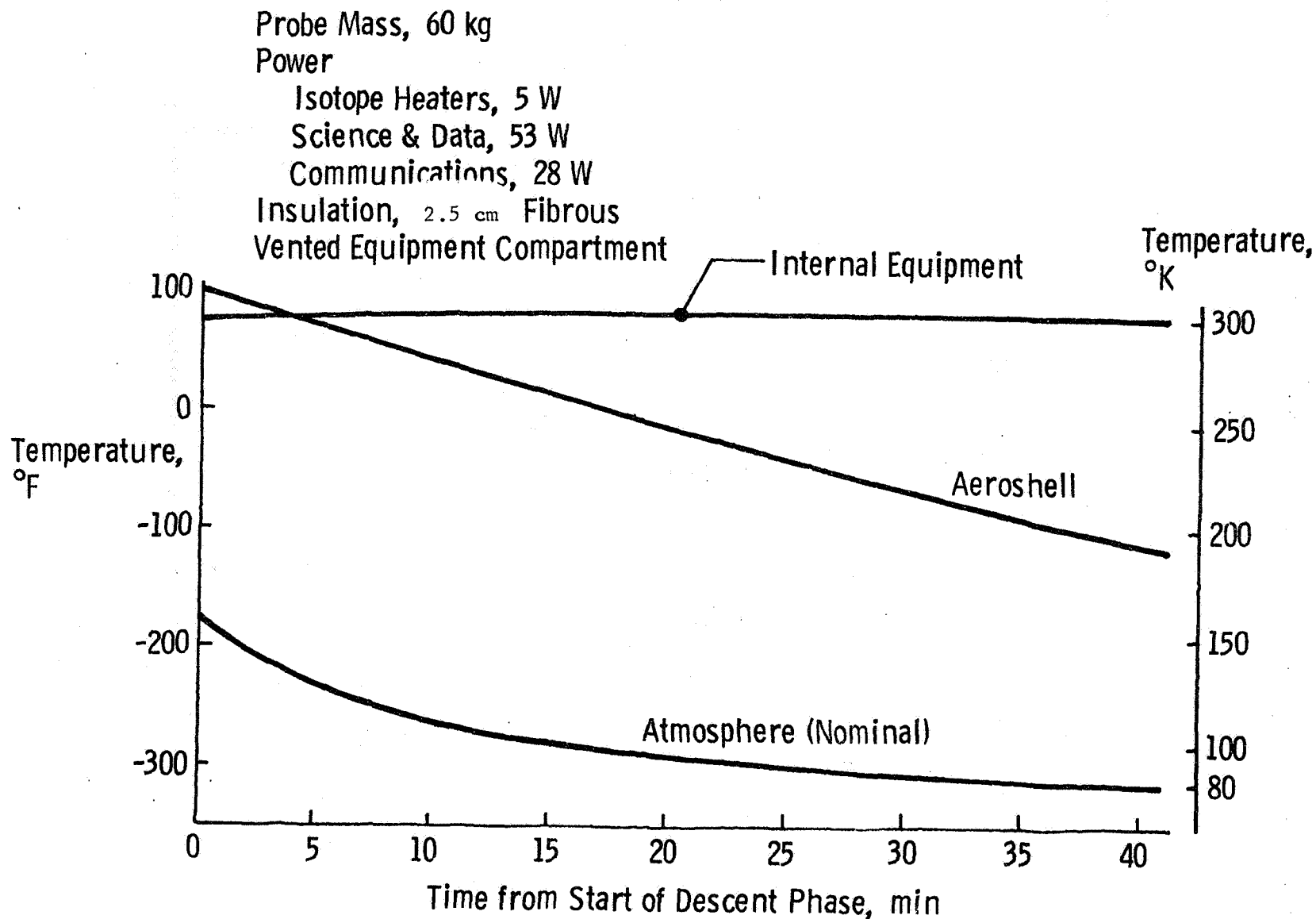
Fig. B-6 Titan Probe Descent Phase Thermal Analysis - Nominal Atmosphere
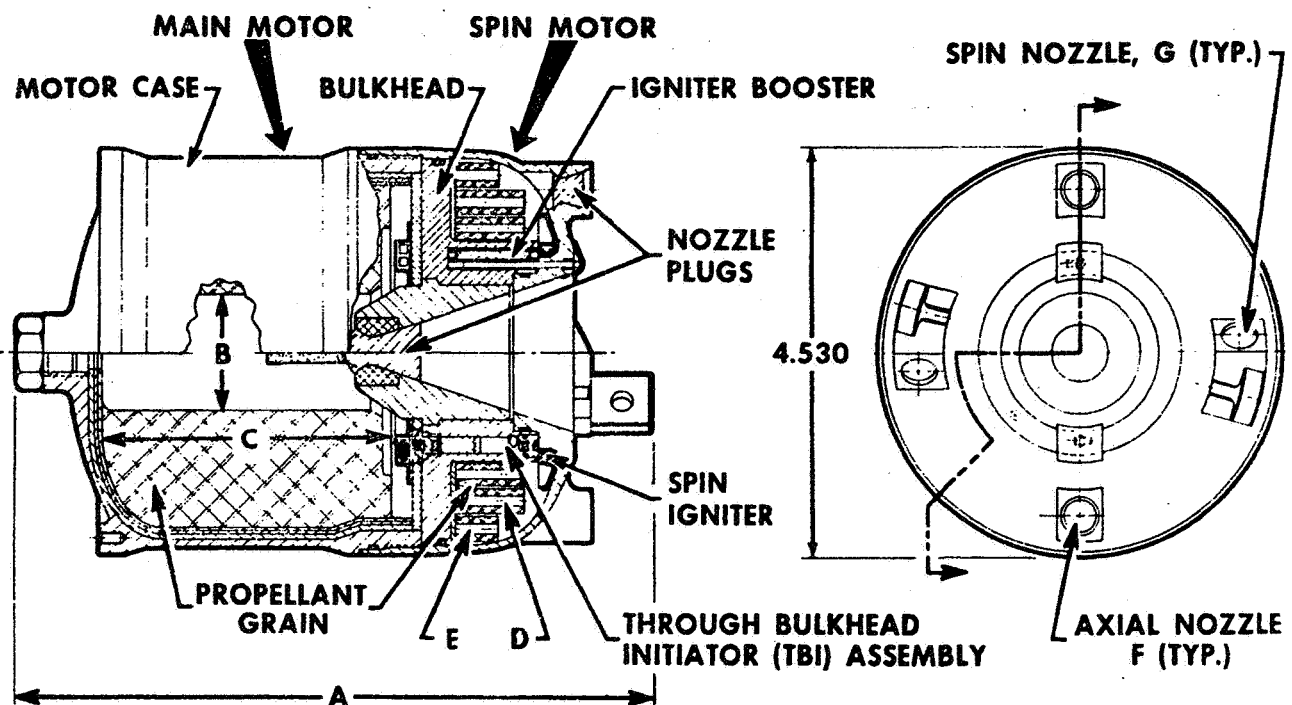
MOTOR FAMILY DESIGN VARIATIONS
(See above drawing)

MARC No.	Main Motor KS Rating	Spin Motor KS Rating	Motor Length (Dimension A) (in)	Grain I. D (Dimension B) (in)	Grain Length (Dimension C) (in)	Long Grains (Area D)	Short Grains (Area E)	Axial Nozzles (Area F)	Spin Nozzles (Area G)
61A (E-1)	3.6-KS-180 (M-1)	0.05-KS-650 (S-1)	7.04	1.30	3.590	2 rows	1 row	2	2
61B (E-2)	3.8-KS-145 (M-2)	0.05-KS-560 (S-2)	7.04	1.30	3.017	2 rows	—	2	2
61C (E-3)	3.7-KS-125 (M-3)	0.05-KS-480 (S-3)	6.23	1.23	3.635	2 rows	—	2	2
61D (E-4)	4.2-KS-90 (M-4)	0.05-KS-400 (S-4)	6.23	1.30	2.114	2 rows	—	2	2
61E (E-5)	2.1-KS-150 (M-5)	0.05-KS-340 (S-5)	6.23	2.340	2.216	2 rows	—	2	2
61J (E-6)	3.8-KS-60 (M-6)	0.06-KS-190 (S-6)	5.06	1.620	1.535	2 rows	—	—	2
61K (E-7)	2.1-KS-70 (M-7)	0.06-KS-160 (S-7)	5.06	2.530	1.435	1 row	—	—	2
61H (E-8)	0.9-KS-85 (M-8)	0.05-KS-140 (S-8)	5.06	3.260	1.219	1 row	—	—	2

Fig. B-7 Existing Solid Rocket Motor Series Suitable for Probe Deflection

can provide this ΔV in addition to providing spinup for thrust vector control. Once the deflection maneuver is complete, the motor assembly would be jettisoned, thus avoiding a blockage of the probe antenna. A weight statement of this probe configuration is shown in Table B-3.

Figure B-8 depicts a typical integration of the trial mission probe into a Pioneer Saturn Orbiter. It is assumed here that planetary quarantine considerations will require the incorporation of a bioshield similar to the arrangement for the MARS Viking Lander Capsule. The probe would attach to the orbiter adapter around the periphery of the aeroshell with the bioshield base having attachment to and being separated with the kick stage adapter. The bioshield cap would remain with the orbiter at the time of probe separation. Although the bioshield complicates the design, the small size of the probe capsule minimizes the impact of its integration into the total spacecraft.

Table B-3

Trial Mission Atmospheric Entry Probe Mass Breakdown

	Mass (kg)
Structure	14.0
Heat Shield	10.0
Heaters/Insulation	7.0
Comm/Data Handling	10.2
Power	8.3
Pyro	3.7
Science	19.0
Science Accommodator	6.0
Instrumentation	1.8
Margin	10.0
Total	90.0

Mechanisms are provided for deploying the sampling devices and their penetrations through the aeroshell/heatshield. Separation devices are required to desplice the bioshield, jettison the deflection motor and separate the entry capsule from the lander. With the exception of the deflection motor separation, these devices can be similiar to the outer planets probe and Viking '75 designs.

MODIFIED PIONEER
JUPITER ORBITER

PROBE RELAY
ANTENNA

TITAN PROBE

KICK STAGE
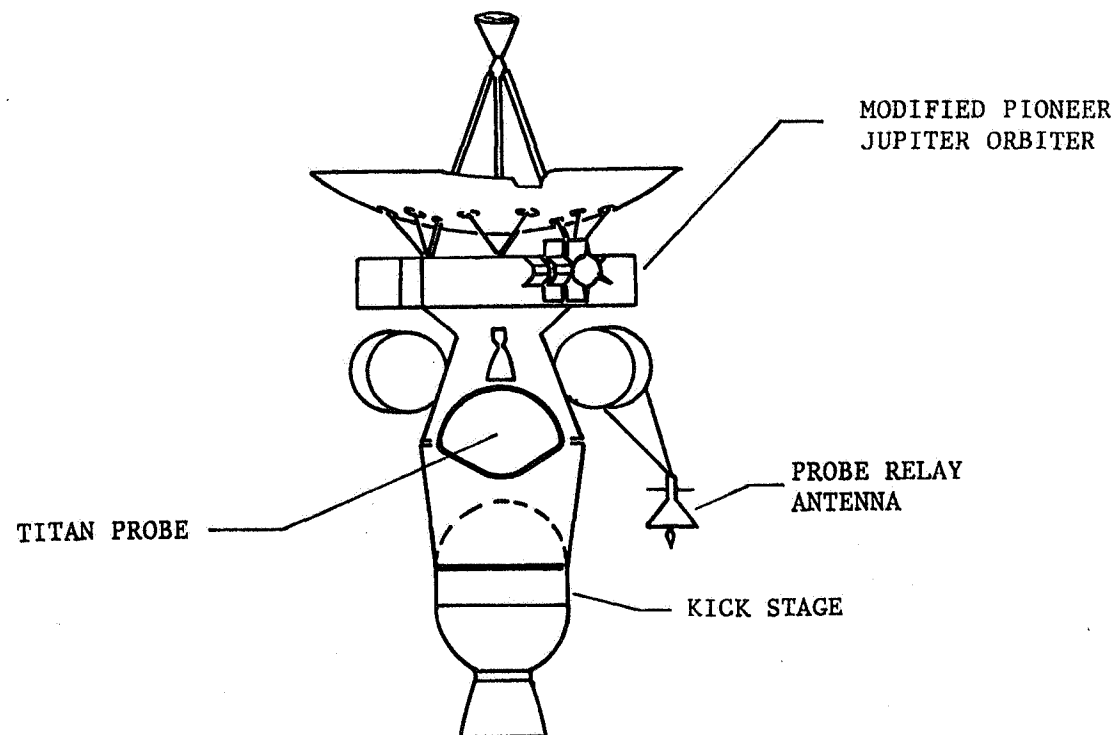
Fig. B-8 Pioneer Saturn Orbiter with Titan Probe

b. Communications and Power - Probe Design

Probe Communications - The probe telemetry system is built around the requirements of the science experiments and impact of the mission geometry. The experiments set the requirements and the mission sets the constraints. The experiments consist of 1) temperature and pressure transducers (3 bps), 2) accelerometers (4 bps), 3) atmospheric mass spectrometer (40 bps), 4) gas chromatograph (15 bps), and 5) μV photometer (15 bps). The raw data rate required for these science experiments is 77 bps. Engineering housekeeping data and formatting brings the rate to 88 bps.

The next question is how to return the probe data to Earth. Past experience in Outer Planet Probes has proven that a direct RF link to Earth is impractical from a power standpoint. Past trade studies have also shown that an optimum relay link frequency is 400 MHz. Non-coherent FSK modulation is also the most efficient for the low data rate. Convolutional coding is also employed for data efficiency and low error rates.

Uncertainties and dispersions in the position of Titan result in a range tolerance of $\pm$ 1000 km and 3-σ angular position tolerances of $\pm$ 3°. These were considered in the link analysis. The optimum probe mission has a radius of closest approach of 3700 km and a lead time of 1 hour. The mean entry communications range is 30,000 km and the probe mission lasts for 43 minutes. RF link conditions improve after entry, with decreasing range and lower probe aspect angles resulting in higher probe antenna gains. Therefore, the worst case condition for the telemetry link is at entry and the RF power required then sizes the transmitter. The entry link table is shown in Table B-4. As seen, 7W of RF power is required to maintain the link at 400 MHz to the flyby spacecraft with a data rate of 88 bps. The link design includes conservative assumptions to cover the uncertainties that presently exist in planet position, noise temperature, and atmosphere effects.

B-16

Table B-4 Probe Telementry Design Control Table

ITEM	PARAMETER	NOMINAL VALUE	ADVERSE TOLERANCE	REMARKS
1.	Total Transmitter Power, dBW	8.4	0.4	400 MHz, 7.0 W
2.	Transmitting Circuit Loss, dB	- 0.8	-0.1	
3.	Transmitting Antenna Gain, dB	3.7	-0.3	Conical,θ=140°,G_m=4.4dB
4.	Antenna Pattern Ripple, dB	- 2.5	-0.1	
5.	Space Loss, dB	-174.0	-0.3	$3 \times 10^4 \pm 10^3$ km
6.	Planet Atmosphere Loss, dB	- 0.2	0.0	
7.	Polarization Loss, dB	- 1.5	-0.1	AR_p=3dB, AR_r= 8 dB
8.	Receiving Antenna Gain, dB	2.9	-0.2	Toroid Pattern, θ=50°,G_m= 3.4dB
9.	Receiving Circuit Loss, dB	- 1.0	-0.1	
10.	Net Circuit Loss,$\Sigma(2 \rightarrow 9)$, dB	-173.4	-1.2	
11.	Total Received Power, (1+10), dBW	-165.0	-1.6	
12.	Receiver Noise Spectral Density, N_o, dBW/Hz	-202.8	-1.0	T_s= 380 $\pm$ 100°K
13.	Received Power/N_o, (11-12), dBW·Hz	37.8	-2.6	

DATA CHANNEL

ITEM	PARAMETER	NOMINAL VALUE	ADVERSE TOLERANCE	REMARKS
14.	Fading Loss, dB	- 0.5	-0.2	
15.	Processing Loss, dB	- 1.0	-0.2	
16.	Received Data Power, (11+14+15), dBW	-163.5	-2.0	
17.	Data Bit Rate, dB	19.5	0.0	Rate = 88 bps
18.	Threshold E_b/N_o, dB	10.6	0.0	BER = 5×10^{-4}
19.	Threshold Data Power, (12+17+18), dBW	172.7	-1.0	
20.	Performance Margin, (16-19) or (13+14+15-17-18), dB	9.2	-3.0	
21.	Nominal Less Adverse Margin, (20-20 adv), dB	6.2		

Conditions: 1. Titan Probe worst-case conditions at Entry.
2. Spacecraft flyby, RCA_t=3700km, γ=-60°, T= 142°, T_L=1 Hr.
3. Radio Guidance employed.
4. Nominal Titan atmosphere model, 100% N_2, 400 mbar pressure.
5. FSK non-coherent modulation, BT=2.
6. Roll-stabilized flyby spacecraft.
7. Convolutional encoding, viterbi decoding, Rate = 1/2, Constraint length = 10, hard decision
8. B = 0.5 slugs/ft^2, Mission completion at Entry + 32 min.

The three atmosphere models currently proposed for Titan contain primarily nitrogen and methane. RF absorption in methane is negligible and for the pure nitrogen model with a pressure of 400 mbar, the effects are similar to the Earth's atmosphere. The absorption at 400 MHz in the Earth's atmosphere is approximately 0.3 dB with the main contributor being from water vapor absorption. Therefore, it is concluded that UHF attenuation in any of the three Titan atmosphere models is negligible ($<$0.1 dB).

The probe antenna is a microstrip disk design with circular polarization and a beamwidth of 140 deg. The peak gain is 3.4 dB and a conical pattern is produced. The spin-stabilized, flyby spacecraft employs a loop-V antenna which is also circularly polarized. It produces a dipole or toroidal pattern centered at an aspect angle of 55 deg. with a beamwidth of 50 deg. and a peak gain of 3.4 dB. Axial ratios for the probe and spacecraft antennas are 3 and 8 dB, respectively resulting in a polarization loss of 1.5 dB.

The approach geometry is such that Saturn is not in the background of Titan during the mission and the only external sources of noise temperature are background cosmic noise and disk noise from Titan. A receiver noise figure of 3.0 dB is assumed for the spacecraft receiver at 400 MHz. The resulting system noise temperature is approximately $400^{\circ}K$ with the major contributor being the internal receiver source. The latest Titan Monograph (Ref B-5) indicates a disk temperature of only $100^{\circ}K$. The spacecraft antenna temperature for the dipole pattern is $50^{\circ}K$.

The telemetry transmitter is an all-solid-state unit capable of 7 W of RF output. The overall efficiency is 25% which results in 28 W of dc power required from the battery. The data handling unit includes an A-to-D converter for the analog accelerometer data, a small, solid-state memory to store entry data prior to transmission, and circuitry to encode the serial bit stream.

Probe Power Subsystem - Evaluation of the science and
mission requirements lead to the selection of an energy source and power
distribution system. The science and engineering subsystems operate
simultaneously during the 42-minute descent and require 96.8 W-hr of dc
energy. The energy requirements of the probe mission are shown in Table
B-5. The science experiments shown in parentheses are not included in
the total energy since they are not in the baseline payload. They re-
flect additional science that might be added if additional weight and
design margins are available.

The power distribution system is shown in Figure B-9. A
remotely activated, 28-volt, unregulated silver-zinc battery of 125 W-hr
capacity is required to provide the necessary margin for sterilization
and long life for this design. A small rechargeable nickel cadmium boot-
strap battery is used to activate the primary silver-zinc power source,
operate a clock after separation from the spacecraft, and initiate the
pyrotechnic remote activation device. The Ni-Cd battery is initially
charged from the spacecraft power through a charger prior to probe
separation.

Power is distributed and controlled to the loads through
a Power Control Unit that is activated by a gravity switch that is
initiated by the entry deceleration. Power sequencing is controlled by
the command memory and logic network.

B. TRIAL MISSION PENETRATOR

The Mars penetrator designed by Sandia Laboratories (Reference B-2)
served as a basis for the trial mission penetrator. The science objectives
for a Titan penetrator, and in particular the desire for a mass spectro-
meter experiment, are not compatible with the size of the Sandia unit.
Consequently, significant design modification became necessary although
due to similarities in estimated surface penetrability coefficients for
Mars and Titan it is desirable to retain the same mass/area ratio and
impact velocity that was selected for the Mars penetrator design. The

Table B-5   Titan Trial Mission Probe Power and Energy Requirements

Coast Phase	Power, W	Time	Energy, Wh
5-day Clock	0.001	5 days	0.12
Entry & Deceleration Switch	0.2	2 hr	0.40

Entry & Descent Phase

Science

	Power, W	Time	Energy, Wh
Temperature & Pressure Transducers	2.5	42 min	1.75
Accelerometers	1.5		1.05
Atmospheric Mass Spectrometer	40.0		28.00
Organic Mass Spectrometer	5.0		3.50
Gas Chromatograph	20.0		14.00
UV Multiband Photometer	5.0		3.50
Impact Indicator	1.0		0.70
(Light Intensity Detector)	(1.0)		(0.70)
(Cloud Particle Size Analyzer)	(20.0)		(14.00)
(X-Ray Fluorescence Analyzer)	(4.0)		(2.8)
(Nephelometer)	(1.0)		(0.70)
(Ion Mass Spectrometer)	(3.0)		(2.10)
(Retarding Potential Analyzer)	(2.5)		(1.75)
Data Management Subsystem	10.0		7.00
Transmitter	28.0		19.00
Ordnance Relays	3.0	0.001 min	0.01
Battery Heater	20.0	42 min	14.00
Equipment Energy			93.11
Distribution Losses (5%)			3.65
Total Energy			96.76

(Items in parentheses are not in baseline payload.)
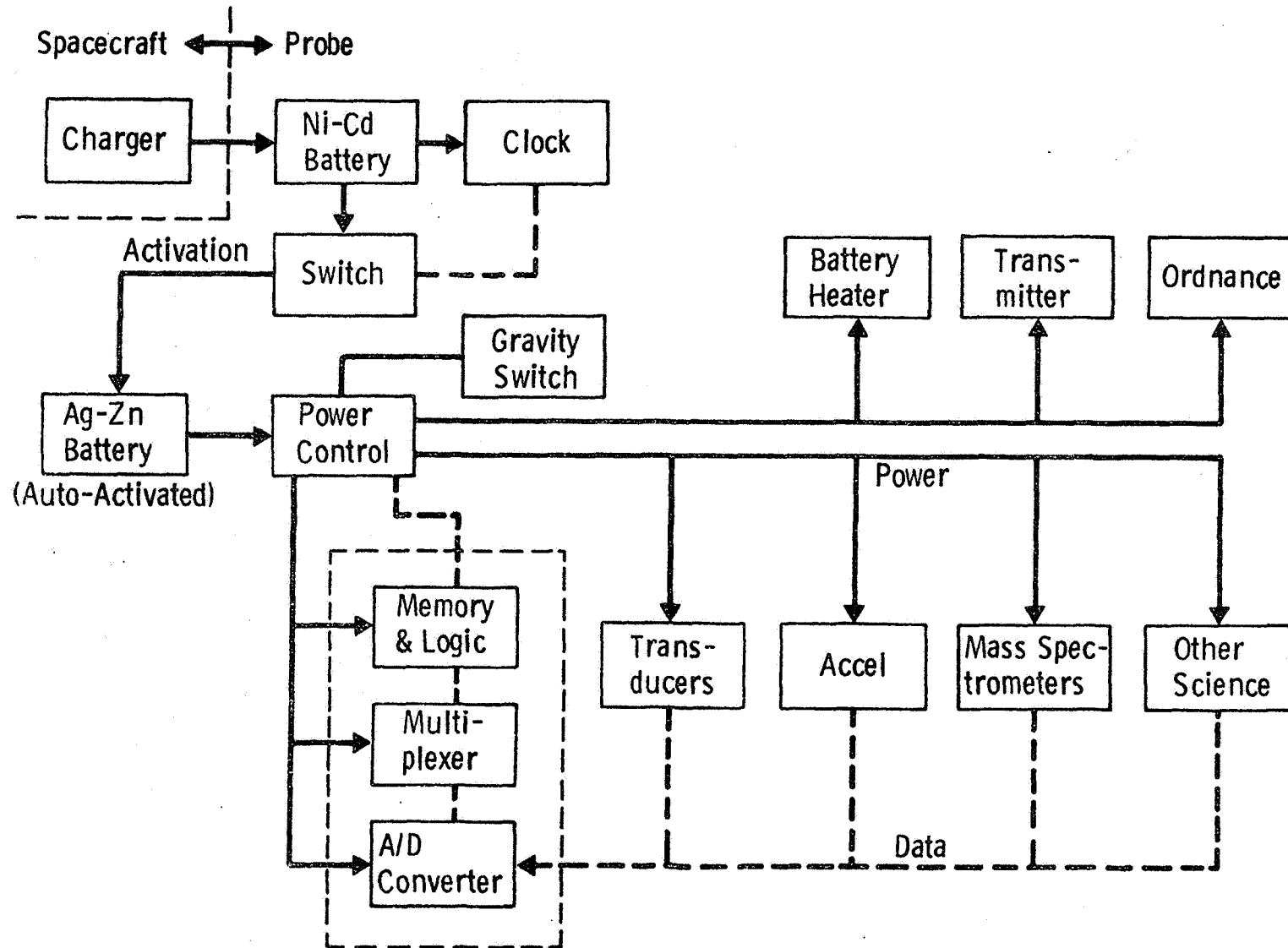
Fig. B-9 Titan Trial Mission Probe Power Distribution

proposed science payload is shown in Table B-6 and discussed in Chapter
II(page II-70).

A summary of the Titan Trial Mission penetrator characteristics is
shown in Figure B-10 and mission analysis and design details are provided
in the following paragraphs.

1. Mission Profile Description - Penetrator

a. Interplanetary Trajectory/Launch Analysis - The trial mission
penetrator has essentially the same mass as the probe described earlier.
Therefore the launch and interplanetary trajectory situation defined for
the probe mission applies also to the penetrator. Using either the
Shuttle/IUS prior to 1985, or the Shuttle/Tug launch vehicles in later
years, a Pioneer/Penetrator mission can be launched in any year. As with
the probe, the optimal years are centered about 1985 and 1998.

b. Approach Trajectory/Deflection Maneuver - The approach
trajectory and the deflection maneuver are also similar to the probe
mission. The penetrator is deflected from the spacecraft on the incoming
hyperbola, by a shared deflection. The approach trajectory is selected
to be compatible with a powered Titan swingby and subsequent orbit inser-
tion about Saturn. The orbit period is 144 days. Deflection occurs at
5×10^6 km and the coast time is 5 days. The deflection maneuver is designed
to maximize the communications time between the penetrator after emplace-
ment in Titan's surface and the spacecraft. Careful design of this man-
euver results in a communication time greater than 45 minutes.

c. Entry and Descent - The penetrator enters the atmosphere of
Titan at a velocity of 5.84 km/sec and a flight path angle of -60°.
Initially the penetrator is enclosed in a protective capsule, which is
staged at a predetermined altitude for final penetrator descent. The
ballistic coefficient of the initial entry configuration is 62.84 kg/m^2
(.4 slugs/ft^2) and the ballistic coefficient of the bare-body penetrator,
after staging, is ~13000 kg/m^2 (82.75 slugs/ft^2). Staging is initiated
by a pressure switch which is activated at an altitude corresponding to

B-22

TABLE B-6   Titan Penetrator Science Payload

INSTRUMENT	CHARACTERISTICS	MASS (Kg)	POWER (Watts)
Accelerometer	Physical Properties of Surface Material	0.3	1.0
Temperature Array	Soil temperature, thermal conductivity	2.0	0.1
MS	10-300 AMU	6.5	27.5
Expanded Organic Analysis *		8.8 Kg	28.6 Watts
Passive Seismometry	Viking		
Active Seismometry	Explosive Charges		
Neutron Activation	Elements, Isotopes		
Passive Gamma-ray Spectrometer	K, U, Activated Nuclides		
XRFS	Elements		
X-ray Diffractometer	Crystal Structures		
Heat Flow	Temperature Profile		
Magnetometer	Sensitivity?		

*The following instruments are optional

Entry

t = 0 sec
h = 594 km
γ_E = -60°
V_E = 5.84 km/s

Separate from Spacecraft

t = -5.2 days
ΔV = 100 m/s

Max g

t = 90 s
10.6 g_E
h = 177 km
B = 63 kg/m^2

Stage Fairings

t = 246 s
h = 100 km
B = 13,000 kg/m^2

Impact

t = 10.5 min
h = 0 km (R = 2700 km)
Aft Section - 18,000 g
Forebody - 1,800 g
V_{impact} = 150 m/s
Data Rate 32 bps
RF Power 2 W
Lifetime 60 min

1 - 15 m

Weights	kg
Science	8.8
Electrical, Electronic	11.5
Structure Mechanical	42.9
	63.2
Entry Fairings	18.0
Margin	10.8
Total	92.0

Dia   = 12.7 cm
Length = 1.82 m

Science

Accelerometer
Temp Array
Mass Spectrometer

B-24

Fig. B-10 Typical Titan Penetrator Mission in Nominal Atm

8.5 mb. The nominal impact velocity is 145 m/sec.

    d. Navigation and Dispersions - The navigation errors and resultant dispersions are the same as those defined for the probe mission.

    2. Design

    a. Configuration and Mechanical Subsystems - Since the selected mission profile is based on completing the science experiments while the orbiter is within communication range in its initial flyby, and since the Titan penetrator contains a mass spectrometer, higher power requirements result. Therefore a much larger battery assembly is required than for the Mars penetrator and an isotope heater would be used instead of the RTG system proposed for the long duration Mars mission. Like the Mars penetrator design however, the afterbody shears off upon surface penetration, leaving the antenna and associated communication hardware at the surface. This design is shown in Figure B-11. The umbilical between the forebody and afterbody could contain the sensors for the heat flow experiment if this method proves to be practical based on current studies for Mars applications.

From an equipment integration and installation point of view, the mass spectrometer experiment provides the biggest challenge. The various elements of the mass spectrometer are capable of being configured to fit a penetrator but additional development would be required to qualify each of them, and particularly the ion source, to the peak impact load (1800 g's). It is desirable to enlarge the penetrator diameter from the Mars penetrator's diameter of 7.5 cm to 12.7 cm to permit housing a mass spectrometer. With this larger diameter, and therefore greater structural mass as well as greater instrument and battery mass, both the mass and area are affected. It turns out that for the Titan penetrator their ratio is the same as for the Mars design, i.e the added mass and area balance out. This is fortunate since the penetrability of a frozen Titan surface is equivalent to a basaltic lava Mars surface and the same mass/area ratio is desired.

An additional area of concern is the acquisition of a vaporized

B-25

MASS SPECTROMETER

BATTERY

ISOTOPE
HEATER

ACCELEROMETER

TRANSMITTER

ELECTRONICS

ANTENNA

UMBILICAL

PLUG RETRACTED
FOR SAMPLING

PENETRATOR

SAMPLE INLET
TO MS

LENGTH   - 1.88 m
WEIGHT   - 63.2 kg
PRINCIPAL DIA - 12.7 cm

PLUG IN
ENTRY LOCATION

SAMPLE VAPORIZING
HEATER

MASS SPECTROMETER
SAMPLING PORT
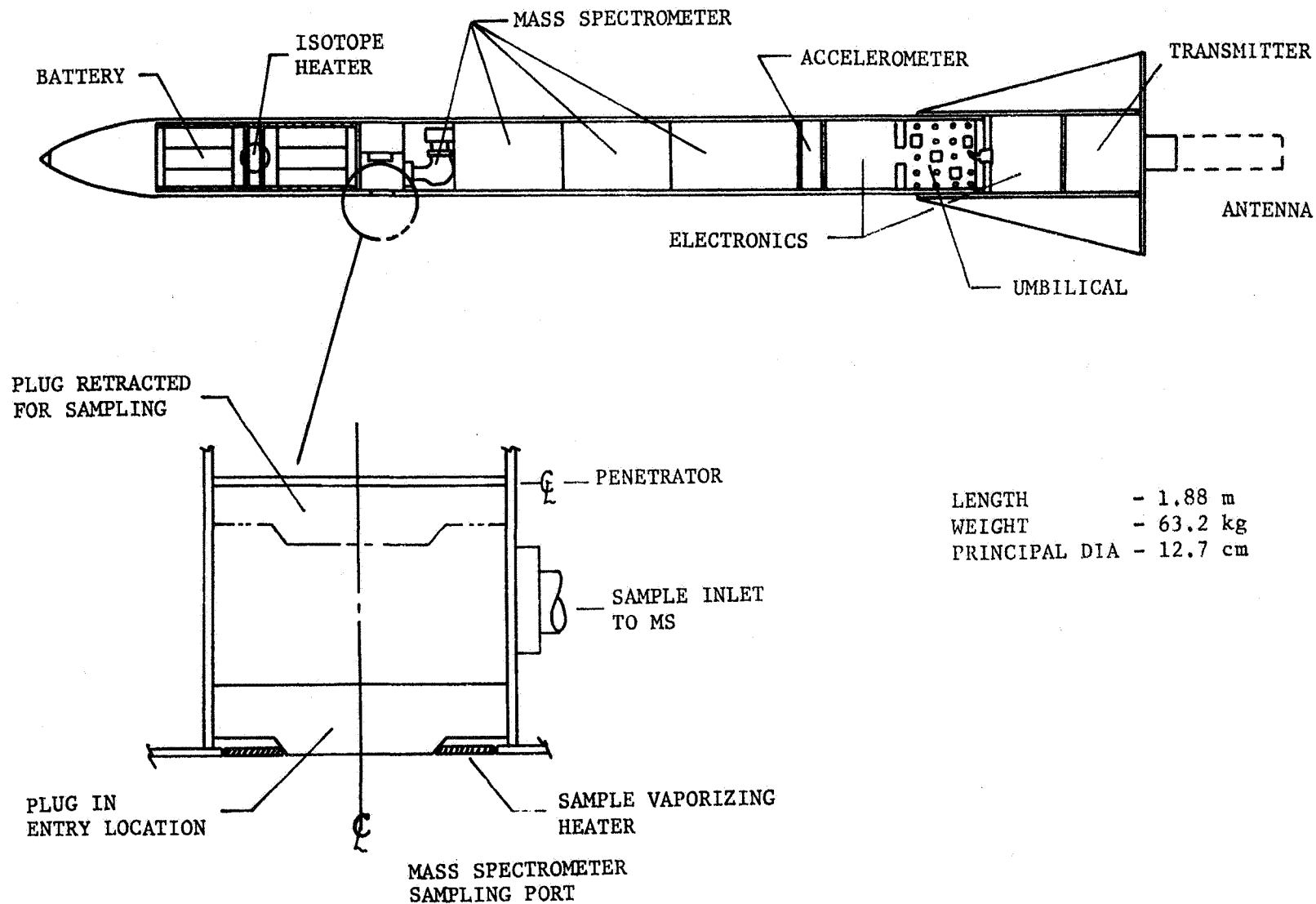
Fig. B-11 Titan Penetrator - Trial Mission Design

sample of the surrounding "soil". A scheme for doing this is also shown in Figure B-11. With this concept, a retractable plug in the wall of the penetrator is surrounded by a heating element as illustrated. Once the penetrator comes to rest, the plug is retracted (with for example a solenoid device) and the heater is energized. As the "soil" is heated, the vapors enter the port and proceed through the instrument for analysis.

The basic reason that the penetrator mission may have to be limited to short duration is the uncertainty in subsurface thermal conductivities and temperatures. The curves of Figure B-12 show the sensitivity of penetrator temperature to the thermal characteristics of some possible Titan surface constituents. The thermal model was run with one dimensional heat conduction only, with a "boundary" node located 100 cm from the penetrator. If there is a "soil" as such on Titan, its thermal conductivity may follow the middle curves, $k_{soil} = 4 \times N_2$ gas, (based on literature thermal conductivity measurements for low density powders in air at cryogenic temperatures). The wide spread indicates the difficulty of insuring that the penetrator will survive after steady state conditions are reached.

The presence of a denser atmosphere than Mars (in the nominal case) and the smaller gravitational acceleration of Titan simplifies the staging requirements, i.e., the bare penetrator ballistic coefficient, 13038 kg/m^2, results in the desired 150 m/s impact velocity. Also, the extendible cylinder used for the entry configuration, $\beta = 63$ kg/m^2, provides sufficient drag to produce a vertical flight path so no "turnover chute" is required.

Prior to entry the cylinder is extended pneumatically, as in Reference B-2 to increase the drag area. The natural stability orients the cylinder crossways to the flow thus providing a high drag configuration. After entry the fairings are staged and the fins on the penetrator afterbody cause the penetrator to assume a near zero angle of attack
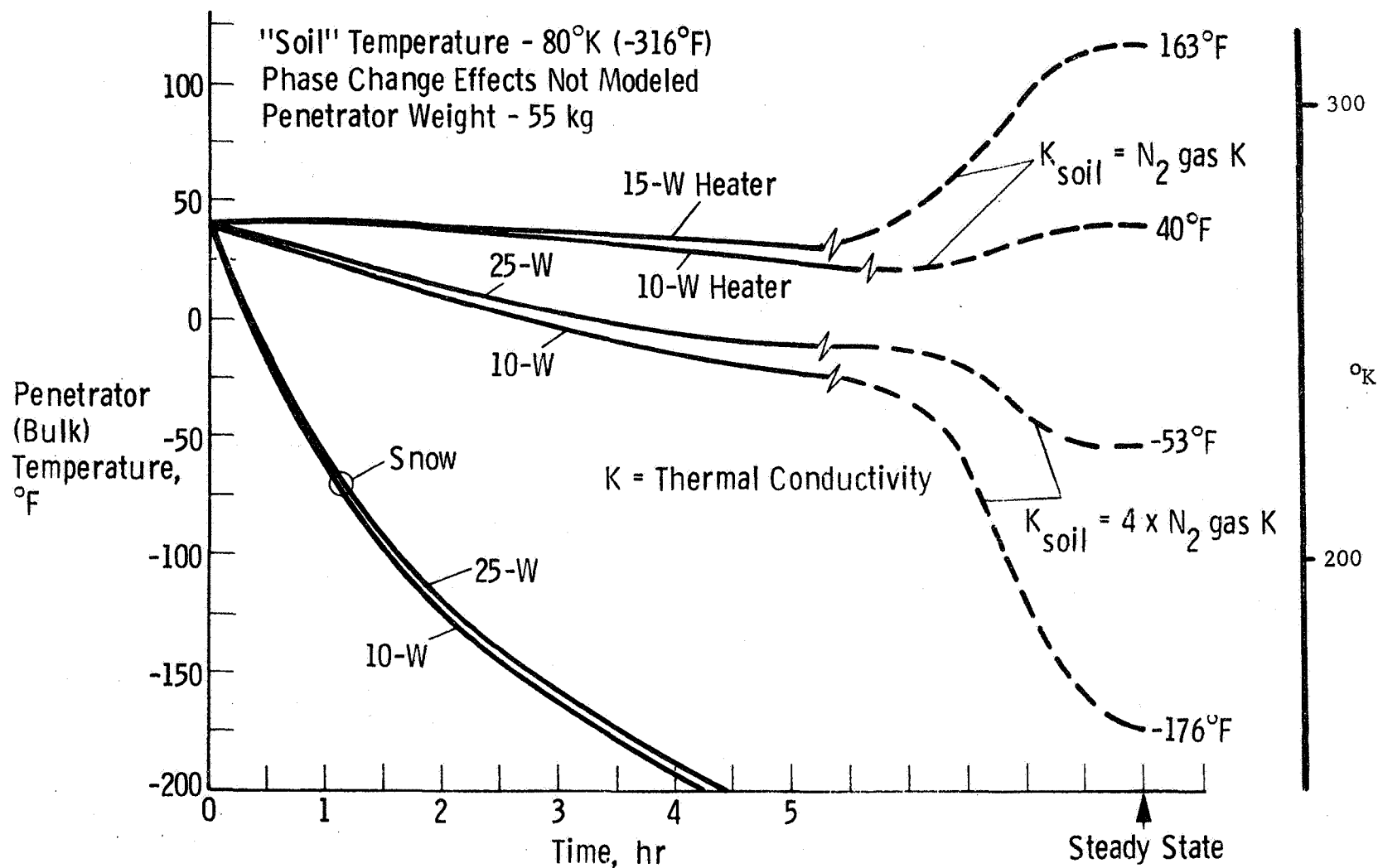
Note: Internal heat dissipation based on 20 W for mass spectrometer operation for 1 hr after impact.

Fig. B-12   Titan Penetrator Temperature Variation with "Soil" Conductivity

prior to impact. Another type of extendible aeroshell for providing increased drag and heat protraction during entry has been suggested for Mars applications. This system employs a carbon cloth extendible forebody somewhat resembling an umbrella. With the low relative velocity (5.8 km/sec) entry mode possible by powered swingby, this type of device also appears to be a possibility for Titan penetrators. Figure B-13 shows that relatively low carbon cloth equilibrium temperatures are experienced, 1500°K to 1800°K, depending on aeroshell diameter. This configuration could be lighter and might provide a more predictable drag than the extendible cylinder at the expense of greater development cost.

The estimated mass breakdown for the trial mission penetrator design is given in Table B-7. Its total mass is almost twice that of the Mars design and is essentially the same as that identified for the trial mission probe.

During cruise, the entry cylinder containing the penetrator is located inside a launch tube with the entire assembly mounted on the spacecraft. Figures B-14 and B-15 illustrate two ways of doing this. The launch tube serves a dual purpose in that it also serves as a bioshield for the penetrator. For penetrators as large as this one carried on Pioneer type (spin-stabilized) spacecraft, an on-axis mounting as illustrated in Figure B-14 is preferred. The single orbit insertion engine configuration normally used would be replaced in this system with four thrusters as shown, and a closed-end launch tube that would protect the spacecraft from exhaust impingement. The penetrator would be spun up within the launch tube with a 2-step solid motor system that delays the main thrust until the penetrator has cleared the spacecraft.

Mariner type (3-axis stabilized) spacecraft would afford more flexibility in mounting provisions as shown in Figure B-15.
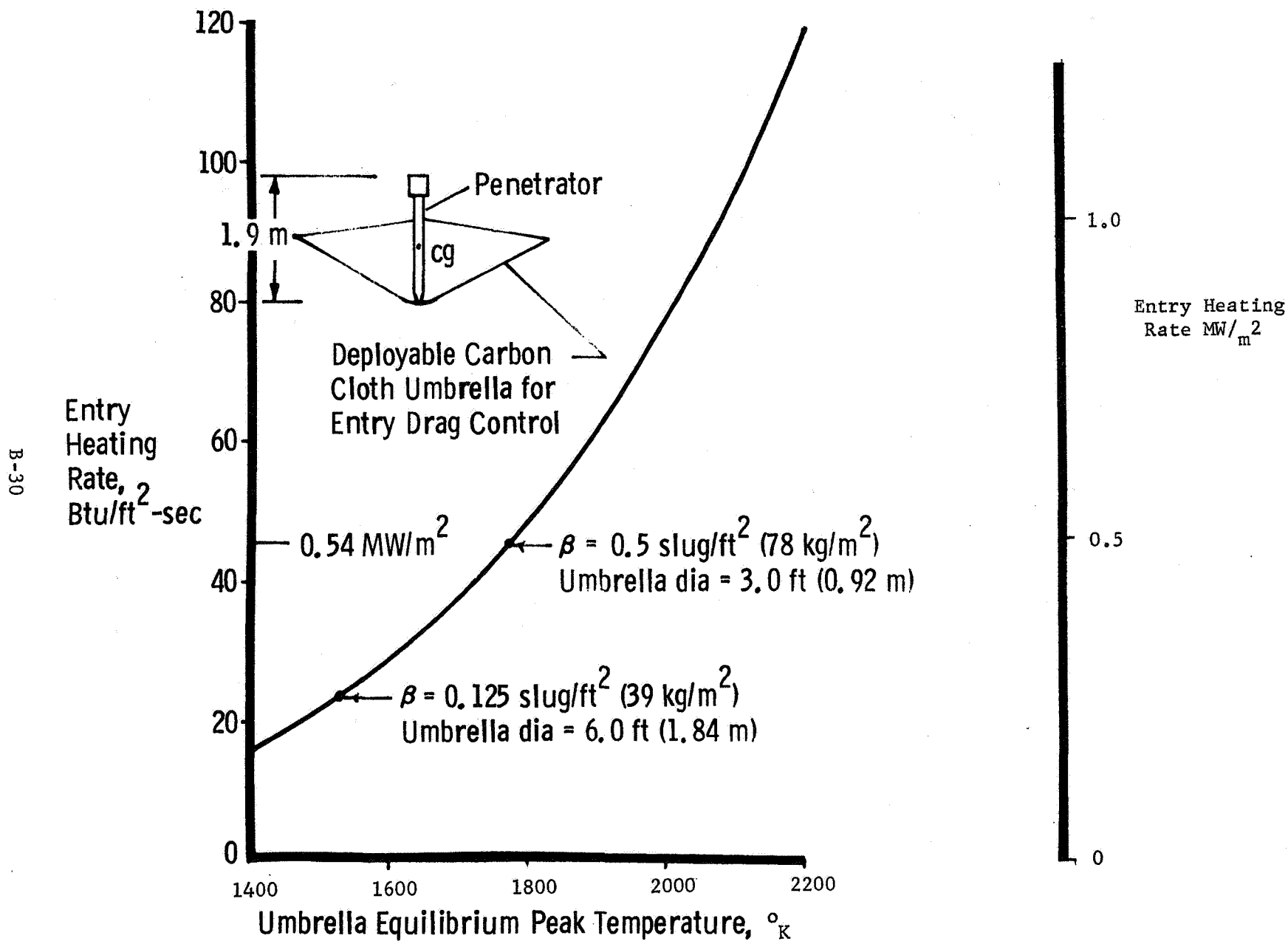
Fig. B-13 Alternative Penetrator Entry Configuration – Temperature/Heating Rate Sensitivity

TRIAL MISSION PENETRATOR WEIGHT STATEMENT

SCIENCE		8.8 Kg
HEAT FLOW EXPERIMENT	1.0	
ACCELEROMETER	0.3	
MASS SPECTROMETER	5.0	
SCIENCE ELECTRONICS	2.5	
ELECTRICAL/ELECTRONIC		11.5 Kg
BATTERY/HEATERS	5.0	
COMMUNICATIONS	3.0	
UMBILICAL	0.5	
ELECTRONICS SUPPORT	3.0	
STRUCTURE/MECHANISMS		42.9 Kg
STRUCTURE	41.4	
MASS SPEC SAMPLER	1.5	
ENTRY FAIRING		18.0 Kg
MARGIN		10.8 Kg
TOTAL		92.0 Kg

Space Storable
Multi-mission
Propulsion Module
(per NASA/ARC/TRW
Study-Ref B-3)

Titan Penetrator

Orbit Insertion
Thrusters (4 PLCS)
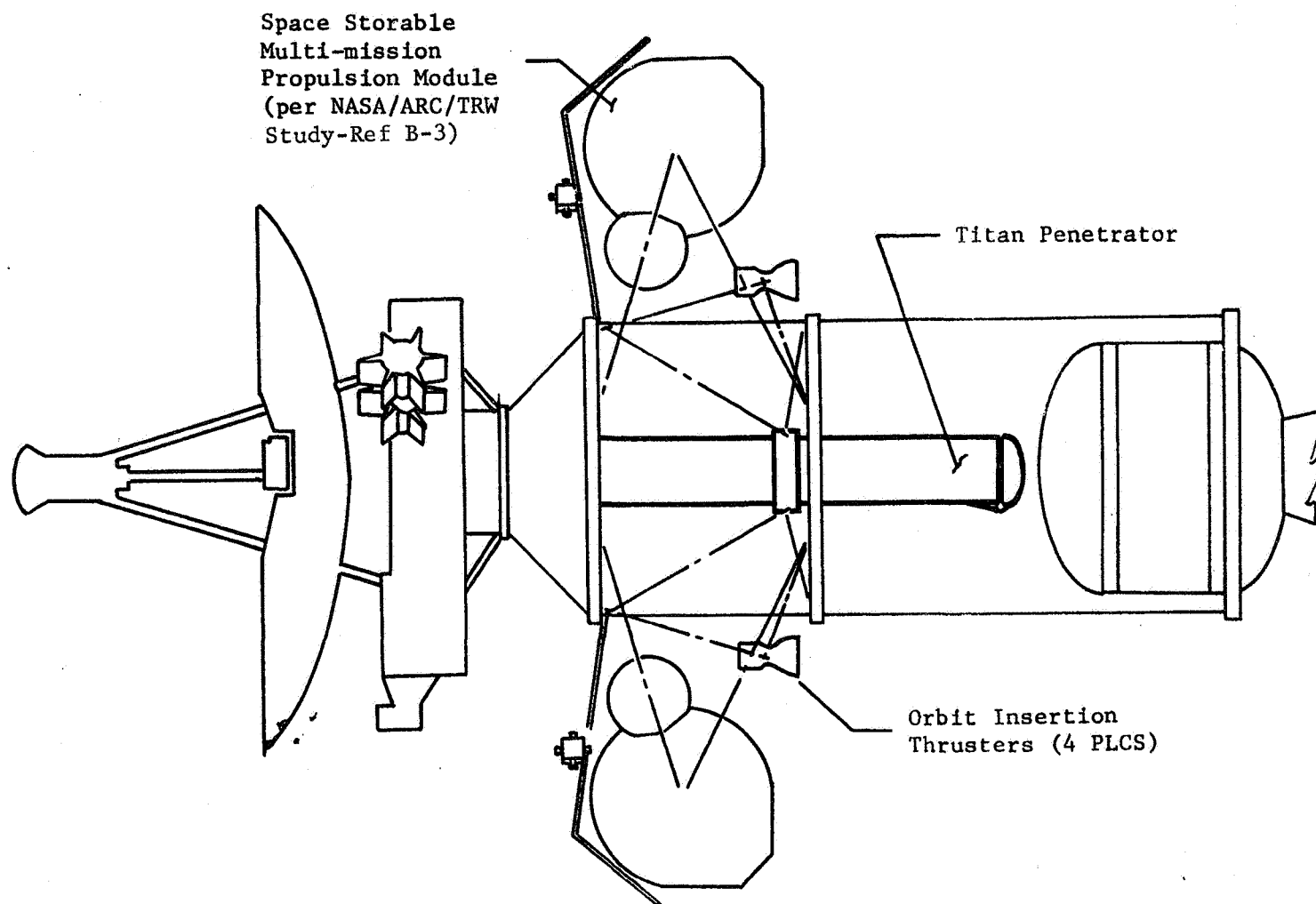
Fig. B-14 Pioneer Saturn Orbiter with Titan Penetrator

MJS'77 MODIFIED AS ORBITER
(PER JPL MJO STUDIES)

TITAN PENETRATOR IN LAUNCH TUBE/BIOSHIELD

ORBIT INSERTION ENGINE

RTGS

ALTERNATIVE
PENETRATOR
LOCATION

ENTRY
CYLINDER
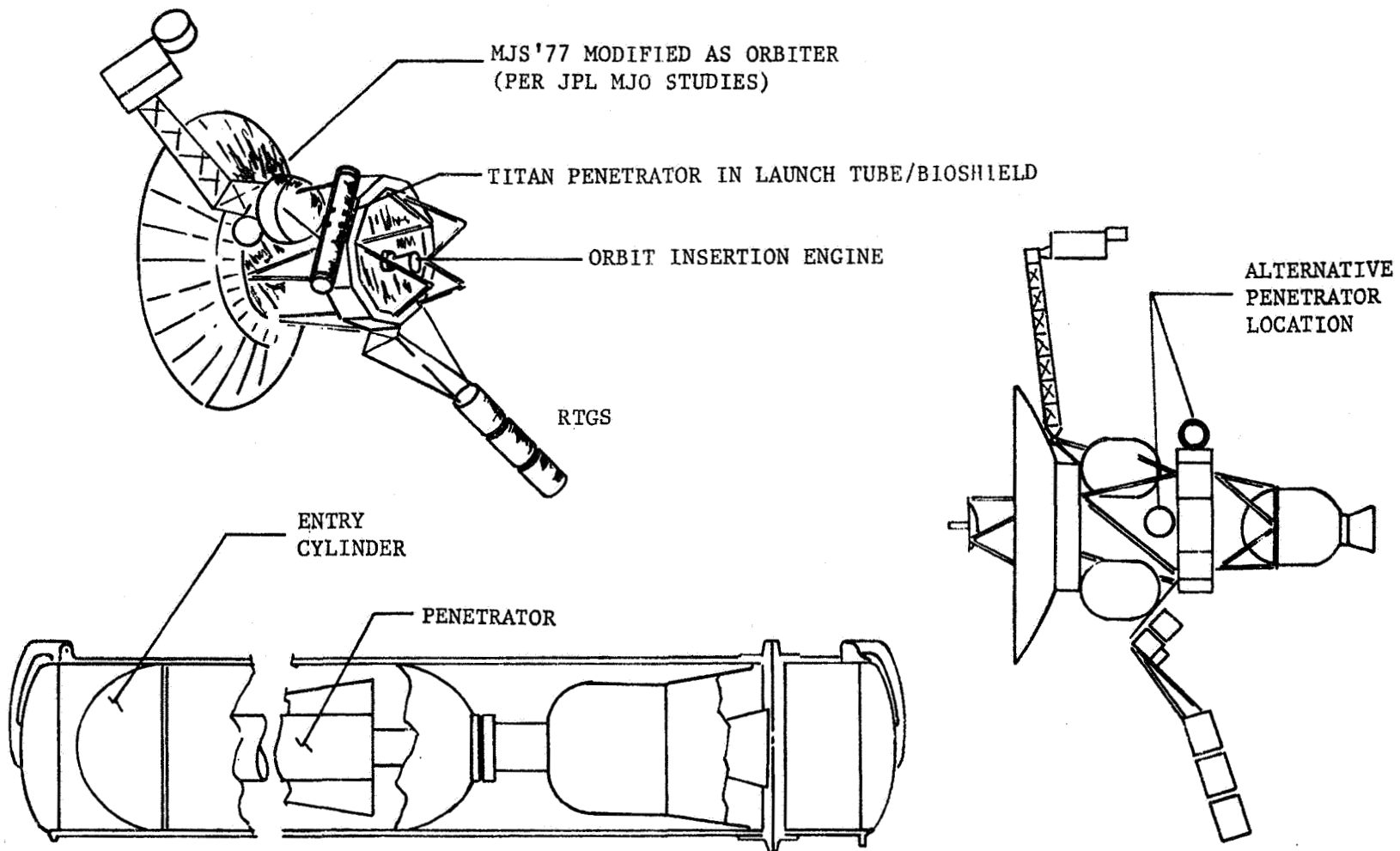
PENETRATOR

Fig. B-15 Mariner Saturn Orbiter with Titan Penetrator(s)

b. Communications and Power - Penetrator Design

Penetrator Communications - To fulfill the requirements of
the Titan penetrator mission, a very compact subsystem of data gathering,
data storage, and transmission is required to support the scientific
experiments and penetrator housekeeping. The science complement consists
of an accelerometer, mass spectrometer, and a heat flow experiment with
a total of 61,500 bits. The accelerometer data during descent/impact
amounts to analog data converted into 31,000 bits and is stored in a
50-kbit solid-state memory. The mass spectrometer experiment produces
25,000 bits of digitized data and the heat flow experiment has 5400 bits
of data. Data transmission begins 32 min. after surface impact and lasts
for 45 min., at which time the flyby spacecraft is over the local horizon.
The stored data and real-time, post-impact data are serialized and trans-
mitted to the flyby spacecraft via a microwave link. The penetrator
mission data are stored on the spacecraft in a memory unit and relayed to
Earth at a convenient time over the spacecraft-Earth microwave link to the
DSN.

The proposed telemetry data link operates at 400 MHz with non-
coherent FSK modulation with a data rate of 32 bps which allows for the
science and housekeeping data. A command and control link is not necessary
since the mission design proposes a single flyover of the mother space-
craft, which released the penetrator.

The worst-link condition occurs at impact when the flyby
spacecraft is farthest away with a range of 32,350 km and at an aspect
angle of 37° from the local vertical. As the spacecraft flies over the
landed penetrator, the communications geometry improves until the space-
craft is over the opposite horizon at 72 min. after entry (45 min. after
impact). The range at this time is only 5000 km. The microwave relay
link table is shown in Table B-8 for the worst-case conditions which
determines the maximum RF output power required from the transmitter. As
seen from the table, 2 W of RF power is required to maintain the telemetry

TABLE B-8

PENETRATOR TELEMETRY DESIGN CONTROL TABLE

ITEM	PARAMETER	NOMINAL VALUE	ADVERSE TOLERANCE	REMARKS
1.	Total Transmitter Power, dBW	3.0	0.0	400 MHz, 2.0 W
2.	Transmitting Circuit Loss, dB	− 0.8	−0.1	
3.	Transmitting Antenna Gain, dB	2.0	−0.2	Hemisphere, Axial, $\emptyset=37°$
4.	Antenna Pattern Ripple, dB	− 2.5	0.0	
5.	Space Loss, dB	−174.7	−0.3	32,350 km
6.	Planet Atmosphere Loss, dB	− 0.2	0.0	Nominal Atmosphere
7.	Polarization Loss, dB	− 3.0	−0.2	Linear-to-Circular
8.	Receiving Antenna Gain, dB	3.1	−0.2	Split-Axial Pattern, $\theta_{hp}=55°$
9.	Receiving Circuit Loss, dB	− 1.0	−0.1	
10.	Net Circuit Loss, $\Sigma(2\rightarrow9)$, dB	−177.1	1.1	
11.	Total Received Power, (1+10), dBW	−174.1	1.1	
12.	Receiver Noise Spectral Density, N_o, dBW/Hz	−200.8	−0.4	$T_s = 600°K$
13.	Received Power/N_o, (11-12), dBW·Hz	26.7	−1.5	

DATA CHANNEL

ITEM	PARAMETER	NOMINAL VALUE	ADVERSE TOLERANCE	REMARKS
14.	Fading Loss, dB	− 1.0	0.0	
15.	Processing Loss, dB	− 1.0	0.0	
16.	Received Data Power, (11+14+15), dBW	−172.1	−1.1	
17.	Data Bit Rate, dB	15.0	0.0	Rate = 32 bps
18.	Threshold E_b/N_o, dB	10.5	−0.3	BER = 5×10^{-4}
19.	Threshold Data Power, (12+17+18), dBW	−175.3	−0.7	
20.	Performance Margin, (16-19) or (13+14+15-17-18), dB	3.2	−1.8	
21.	Nominal Less Adverse Margin, (20-20 adv), dB	1.4		

Conditions: 1. Titan Penetrator impact conditions, worst-case power.
2. Spacecraft flyby mission, RCA=50,000 km
3. Nominal Titan atmosphere model, 100% N_2, 400 mbar pressure.
4. FSK non-coherent modulation, BT=2.
5. Roll-stabilized flyby spacecraft.
6. Convolutional encoding, Viterbi decoding, Rate = 1/2.

link at 400 MHz to the flyby spacecraft with a data rate of 32 bps.

The telemetry transmitter is an all-solid-state unit capable of 2 W of RF output. The overall efficiency is 25% which results in 8 W of dc power required from the battery. Data management includes an A-to-D converter for the analog accelerometer data, a 50-kbit solid-state memory, and circuitry to encode the serial bit stream. The dipole antenna and transmitter are separated during impact and remain on the surface. Antenna deployment is powered by a coiled spring. When released, the antenna assembly is driven out of a storage tube and the rigid, spring-loaded dipole elements unfold and the flexible counterpoise arms deploy.

The flexible ground plane arms are made of steel. The ground plane height is 25 cm and the antenna provides a linearly polarized, hemispherical pattern. The transmitter and antenna is packaged in the aft end of the penetrator and after impact, an umbilical connects the transmitter to the penetrator body and provides dc voltages and signals from the data processing unit.

Penetrator Power Subsystem - Penetrator energy requirements are determined from the science equipment and engineering subsystem power loads. The energy requirements of the penetrator mission are shown in Table B-9. Power is required from pre-impact (descent) to 72 minutes after entry when the mission is completed. The science and engineering subsystems operate simultaneously and the transmitter begins operation 32 minutes after impact and lasts for 45 minutes. The total energy required is 34.7 W-hr. With the addition of design margins for sterilization and other factors, the battery energy requirement is 45 W-hr.

The power distribution system is shown in Figure B-16. A sterilizable, nickel- cadmium battery was chosen for the power source. The battery is located in the forebody of the penetrator and will experience a maximum deceleration of about 1800 Earth g's. The battery is charged by the spacecraft bus prior to separation at about 5 days prior to entry. Battery recharge on the surface of Titan is not necessary due

Table B-9 Titan Trial Mission Penetrator Power & Energy Requirements

Entry Cylinder	Power, W	Time, min	Energy, Wh
Pyro System	1.0	--	0.25
Gas Valve			
Cylinder Release			
Deceleration Switch	0.2	120	0.4
Pressure Switch	0.2	120	0.4
Afterbody			
Antenna			
Transmitter	8.0	60	8.0
Forebody			
Accelerometer			1.0
Temperature Array	0.1	60	0.1
Mass Spectrometer	20.0	60	20.0
Sample Heater	15.0	10	2.5
Data Management	0.2	75	0.25
			32.9
Power System Losses (5%)			1.8
Total			34.7
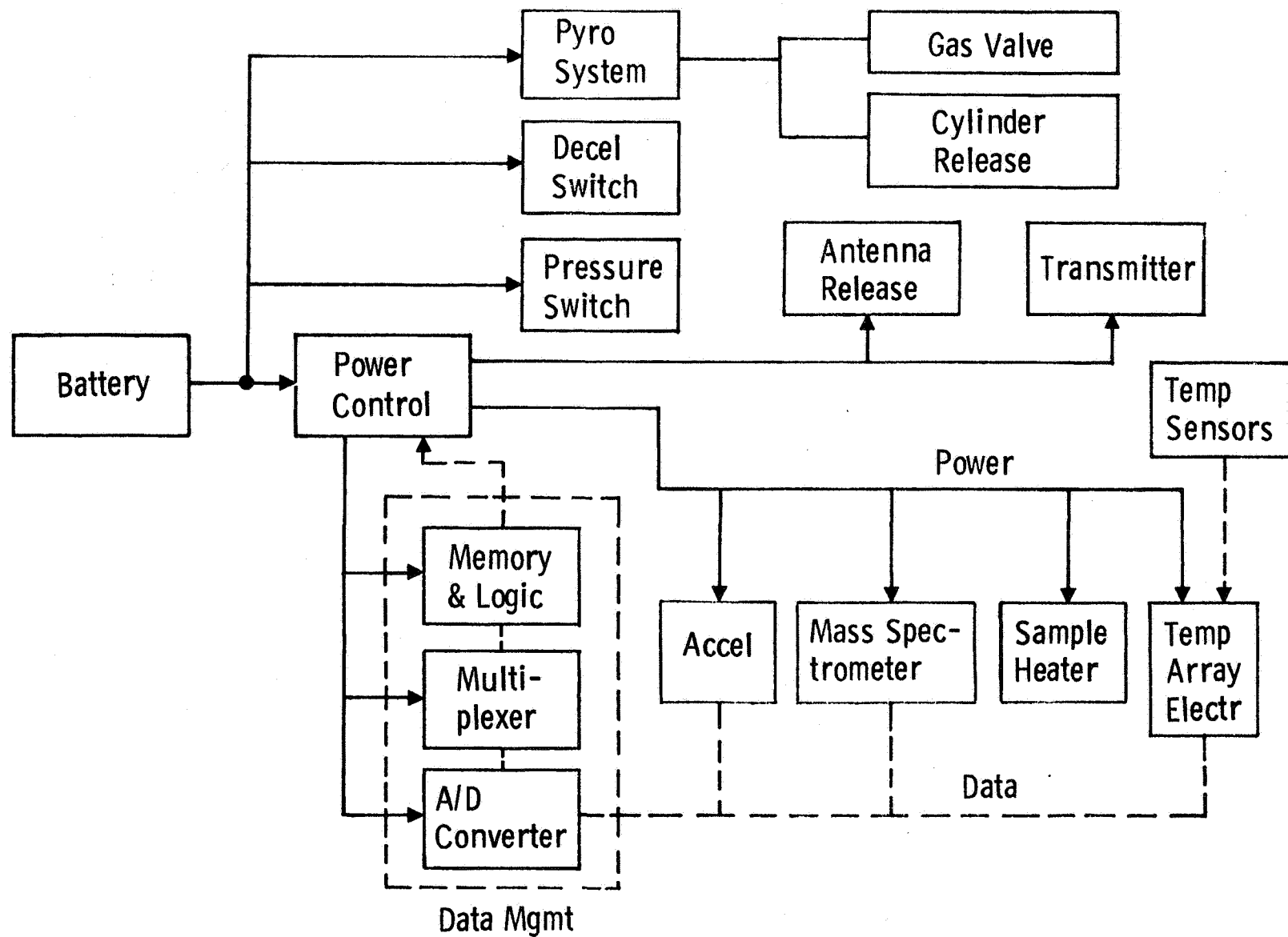
Fig. B-16   Penetrator Power Distribution

to the short mission time. An optional approach is to use a remotely activated silver-zinc battery.

The penetrator sequence of events requires pyrotechnic device actuation to release the heat shield/cylinder after entry and the accelerometer and data storage system are active during impact and penetration. After impact, power is sent to the required systems through a Power Control Unit to complete the sample acquisition and data transmission to the orbiting bus.

The UHF transmitter is in the afterbody and remains on the surface after impact. Power is supplied to the transmitter via an umbilical cable from the penetrator forebody which is imbedded into the Titan surface.

C. TRIAL MISSION SOFT LANDER

A soft lander was configured to accommodate the science payload described in Table B-10 with various subsystem components essential to the operation and support of the science instruments.

An assumption was made that planetary quarantine requirements would dictate bioshield encapsulation of the lander in a manner similar to the Viking '75 lander. Also, it was assumed that some deflection capability would be required of the lander to avoid having to sterilize the bus spacecraft or having to insure that the bus deflection maneuver was reliable enough to permit targeting it within the possible Titan impact zone. An attempt was made to keep the capsule size small in order to facilitate its integration into as wide a range of spacecraft configurations as possible. The resulting mission profile and system characteristics are summarized in Figure B-17 with details provided in the paragraphs below.

1. Mission Profile Description - Lander

a. Interplanetary Trajectory/Launch Analysis - In a systematic exploration of Titan, the lander mission would follow after both the probe and penetrator missions. Mission opportunities to Saturn occur once every

TABLE B-10 Titan Lander Science Payload

INSTRUMENT	CHARACTERISTICS	MASS (Kg)	POWER (Watts)
Combined GCMS/Life Detection	Viking GCMS + Kok experiment	29.9	7 Standby
Meteorology	T, P, wind	4.5	15 Scans
Sunlight Monitor	Visible, UV?		5
Imagery	One panorama	7.3	15
Surface Sampler	Scoop/Chisel (viscid surface?)	9.1	40
Wet Chem. Amino Acid Analysis *	ABLDI	50.8 Kg	75 Watts
Expanded Organic Analysis			
Seismometer	Passive, Active?		
Neutron Activation, Scatter	Elements, Isotopes		
Passive Gamma-ray Spectrometer	K, U, cosmic ray, nuclides		
XRFS, X-ray Diffraction	Heavy elements, crystal structure		
Heat Flow	Temp., gradient, thermal conduct.		
Microwave Radiometer	Subsurface temperature profile		
Sonar Sounder	Layer detection		
Drill Sampler	1-10 meters		
Particle Size Analyzer	Regolith characteristics		
Age Dating	Ices, organics?		
Upper Atmosphere Life Detect.	Sampler		
Listening Devices	Audio, Em, lightning, thunder		

*The following instruments are optional

Separate from S/C
t = -5 days
ΔV = 150 m/s

Entry

t = 0 s
h = 594 km
γ_E = 60°
V_E = 5.84 km/s

Max g

t = 90 s
h = 179 km
11.3 g_E
B = 47.1 kg/m²

Deploy Chute,
Stage Aeroshell

t = 53 min
h = 2 km
B = 5.5 kg/m²

Impact

t = 63 min
h = 0 km (R = 2700 km)
V_{impact} = 3 m/s
Data Rate = 16 - 88 bps
RF Power = 10 - 40 W
S-Band Direct Link

Weights	kg
Science	37.9
Electronic/Electrical	80.1
Structural/Mechanical	48.6
Landed Weight	166.6
Parachute/Mortar	13.2
Aeroshell, H/S	45.4
Deorbit Propulsion	15.0
Margin	39.0
Total	279.2

Science

GCMS/Life Detection
Atmospheric Sensor Array
   (P, T, Wind, Sunlight)
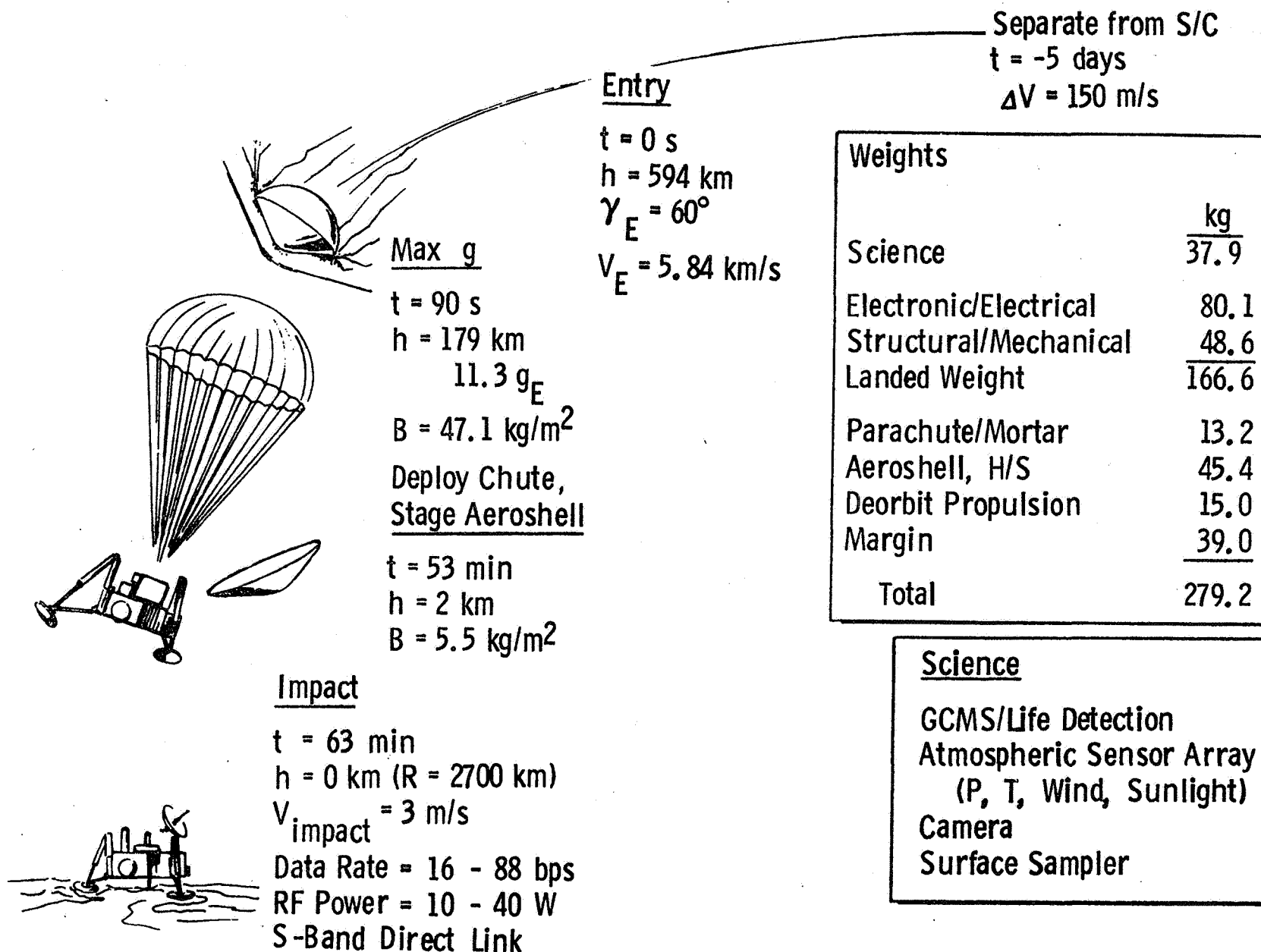Camera
Surface Sampler

B-41

Fig. B-17 Typical Titan Soft Lander Mission into Nominal Atm

13 months. In the interval of interest 1983 - 2000 the two best launch years are 1985 and 1998; 1992 is the worst launch year. The first is too soon and 1998 may be too late. Launch dates which would yield reasonable weight margins and yet allow for either probe or penetrator mission results to be incorporated into the lander design must occur after 1993. Therefore for purposes of the trial mission design a 1994 launch date was assumed. Launch occurs on 5/8/94 and the lander/spacecraft combination encounters Titan on 11/16/98 with a flight time of 4.5 years. The spacecraft is a Pioneer which when combined with a lander has a total mass of approximately 1200 kg including propellant for Saturn orbit insertion after Lander deployment. The Shuttle/Tug launch capability for the indicated trajectory is in excess of 1700 kg. A Mariner derivative spacecraft is not compatible with this trial lander mission since the corresponding total system mass of 2600 kg is greater than the Shuttle/Tug launch capability.

      b. <u>Titan Approach Trajectory</u> - The same considerations that went into the selection of the approach trajectory for the probe mission are also applicable for selection of the Lander approach trajectory. Since the lander weighs $\sim$300 kg, the idea of taking the lander/spacecraft combination into Saturn orbit before separation does not appear to be a viable option. Therefore the lander is deflected from the spacecraft on the incoming trajectory. The deflection radius of 5×10^6 km results in a coast time of 5 days. The deflection maneuver is performed in a shared mode. The spacecraft with the lander before deflection is targeted to fly within 1000 km of Titan. This distance is selected to minimize the requirements for on-board lander propulsion while still preventing the spacecraft from impacting Titan (for quarantine reasons) in the event of a spacecraft deflection maneuver failure. The lander solid rocket deflection motor is ignited after separation from the spacecraft and the desired landing site is acquired. The deflection maneuver is designed to enhance the spacecraft communication link both during

descent and after touchdown. The spacecraft lander range at entry is 100,000 km.

    c. <u>Entry and Descent</u> - The entry portion of the lander mission is identical to the entry portion of the probe mission. Entry angle, entry velocity, peak "g's" and maximum dynamic pressure are illustrated below:

Lander Entry Analysis Summary			
Entry Angle, deg		-60	
Entry Altitude, km		594	
Entry B, slugs/ft^2		.5	
kg/m^2		78	
Final B slugs/ft^2		.035	
kg/m^2		5.5	
Max Deceleration, g's		11.3	
	Thin	Nominal	Thick
Staging Altitude, km (chute deployed)	2	2	2
Touchdown Velocity, m/sec	23.7	3	2.2
Total Mission Time, min	7.5	51	85

    The key difference between probe entry and lander entry is the design of the staging event. A parametric analysis of staging altitude indicated that 2 km was a good compromise between long descent times (high altitude) and large touchdown velocities (low altitude). It should be noted however, that large variations in descent time (7.5 minutes to 85 minutes) do occur for the extreme atmospheres.

    d. <u>Navigation and Dispersions</u> - The navigation errors and associated dispersions used in sizing the communications and entry subsystems for the lander are the same as those used for the probe trial mission design.

2. Design

a. <u>Configuration and Mechanical Subsystems</u> - Figures B-18 through B-20 depict the overall configuration and external and internal configurations of the trial design. A three-legged configuration was selected with the leg assemblies being similar to the Viking '75. In order to ensure landing stability the radial spacing of the footpads should be twice the c.g. height. For the trial mission design, extendable legs were selected that recess into the lander body for stowing. The hexagonal lander body (60 cm along a side) provides an environmentally protected compartment for components requiring survivability on Titan's surface as well as provisions for mounting sensors, antennas, a camera, thrusters, and landing support equipment whose function is complete once landing has been accomplished. To minimize thermal shorts between the inside and outside of the lander, penetrations would be limited to a single electrical interface point and a sample acquisition drill.

The major lander thermal problem is how to effect sufficient thermal coupling to the RTG waste heat to survive after landing and yet not overheat during the cruise mode. A thermal switch could do the job, as illustrated in Figure B-21, however it is not a particularly light-weight device. Other options include: variable conductance heat pipes, fluid loops/pumps, and controlled heat "shorts" in the lander insulation. The latter device would require new technology development.

Assuming the cruise phase RTG heat rejection can be accomplished, the trial lander design with 5 cm insulation (occupying 23% of lander volume) would require 390 watts to maintain a $283^{\circ}K$ ($50^{\circ}F$) payload temperature on Titan's surface with infinite coupling to atmosphere. This is consistent with a 35 watt (electrical power) RTG, or 2 of the new 20 watt selenide RTGs currently under development.

Due to the relatively dense atmosphere, an 8 meter diameter parachute can be used to slow the lander to the 3 m/s landing velocity. Thus the terminal descent propulsion and attitude control systems used

BIOSHIELD
FILTER

BIOSHIELD

LANDER LEG
(STOWED)
3 TOTAL

MAIN CHUTE
8 m DIA

PILOT CHUTE/MORTAR

Relay Antenna

SPIN UP
THRUSTERS

LAUNCH LOAD
REACTION FITTING

HEAT SHIELD/AEROSHELL

DIA: 173 cm
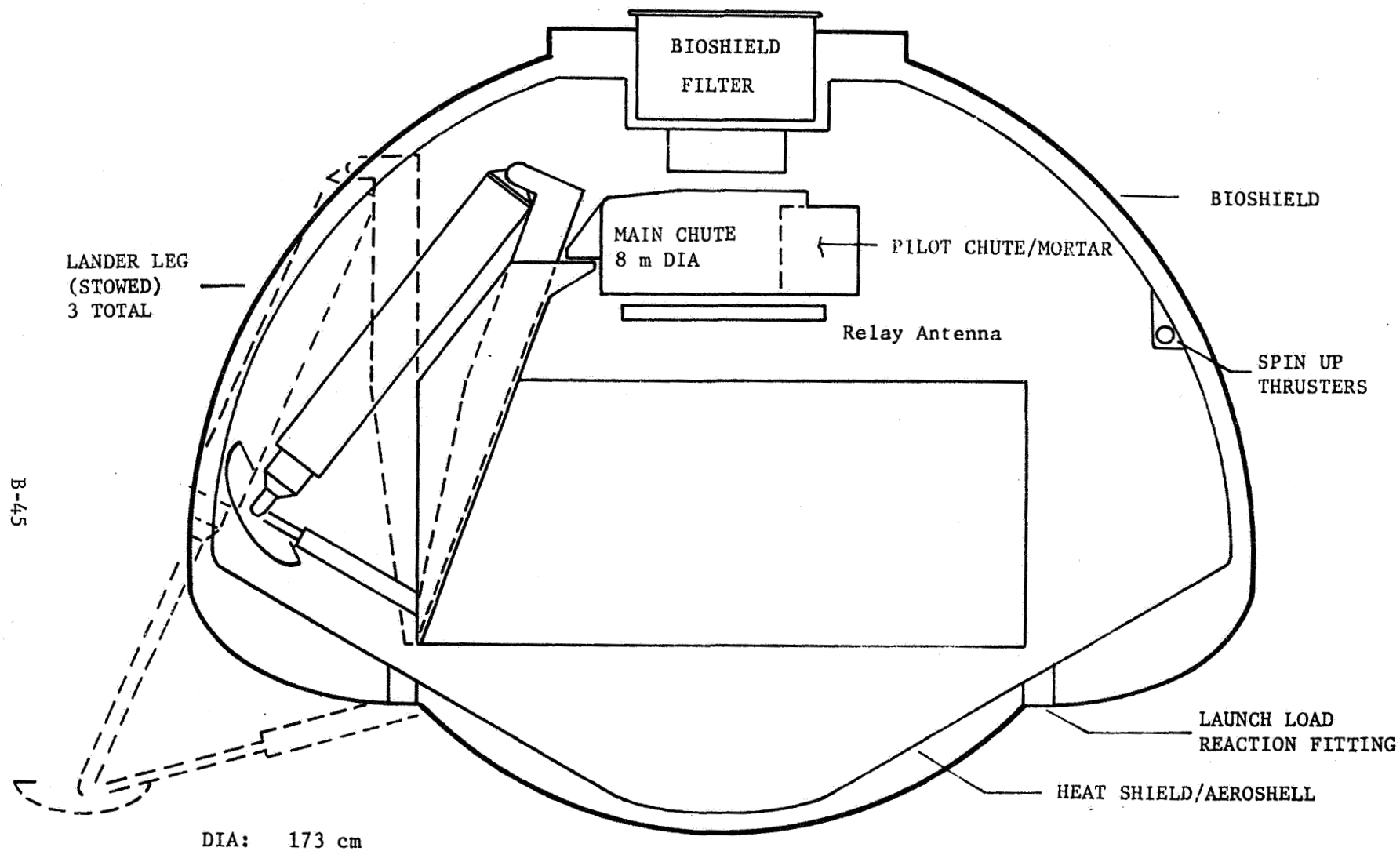
Fig. B-18   Titan Lander - Trial Mission Configuration

ATMOSPHERIC SENSOR ARRAY

Direct Antenna (Stowed Position)

RELAY ANTENNA

RTG (2 PLCS)

PARACHUTE/MORTAR ASS'Y

Command Antenna

DEFLECTION MOTOR
(3 PLCS)

LANDING LEG ASS'Y (3)

FAX CAMERA

LANDER BODY/
EQUIPMENT COMPARTMENT
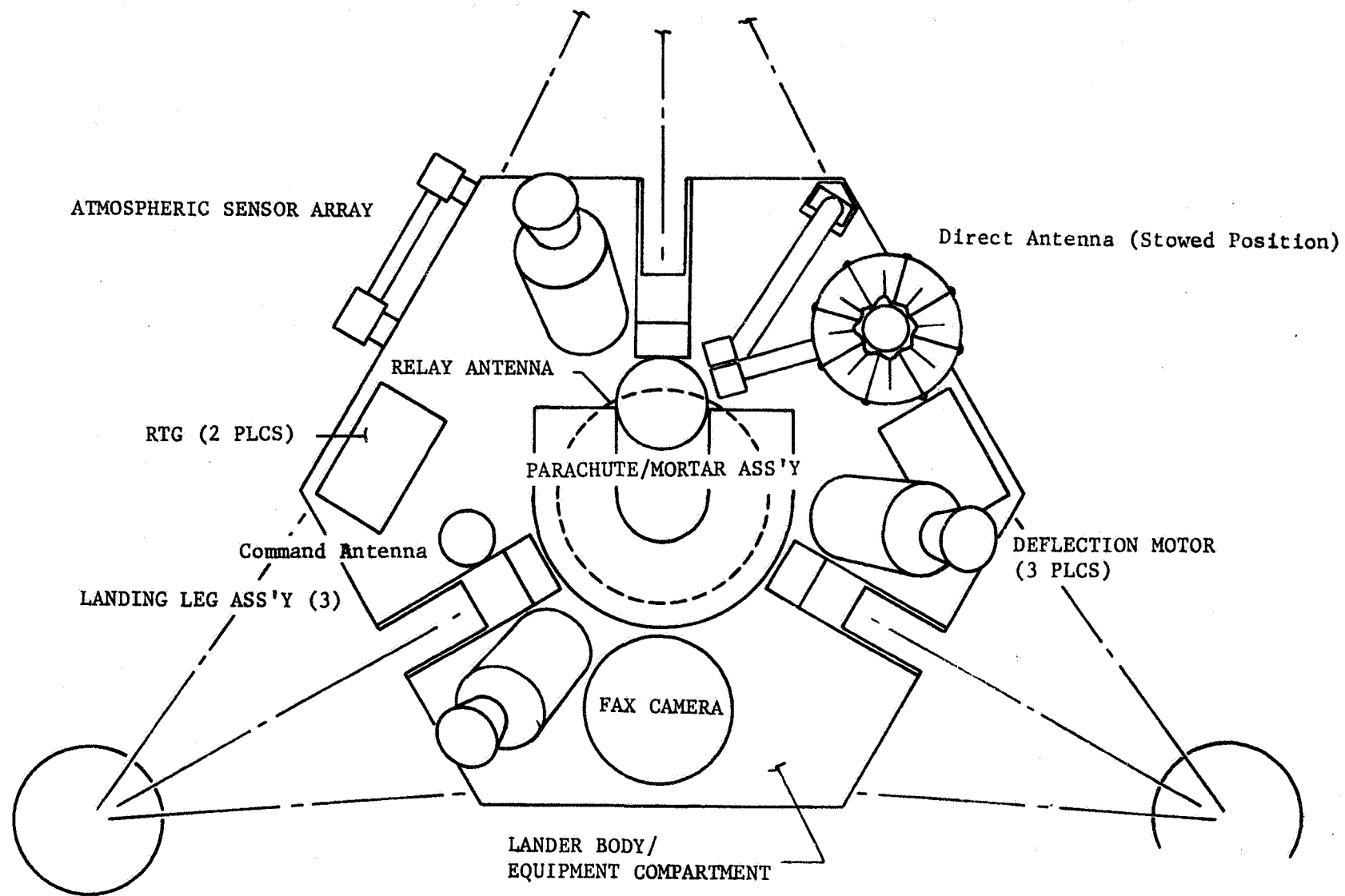
Fig. B-19 Titan Lander - Outboard Profile

B-46

INSULATION

SUPPORT MODULE

RADIO ASS'Y

BATTERY

MEMORY

MASS SPECTROMETER/
LIFE DETECTION

SURFACE SAMPLER
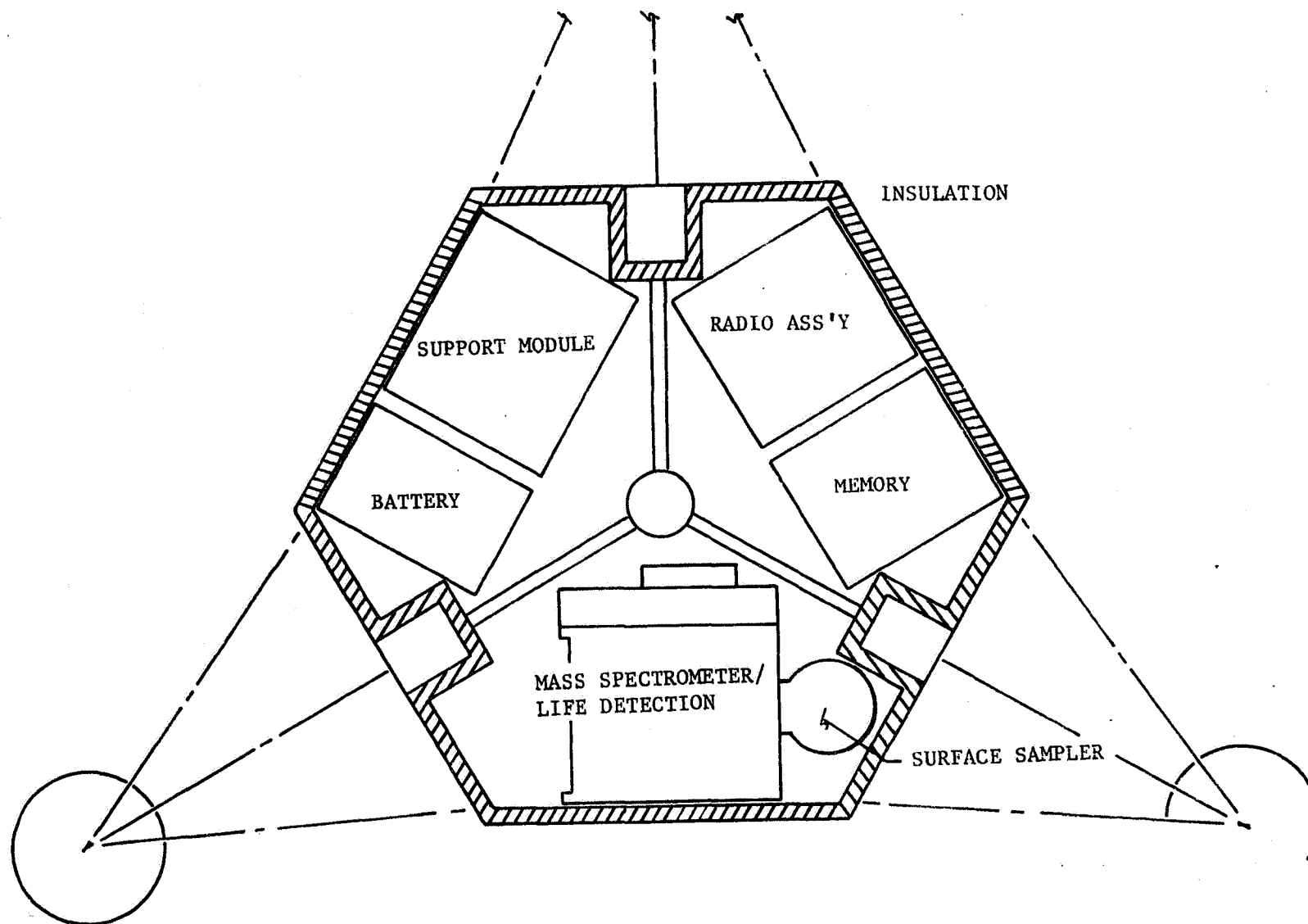
Fig. B-20 Titan Lander - Inboard Profile

Surface Operations Mode

2-in. Fiberous Insulation May Require Higher Density than Viking to Eliminate Convection

Thermal Switch 390 Watts Capacity

RTG End Cap Temperature Regulator Based on Variable Convector Area (New Technology Item)

$Q_{insul} \approx$ 330 Watts

Equipment Shelf

RTG 620 Watts Waste Heat

$Q_{science\ penetrations} \approx$ 320 Watts

Insulation Required on RTG to Maintain High Fin Root Temperature 450°K Max

$Q_{structure} \approx$ 230 Watts

Cruise Mode

Pioneer S/C Earth Oriented

S/C

S/C Adapter

Bioshield

Base Cover

RTG

Bioshield

Heat Shield

Alternative Approach - Jettisonable Space Radiator with Fluid Loop

Removable Radiator Required to Reject RTG Heat (New Technology Item)

Fig. B-21 Titan Trial Mission Lander Thermal Control Concepts

for Mars are not required. If significant lateral winds are identified, the parachute will have to be released before touchdown and a small, landing-propulsion system and ACS will then hav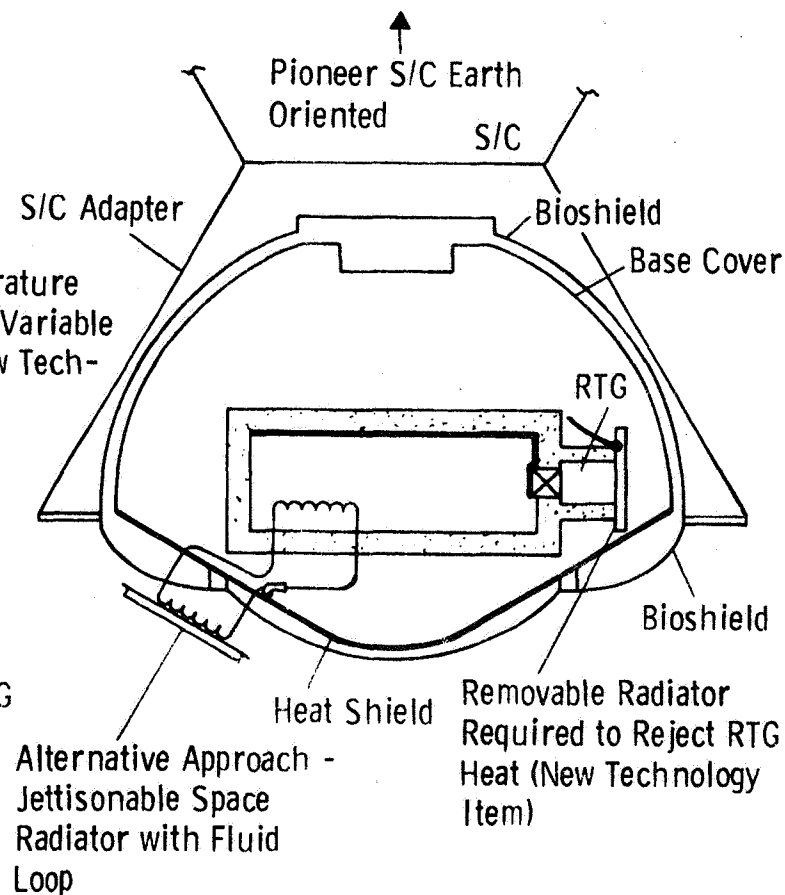e to be included. This chute is deployed at 2 km altitude by means of a radar altimeter, the low altitude being selected to minimize the variation in descent time due to uncertainties in atmospheric density.

In order to install all the components within the envelope of the capsule, it was necessary to locate the relay antenna beneath the parachute canister and to fold and stow the direct link antenna. An estimate of the mass breakdown for the trial mission lander is shown in Table B-11.

Three larger solid propellant motors would be used to deflect the lander onto its entry trajectory once it has left the bus, $\Delta V = 88$ m/s. This "shared" deflection mode permits the bus to miss Titan even if the portion of the deflection maneuver to be performed by the bus fails to function properly.

Figures B-22, B-23 and B-24 show the lander capsule integrated into Pioneer, and Mariner spacecraft. These spacecraft configurations are based on results of studies performed by TRW and JPL to modify the outer-planet versions of these flyby spacecraft into orbiter configurations, see References B-3 and B-4. The integration of the lander into the version of the Pioneer spacecraft proposed as an outer-planet orbiter in Ref B-3 resulted in an unacceptably large value for pitch-to-roll axis inertia ratio prior to boom deployment. This problem is relieved by modifying the configuration shown in Figure B-22. Although not as critical for the 3-axis spacecraft designs, Figures B-23 and B-24, the increased pitch inertia caused by the addition of the lander will require redesign of the ACS system and the inclusion of more propellant.

In all of the configurations, the capsule is supported around the periphery of the aeroshell for all but launch loads. A separate support structure would be used to carry the launch loads and separate the bio-

Table B-11

Trial Mission Lander Mass Properties

SCIENCE		50.8 Kg
ATMOSPHERIC SENSOR ARRAY	4.5	
CAMERA	7.3	
MASS SPEC/LIFE DETECTION	29.9	
SAMPLE ACQUISITION	9.1	
COMMUNICATIONS		28.3 Kg
S-BAND RADIO ASSEMBLY	11.3	
S-BAND DIRECT ANT/DRIVES	11.3	
S-BAND COMMAND ANTENNA	.2	
UHF RADIO ASSEMBLY	4.5	
UHF RELAY ANTENNA	1.0	
POWER		44.5 Kg
BATTERY ASSEMBLY	22.7	
POWER DISTRIBUTION	13.6	
RTG (2-20 WATT)	8.2	
DATA HANDLING		10.0 Kg
DATA ACQUISITION	5.5	
MEMORY AND/OR RECORDER	4.5	
GUIDANCE AND CONTROLS		5.4 Kg
COMPUTER/SEQUENCER	1.4	
PYRO CONTROL ASSEMBLY	4.0	
STRUCTURE		105.0 Kg
BASECOVER	13.6	
AEROSHELL, H/S	45.4	
LANDER BODY/BOTTOM PLATE	46.0	
PARACHUTE & MORTAR		13.2 Kg
DEORBIT PROPULSION		15.0 Kg
THERMAL CONTROL		6.8 Kg
INSULATION	3.6	
HEATERS	1.4	
PAINT	1.8	
SUB TOTAL		279.0 Kg
BIOSHIELD		59.0
TOTAL		338.0

Space Storable
Multi-mission
Propulsion Module
(per NASA/ARC/TRW
Study-Ref B-3)

Titan Lander

SPM
(1800)

Orbit Insertion
Thrusters (4 PLCS)

Outer Planets
Pioneer

B-51

Fig. B-22 Pioneer Saturn Orbiter with Titan Lander

Space Storable
Multi Mission
Propulsion Module
(per NASA ARC/TRW
Study-Ref B-3)
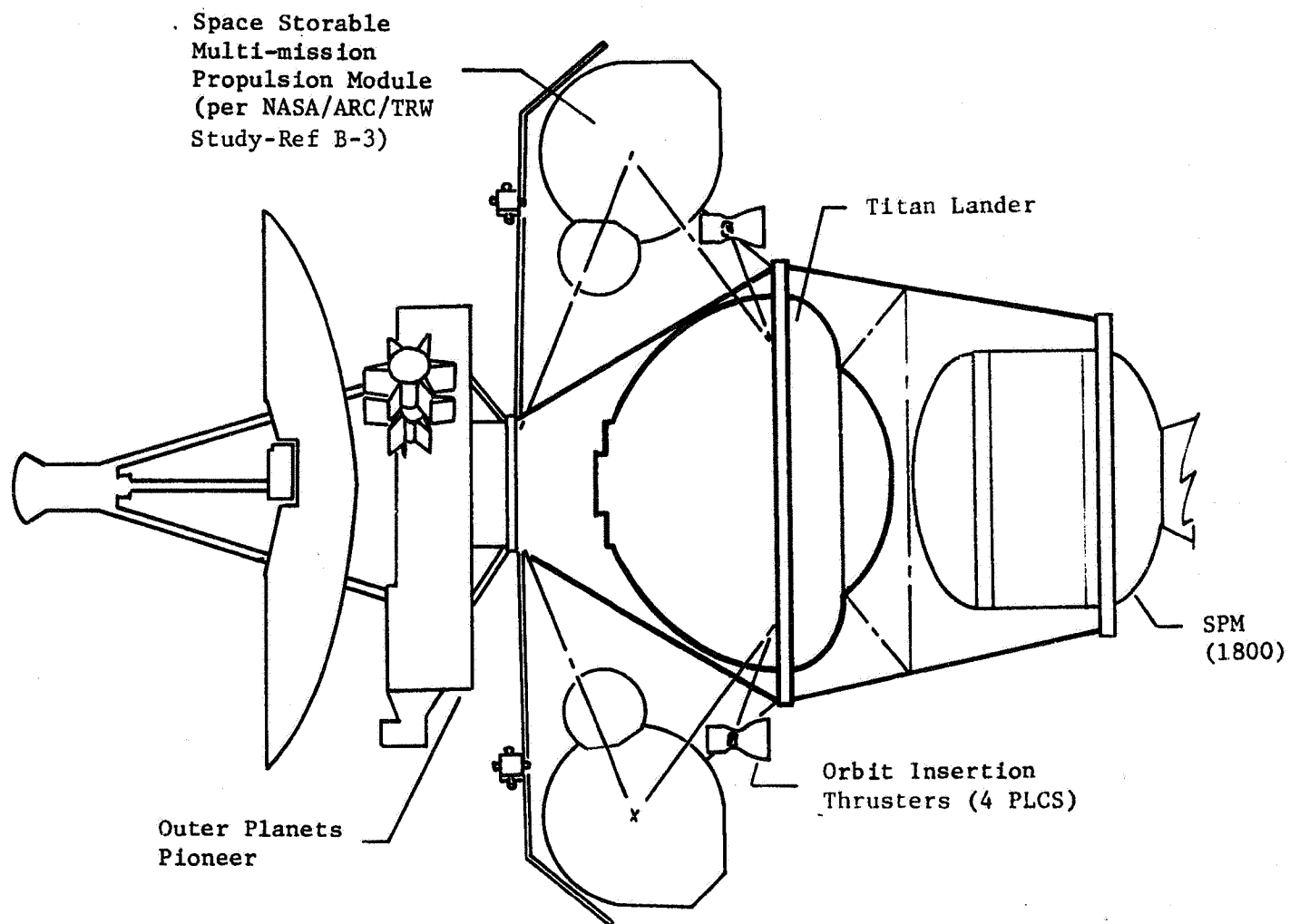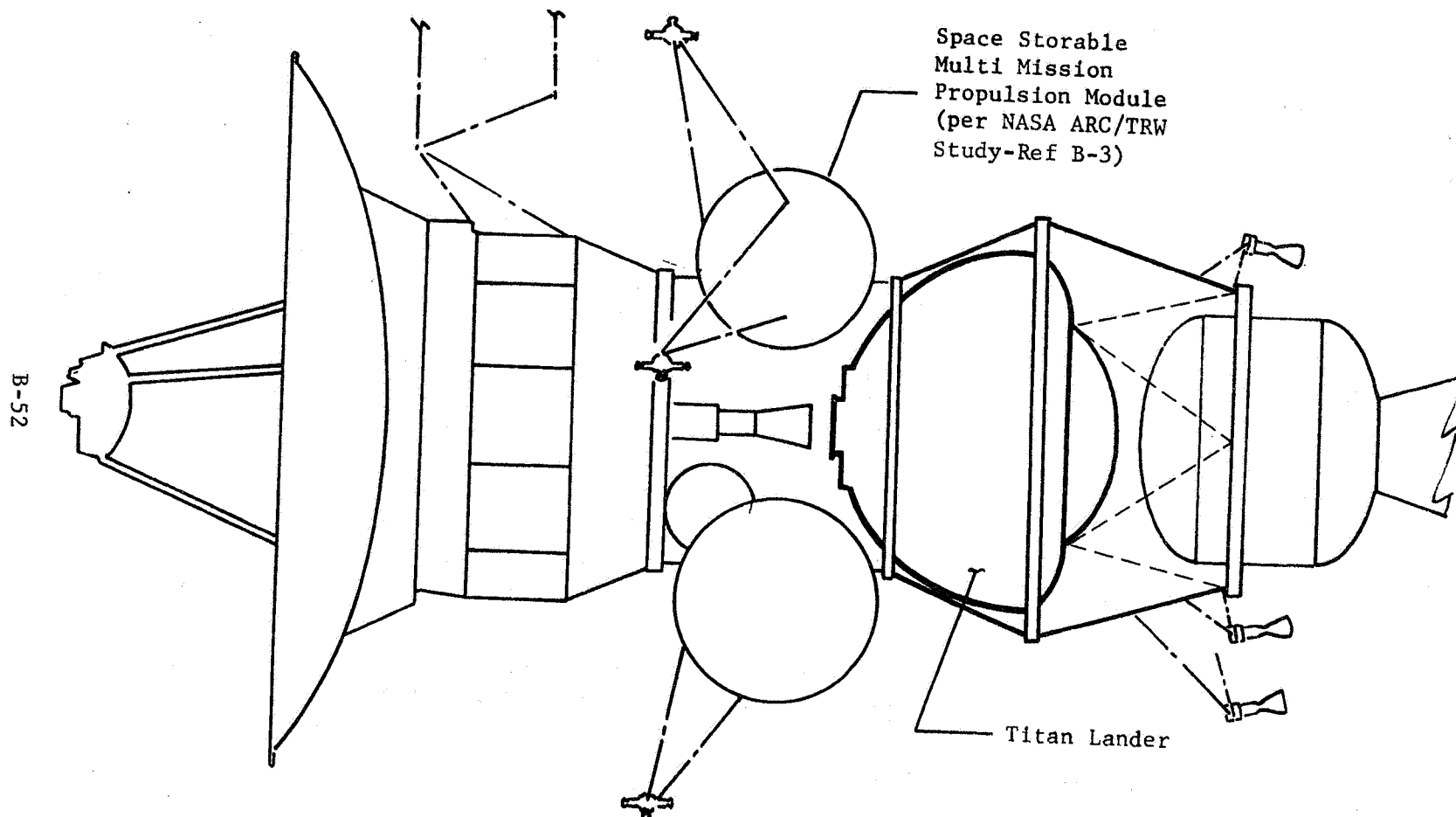
Titan Lander

Fig. B-23 Multi-Mission Propulsion Module Version of a Mariner Saturn Orbiter with a Titan Lander

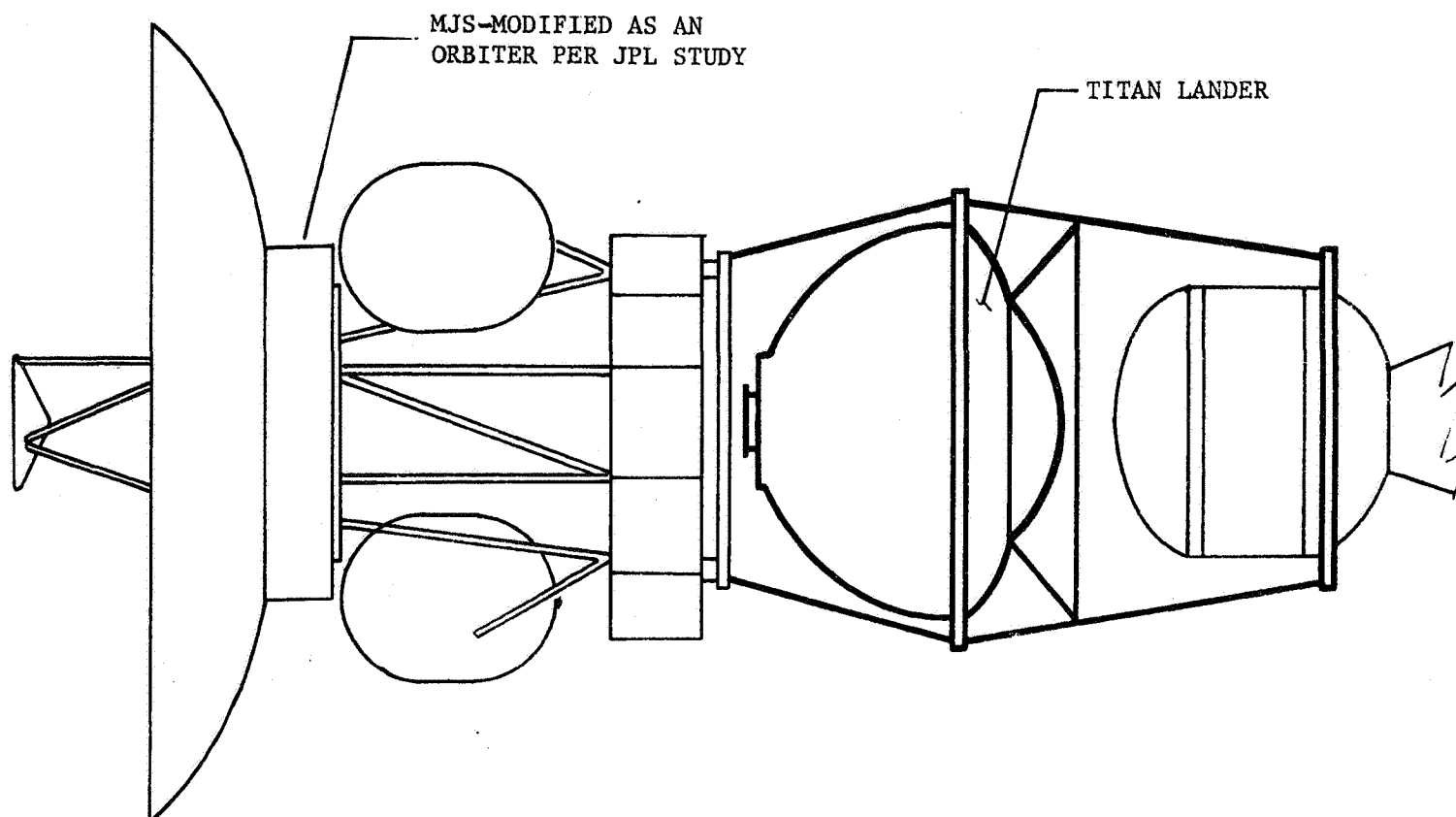MJS–MODIFIED AS AN
ORBITER PER JPL STUDY

TITAN LANDER

Fig. B-24 Mariner Saturn Orbiter with Titan Lander (Ref B-4 Orbiter Version)

shield base. This structure is jettisoned with the kick stage adapter. Upon lander capsule separation from the spacecraft, spin thrusters are fired to provide capsule stability until entry is accomplished. These thrusters are mounted on the basecover as shown earlier in Figure B-18. The bioshield cap remains with the orbiting spacecraft.

Mechanisms & Separation Devices - The trial mission lander requires the mechanisms and separation devices listed below. Of these, the subsurface drill and possibly the antenna deployment are areas that would require new technology development.

Lander Mechanical Operation Requirements

o Deploy the landing leg assemblies for touchdown
o Acquire a surface or subsurface sample (possibly a drill based on the Apollo drill)
o Unfurl and erect the direct link antenna
o Deploy the atmospheric sensor array

Devices would be required to accomplish the following separations:

o Bioshield base from cap
o Lander capsule from bioshield cap/orbiter
o Aeroshell/heat shield from lander/basecover
o Basecover/parachute canister from lander

b. Communications and Power - Soft Lander Design

Lander Communications - The lander mission utilizes two links to communicate telemetry data to Earth. The orbiter provides a UHF relay link with the lander during initial touchdown and at selected days as dictated by the rotational period of Titan. The orbiter is in a highly eccentric orbit with a period of 112 to 144 days around Saturn and encounters Titan. After touchdown, the orbiter is overhead from 1 to 2.7 hrs and only 2W of RF power are required at 400 MHz for a data rate of 128 bps, due to the close range (70000 km). At E+2 days, the orbiter is again above the local horizon and remains for 10 days but the range is rapidly increasing to 2.5 Mkm. The usefulness of the relay link to the orbiter

rapidly diminishes after periapsis. At apoapsis, the lander is again
in view with a range of 9 Mkm. The relay link is based on technology
developed by NASA/ARC for Outer Planet Probes. FSK modulation is con-
volutionally coded on the 400 MHz link. RF power up to 40 W is avail-
able with a solid-state transmitter. The lander relay antenna is a
compact microstrip disk antenna 14 in. in diameter and 0.5 in. thick.

A direct RF link to Earth is also possible when Earth is
in view which is approximately 4 days of each 16-day period. Transmission
cannot occur when the Earth and Saturn are in superior conjunction.
Transmissions can occur; however, when the sun is behind Earth as viewed
from Titan. The long communication range to Earth of 10 A.U. limits the
data rate at S-band for reasonable (<50 W) transmitter power levels.
The lander battery also cannot support higher power levels for a
long period of time (>2 hours).

An analysis was performed for the direct link with an
arbitrary RF power level of 40 W at S-band using the DSN with PSK modula-
tion and block coding. Two periods of 2 hours each, on two consecutive
days are required to transmit 1.2 Mbits of data at 88 bps stored on the
lander tape recorder. This includes one picture, a GCMS/biology sample,
six mass spectrometer runs, six atmosphere sensor runs, and lander engineer-
ing and housekeeping data. The S-band performance is shown in Table B-12.
The link relies on a high gain lander antenna. A deployed and automatic-
ally controlled parbolic dish with a 0.76 m (30 in.) diameter and
circular polarization is employed on the lander. The antenna control
system options are described elsewhere. The antenna is a flex-rib
design that occupies a small volume when stowed and is self-erecting
after release.

Reflector curvature tolerances are not critical for this
size of dish and the beamwidth is 0.2 rad (12 deg) at S-band. A low
gain, omni antenna is also employed on the lander for reception of low
rate (8.3 bps) commands from Earth for lander control. 40 W at S-band

Table B-12   DSN Direct Data Link Frequency Comparison

NO	PARAMETER	S-BAND		X-BAND	
		NOMINAL	NOTE	NOMINAL	NOTE
1	TOTAL TRANSMITTING POWER (DBW)	- 16.0	40W	16.0	40W
2	TRANSMITTING CIRCUIT LOSS (DB)	- 1.0		- 1.0	
3	TRANSMITTING ANTENNA GAIN (DB)	21.3	76 cm Dish	34	76 cm Dish
4	COMMUNICATIONS RANGE LOSS (DB)	-283.4	10AU,2.3GHz	-294.5	8.4GHz
5	PLANET ATMOSPHERIC - DEFOCUSING LOSSES (DB)	0		0	
6	POLARIZATION LOSS (DB)	- 0.1	RHC	- 0.1	RHC
7	MULTIPATH & OTHER LOSSES (DB)	0		0	
8	RECEIVING ANTENNA GAIN (DB)	61.3	64 m DSN	71.2	DSS
9	RECEIVING CIRCUIT LOSS (DB)	0	Included	0	
10	NET LOSS (DB) (2+3+4+5+6+7+8+9)	-201.9		-190.4	
11	TOTAL RECEIVED POWER (DBW) (1+10)	-185.9		-174.4	
12	RECEIVER NOISE SPECTRAL DENSITY - (DBW/HZ)	-213.8	$T_S=30^\circ K$	-212.4	$T_S= 41^\circ K$
13	TOTAL RECEIVED POWER/NO (DBW.HZ) (11-12)	27.9		38.0	
	CARRIER TRACKING				
14	CARRIER POWER/TOTAL (DB)	- 5.8	θ= 1 rad	- 10.0	θ=1.3 rad
15	ADDITIONAL CARRIER LOSSES (DB)	0		0	
16	THRESHOLD TRACKING BANDWIDTH - $2B_{LO}$ (DB)	10.0	10 Hz	10.0	
17	THRESHOLD SNR (DB)	10.0		10.0	
18	PERFORMANCE MARGIN (DB) (13+14+15-16-17)	2.1	Adv = -2.1	8.0	
	DATA CHANNEL				
19	DATA POWER/TOTAL (DB)	- 1.4		- 1.4	
20	ADDITIONAL DATA CHANNEL LOSSES (DB)	- 1.1		- 1.1	
21	DATA BIT RATE - BPS (DB)	19.4	88 bps	29.5	900 bps
22	THRESHOLD ENERGY PER DATA BIT - E_b/N_o (DB)	3.0	BER=5×10^{-3}	3.0	BER=5×10^{-3}
23	PERFORMANCE MARGIN (DB) (13+19+20-21-22)	3.0		3.0	

NOTES: 1. PCM/PSK/PM Modulation, Block Coding.
2. X-band losses based on latest DSN information.
3. RF power and both antenna sizes remain fixed.
4. Transmit antenna beamwidth is 12 deg. at S-band and 3.4 deg. at X-band.

is within the state-of-the-art for space qualified transmitters.

Direct link operation at X-band was also investigated to evaluate the data rate advantage of the higher frequency. The DSN will have X-band reception operable for the MJS '77 spacecraft, using a new feed on the 64 m antenna. Performance at X-band is also depicted in Table B-12 in order to show the comparative advantage over S-band. As shown, for the same amount of RF power transmitted and same size antenna dish, the improvement in data rate is tenfold (10 dB). Any further weight savings by reducing the size of the lander antenna would reduce the advantage of the higher frequency. *The increase in space loss is offset by the increase in gain of the DSN. The system noise temperature* at X-band and the susceptibility to adverse weather is also slightly greater. The major advantage is in the increase gain of the lander transmitting antenna for the same dish size *at the higher frequency.*

Data rates could also hypothetically be improved by another factor of ten by going to 30 GHz (K_a -band). At this frequency a 76 cm lander dish antenna has a gain of 45 dB with a beamwidth of only 0.92 deg. Now antenna pointing becomes a major problem and the data rate advantage of this frequency could easily be offset by the added complexity of the antenna tracking system. JPL has no immediate program plans to implement K-band reception on the DSN but it could be possible by 1985. This exercise in data rate improvement shows what rates could possibly be achieved for a nominal power level and lander antenna size. The Titan Lander would benefit from increased rates of science data return, since the S-band link with 40 W has a data rate that only marginally supports the baseline science objectives.

To carry the data rate improvement one step further, Figure B-25 depicts data rate versus operating frequency for two lander antenna dish sizes and shows the relationships of the primary variables for 40 W of RF power. As mentioned previously, the practicality of such a large
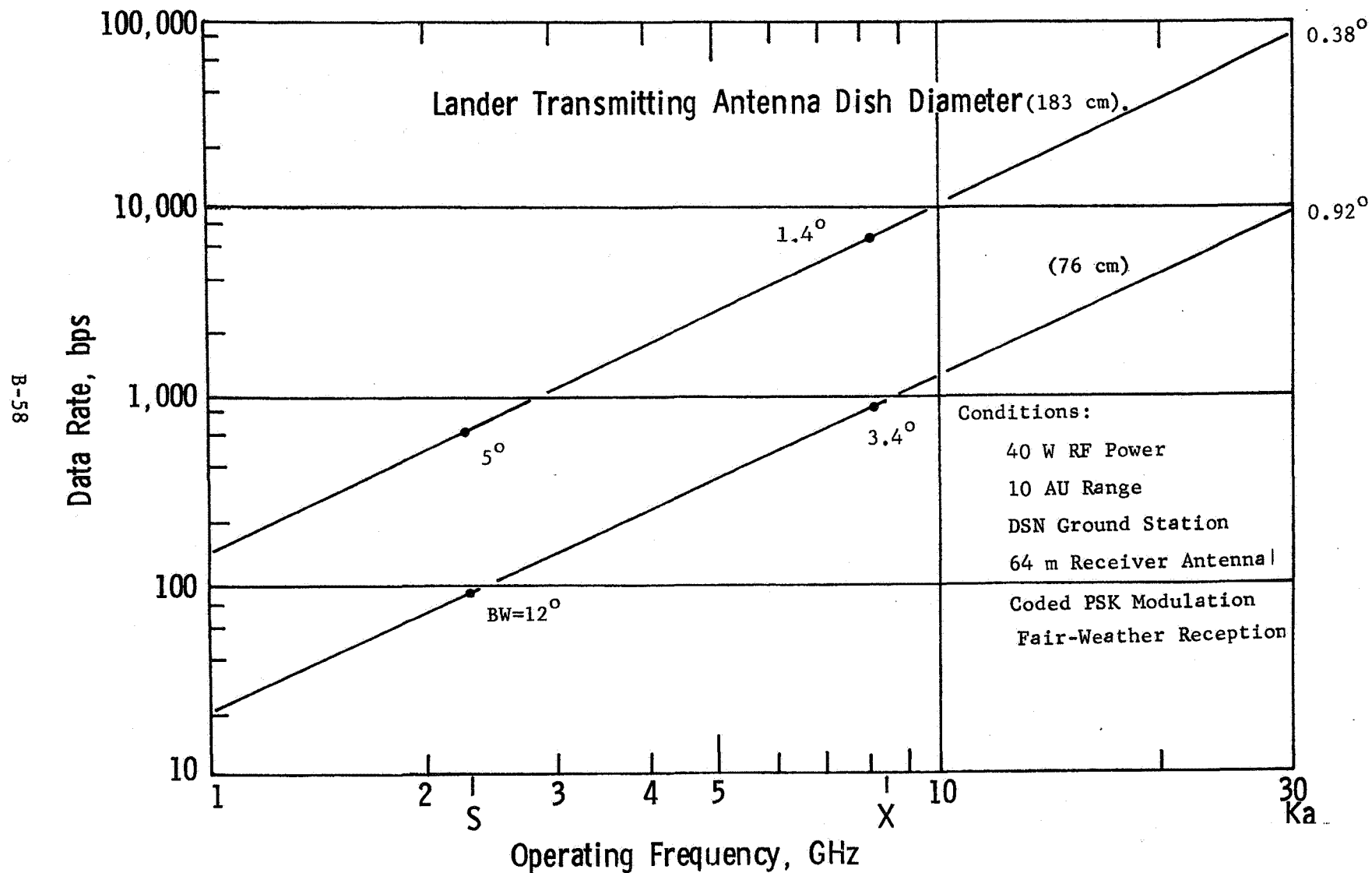
B-57

Fig. B-25   Titan Lander Direct RF Data Link to Earth

antenna above 10 GHz is doubtful, due to the small beamwidth and attendant pointing problem.

Characteristics and operating sequences for the lander science are shown in Table B-13. Biology and image experiments are not performed simultaneously and a typical operating day (24-hour period) consists of the MS and atmosphere sensor AS scans six times a day. A tape recorder on the lander stores the encoded digital data until transmission to Earth via the direct or relay RF links, depending on Earth viewing. Recorder capacity is 2 million bits to accommodate the several days when neither Earth or the orbiter is within view of the lander.

The surface sampler provides the sample material for the GCMS and operates once each biology cycle. GCMS sampling then would be required for 15-20 consecutive days to complete the sample cycle with daily sample monitoring at a low data rate. The total GCMS data output is 100,000 bits.

Lander engineering functions are monitored daily at a low rate and are stored on the tape along with the science PCM encoded serial bit stream. The engineering data are transmitted to Earth on a separate subcarrier and may or may not be transmitted simultaneously with the science subcarrier, depending on the RF link margin during the transmission.

Lander Power Subsystem - Power is required for the lander science and engineering subsystems while on the Titan surface. Power is also required during the coast phase to operate a 5-day clock. The mission timeline meets the science requirements and provides sufficient time to transmit the data. Considerable variation in the timeline is possible. The power and energy requirements are shown in Table B-14. Note that either the S-band direct RF link or the UHF relay link is used, but not simultaneously.

The lander power distribution system is shown in Figure B-26. A typical timeline sequence requires 40 W from the RTG's and a 615 W-hr

Table B-13   Titan Lander Science Data Sequence

Abbreviation	Science Equipment	Use	Scan Time (min)	Data/Cycle (kbits)
MS	Mass Spectrometer	6 scans/day	15	2
AS	Atmosphere Sensor	6 scans/day	15	2
GCMS	GCMS Biology	3 cycles/mission	180	100
SS	Surface Sampler	3 cycles/mission	20	8
C	Imaging	20 pictures/mission	15	1,000

Data Format	Science On	Total Bits	Days Used	Note
1	AS, MS	24K	Others	Typical Day
2	GCMS, SS, AS, MS	132K	3	Biology Exp. Day
3	C, MS, AS	1.024×10^6	20	Camera Day

Table B-14 Titan Trial Mission Lander Power and Energy Requirements

	Power, W	Time per Sample or Activity, min
Coast Phase		
5-day Clock	0.001	5 days
Deceleration Switch	0.2	120.0
Landed Phase		
Science:		
GCMS/Life Detection		
Standby	7.0	--
MS Scan	15.0	15
GCMS Mode	50.0	180
Atmospheric Sensor Array	5.0	15
Camera	15.0	15
Surface Sampler	40.0	20
Data Management	10.0	
Transmitter, S-Band	160.0	120*
Transmitter, UHF	(40.0)	(60)
Ordnance Relays	3.0	0.01
Attitude Reference	10.0	30
Antenna, Deploy & Track	10.0	120

*Note: Timeline includes a 2-hr transmission directly to Earth
every 24 hr. Science acquisition and data storage are
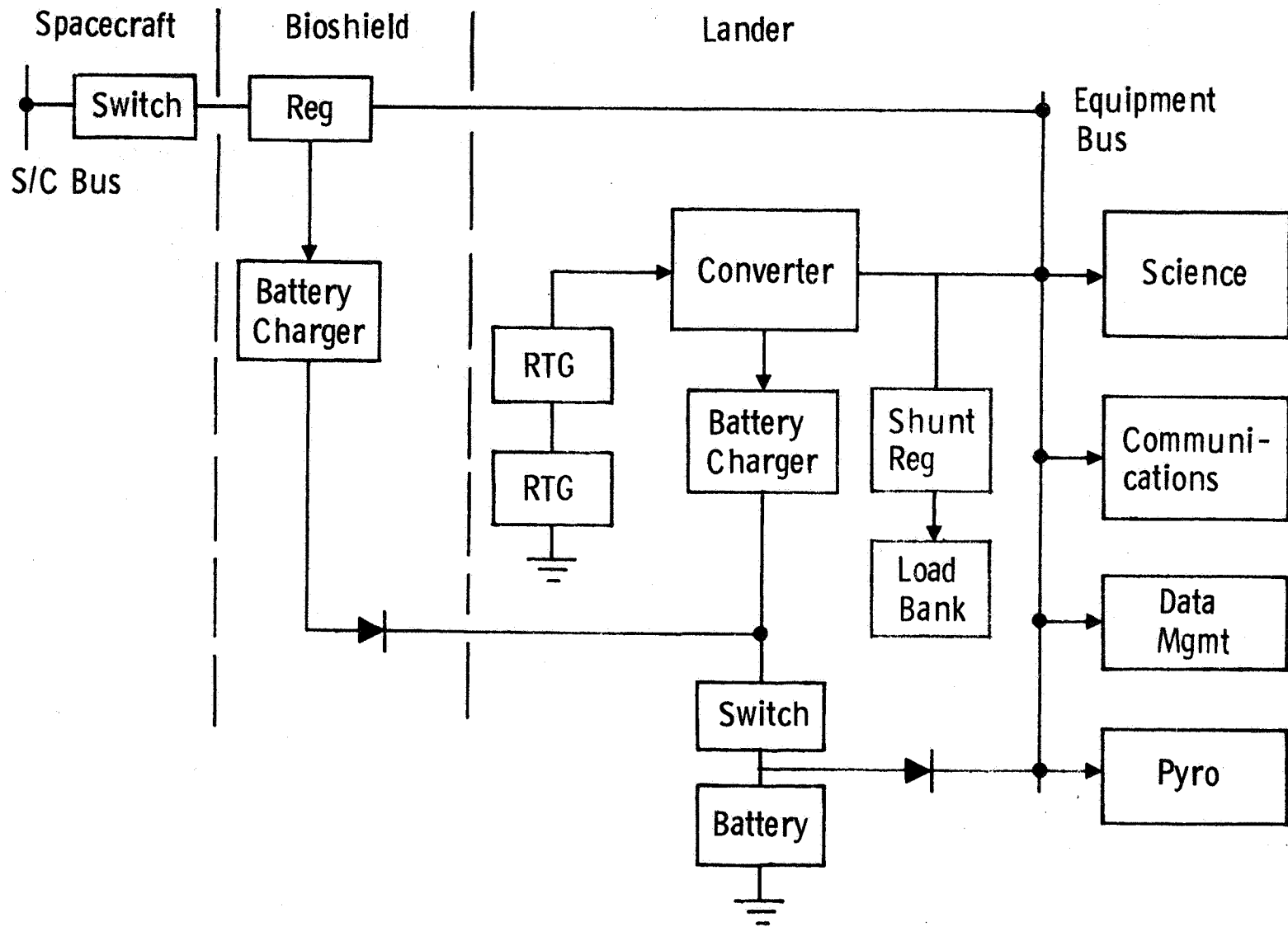carried out during remaining 22-hr period.

Fig. B-26 Titan Lander Power Subsystem

rechargeable nickel-cadmium battery. This provides sufficient power
for a 2-hr data transmission directly to Earth over the S-band link to
the DSN every 24 hours and science data acquisition and storage during
the remaining 22 hours.

Upon impact, the high gain S-band antenna is deployed and
directed to the Earth line of sight. Thereafter, the antenna is
repositioned and slewed as required during the 2-hr data transmission
period. When the orbiter is within view and at a favorable range, data
are also relayed to it on the UHF link as a redundant mode.

The spacecraft provides the initial battery charge prior
to lander separation. Periodic recharging after impact occurs from
the RTG's as required. The power system provides unregulated, 28 V
power to the loads and a Power Control Unit controls battery charging
and power distribution. Time sharing is also utilized to minimize peak
loads and total energy requirements.

Long storage life in a remotely activated battery is achieved
by holding the electrolyte in reserve from the plates until power is
needed. Still some capacity will be lost by sterilization because of the
unstable nature of the silver oxides making up the positive plates.
There are many complex oxide levels in a silver oxide plate. The primary
composition consists of two higher oxides, AgO and Ag_2O_2, and a monoxide
level of Ag_2O. In a fully charged plate approximately 70 percent of the
available capacity is obtained at the monoxide level and the remainder
in the higher oxide or peroxide levels. The higher oxides are relatively
unstable and chemical decomposition into gaseous oxygen and Ag_2O occurs
at a rate dependent on temperature, humidity, and residual electrolyte.
The more stable monoxide also decomposes but at an extremely low rate
and over many years. In our previous investigations we have not
discovered any programs carrying out sterilization of reserve batteries.
Despite lack of test data, most battery authorities feel that the loss
due to sterilization can be expected to be about 25 percent, as seen in

Figure B-27. Earlier sterilization criteria specified a temperature of 110°C; however, recent findings of "hardy" organisms on Viking components have indicated that a sterilization temperature of 120°C may be required.

D. IMPACT ON TRIAL MISSION DESIGNS AND SCIENCE ACCOMPLISHMENT OF UNCERTAINTIES IN TITAN'S ATMOSPHERE AND SURFACE CONDITIONS

The variations in touchdown velocity and descent time for probes, penetrators, and landers encountering the various atmosphere models are summarized in Table B-15. Designing these vehicles to perform satisfactorily regardless of the atmosphere encountered results in significant design penalties and reduced scientific payloads.

Entry Probe - In the case of the atmospheric entry probe, the main problem is in dealing with the thin model atmosphere; i.e., the descent would be too rapid (6 minutes total) to obtain and process even a single gas chromatograph sample, and telemetry data rates would exceed transmission capability. One solution to this problem would be to equip the probe with an auxiliary parachute to be deployed if a thinner than nominal atmosphere is encountered. Figure B-28 shows the growth required in the nominal probe design to incorporate the 8 meter diameter parachute that would be required. Mass increase to account for afterbody staging, chute deployment, and chute mass is estimated at 20 to 30%. Also, some means would be required for determining whether, and when, to deploy the chute; e.g., an onboard system capable of calculating the density profile from entry accelerometer data or from radar altimeter and pressure/temperature data.

The existence of a heavy atmosphere model also degrades the probe mission performance. It requires the phasing between the bus flyby and the probe entry to be biased such that the longer descent time (74 min) does not result in the relay communication spacecraft having gone over the horizon before the probe reaches the surface. This, however, is not as severe a problem as is the too-rapid descent in the thin atmosphere. A somewhat higher aerodynamic heating rate is caused during the more rapid density buildup (lower scale height) of the thick atmosphere model but the effect on total probe mass is less than 5%.
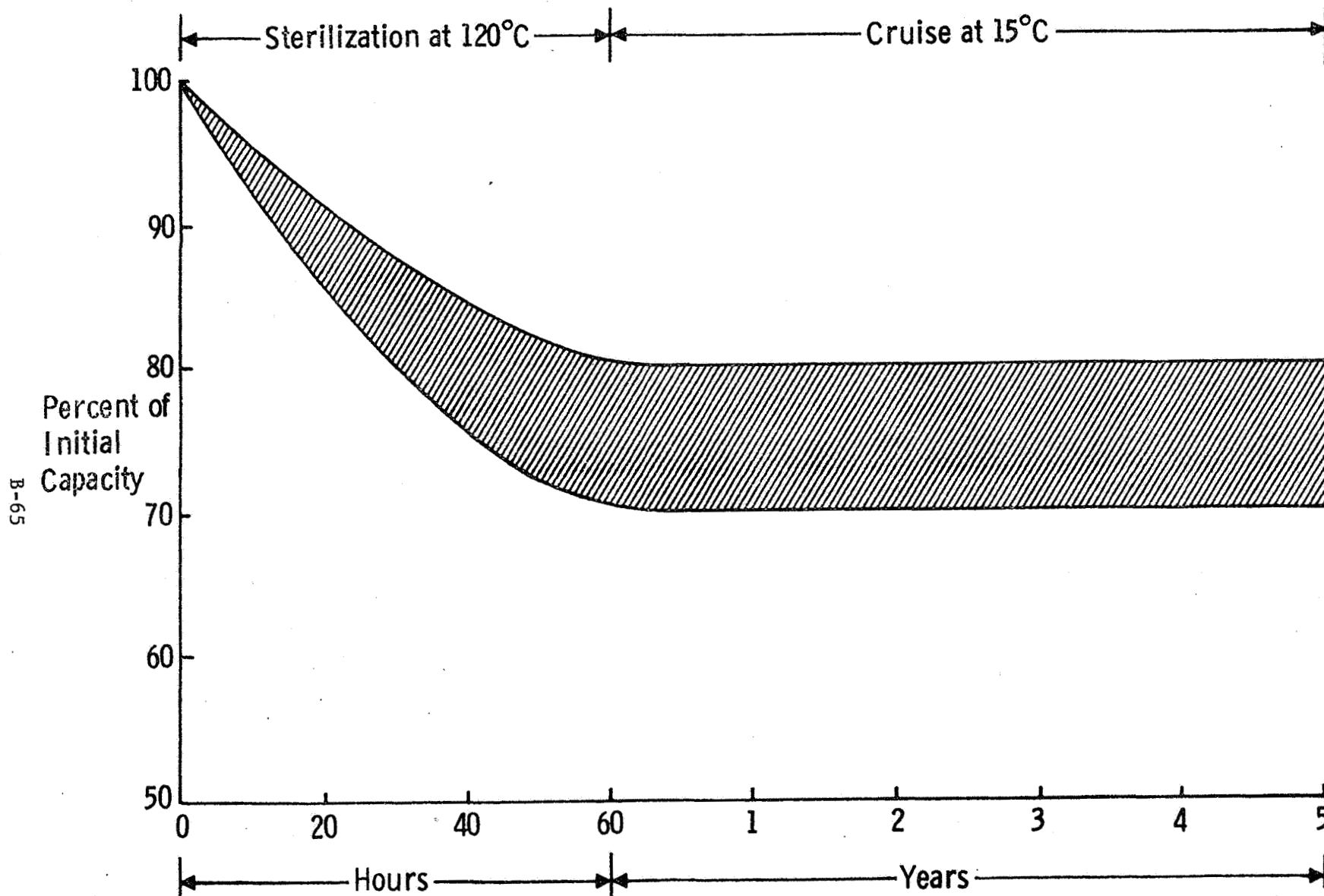
B-64

Fig. B-27 Effect of Sterilization and Storage Life on Remotely-Activated Ag-Zn Batteries

	Probe			Penetrator			Lander		
Entry Angle	-60			-60			-60		
Entry Attitude	594			594			594		
Entry B, slugs/ft^2	.5			.4			.5		
kg/m^2	78			63			78		
Final B, slugs/ft^2	.84			83			.035		
kg/m^2	135			13038			5.5		
Max Deceleration, q	11.3			10.5			11.3		
	THN	NOM	THK	THN	NOM	THK	THN	NOM	THK
Staging Altitude, km	N/A	N/A	N/A	35	100	112	2	2	2
Touchdown Velocity, m/sec	114.8	14.8	11.1	330	146	110	23.7	3	2.2
Total Mission Time, min.	6.2	42	74	9.5	10	13	7.5	51	85

THN = Thin Atmosphere

NOM = Nominal Atmosphere.
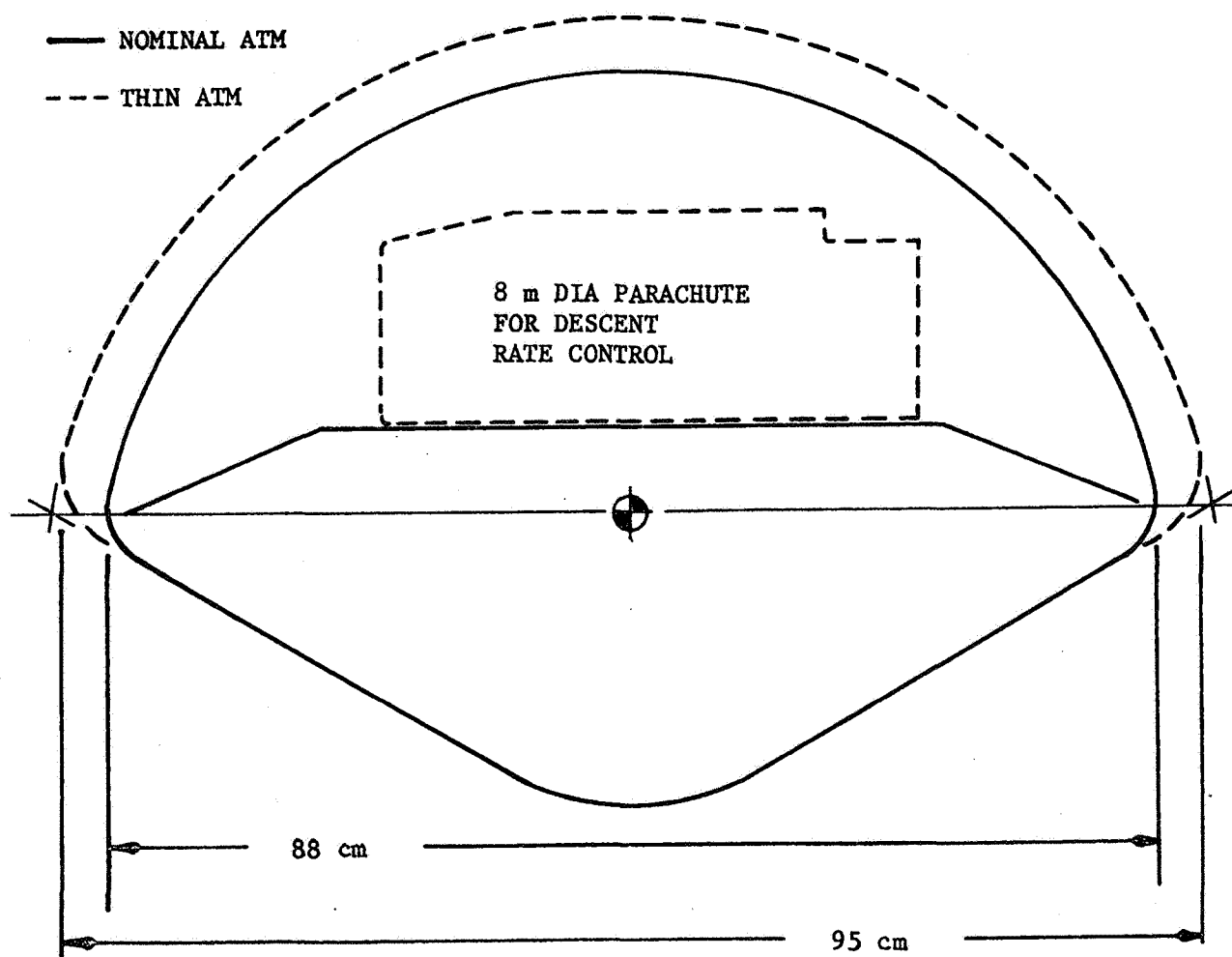
THK = Thick Atmosphere

Fig. B-28 Probe Design for Thin Compared to Noninal Model Atmosphere

Penetrator Missions - The penetrator is more sensitive to atmospheric uncertainties than is the entry probe since it must also deal with a wide range of uncertainty in the penetrability of the surface material. The spread in impact velocity as seen in Figure B-29 varies from 100 m/s in the thick model atmosphere to over 300 m/s for the Thin model. This compares to a much narrower velocity spread for the Mars penetrator, 140 m/s to 160 m/s (see Reference B-2). The disadvantages of the wide spread in the Titan case stem from the fact that obtaining a mass/area ratio for the penetrator large enough that the lowest impact velocity will produce an acceptable penetration depth (one meter) requires either a much smaller cross sectional area than is practical, or a much greater mass than is desirable. Even if these penalties are tolerated, the upper side of the velocity spread results in supersonic impacts and correspondingly high g levels unless an auxiliary drag device is carried with appropriate sensing systems to determine when to deploy it.

An attempt to narrow the Titan impact-velocity spread by selecting a different predetermined pressure for entry cylinder staging reveals that this can only be accomplished if the two extreme models are considered, but that denisty models between the extremes will result in penetrator impact velocities that exceed the Thin model impact velocity. This is due to the penetrator reaching a greater fraction of its terminal velocity at impact in those cases since staging will occur at higher altitudes. Selecting the appropriate altitude for staging the entry cylinder to achieve the desired impact velocity requires an on-board, real time system for determining the atmospheric density profile that exists.

Landers - Similar problems exist with landers. One way of dealing with the higher touchdown velocity experienced by a lander that encounters a Thin model atmosphere, 24 m/s vs 3 m/s nominal is to increase the stroke of the landing gear. However, for a given g level the stroke required is proportional to the velocity squared and thus even with a major redesign of the landing gear, much higher g levels would have to

Legend:

Terminal Velocity Profiles —x—x—

Thick ——————
Nominal —————— } Descent Profiles
Thin —·——·—

Penetrator Descent Trajectories in Various Model Atmospheres

$m/C_D A = 63$ kg/m^2 before staging and 13083 after staging

In each case staging occurs at a pressure of 6.5 millibars

Terminal Velocity Curve for thick Atm

Terminal Velocity Curve for Nominal Atm Model
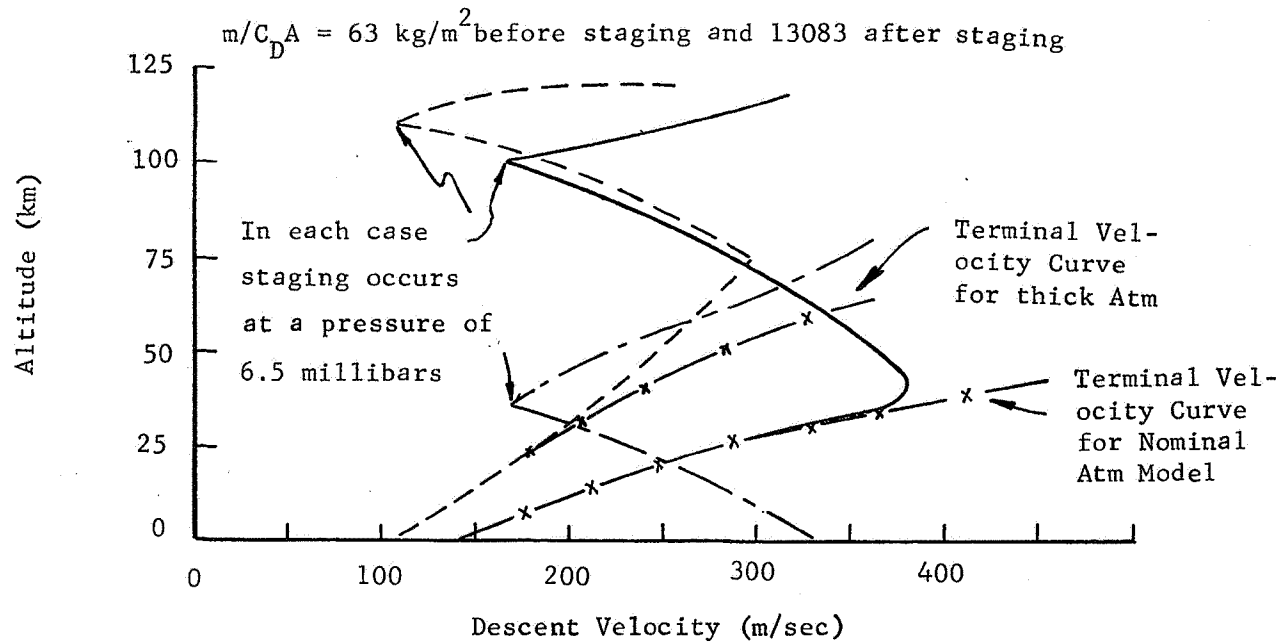
Altitude (km)

Descent Velocity (m/sec)

Fig. B-29 Penetrator Altitude-Velocity Profiles

be tolerated. Alternatively, as in the case of the entry probes and penetrators, an auxiliary parachute could be carried or the basic chute could be made larger. In the case of the thinnest density model atmosphere, which at the surface is similar to the very tenuous atmosphere found on Mars, it might be necessary to add a terminal propulsion system similar to that used on the Viking '75 lander, see Figure B-30, and compare with Fig. B-19. Such a system would be required in any case if winds turn out to be an appreciable fraction of the lander's sink speed (in order that the chute can be jettisoned to avoid high incidence angles and tipover problems at touchdown). The additional mass required for such a landing propulsion system, exclusive of propellant, is shown in Table B-16.

In addition to inducing a requirement for greater system masses which means less mass available for science, the atmospheric uncertainties degrade the achievement of science objectives since with conventional techniques instrument settings have to be preestablished to cover the range of possible conditions and accuracy is thereby sacrificed.

Consequently, adaptive designs are desirable for science instruments and data processing systems as well as for engineering systems in order to preclude having to conduct a long series of sequential missions. Ideas for such techniques are discussed in Chapter III.

Table B-16
Thin Model Atmosphere Lander Dry-Mass Breakdown

BASELINE LANDER   337.3 Kg

PROPULSION SYSTEM   8.3 Kg
      PROPELLANT TANKS (2)   3.2
      LATERAL ENGINES (6)   1.4
      LINES   1.4
      COMPONENTS   1.4
      TERMINAL DESCENT (3)   .9

GUIDANCE & CONTROLS   14.5 Kg
      PROCESSOR & SET   .9
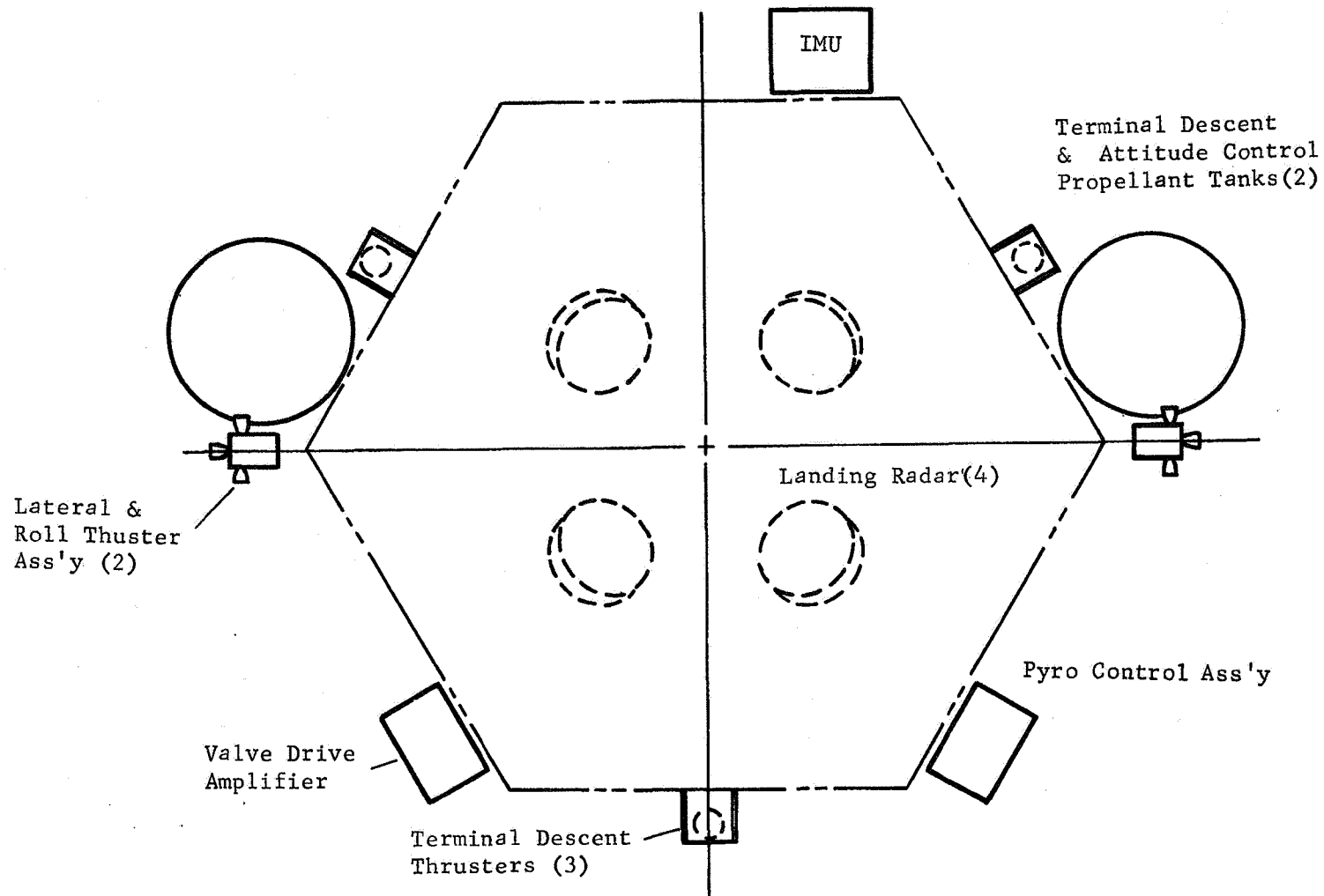   IMU   3.6
      VALVE DRIVE AMPLIFIER   3.2
      LANDING RADAR   6.8
                                                          _____
                  TOTAL   360.1 Kg

IMU

Terminal Descent
& Attitude Control
Propellant Tanks(2)

Lateral &
Roll Thuster
Ass'y (2)

Landing Radar(4)

Pyro Control Ass'y

Valve Drive
Amplifier

Terminal Descent
Thrusters (3)

Fig. B-30 Thin Atmosphere Model Lander

E. <u>REFERENCES</u>

B-1 "Outer Planet Atmospheric Entry Probe - System Description",
Ames Research Center, NASA, Moffett Field, California, July
1975.

B-2 "Mars Penetrator Subsurface Science Mission" SAND 74-0130,
Sandia Laboratories, Albuquerque, New Mexico, August 1974.

B-3 "Design of Multi-Mission Chemical Propulsion Modules for
Planetary Orbiters", TRW System Division, Contract NAS2-8370
for NASA Ames Research Center, August 1975, NASA CR 137789
through 137791.

B-4 R. F. Draper et al., "The Outer Planet Mariner Spacecraft",
Jet Propulsion Laboratory, Contract NAS-7-100, September 1975.

B-5 NASA Space Design Criteria (Environment) "The Environment of
Titan (1975)" August 1975, NASA SP-81XX (to be Published).